EXPLOSIVE PRODUCTION OF NEW MATERIALS: SCIENCE, TECHNOLOGY, BUSINESS, AND INNOVATIONS

Edited by

M. I. Alymov

O. A. Golosova

TORUS PRESS   MOSCOW 2018

Mikhail I. Alymov
Merzhanov Institute of Structural Macrokinetics and Materials Science
Russian Academy of Sciences
Chernogolovka, Moscow, 142432 Russia

Olga A. Golosova
Merzhanov Institute of Structural Macrokinetics and Materials Science
Russian Academy of Sciences
Chernogolovka, Moscow, 142432 Russia

This book is a collection of revised, edited, and formatted abstracts submitted to the 14th International Symposium on Explosive Production of New Materials: Science, Technology, Business, and Innovations (EPNM-2018) held in Saint Petersburg, Russia, May 14–18, 2018. The contents of the book include recent worldwide accomplishments in basic and applied research on application of explosives (explosion, shock, and impact) to materials synthesis and processing. The book is addressed to practicing engineers, research workers, and graduate students active in the field.

Preface

The series of symposia on Explosive Production of New Materials (EPNM) continues the tradition laid down at the international meetings held in 1970s-1990s, such as HERF (held in USA and former USSR), EXPLOMET (held in USA) and EWM (International Symposium on Explosive Working of Metals held in former Czechoslovakia). The countdown of EPNM symposia is from the last (7th) EWM meeting held in Pardubice (Czechoslovakia) in 1988. After a long break, the tradition was restored in 2006 by holding the 8th symposium in Moscow (EPNM-2006). Prof. Yuri Gordopolov, Prof. Andrei Deribas and other employee of Merzhanov Institute of Structural Microkinetics and Materials Science of Russian Academy of Sciences (ISMAN) made a crucial contribution to the organization of EPNM-symposia as a meeting platform for researchers, engineers and businessmen using the explosion in research and production.

After 2006, several EPNM-events took place in different European countries outside of Russia. Now, after 12 years, symposium returned to Russia and is held in a picturesque city of Saint-Petersburg. The scope of EPNM-2018 is traditional and includes explosive welding, commercial explosion metalworking, processing of welded bimetal, synthesis of new materials, shock activation, high-strain rate deformations associated with explosive loading, explosive compaction/consolidation of powders, self-propagating high-temperature synthesis, combustion and chemical conversion of powder mixtures, etc. The abstracts concerning all these areas, submitted by participants from the different countries (Russia, USA, China, Germany, Poland, Japan, Portugal, Ukraine, Czech Republic, etc.) are included in this book. Attention was given to the current trends in the explosion metalworking, post-welding treatment of bimetal and multilayered composites, and formation of interface structure during explosive welding and other processing methods. The reports on the synthesis of new materials (including graphene-like carbon) by detonation, combustion and shock wave techniques prove the importance and prospects of this research area.

The present and previous EPNM symposia confirm that high-pressure and high-temperature methods of impact on materials continue to develop, and EPNM-events are important for the appropriate scientific and business community worldwide.

<div align="right">

A. A. Shtertser

M. I. Alymov

</div>

Organizers

Merzhanov Institute of Structural Macrokinetics and Materials Science, Russian Academy of Sciences (ISMAN)
Chernogolovka, Russia

EnergoMetall Co.
Saint Petersburg, Russia

Acknowledgments

Symposium Sponsors

NobelClad
A DMC Company
5405 Spine Road, Boulder, CO 80301 USA
www.nobelclad.com
tel.: +1 800 821-2666

NobelClad, a DMC Company, is the world's leading provider of explosion-welded clad metal plates. Its Detaclad TM products are used in a variety of industries, including petrochemicals, refining, hydrometallurgy, aluminum smelting, and shipbuilding. Most recently known as DMC, the Boulder, Colorado, USA based company began business in 1965 as an explosion forming specialist, producing complex three-dimensional parts for aerospace equipment manufacturers. NobelClad became a publicly traded company in 1976 under the ticker symbol "BOOM" and shortly thereafter licensed technology from E. I. DuPont de Nemours and Company ("DuPont") to explosively bond, or clad, two or more dissimilar metal plates together. The explosion-bonded clad metal business remains NobelClad's core business today. The acquisitions of DuPont's Detaclad Division in 1996, Nobelclad Europe in 2001, and DynaEnergetics in 2007 have strengthened the Company's world-wide position in explosion cladding. In 2013, Dynamic Materials Corporation became DMC to serve as the parent company for its subsidiary businesses. The explosion welding entities (DMC Clad Metal U.S., Nobelclad France, DynaPlat Germany) now operate under the single global trade name of NobelClad.

The company is located in an area of strong, wide co-operating companies. Explomet has the ability to perform explosive works on own cladding area and possesses own production technology of explosives.

The Company's structure, adapted to the scale and scope of production ensures efficient implementation of orders received from domestic and foreign customers. Production is under constant supervision of the quality control department. Produced cladding materials are subject to standard test and control procedures compatible with European regulations, AD-2000 Merkblatt W0-W8, ASME / ASTM rules or other designated by the customer. Each batch of manufactured products receives full documentation attesting the production process and quality.

Dimensional assortment of offered cladding products is very wide. We are using practically all of material's grades, applied in this technology. For industrial purposes, thickness of the clad material is mostly more than 1 mm and not more than 25 mm, in one shot. The maximal area of a single cladding element, depending on the thickness of the component materials can be more than 20 m^2.

EnergoMetall Co.
St. Petersburg, Russia
tel. +7 (812) 535-7243, 336-6465
fax +7 (812) 534-1919
e-mail: info@emet.ru
http://emet.ru

EnergoMetall Co., St. Petersburg, Russia. Production of two- and multilayer clad metals by explosive welding, their subsequent machining, and manufacturing industrial products.

EnergoMetall was established in 2003. In 2007, the Company produced first bimetallic products for the European customer on the basis of the Finnish subsidiary company "Energometall Oy". Since 2012, the Company has been producing bimetallic products in Saint Petersburg using its own production area and testing ground.

Over the past ten years, EnergoMetall has mastered the manufacture of multilayer metals to various industrial sectors including power, chemical, petrochemical and shipbuilding, and has become a supplier of bimetal plates for the international project, ITER.

EnergoMetall is certified by the European Office of BV and has experience in exports of products to the countries of EU, Asia, and Latin America.

Contents

EXPLOSIVE WELDING AND ITS APPLICATION

A. A. Deribas

Joint Institute for High Temperatures, Russian Academy of Sciences, Moscow, 125412 Russia

e-mail: aderibas@mail.ru

Multilayer metallic materials were first discovered upon penetration of armour plates by high-explosive projectiles. Such projectiles were invented at the end of XIX century and used in World War II to fight tanks. The projectiles with hollow conical shells upon impaction with a barrier create a high-rate jet from shell metal, which breaks through the barrier. The external part of the shell forms the so called slug. If the materials of jet and shell differ, a two-layer slug is obtained. This is apparently the first way to produce two-layer materials by explosion welding. During the war, researchers focused on armor-piercing studies and neglected this effect.

In 1944, L. R. Carl reported in the Metal Progress magazine a brief publication on the explosion welding of metallic plates. However, we did not find any more publications on this subject, as well as other works of this author. Explosion welding was not actually used until the 1960s. In 1960, G. R. Cowan, J. Douglas, and A. Holtzman, American researchers, published a patent on the explosive welding process.

The Institute of Hydrodynamics, Siberian Branch of the USSR Academy of Sciences was founded in 1957. The Institute headed by M. L. Lavrent'ev engaged in the studies of explosive processes. I led a small group that carried out the explosive experiments. Once, it was in 1960, E. I. Bichenkov and Yu. A. Trishin, employees of group, showed me a "by-product" of one of the experiment — stuck together pieces of steel and copper. I brought this sample to V. S. Sedykh, welding specialist and senior researcher of the Institute, and asked what it was. He looked closely, felt the seam, and said that this is

welding. This sample was the same as the piece of stamp that M. A. Lavrent'ev found at once after the war near Kiev.

We began to analyze the welding process. The pieces of steel and copper lied one above the other. As a result of explosion, one metal penetrated into another and in the boundary layer, an alloy based on these metals was obtained. We carried out experiments successful and become to develop purposefully the explosion welding of metals. We found out that almost any metals can be welded using an explosion, you only need to choose conditions: distance between plates, collision velocity equal to a ratio of charge mass to flyer plate mass, and other parameters.

In 1962, V. S. Sedych, A. A. Deribas, E. I. Bichenkov, and Yu. A. Trishin issued a first publication devoting to the explosion welding in USSR (in *Svarochnoe proizvodstvo*).

Thus, two centers for R & D in explosion welding — USA and USSR — were formed in the early 1960s. The number of studies and industrial applications of new process in the 60s and 70s in the USA and USSR was approximately the same. Then, American researchers stopped publishing for reasons unknown to us.

Explosion welding has been significantly developed in Europe (Germany, Poland, France, Netherlands, etc.). All these works were the result of cooperation with us. Based on our results and personal contacts, explosion welding process has been applied and developed significantly in China, India, and Japan.

Let us consider the application of explosive welding to produce multilayer materials for different purposes in Russia.

(1) The first practical application of explosive welding has been implemented at the Institute of Hydrodynamics. We produced an experimental batch of bimetallic sheets for the spacecraft. The Deputy General Designer of S. P. Korolev came to the Institute for conversations. He said that they have not managed to weld metal sheets using the traditional method to a scheduled appointment of the launching of spacecraft and suggested us to apply the explosion welding. After the positive results of tests, we received an order for 500 sheets. The order was executed in a week at the testing ground, near Novosibirsk and was sent to Moscow. Then, we received a telegram signed by S. P. Korolev: "Thank you for your astute work".

A. A. Deribas

(2) During the late 1970s, A. A. Shtertser, B. S. Zlobin, V. M. Ogolikhin, and others, young workers of the Siberian Branch of the USSR Academy of Sciences (joined to works on the explosive welding. Soon, B. S. Zlobin and A. A. Shtertser led the team that developed the welding process between steel and aluminum–tin alloy with clad aluminum for the production of billets of the friction bearings of large-scale diesel engines of railway locomotives, ships, diesel generators and other devices. Specialized technological equipment for explosion welding and subsequent stamping of flat bimetal billets in a semi-ring using a hydraulic press was designed and manufactured, all the necessary tests were carried out, approval was obtained, and the production of bimetal billets of friction bearings was organized. The production of more than 20 sizes was mastered. Works continue, and to date, about 115 thousand blanks of bearings were produced.

(3) In CRISM Prometey, a group headed by I. I. Sidorov develops technologies and produces bimetallic products for marine vessels for various purposes since the mid-1960s. It is known that more than 2000 steel–copper, steel–aluminum, and steel–titanium billets were made.

As of now, JSC United Shipbuilding Company, JSC PO Sevmash, CRISM Prometey, and Rubin and Malakhit Design Bureaus with the participation of Bitrub International Ltd use the explosive welding to form joining between titanium and steel in a protective gas environment.

(4) In 1964, JCS Anitim in cooperation with JSC RPA CNIITMASH, then Bitrub International Ltd and Altai State Technical University (ASTU, Barnaul) began to use explosive welding. The most famous achievements are the corrosion resistance steel cladding of blades of hydroturbines for Krasnoyarsk, Sayano-Shushenskaya, Charvakskaya HEPs and HEP Site 1 (Canada), tube plates for chemical reactors, bimetal for steam separators and hydraulic accumulators of Bilibino and Chernobyl NPPs. Welding processes of steel with copper, aluminum, titanium, as well as the technology of production of a three-layer corrosion resistance sheet by the explosion welding method with subsequent rolling have been developed and mastered.

Before 1991, the total volume of production was more than 17 thousand tons, the volume of output of a three-layer billet reached 30 thousand square meters.

Bitrub international Ltd (founded by Prof. L. B. Pervukhin in 1992 in Barnaul) in cooperation with ISMAN at the Geodesy Research Institute base began industrial production of bimetal by welding explosion in Krasnoarmeisk (Moscow) in 2004. Together with ASTU, the unique technology for manufacturing large-size steel/titanium sheets in the environment of argon was developed and mastered industrially. The processing was highly appreciated by John Banker (DMC, USA). This technology allowed producing more than 200 sheets (12 sq. m) for tube sheets of condensers of nuclear power plants.

In 2015, Bitrub Ltd was established to develop new technologies of production of explosively welded bimetal. The volume of production of bimetallic sheets of various compositions and dimensions largely for petrochemical engineering and NPPs was more than 32 thousand sq. m in all.

In 2017, Bitrub Ltd produced and supplied 6,000 products (two-layer rods) for current leads of electrolyzers for Kola Mining and Metallurgical Company.

(5) Since 1995, Pulsed Technologies Ltd (Krasnoyarsk, Russia) fabricates aluminum–steel and aluminum–copper bimetallic inserts and copper–aluminum adapters by explosion welding, and applies explosive welding to produce aluminum current leads of large cross section. Performed is a joining of electrical wires using aluminum or steel shunts welded by explosion welding to the surface of the wires. Customers are all Russian aluminum plants (RUSAL). To data, Pulsed Technologies Ltd has delivered about 200 thousand bimetal adapters.

(6) EnergoMetal JSC (St. Petersburg) has been registered in 2003. In 2005, EnergoMetall in co-operation with the research center Prometey have developed and implemented the technological process of explowelding for large size metal plates with clad titanium layer. Further development of the technology was carried out by subcompanies in Finland and Estonia. Since 2013, the production facilities moved to Saint Petersburg.

The first products have realized in 2007 in Finland. Currently, EnergoMetal JSC has a wide range of bimetallic products with an area of sheets up to 30 m^2 for the needs of energy, chemistry, petrochemistry, shipbuilding, and is a supplier of bimetallic parts for

diverter hull and superconducting contacts for the international project of the thermonuclear reactor ITER. Export orders are executed.

In just 10 years, 1100 sheets of bimetal were produced under the order.

Pilot-scale batches of bimetals were manufactured by explosive welding in many EU countries at our initiative and with our support. Americans learned about welding explosion from us — for some reason they did not known early works of their compatriots — and created the ground in the South of France where successfully make bimetal. As a result of personal contacts with the Lavrent'ev Institute of Hydrodynamics (LIH), the explosion welding has been successfully used in India, China, and Japan.

Thus, the explosive welding technique elaborated in the LIH is well developed and applied in various fields of industry for more than 50 years.

The main advantage of explosive welding is in joining metals that would frequently be incompatible. Whereas the usual way requires to develop the technology individually for each combination using complex expensive equipment.

In the future, this process must evolve and the volume of production of multilayer metallic materials will multiply.

ISMAN – NEW RESULTS ON THE SYNTHESIS OF NEW MATERIALS

M. I. Alymov

Merzhanov Institute of Structural Macrokinetics and Materials Science, Russian Academy of Sciences, Chernogolovka, Moscow, 142432 Russia

e-mail: alymov@ism.ac.ru

Merzhanov Institute of Structural Macrokinetics and Materials Science, Russian Academy of Sciences (Russian acronym ISMAN) was founded in 1987. ISMAN has a status of the Federal State Budgetary Institution of Science. It operates under the authority of the Federal Agency for Scientific Organizations (FASO Russia). The purpose and scope of Institute activities is to carry out fundamental, research, and applied scientific studies in the field of physics and chemistry of combustion and explosion processes, physicochemical transformations of substances under high temperatures and pressures, and materials science.

In Shock-Driven Processes Laboratory, high-strength steel (30KhGSA)/special steel (60G40D) bimetal sheets possessing high strength and good damping capacity were fabricated by the explosive welding. To restructure fusion zones and to produce explosively welded high-strength joint between ferritic steel and pig iron, annealing regimes were found. It was experimentally shown that the explosive welding of titanium/steel sheets having an area of above 9 m^2 provides the joint strength of more than 300 MPa over the entire sheet surface [1].

The influence of preliminary mechanical activation on SHS of sialon powders and their sintering was explored. Dependencies of physicomechanial characteristics of products on the properties and composition of initial components were revealed. It has been

determined that the external factors (initiation temperature of synthesis, heat removal presence, etc.) affect the synthesis process [2].

Experimental and theoretical studies of the physicochemical transformation of mixtures of trinitrotoluene (TNT) in shock wave processes were carried out. A new set of equations of motion for reacting medium was obtained. Parameter determining the decay rate is a deformation rate rather than temperature.

Theoretical calculations of the wave pattern of the bands of localized deformation showed that the necessary condition of the localization of plastic deformation is an oscillation of the sample in the nodes of standing waves, in which the localized deformation band is nucleated and developed [3, 4].

V. A. Shcherbakov and co-workers established experimentally the possibility to produce ceramic composites by SHS compression method allowing simultaneously to synthesize ceramic material based on refractory compounds (ZrB_2, CrB) and to press it to obtain minimal residual porosity [5–8]. The SHS-pressed ceramic composite possesses high thermal conductivity, hardness, and wear resistance. The heat, electric and kinetic regularities of electrothermal explosion (ETE) of titanium–carbon soot mixture under quasi-isostatic compression conditions were first studied. It has been shown that the electric resistance of the investigated sample at the stage of pre-explosive heating decreases by 90–95%.

The principal possibility of obtaining metal–ceramic composites based on TiC–Fe system by ETE method under a pressure was shown [9]. The introduction of metal binder (Fe) into initial system provided the production of the high-density SHS composite. It has been shown that an increase in the pressing pressure favors to an increase in the density of SHS composites from 5.4 to 5.85 g/cm^3 and to a decrease in their total porosity from 10.6 to 1.6%. Depending on the metal–ceramic composite density, Vickers microhardness are changed from 19 to 30 GPa.

Prof. A. M. Stolin and co-workers developed the technological process of production of electrodes with a diameter of up to 10 mm and a length of more than 100 mm by SHS extrusion and free SHS compression. Scale factor problem related to the fabrication of a special tool taking into account features for obtaining such samples was solved [10–12].

V. Yu. Barinov and co-workers showed that kinetic scheme for synthesis of zinc sulfide in conditions of air atmosphere with water vapor should be supplemented by the stage of oxidation of zinc particles, which occurs at the interphase boundary and is extremely exothermic one strongly accelerating both chemical heat release and propagation rate of heat front over the reacting sample. Numerical calculations carried out within the frame of modified two-temperature model allowed to determine the combustion regime with stationary values of temperatures of gas and solid phase, which differ significantly from one another [13].

1. N. L. Fedotova, I. B. Chudakov, I. A. Korms, S. Yu. Makushev, L. B. Pervukhin, I. V. Saikov, N. A. Arutyunyan, Preparation of bimetal with good damping properties, *Metallurgist*, 2017, vol. 61, no. 1–2, pp. 63–71.
2. K. L. Smirnov, Combustion synthesis and luminescent properties of Eu-doped Ca-α-SiAlON, *Int. J. Self-Propag. High-Temp. Synth.*, 2016, vol. 25, no. 2, pp. 107–113.
3. V. S. Trofimov, V. A. Veretennikov, On mechanism of detonation of solid explosives, *Gorenie and vzryv*, 2017, vol. 10, no. 2, pp. 121–128.
4. S. N. Buravova, E. V. Petrov, M. I. Alymov, Chemical transformations in the zone of spall damageability, *Dokl. Phys.*, 2016, vol. 61, iss. 7, pp. 309–312.
5. V. A. Shcherbakov, A. N. Gryadunov, M. I. Alymov, Synthesis and characteristics of the B_4C–ZrB_2 composites, *Lett. Mater.*, 2017, vol. 7, no. 4, pp. 398–401.
6. A. N. Gryadunov, V. A. Shcherbakov, Production and properties of B_4C–TiB_2 and B_4C–ZrB_2 ceramic composites, *Fundamen. Issled.*, 2017, no. 10 (part 1).
7. A. V. Shcherbakov, V. Yu. Barinov, A. S. Shchukin, I. D. Kovalev, V. A. Shcherbakov, T. D. Malikina, A. I. Al'khimenok, Synthesis of TiB_2–30CrB composite by electrothermal explosion uder pressure, *Fundamen. Issled.*, 2017, no. 11 (part 2).
8. V. A. Shcherbakov, A. N. Gryadunov, V. Yu. Barinov, O. I. Botvina, Synthesis and properties of composites based on borides of zirconium and chromium, *Izv. Vuzov. Porosh. Metall. Funk. Pokryt.,* 2018, no. 1, pp. 18–25.

9. V. T. Telepa, V. A. Shcherbakov, A. V. Shcherbakov, Production of TiC–30Fe composite by ETE under pressure, *Lett. Mater.,* 2016, vol. 6, no. 4, pp. 286–289.

10. P. M. Bazhin, A. M. Stolin, M. V. Mikheev, M. I. Alymov, Self-propagating high-temperature synthesis under the combined action of pressure and shear, *Dokl. Chem.*, 2017, vol. 473, pp. 95–97.

11. A. M. Stolin, P. M. Bazhin, O. A. Averichev, M. I. Alymov, A. O. Gusev, D. A. Simakov, Electrode materials based on a Ti–Al–C MAX phase, *Inorg. Mater.*, 2016, vol. 52, no. 10, pp. 998–1001.

12. P. M. Bazhin, A. M. Stolin, SHS extrusion of materials based on Ti–Al–C MAX phase, *Dokl. Acad. Nauk*, 2011, vol. 439, no. 5, pp. 630–632.

13. V. Yu. Barinov, L. M. Umarov, A. A. Markov, I. A. Filimonov, To conditions of chain spontaneous ignition and to comparative characteristics of combustion synthesises with that for ZnS in open air at the limited range of humidity, *Mezh. Zhur. Prikl. Fundamen. Issled.*, 2017, no. 9, pp. 45–48.

INFLUENCE OF ALUMINUM ADDITIVES ON IGNITION OF TUNGSTEN/TEFLON POWDER MIXTURE

M. I. Alymov, S. G. Vadchenko, and I. S. Gordopolova

Merzhanov Institute of Structural Macrokinetics and Materials Science, Russian Academy of Sciences, Chernogolovka, Moscow, 142432 Russia

e-mail: gis@ism.ac.ru

The aim of the work is to study the effect of additives of aluminum on ignition of mixtures of tungsten with Teflon to obtain more high-density condensed products. The combustion experiments of W–Teflon–Al mixtures were performed based on the preliminary thermodynamic calculation. Results of calculations carried out using a THERMO program are presented in Table 1.

Table 1. Results of thermodynamic calculations.

	Initial components, wt %			ρ, g/cm³	T_{ad}, K	Combustion products		
	Al	W	Tf			Gas phase volume, liters	Solid phase products, wt %	Liquid phase products, wt %
1	5	76	19	6.93	3050	75	53 (C; W₂C)	24 (W₂C)
2	10	72	18	6.40	3130	99	2 (C)	74 (W₂C)
3	20	64	16	5.56	1985	106	71 (C; W₂C; Al₄C₃)	0
4	30	56	14	4.91	1660	75	64 (Al₄C₃; W₂C)	11 (Al)
5	40	48	12	4.34	1520	45	55 (Al₄C₃; W₂C)	26 (Al)
6	50	40	10	3.98	1460	22	51 (Al₄C₃; AlF3; W₂C)	41 (Al)
7	60	32	8	3.63	1450	0	45,5 (Al₄C₃; AlF₃; W₂C)	54,5 (Al)

Here, ρ is the theoretical density of material and T_{ad} is the adiabatic combustion temperature.

The prepared mixtures after mechanical activation were pressed in tablets and heated in a special crucible. The crucible heating rate was

M. I. Alymov et al.

varied. Thermograms of combustion at different heating rates are presented in Fig. 1. It is shown that an increase in the heating rate leads to an insignificant change in the ignition temperature of mixtures.
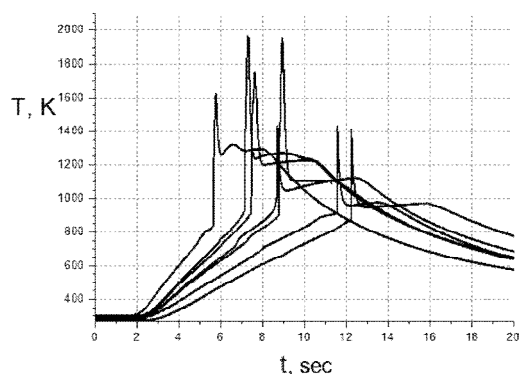
Fig. 1. Thermograms of combustion of 0.90(0.8W + 0.2Tf) + 0.1Al mixture at different heating rates.
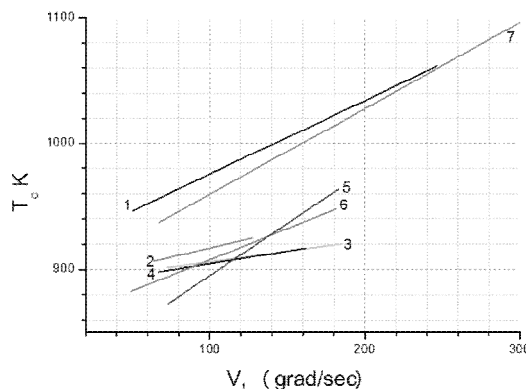
Fig. 2. Critical ignition temperature vs. heating rate of mixtures *1–7* indicated in Table 1.

The calculations show that during ignition and combustion mixtures with small addition of aluminum form a high amount of gaseous products, which completely fly out, or form a high-porous structure. At aluminum high concentration, results of thermodynamic calculations and experiments differ significantly that is explained by the fact that there are no thermodynamic data for tungsten aluminides in the program and the real reaction conditions are far from the equilibrium and adiabatic ones. The dependence of the ignition temperature as a function of heating rate, which was constructed by the method of least squares, is given in Fig. 2.

The experimental and calculated data show that to produce high-density melted products ($\rho(W_2C)$ = 17.2 g/cm^3) an optimal aluminum concentration is about 10 wt %. At the higher aluminum concentrations, the formed main product (tungsten aluminide WAl_4) has a noticeably lower density ($\rho(WAl_4)$ = 6.6 g/cm^3).

EFFECT OF MECHANICAL ACTIVATION ON THE THERMAL AND SHOCK-WAVE INITIATION OF THE REACTION BETWEEN REFRACTORY METALS AND TEFLON

M. I. Alymov, S. G. Vadchenko, I. S. Gordopolova, and I. V. Saikov

Merzhanov Institute of Structural Macrokinetics and Materials Science, Russian Academy of Sciences, Chernogolovka, Moscow, 142432 Russia

e-mail: gis@ism.ac.ru

The powder mixtures of high-melting metals with Teflon and energetic admixtures have been studied. The thermodynamic analysis was carried out, as well as the processes of ignition and product structure formation were investigated. Tungsten or tantalum was used as the mixture component to obtain the high-density condensed products. Aluminum and zirconium were used as the energetic admixtures to decrease ignition temperature and increase mixture combustion temperature. We studied some compositions, which were selected based on thermodynamic calculations to obtain more high-density condensed products with high combustion temperature. The mixtures were prepared by two methods: dry mixing of components and mechanical activation in an AGO-2 apparatus under hexane atmosphere at an acceleration of balls of 60 g for 5 min. Then, we pressed mixtures into tablets for ignition experiments (diameter of 3 mm, weight of 0.01–0.02 g), heated in a boron nitride crucible at atmospheric pressure of argon with regulated heating rate. In the present paper, four reactive compositions have been studied. The experimental thermograms for the thermal initiation of mixtures are presented in Fig. 1. For shock-wave experiments, the equidistant hollows (10 mm in diameter and 10 mm in depth) were made in a steel matrix (with a diameter of 90 mm) to place preliminary pressed tablets. The shock-wave loadings were carried out by throw of a steel

impactor toward the matrix and sample surface. The detonation initiation was made by electric detonators placed in the center of matrix along the axis, and thus, the conversation cell construction is maintained the same loading conditions for all samples. Green mixtures and actual phase composition of products are presented in Table 1.
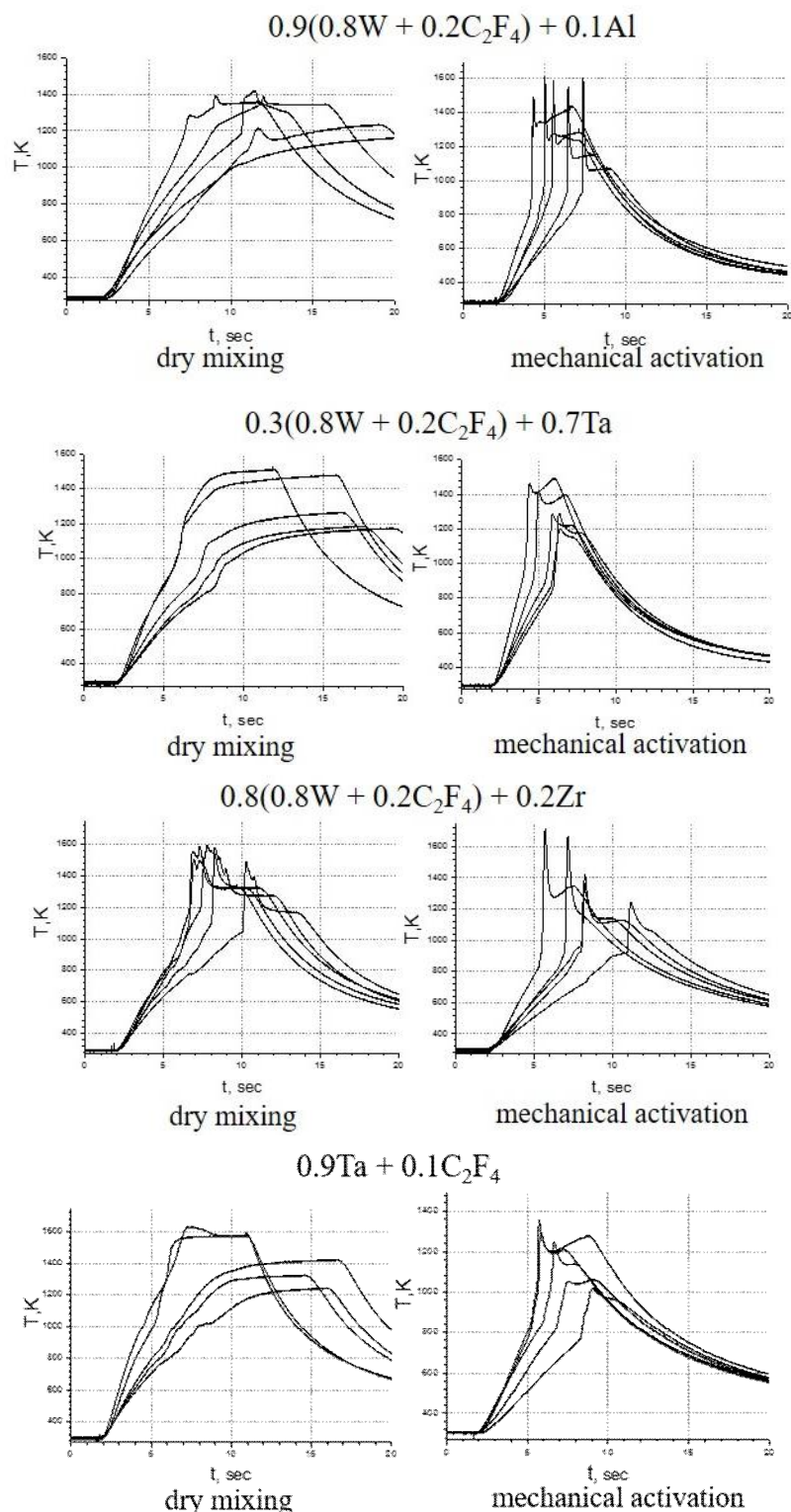
Fig. 1. Thermograms of studied mixtures.

Overall view of ampules for the initial and mechanically activated compositions differs (Fig. 2). In first case, the most part of material is remained in cells; in second case, the material flew away completely. We were able to obtain only mechanically activated $0.9Ta + 0.1C_2F_4$ mixture for XRD analysis.

Table 1. Green mixture and product phase composition after the shock-wave loadings.

Green mixture	Product phase composition	
	Dry mixing	Mechanical activation
$0.9(0.8W + 0.2C_2F_4) + 0.1Al$	32% W; 26% W_2C; 34% AlF_3	Product was scattered
$0.3(0.8W + 0.2C_2F_4) + 0.7Ta$	Initial	Product was scattered
$0.8(0.8W + 0.2C_2F_4) + 0.2Zr$	Initial	Product was scattered
$0.9Ta + 0.1C_2F_4$	Initial	84% Ta_2C; 10% TaC; 6% Ta

Fig. 2. Overall view of matrices after the shock-wave loadings of the initial (left) and mechanically activated (right) compositions.

M. I. Alymov et al.

COMPOSITE COATINGS MANUFACTURED IN THE RESULT OF THE DETONATION SPRAYING OF THE COPPER POWDER COATED WITH GRAPHENE

T. Babul and A. Olbrycht

Institute of Precision Mechanics, Duchnicka 3, Warsaw, Poland

e-mail: tomasz.babul@imp.edu.pl

The detonation spraying is one of the methods of thermal spraying, enabling to manufacture the coatings, which are characterised by high hardness, low porosity, good adherence and increased wear resistance. The essence of the denotation spraying is the utilization of the explosive combustion energy of a gaseous mixture to heat the particles of the powdered coating material and to give them the specified high kinetic energy [1]. Then, following spraying parameters were used: oxygen pressure – 0.06 MPa, propane-butane pressure – 0.001 MPa, nitrogen pressure – 0.008 MPa, detonation frequency – 4 Hz.

With use of a detonation method the copper powder coated with graphene – Graphene 3D^{IMP} was thermally sprayed in order to manufacture a composite coating.
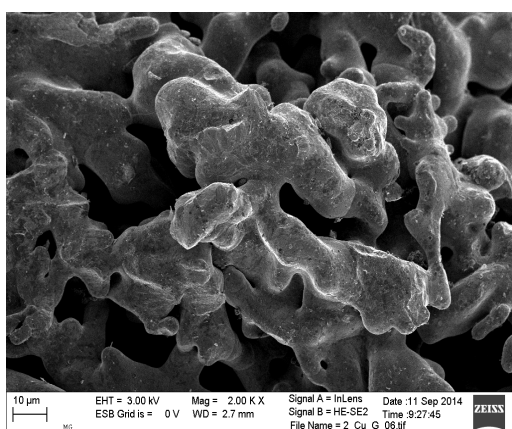
Fig. 1. Dendritic copper powder particles after graphene processing (SEM).
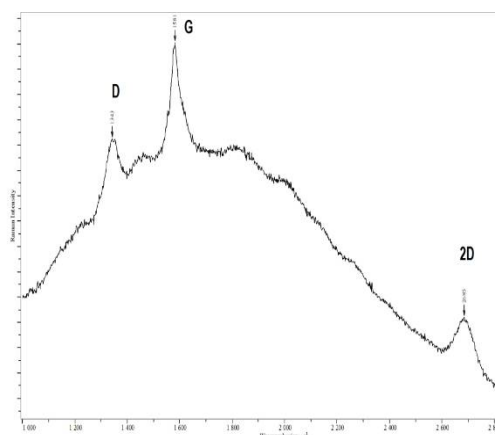
Fig. 2. Raman spectrum of graphene deposited on copper powder.

The basis of this modern composite material is graphene coated on copper powders, so called the 3D^{IMP} Graphene, which has been manufactured at the Institute of Precision Mechanics [2–5]. Formation of the graphene structures on the surface of the copper powder comes into being as a result of thermal chemical processes taking place in the atmosphere of hydrocarbons in a fluid deposit. The copper powder together with graphene was studied using scanning electron microscopy (Fig. 1) and a Raman spectroscopy (Fig. 2). In the Raman spectrum, 2D and G peaks characteristic of graphene spectrum are clearly visible, which confirms its presence in the tested powders (Fig. 2).

The fundamental advantage of the Cu–G composite coating obtained by detonation spray method as compared to Cu coating is the cohesion of the structure, which results from the much fewer number of oxides and from the good connection of the grains among one another (Fig. 3). There is a good connection of the coating to substrate.
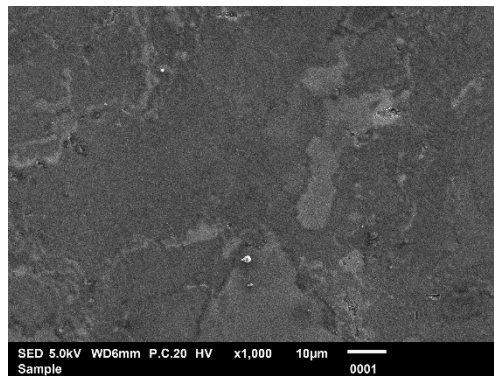
Fig. 3. SEM image of the exemplary microstructure of the Cu/G coating sprayed by means of the detonation method.

The pure copper powder is strongly oxidized during the process of spraying. A large number of oxides, which are included in the coating and are arranged in the bands between the copper grains, causes a significant decrease in the cohesion of the coating and makes the connection with the substrate worse. During the spraying of the copper powder with graphene, the carbon structures protect the particles of the copper powder against the excessive oxidization and therefore there are much fewer oxides in this coating than those in the sprayed Cu powder coating.

T. Babul and A. Olbrycht
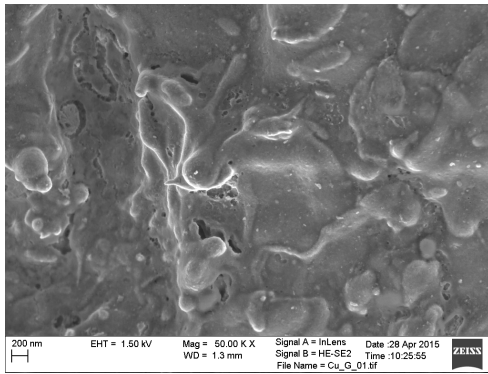
Fig. 4. SEM image of the surface of the Cu/G coating sprayed by means of the detonation method
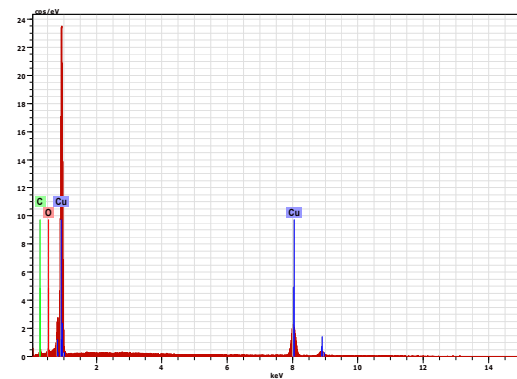
Fig. 5. X-ray diffraction pattern of the Cu/G coating sprayed by means of the detonation method

Figure 4 illustrates the SEM image of the surface of the Cu/G sprayed coating and figure 5 shows the X-ray diffraction pattern of this coating. The analysis of the chemical composition showed that the analysed area contains 99.92% Cu, 5.60% C and 1.48% O.

1. T. Babul, *Podstawy procesu natryskiwania detonacyjnego powłok NiCrBSi i WC/Co*, Warszawa: Instytut Mechaniki Precyzyjnej, 2011.
2. T. Babul, Z. Obuchowicz, S. Kowalski, J. Błaszczyk, *Sposób wytwarzania struktur węglowych zawierających grafen na proszkach miedzi z wykorzystaniem obróbki cieplno-chemicznej*, Zgłoszenie patentowe nr P.409141, 2014/
3. Z. Obuchowicz, M. Baranowski, T. Babul, N. Sobczak, Kompozyty Cu-Grafen 3D[IMP"], *Inżynieria Powierzchni*, 2015, no. 2, pp. 10–14.
4. T. Babul, M. Trzaska, J. Jeleńkowski, A. Wojciechowski, Potencjał Grafenu 3DIMP, *Logistyka*, 2015, no. 4, pp. 2282–2291.
5. T. Babul, M. Baranowski, N. Sobczak, M. Homa, W. Leśniewski, Thermophysical properties of cu-matrix composites manufactured using cu powder coated with graphene, *J. Mater. Eng. Perform.*, 2016, vol. 25, no. 8. Pp. 3146–3151.

GLOBAL EVOLUTION OF THE COMMERCIAL EXPLOSION METALWORKING INDUSTRY: PAST, PRESENT AND FUTURE

J. G. Banker

Clad Metal Consulting, USA

e-mail: Jbankercladmetal@gmail.com

The presentation looks back at the evolution of the commercial explosion metalworking production opportunities from the mid 1950's through today. It presents a brief look at the technical and commercial aspects driving the major phases of the Explosion Metalworking industry which include (in somewhat chronological order): Forming, Hardening, development of welding/cladding technology, US coinage production, development of the chemical process markets for clad and development of transition joints markets, globalization of DuPontian process technology, the Bang and Roll era, transition into a globally competitive similar-metal clad manufacturing industry, the evolution of the eastern European/Russian commercial operations and the emergence of a huge new type of explosion cladding industry in China. The presentation moves to a forward looking discussion of the needs of the industry to assure continuation into its 2nd Century. One of the many challenges will be learning how to continue evolving the industry in a way that it remains a relevant technical, socially acceptable and commercially viable solution of choice for support to emerging future needs.

SUPERHIGH COOLING RATES AND FORMATION OF STRUCTURE AT THE INTERFACE OF EXPLOSIVELY WELDED MATERIALS

I. A. Bataev

Novosibirsk State Technical University, pr. K. Marksa 20, Novosibirsk, 63073 Russia

e-mail: ivanbataev@ngs.ru

The properties of explosively welded bimetals and multilayer composites significantly depend on structures, which appear at the interface between the plates. This study aims to understand the formation of these structures in detail.

The study consists of two mutually interconnected parts: numerical simulation of high velocity oblique collisions and experimental study of material structures using various microscopy techniques.

The numerical simulation was carried out in Ansys AUTODYN software using smooth particle hydrodynamic approach. The simulations allowed to understand better deformation processes near the interface of explosively welded materials. A self-developed model was proposed to analyze the cooling processes after the welding. Based on the simulation, it was concluded that the severe plastic deformation is localized to a very narrow area close to the interface. Under specific collision parameters, a jetting phenomenon, a wave formation phenomenon and vortexes formation phenomenon were observed. The simulation predicted that the cooling rate near the interface may exceed 10^6 K/s.

In the experimental section, a number of explosively welded combinations were studied. Namely steel/steel, steel/copper, steel/Nb, steel/Ta, steel/Al, Al/Ti, Al/Mg, Al/Ni, etc. were thoroughly investigated. The structure of the welded materials was characterized using scanning electron microscopy (SEM), transmission electron

microscopy (TEM), energy dispersive X-ray spectroscopy (EDX) and some other techniques.

The high velocity collision led to significant heating and deformation of materials at the interface. At some local points the temperature at the interface exceeded melting temperature and the mixing zone were formed. Due to the specific turbulent flow of metal, these zones are frequently referred to as vortices. The structure of the vortexes forms due to the liquid state mixing and subsequent rapid solidification. It was found that in most of the cases some kind of metastable structures appeared in mixing zones. For materials with negative heat of mixing, the formation of metallic glasses and various quasicrystals was observed. For materials with highly positive heat of mixing possessing miscibility gap, a nanometer scale mechanical mixture was observed at the interface. The observed phenomena were explained by superhigh cooling rate achieved at the solidification stage.

The material, which was adjacent to vortices, was not melted, however, it was also significantly heated. The formation of its structure was explained using classical metallurgy approaches to high temperature deformation of metals. Due to the high strains, the material near the interface is significantly hardened. However, due to the high temperatures the softening of materials occurs due to recrystallization, polygonization and related phenomena. Thus, the final structure at the interface appears in the competition of strain hardening and temperature softening.

The structure of materials at a distance from the interface was also changed due to the propagation of the shock waves. Dislocation cells, deformation twins, stacking faults and some other defects were observed in this area.

In contrast to convenient welding techniques based on materials fusion (arc welding, plasma welding, etc), the heated area in explosively welded materials is localized near the interface. Thus, the heat affected zone is extremely narrow. However, the pressure of affected zone is high. Virtually all material experiences a deformation during the explosion welding.

I. A. Bataev

SHS OF POWDER MATERIALS OF REFRACTORY INORGANIC COMPOUNDS UNDER THE COMBINED ACTION OF PRESSURE AND SHEAR

P. M. Bazhin and A. M. Stolin

Merzhanov Institute of Structural Macrokinetics and Materials Science, Russian Academy of Sciences, Chernogolovka, Moscow, 142432 Russia

e-mail: olimp@ism.ac.ru

The technology of self-propagating high-temperature synthesis (SHS) makes it possible to obtain various ceramic, nonmetallic and intermetallic compounds in a few seconds due to the use of an exothermic synthesis reaction. The possibility of obtaining high-quality product and the speed and simplicity of the process make this technology attractive for the use in the production of materials and products [1]. Recently, new methods based on the combination of SHS and traditional methods of powder metallurgy have been developed. However, in SHS-technology, as well as in the powder metallurgy, the most progressive methods of material processing using high-temperature shear deformation of the products have not yet found wide application. Such deformation induces grain refinement leading to an increase in the hardness and strength of final products [2]. The combined action of shear deformation and pressure in the SHS process was first realized in the so-called SHS-grinding process to prepare powders of refractory compounds [3]. The idea of this process lies in the fact that hot combustion products heated during synthesis are refined due to the application of different mechanical actions [4]. Under such an approach, powders of refractory compounds can be prepared in one technological stage, avoiding the difficulties associated with the complexity of refinement of cold synthesized products.

The initial powder reagents of molybdenum, silicon, titanium, boron, and carbon black were used as the research objects. As a result of SHS, materials based on $MoSi_2$, TiB, TiB_2, and TiC were formed. These materials are supposed to be used upon creation of heat-resistant composite materials and during magnetic-abrasive treatment of surfaces of gas turbine engines blades.

Two types of installation combining combustion processes in the SHS regime and shear deformation are proposed. The first type of installation refers to the open type of reactor (displacement reactor), differing in equalizing of the concentration of the reactants in the entire volume. The second one refers to the close type of reactor of continuous action (mixing reactor), which is characterized by a limited exposure time to the synthesis products. The mixing reactor can be consider as semi-industrial installation. The practical possibility of carrying out of the SHS technological process under the action of pressure with shear makes it possible to realize the synthesis of refractory metals and the grinding of reaction products, which do not have time to cool down to room temperature in a single technological cycle. It has been established that shear loads applying to material unformed yet upon synthesis can significantly affect the grain size, morphology and mutual arrangement of grains throughout the volume. The quality of the obtained powder was analyzed by comparing the obtained dispersion and microstructure with dispersion, composition and microstructure of powders produced by SHS method without mechanical effects. The results of the granulometric analysis showed that the powder obtained by SHS with shear deformation is not bimodal and contains a higher amount of fine fraction than powders obtained by the traditional SHS method.

1. A. G. Merzhanov, History and recent developments in SHS, *Ceram. Int.*, 1995, vol. 21, no. 5, pp. 371–379.
2. P. M. Bazhin, A. M. Stolin, M. I. Alymov, A. P. Chizhikov, Peculiarities of the production of elongated items from a ceramic material with nanoscale structure by the SHS extrusion method, *Inorg. Mat. Appl. Res.*, 2015, vol. 6, no. 2, pp. 187–192.
3. A. G. Merzhanov, A. M. Stolin, A. V. Mazelia, SHS-grinding, *Dokl. Acad. Nauk.*, 1995, vol. 342, no. 2, pp. 201–204.
4. P. M. Bazhin, A. M. Stolin, M. V. Mikheev, M. I. Alymov, Self-propagating high-temperature synthesis under the combined action of pressure and shear, *Dokl. Chem.*, 2017, vol. 473, pp. 95–97.

FEATURES OF FORMATION OF LOCALIZED DEFORMATION BANDS UPON PULSE LOADING

A. F. Belikova, S. N. Buravova, and E. V. Petrov

Merzhanov Institute of Structural Macrokinetics and Materials Science, Russian Academy of Sciences, Chernogolovka, Moscow, 142432 Russia

e-mail: svburavova@yandex.ru

Impulse loading of the sample was carried out by the classical well-known scheme of impact with a thin metal plate, which was accelerated by a superimposed explosive charge. The interference of unloading waves forms a spall crack (a spall is a dynamic form of destruction) inside the sample if the tension stress exceeds the dynamic strength of the material. When the tension stress in the zone decreases, the crack passes into the localized deformation bands (LDB is synonym of the adiabatic-shear band). Numerous experiments [1, 2] have substantiated the spall nature of the deformation localization under pulse loading. A necessary condition for deformation localization is the presence of two free surfaces, the sources of unloading waves. Analysis of wave pattern of LDB formation reveals the features of the deformation localization process.
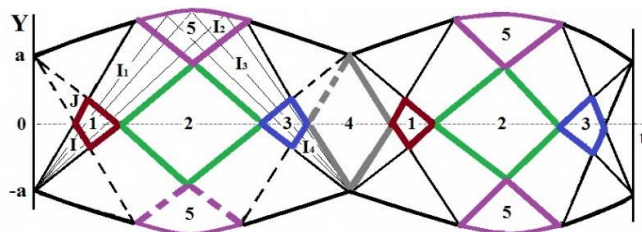
Fig. 1. Wave pattern of the LDB formation.

Two opposing unloading waves I and J are seen in Fig. 1 to across over the entire transverse section of the sample and return to the starting position. Such cycle is repeated many times. In Fig. 1, I, I_1, I_2, J, J_1, J_2 are waves of unloading (expansion); I_3, I_4, J_3, J_4 are waves of

compression (loading); marked regions *1* and *3* are zones of interference of unloading and compression waves, respectively; *2* and *4* are rest zones where the material is in the stretched or compressed state, respectively; *5* is the region of reflections of unloading waves on the sides of the sample. It is known [3] that the interaction of unloading waves with the sample sides and between them leads to stress oscillations, which come in the form of standing waves (Lamb waves). Ultrasonic oscillation frequency $\gamma = c_0/4a$ depends on the thickness of the sample $2a$ and the speed of sound c_0. On the axis of symmetry $(y = 0)$, where particle velocity is equal to zero, node is formed; at the free surface $(y = a)$, where the stress is zero, the antinode of the standing wave is formed. The length of the standing wave is $4a$. The duration of interaction of waves of unloading and compression on the axis is extremely small and $\Delta = c_0 t/a = 2bs_0$, where b is the coefficient in the dependence of the shock wave speed on the bulk velocity u_0; $s_0 = u_0/c_0$. For metals, the maximum tension strain, at which deformation localization takes place, does not exceed the spall strength of material, therefore, the values of $s_0 \approx 0.01$ and $\Delta \approx 0.03$ are small, while the duration of the cycle $T_0 = c_0 T/a = 4[1 - (b - 1)s_0] \approx 4$. Here, in the standing wave nodes, LDBs nucleate and evolve, their width $d/a = 2bs_0$. Analysis of the wave pattern showed that LDB is in a rest state for a long time (almost half period of the standing wave) at maximum tension of material -σ_0 (position *2* in Fig. 1) and during this time at the maximum compression σ_0 (position *4* in Fig. 1). The result was unexpected. The process of oscillation continues as long as the waves do not damp as the result of irreversible losses. The estimation of attenuation time of waves, which is based on the geometric interpretation of the conservation laws, shows a weak attenuation. The duration of impulsive deformation of the sample in the standing waves is increased by 2–3 orders as compared to the duration of initial impulse of compression.

1. A. F. Belikova, S. N. Buravova, Yu. A. Gordopolov, Strain localization and its connection with the deformed state of the material, *Techn. Phys.*, 2013, vol. 58, no. 2. pp. 302–304.
2. S. N. Buravova, *Etudes on the topic of localization of dynamic deformation: a spalling model for the localization of plastic deformation*, Saarbrücken: Palmarium Academic Publishing, 2014.
3. G. V. Stepanov, *Elastic-plastic deformation of materials under the action of impulse loads*, Kiev: Naukova dumka, 1979.

A. F. Belikova et al.

DETECTION OF INTERLAYER DEFECTS IN BIMETALLIC MATERIALS BY ELECTRIC FOUR-PROBE METHOD

V. O. Belko, P. N. Bondarenko, K. A. Kurkin, and A. D. Lukyanchikov

Peter the Great St. Petersburg Polytechnic University,
St. Petersburg, 195251 Russia

e-mail: vobelko@gmail.com, bonpetnik@yandex.ru

The four-probe method is widely used in measuring the properties of conductor (in the form of linear products with an arbitrary cross-section) and semiconductor materials (in the form of semi-infinite bulk bodies or thin-layer coatings) [1, 2]. The method is known to be also applied in geological prospecting to search for underground anomalies in the potential profile [3]. In all listed cases, the measurement can be made at DC or AC voltages. As preliminary experiments have shown, the measurement in alternating current with a frequency of 50 Hz is optimal in application to bimetallic systems.

A variant of the test installation scheme is shown in Fig. 1. The object of investigation is a bimetallic strip obtained by the explosive technology and consisting of layers M1 and M2. Two current contacts are applied to the strip - movable and terminal contacts. When the current flows through the strip, a potential gradient near the movable contact appears and it can be measured with needle probes. Moving the movable contact and probes along the surface of the strip, it is possible to obtain a potential distribution along the length of the sample. The COMSOL Multiphysics software was used to simulate the potential distribution along the surface of a bimetallic strip of stainless steel and an AMg alloy. Between the layers of metals, two defects (air gaps) of different sizes are placed. Figure 2 shows the results of the simulation. It can be seen that a larger potential corresponds to a defect of a larger area.
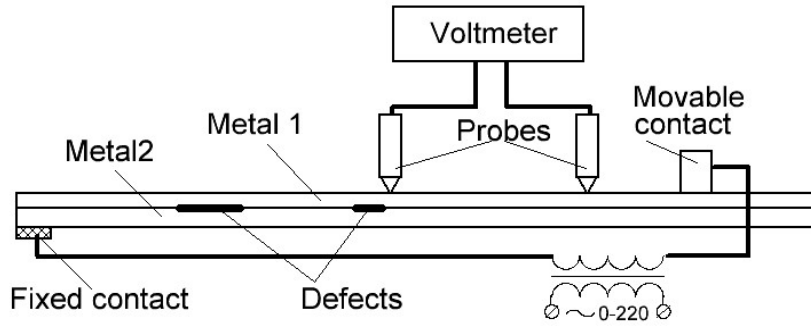
Fig. 1. Test installation scheme.
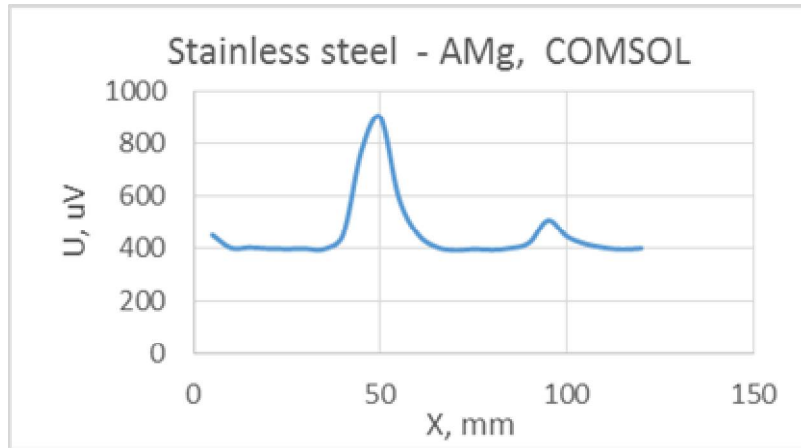
Fig. 2. Simulation of the potential distribution in the bimetallic strip with defects.

A physical modelling of a system of two 5 mm thick plates made of copper and stainless steel was also performed. Parallel copper foil strips with a width of 10 mm are laid between the plates. The distance between the strips is 40 mm. The result of scanning is shown in Fig. 3. It can be seen that in the area of the foil, a decrease in the potential is observed, and, conversely, in the intervals between the foil strips, the potential rises sharply.
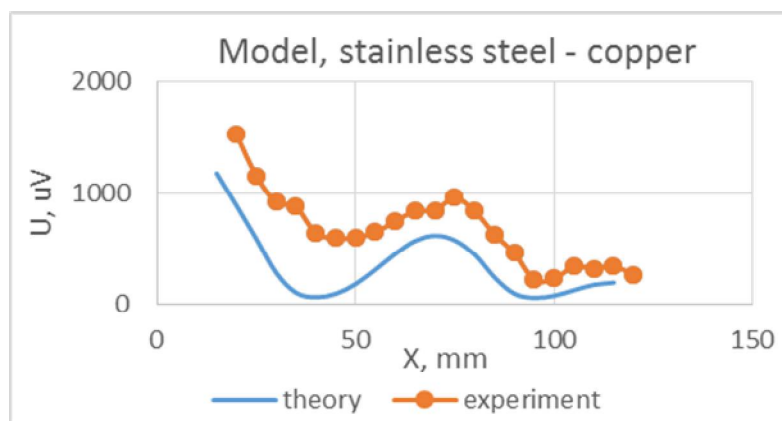
Fig. 3. Scanning of the physical model.

V. O. Belko et al.
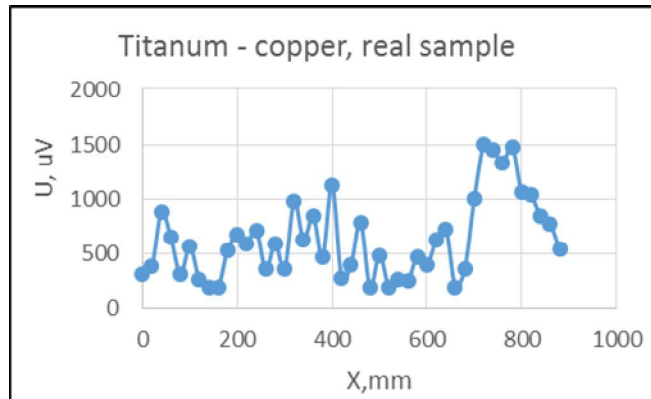
Fig. 4. Scanning of the real object.

Figure 4 shows the results of Cu–Ti bimetallic strip (real objejct). The presence of defects in the real object sample and the correspondence of their position to the probe data was confirmed by ultrasonic flaw detection.

1. GOST 24392–80. Silicon and germanium monocrystalline. Measurement of the resistivity by the four-probe method.
2. N. A. Poklonskiy et al, *Four-probe method for measuring the resistivity of semiconductor materials*, Minsk: Belgosuniversitet, 1998.
3. A. G. Sokolov, N. V. Chernyh, *Geophysical methods of prospecting and exploration of mineral deposits*, Orenburg: OGU, 2015.

REVIEW OF HYDROGEN INDUCED CLAD DISBOND TESTING

M. Blakely

NobelClad, Boulder, Colorado, USA

e-mail: MBLAKELY@dynamicmaterials.com

Clad materials are regularly used in corrosive, high temperature, high pressure process environments. When there are high partial pressures of hydrogen are also present, as is witnessed in modern oil refineries, the stakes are raised considerably. When hydrogen charging conditions are present and subsequent operations causing rapid cooling are considered, disbonding becomes a valid concern. The ability of clad material to resist disbonding is a key consideration when selecting appropriate materials of construction for critical process equipment. In this paper, a sampling of test data that has been generated over many years will be reviewed. To build a foundation for that discussion, a brief examination of the ASTM G146-01 standard practice for evaluating clad materials for hydrogen induced disbonding will be undertaken. In addition, the paper will include a review of the choices for producing clad for this type of service. The results give equipment designers and materials selection experts some guidance on appropriate cladding techniques for the materials of construction in these service environments.

ZSM-5 SUPPORTED CATALYSTS PRODUCED BY LOW-TEMPERATURE COMBUSTION

V. N. Borshch and I. M. Dement'eva

Merzhanov Institute of Structural Macrokinetics and Materials Science, Russian Academy of Sciences, Chernogolovka, Moscow, 142432 Russia

e-mail: borsch@ism.ac.ru

Traditional processes of supported catalyst synthesis are multi staged and power consuming. Low-temperature combustion is a new approach to the production of supported catalysts. By this method supports are impregnates by mixture solutions of nitrates of catalytically active metals as the oxidants and some heteroatomic organic compounds as reducing agents (fuels). After drying of impregnated support, the combustion process was initiated to form active phase (AP). High temperature of the process can destroy support, therefore, to reduce the temperature AP content in the catalysts should not exceed 10–15 wt %. AP of such catalysts consisted of highly dispersed metals and metal oxides.

Mesoporous zeolite ZSM-5 with a diameter of pores 0.45–0.60 nm and a specific surface of 560 m^2g^{-1} was used as support. Cobalt, nickel and manganese nitrates, and urea were used as the oxidants and fuel, respectively. Pattern of ZSM-5 after impregnation was dried at 90°C and heated in argon flow. Time dependence of temperature during combustion process is shown in Fig. 1.

Temperature of ignition was ~ 150°C. After combustion, the catalysts were stabilized by 5% solution of H_2O_2 to prevent full oxidation of AP metal on air, washed by distilled water and dried. Catalysts with AP of Co5%–Mn5%, Co5%–Ni5%, and Co5%–Ni5%–Mn5% were synthesized.
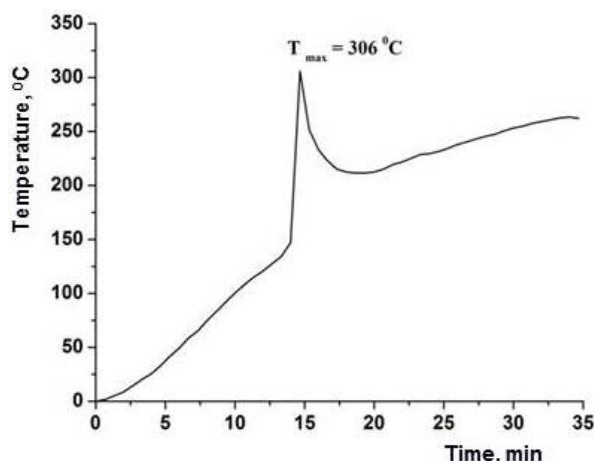
Fig. 1. Temperature vs. time of synthesis of the catalyst Co5%–Ni5%/ZSM-5.

Figure 2 shows the SEM image and EDS data of the catalyst Co5%–Ni5%/ZSM-5.
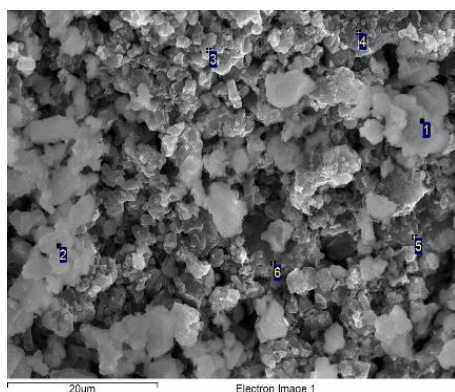
Spot.	O% wt.	Al% wt.	Si% wt.	Co% wt.	Ni% wt
1	49.2	10.5	31.8	3.7	4.8
2	59.1	8.7	26.5	3.0	2.7
3	56.9	9.9	23.7	5.0	4.4
4	42.4	13.7	24.7	9.1	10.1
5	55.1	6.1	33.3	2.9	2.6
6	53.5	7.8	33.0	2.6	3.1

Fig. 2. SEM image and EDS data of the catalyst Co5%–Ni5%/ZSM-5.

BET specific surface of the catalysts was 188 m^2g^{-1} for Co5%–Mn5%/ZSM-5, and 235 m^2g^{-1} for Co5%–Ni5%/ZSM-5.

Patterns of the catalysts were tested in the process of deep oxidation of CO and propane, and hydrogenation of CO_2. Quartz catalytic flow reactor was used. Gaseous mixtures for deep oxidation contained (vol %) 0.2% propane, 0.7% CO, 2.3% O_2 and N_2 being the rest, and 2.7% CO_2, 10.8% H_2, and He being the rest for hydrogenation. Results of these experiments were demonstrated in Figs. 3 and 4. Complete conversion of CO takes place at 200°C and conversion of propane reached ~ 85% at 400°C. Main product of CO_2 hydrogenation was methane with maximum yield at 350°C.

V. N. Borshch and I. M. Dement'eva
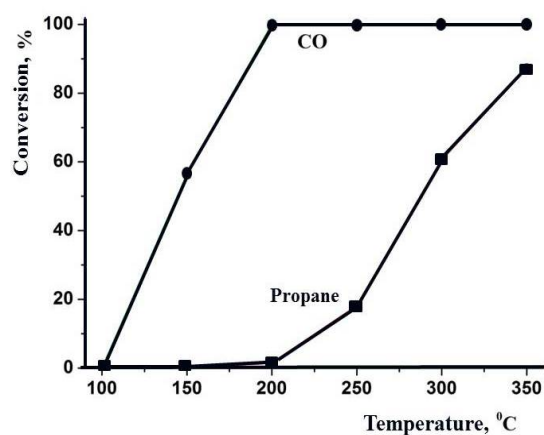
Fig. 3. Conversion in deep oxidation of CO and propane for Co5%–Ni5%/ZSM-5 catalyst as a function of temperature.
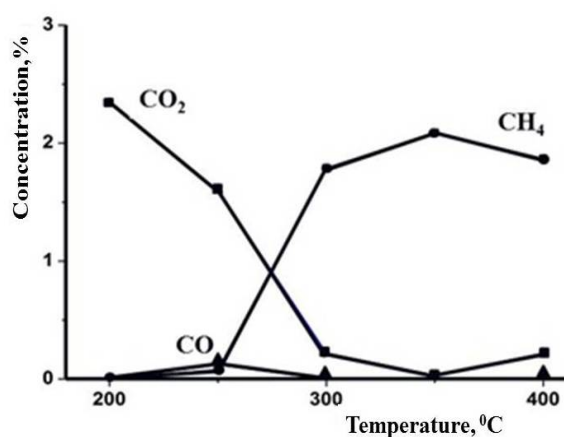
Fig. 4. Concentration of CO_2, methane, and CO vs. temperature in hydrogenation of CO_2.

Catalysts Co–Ni/ZSM-5 were more active both in deep oxidation and in hydrogenation of CO_2 than Co–Mn/ZSM-5 and Co–Ni–Mn/ZSM-5. On the contrary, Ni-containing catalysts on such supports as silica-gel, γ-alumina and other zeolites, were less active in these processes.

Thus, the catalysts on ZSM-5 support produced by low-temperature combustion demonstrated high activity in oxidation and reduction processes.

STRUCTURE FEATURES OF SHS INTERMETALLICS AS PRECURSORS FOR HIGHLY ACTIVE POLYMETALLIC CATALYSTS

V. N. Borshch, E. V. Pugacheva, S. Ya. Zhuk, V. N. Sanin, D. E. Andreev, and V. I. Yukhvid

Merzhanov Institute of Structural Macrokinetics and Materials Science, Russian Academy of Sciences, Chernogolovka, Moscow, 142432 Russia

e-mail: borsch@ism.ac.ru

Novel class of highly active polymetallic catalysts was proposed and investigated. Complex multicomponent intermetallic compounds (aluminides) produced by one-stage short-term SHS were used as the precursors for these catalysts. The intermetallics consisted of catalytically active metals such as iron group metals (Fe, Ni, Co) as main components and other d-metals and rare-earth elements (V, Mn, Cu, Zr, Mo, La, Ce etc.) as promoters. Intermetallic compounds were synthesized by highly exothermic liquid phase process from oxides of metals according to the following reaction scheme:

$$\Sigma(Me_KO_L) + \alpha Al \rightarrow \Sigma(Me_XAl_Y) + \beta Al_2O_3$$
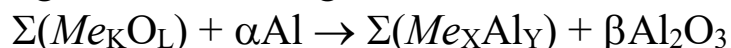
The temperature of this process exceeded $2500°C$. SEM image and EDS results of Ni–Co–Mn–Al intermetallic are presented in Fig. 1. Figure 2 shows the XRD pattern of this intermetallic compound.

As shown in Fig. 1, the microstructure of the intermetallic compound consists of grains of lower intermetallic compound of basic metal (Ni), which are surrounded by higher intermetallic compounds of promoter metals (Co, Mn). Various aluminides of Ni, Co, and Mn were detected by XRD analysis (Fig. 2). The catalysts were produced by leaching of intermetallic alloys with alkaline solutions and then were stabilized with H_2O_2. Lower intermetallics with Al content of less than 50 wt % were leached very slowly. They served as supports for highly disordered nanostructured oxo-metallic active phases (AP)

consisted mainly of promoters. As a result, the catalysts were composite materials. Specific microstructure of SHS-intermetallics resulted in specific features of the structure of catalysts, which was the main reason of their high activity both in oxidation and reduction processes [1–3].

Points	Al, % wt.	Mn, % wt.	Co, % wt.	Ni, % wt.
1	41.0	-	4.5	54.4
2	40.9	-	5.1	53.9
3	61.9	22.4	2.1	13.5
4	62.1	21.9	1.7	14.2
5	50.3	1.1	10.7	37.9
6	51.4	1.2	11.1	36.3
7	55.2	3.9	4.4	36.4
8	56.4	0.4	3.8	39.4
9	56.4	1.2	3.2	39.2
10	55.5	0.3	3.7	40.4
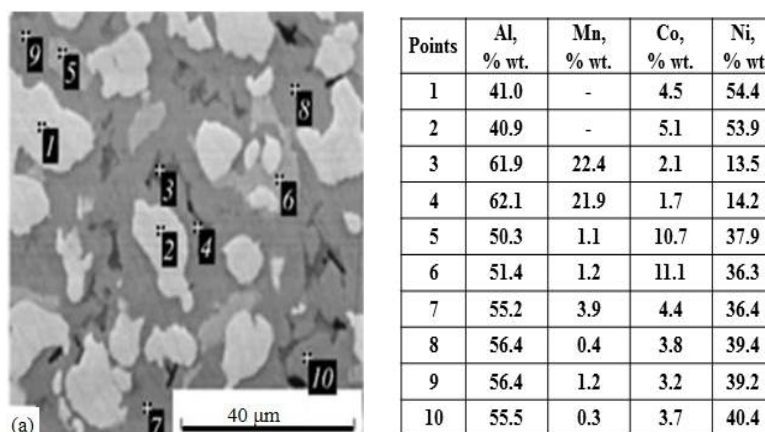
Fig. 1. SEM image with EDS data of Ni–Co–Mn–Al intermetallic surface.
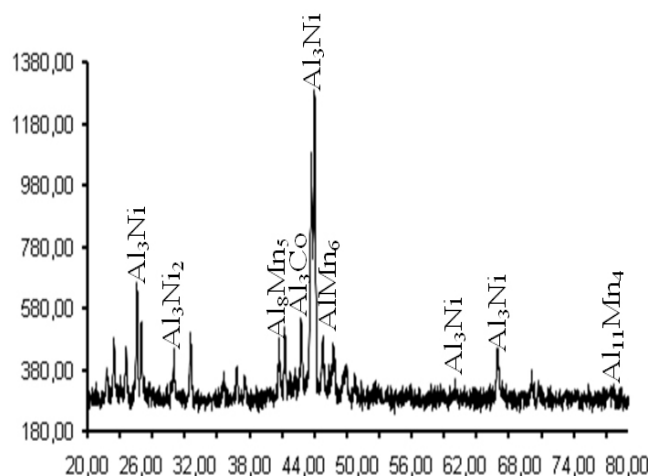
Fig. 2. X-ray diffraction pattern of Ni–Co–Mn–Al intermetallic.

The formation of two-level nanostructures on the AP surface was the most promising feature of all investigated catalysts. An example of this structure is shown in Fig. 3. High activity of Co catalyst during deep oxidation of H_2 is demonstrated in Fig. 4.

Consequently, peculiarities of microstructure of SHS-intermetallics as a result of high temperature of process, short times of combustion and crystallization, allow to use them as precursors for a new class of highly active polymetallic catalysts for various processes.
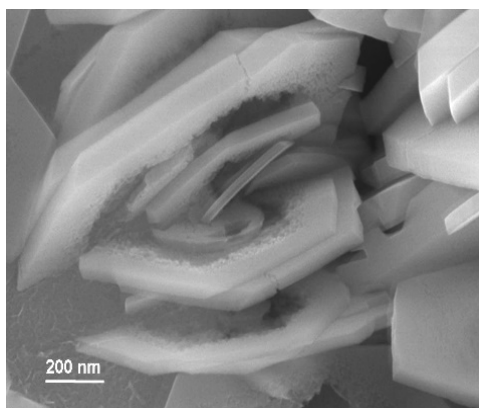
Fig. 3. SEM image of the Fe–Ni–Co–Mn catalyst surface.
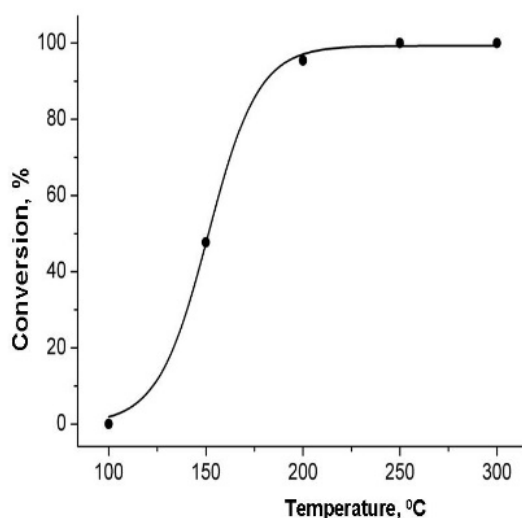
Fig. 4. Deep oxidation of H_2 on Co catalyst. Hydrogen-air mixture with 1 vol % H_2, flow rate 60 000 h^{-1}.

1. E. V. Pugacheva, V. N. Borshch, S. Ya. Zhuk, V. N. Sanin, D. E. Andreev, V. I. Yukhvid, Iron-based polymetallic catalysts with a nanostructured surface for deep oxidation processes, *Nanotech. Russ.*, 2015, vol. 10, pp. 841–849.
2. V. N. Borshch, E. V. Pugacheva, S. Ya. Zhuk, V. N. Sanin, D. E. Andreev, V. I. Yukhvid, O. L. Eliseev, R. V. Kazantsev, S. I. Kolesnikov, I. M. Kolesnikov, A. L. Lapidus, Polymetallic catalysts for the Fischer–Tropsch synthesis and hydrodesulfurization prepared using self-propagating high-temperature synthesis, *Kinet. Catal.*, 2015, vol. 56, pp. 681–688
3. V. N. Borshch, E. V. Pugacheva, S. Ya. Zhuk, V. N. Sanin, D. E. Andreev, V. I. Yukhvid, Deep oxidation catalysts based on SHS-produced complex intermetallics, *Int. J. Self-Propag. High-Temp. Synth.*, 2017, vol. 26, pp. 124–128.

THE EXPLOSION WELDING OF Ti + SS + Ti TRIMETAL FOR MANUFACTURING LINEAR COLLIDER ADAPTORS

A. G. Bryzgalin[1], E. D. Pekar[1], P. S. Shlonskii[1], G. D. Shirkov[2], Yu. A. Budagov[2], and B. M. Sabirov[2]

[1] E.O. Paton Electric Welding Institute, Kiev, Ukraine
[2] JINR, Dubna, Russia

e-mail: bag60@mail.ru

The adapter of the cryogenic module of the linear collider is presented by a stainless steel (SS) disk in the center of which a niobium pipe is welded. The join of niobium with SS should ensure the vacuum and helium tightness and operability under conditions of high-frequency electromagnetic loads at cryogenic temperatures [1].

Fusion welding for joining niobium and SS is unsuitable for solving the problem associated with the formation of intermetallic compounds such as Nb_xFe_y, which obstruct the achievement of the required tightness of adapters.

We made an adapter using explosion welding of Nb pipe directly into the SS disk. An amount of intermetallic compounds was expected to be significantly lower than that upon fusion welding because of the lower heating and they would not break the tightness due to the larger area of the joint [2]. In order to prevent the destruction of the niobium pipe during explosion, the width of the steel billet should not be less than that of Nb pipe. In Fig. 1, red lines indicate the size of the steel billet before the explosion; black lines show the expected shape of the adapter.

The welded adapter is shaped by machining. To ensure the required geometric dimensions of the adapter, taking into account the inevitable deformations of Nb pipe upon explosion, it will be necessary to use Nb pipe with a smaller outer diameter and a larger wall thickness. However, this is not suitable for industrial applications

due to high labor-consuming, high cost and high consumption of scarce niobium. In this case, the helium tightness of the compound was not investigated.

Earlier experiments showed that electron-beam welding of niobium to titanium does not form intermetallic compounds and ensures the necessary helium and vacuum tightness. Considering this, the following adapter manufacture procedure was proposed.

First, the SS disc is clad with titanium on both sides by explosion welding, then, after machining to the desired shape (using straightening and turning to the size) a hole is cut out for Nb pipe. The pipe is inserted into the hole and electron-beam welded to titanium (Fig. 1b). The possible formation of intermetallic compounds in the explosive welded joint between titanium and steel does not affect the operability of the adapter, because helium is located outside the Nb pipe, and cannot get into it.

(a) (b)
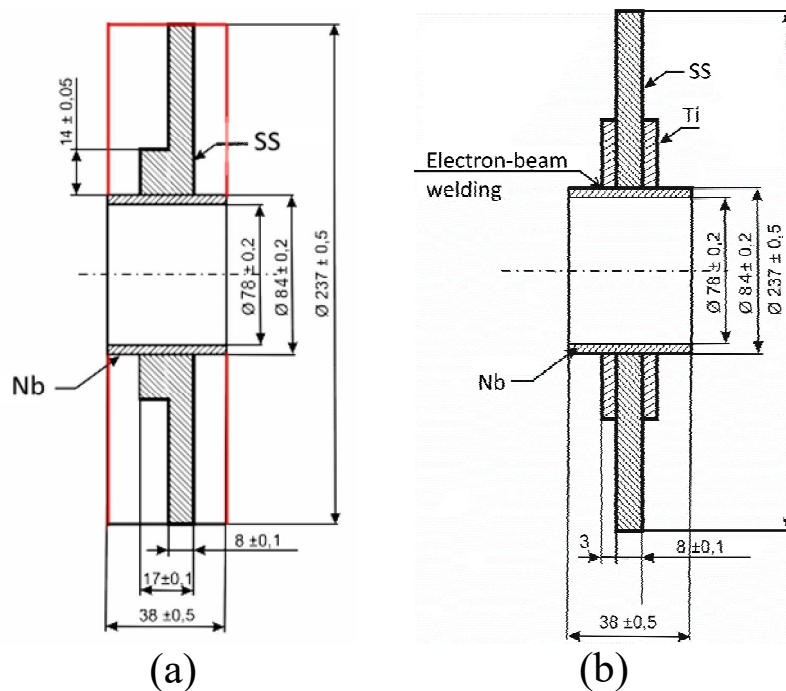
Fig. 1. Design of adapter manufactured by: (a) explosion welding of Nb to SS, (b) explosion welding between SS and Ti and electron-beam welding of Ti to Nb.

Advantages of the proposed method of manufacture of the adapter are as follows:

- helium tightness is provided by welding of niobium with titanium, which have good weldability;

A. G. Bryzgalin et al.

- Nb pipe is used in the factory delivery condition;

- possible formation of intermetallic compounds in the explosive welded steel–titanium joint does not affect the helium tightness;

- explosion welding of flat samples is technologically much simpler than welding of pips and makes it possible to obtain joints with the greatest possible stability of quality, which reduces the probability of rejection;

- after explosion welding, if necessary, cheaper steel–titanium billets will be rejected;

- steel–titanium flange can be heat treated to reduce residual stresses in a conventional (non-vacuum) furnace;

- expenditure of steel and niobium decreases.

1. B. Sabirov, Explosion welding: New Design of the ILC Cryomodule, *JINR NEWS*, 2010, 3, p. 16.
2. V. I. Lysak, S. V. Kuzmin, *Explosion Welding*, M.: Mashinostroenie, 2005, (in Russian).

PROBLEMS OF EXPLOSION WELDING OF LONG-LENGTH COAXIAL Cu + Al RODS WITH A THIN CLADDING LAYER

A. G. Bryzgalin, P. S. Shlonskii, S. D. Ventsev, and E. D. Pekar

E. O. Paton Electric Welding Institute of NAS of Ukraine, ul. Kazimira Malevicha 11, Kyiv, 03150 Ukraine

e-mail: shlensk@ukr.net

A practical solution to the problem of the production of long-length (more than ten diameters) co-axial bimetallic bars is topically for aircraft building (current conductors of control systems for aircraft) and the metallurgical industry (cathode matrix for the electrolysis of copper).

To study the possibility of production of such bars, a copper-aluminum coaxial rods with a length of 1 m were subjected to explosion welding. Copper cladding pipe had a thickness of 1 mm with an outer diameter of 28 mm (Fig. 1),

For uniform distribution of explosive along the length of the billet, the container for the explosive was made from several pieces of pipes.

<table>
<tr><td>(a)</td><td>(b)</td></tr>
</table>
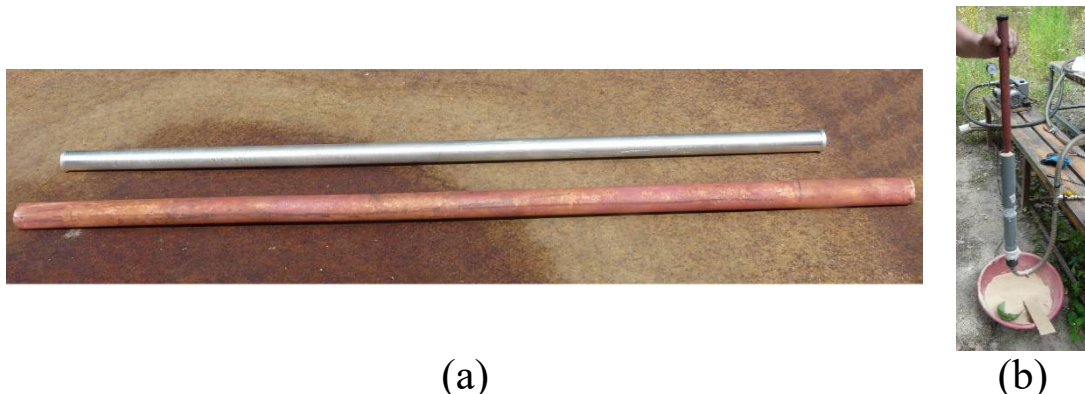
Fig. 1. (a) Extended billets for explosion welding; (b) backfilling of explosives into a compound container.

In the welding process, the air in the gap must flow through the outlet at the end of the assembly with a speed exceeding the detonation velocity (D). The air will be considerably compacted and heated and a shock wave will form in it. This can significantly affect the quality of the welded joint. In addition, at some length of the coaxial assembly, the speed of air outflow from the gap, which depends on the area of the exit opening (welding gap) and contact speed (V_k), becomes lower than V_k ($V_k = D$). A certain volume of air remains between the welding surfaces and the collapse with forming bubbles. To avoid this, vacuuming of the welding gap is needed.

Experiments were carried out using samples shown in Fig. 1 in the modes with vacuuming of the welding gap and without it; the residual pressure upon vacuuming was 1×10^{-5} atm.

After the explosion welding of a long-length billet with vacuuming, the defects appeared beginning from the distance of about 500 mm from the start of detonation, a rupture of the cupper clad layer and damage to the aluminum surface were observed (Fig. 2). A similar situation is observed in the case of lack of vacuuming, but the defects appeared closer to the start of detonation at a distance of approximately 250 mm.

Fig. 2. Long-length coaxial billets after explosion welding: from above - with vacuum, from below - without vacuum; the direction of detonation from left to right.

A characteristic feature of both samples is that most bubbles and all defects in the form of discontinuities are concentrated on one generatrix. This is due to the fact that the front of detonation is nonuniform along one of the generatrix, it will always lag behind creating of a cumulating effect at the apex of the nonuniform front. Such nonuniformity will depend on the displacement of the center of initiation of the explosive charge from the center of the welding

assembly, as well as on the nonuniformity of the detonation velocity and thickness of the charge along the length of the assembly.

It is also characteristic that during welding with vacuuming of the gap, intermetallic compounds are formed at smaller area and have smaller size.

Therefore, to obtain long-length coaxial bimetallic billets with small diameter and thin cladding layer by explosion welding, special measures must be applied, in particular, in our opinion, it is necessary to ensure:

- maximum uniformity of detonation front along the transverse section of the coaxial assembly for welding;

- stability of the detonation velocity of explosives;

- uniformity of geometric characteristics (welding gap, charge height) along the length of the assembly;

- removal of the air from the gap, if possible.

A. G. Bryzgalin et al.

DISSOLUTION OF STRENGTHENING PHASE PARTICLES IN THE LOCALIZED DEFORMATION BANDS

S. N. Buravova, E. V. Petrov, N. I. Mukhina, and A. S. Shchukin

Merzhanov Institute of Structural Macrokinetics and Materials Science, Russian Academy of Sciences, Chernogolovka, Moscow, 142432 Russia

e-mail: svburavova@yandex.ru

This work studied dispersion-strengthened aluminum alloy. The structure of the samples after explosive treatment was examined using a Neophot-30 optical microscope, a LEO 1450 scanning electron microscope, and a Zeiss Ultra Plus electron microscope of super high resolution. The explosive loading of samples in the form of a thick-walled hollow or solid cylinder was carried out by the impact of a thin aluminum plate accelerated by a charge of 6ZhV ammonite or hexogen of pour density. The shock wave pressure was 7–15 GPa. Alloying additives containing magnesium, manganese, and copper were located in colonies formed during technological rolling. The distance between the colonies of intermetallic microparticles varied from 15 to 40 μm. The individual size of particles was 0.5–2 μm, but many particles clumped, forming conglomerates of fine particles with a size of 5–10 μm. Coarse particles (Fig. 1.) consisted of insoluble intermetallics based on iron and silicon, which are surrounded by soluble copper-based intermetallics. Fine soluble particles had an irregular polygon shape.

As a result of high-rate tension in the zone of the interference of unloading waves where localized deformation bands (LDBs) are formed, the material is refined, the phase composition of intermetallic compounds was changed (Fig. 2). Fine soluble intermetallic particles 0.5–2.0 μm in size with two-component $\theta(Al_2Cu)$ and three-component $S(Al_2CuMg)$ compositions, which had a shape of irregular

polygons in the initial alloy, become rounded, their size is decreased. An amount of particles in BLD with a size of less than 500 nm significantly increased as compared to the undisturbed material. This indicates partial dissolution of intermetallic compounds in BLD.
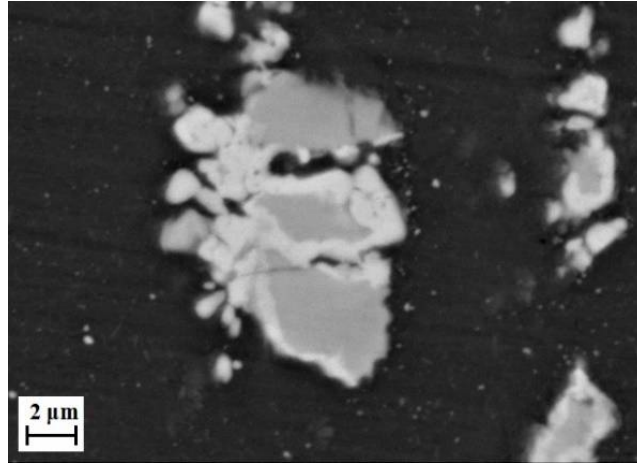
Fig. 1. Microstructure of the alloying phase particles.
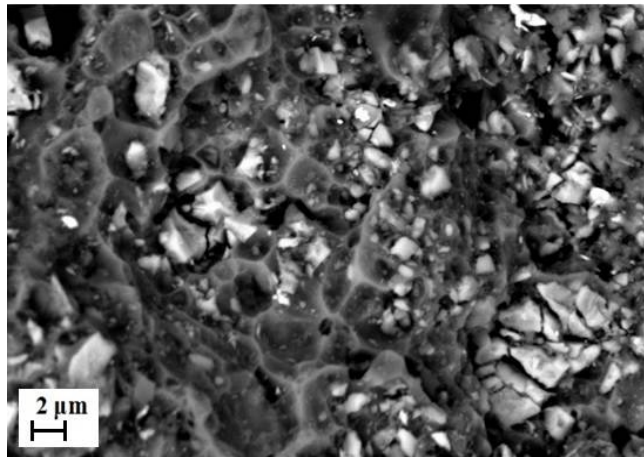
Fig. 2. Microstructure of the LDB in aluminum alloy near the region of transition of the spall crack into the BLD.

WELDING STAINLESS STEEL AND ALUMINIUM BY EXPLOSION WELDING: EFFECT OF THE MATERIALS POSITION

G. H. S. F. L. Carvalho[1], I. Galvão[1,2], R. M. Leal[1,3], R. Mendes[4], J. B. Ribeiro[4], and A. Loureiro[1]

[1] CEMMPRE, Department of Mechanical Engineering, University of Coimbra, Rua Luís Reis Santos, 3030-788 Coimbra, Portugal
[2] ISEL, Department of Mechanical Engineering, Polytechnic Institute of Lisbon, Rua Conselheiro Emídio Navarro, 1959-007 Lisboa, Portugal
[3] ESAD.CR, Polytechnic Institute of Leiria, Rua Isidoro Inácio Alves de Carvalho, 2500-321 Caldas da Rainha, Portugal
[4] ADAI, LEDAP, Department of Mechanical Engineering, University of Coimbra, Rua Luís Reis Santos, 3030-788 Coimbra, Portugal

e-mail: altino.loureiro@dem.uc.pt

Austenitic stainless steel (SS) has been widely applied in applications, which require a combination of strength, high toughness in low temperature and corrosion resistance. On the other hand, aluminium alloys have been used for applications where is needed a combination of resistance and low weight due to its low density. The use of both alloys is growing considerably for applications that need the combination of their properties. However, the manufacture of components combining these two materials is still challenging since these alloys possess extremely different physical properties that difficult the welding through conventional arc welding processes. Thus, the joining between these materials usually achieves success through solid state welding processes.

Explosion welding (EXW) is an interesting process to join materials with different physical properties. It is characterized by an impact between materials as the result of a controlled detonation of an explosive [1, 2]. Progress has been achieved in works addressing

dissimilar explosive welding [3, 4] and some woks addressing the joining between aluminum and SS have also been carried out [5]. However, few works address weldability problems and the aspects that should be considered when choosing parameters and configurations for this combination.

The objective of this work is to characterize the main aspects regarding the weldability of SS to aluminium alloys by EXW. Different position of the alloys (as the flyer or base plate) and different welding parameters/explosive mixtures for the combination of AISI 304 stainless steel and 6082-T6 aluminium alloy were tested.

It was verified that welding SS with aluminium by EXW can only be achieved with the steel positioned as the base plate. When used as flyer plate, the plates separate at the end of the process and intermetallic compounds layers are formed on the surface of the plates (Fig. 1). The separation happened for all tests with SS flyer however, the quantity of intermetallic compounds changed depending on the parameters. The welding failure seems to be related to the time that is needed to the interface solidify, with the shock waves arriving at the interface before the complete solidification of the localized melting.

However, changing the plate position and placing the aluminium as the flyer it was possible to achieve a consistent weld. The same parameters were used for this configuration and consistent weld was achieved (Fig. 2) The weld displayed good appearance though all the length, as Fig. 2 shows, but the interface is nearly flat since it was used an explosive of low detonation velocity. Some intermetallic compounds can be seen at the interface, but there is no continuous intermetallic layer.
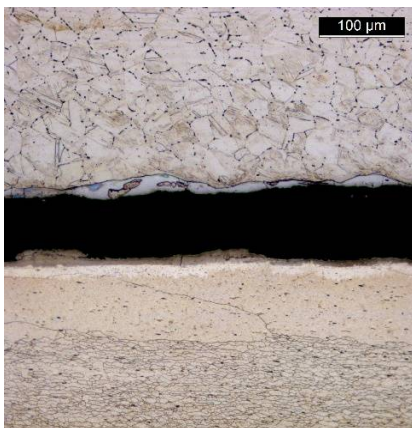
Fig. 1. Appearance of the stainless steel–aluminium failed welds.
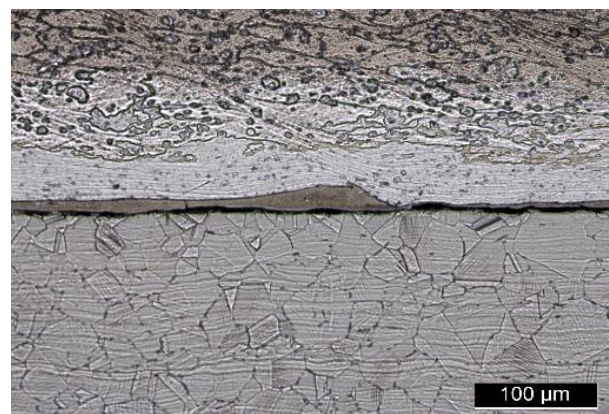
Fig. 2. Aspect of the aluminium–stainless steel welds.

G. H. S. F. L. Carvalho et al.

It can be concluded that welding stainless steel to aluminium alloys by EXW could only be achieved if the stainless steel is the base plate. The failure in welding stainless steel flyer to aluminium alloys seems to be related to the tensile stresses resulting from the shock waves that arrive at the interface before the complete solidification of the localized melting.

1. H. El-Sobky, Mechanics of Explosive Welding, *Explosive Welding, Forming and Compaction*, 1983, pp. 189–217.
2. A. A. Deribas, V. M. Kudinov, F. I. Matveenkon, V. A. Simonov, Explosive Welding, *Fiz. Goreniya I Vzryva*, 1967, vol. 3, n.1, pp. 111–118.
3. G. H. S. F. L. Carvalho, I. Galvão, R. Mendes, R. M. Leal, A. Loureiro, Influence of base material properties on copper and aluminum–copper explosive welds, *Sci. Technol. Weld. Joining*, 2018, in press.
4. G. H. S. F. L. Carvalho, R. Mendes, R.M. Leal, I. Galvão, A. Loureiro, Effect of the flyer material on the interface phenomena in aluminium and copper explosive welds, *Mater. Des.*, 2017, vol. 122, pp. 172–183.
5. K. Hokamoto, T. Izuma, M. Fujita, New Explosive Welding Technique to Weld Aluminium Alloy and Stainless Steel Plates Using a Stainless Steel Intermediate Plate, *Metall. Trans. A*, 1993, vol. 24, pp. 2289–2297.

BONDING INTERFACE CHARACTERISTICS OF STEEL-TO-ALUMINIUM EXPLOSION WELDS

G. H. S. F. L. Carvalho[1], I. Galvão[1, 2], R. M. Leal[1, 3], R. Mendes[4], J. B. Ribeiro[4], and A. Loureiro[1]

[1] CEMMPRE, Department of Mechanical Engineering, University of Coimbra, Rua Luís Reis Santos, 3030-788 Coimbra, Portugal
[2] ISEL, Department of Mechanical Engineering, Polytechnic Institute of Lisbon, Rua Conselheiro Emídio Navarro, 1959-007 Lisboa, Portugal
[3] ESAD.CR, Polytechnic Institute of Leiria, Rua Isidoro Inácio Alves de Carvalho, 2500-321 Caldas da Rainha, Portugal
[4] ADAI, LEDAP, Department of Mechanical Engineering, University of Coimbra, Rua Luís Reis Santos, 3030-788 Coimbra, Portugal

e-mail: altino.loureiro@dem.uc.pt

The welding of dissimilar materials, such as steel (Fe) to aluminium (Al), has high interest for transport industries. However, the fusion welding technologies are not appropriate for joining these metals, but other processes, such as explosion welding (EXW), have high potential [1]. Even so, the different physical properties of both metals and the high susceptibility to the formation of intermetallic phases also become their joining by EXW difficult. The characterisation of the interfacial weld zones, where Al–Fe interaction occurs, is mandatory to understand the metallurgical phenomena occurring during welding.

This research is aimed to characterise the bonding interface of explosion welds in 3 mm-thick plates of EN DC06 steel to 15 mm-thick plates of AA6082-T6. The welds were produced in a full overlap joint configuration, using ANFO and emulsion-based explosive mixtures. Several explosive ratios were used. The welds produced with ANFO were identified as A welds, whereas the welds produced with the explosive emulsion were identified as E welds.

The surface appearance of the welds is shown in Fig. 1. Figure 1a shows that no effective joining occurred in the E welds. However, the un-bonded surfaces present a whitish and dull appearance, suggesting the formation of a layer of a new material. As illustrated in Fig. 1b, unlike to the E welds, effective joining was achieved in the A welds, which were produced using a much lower detonation/collision point velocity.

(a)   (b)
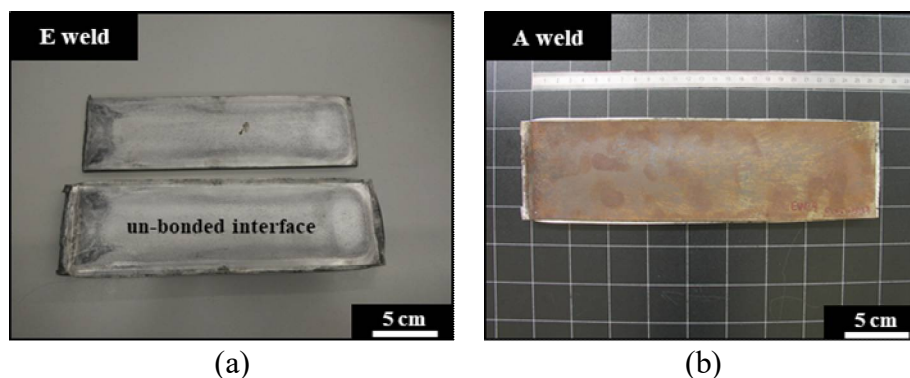
Fig. 1. Surface appearance: (a) E weld; (b) A weld.

Figure 2 illustrates micrographs of the weld longitudinal cross-sections. As shown in Fig. 2a, a continuous layer of a new material was formed at the interface of the E welds. The formation of this molten layer, which resulted from Al–Fe interaction, avoided the interfacial bonding [2]. The figure also shows that several cracks are present in this layer, which indicates that it is composed of a brittle material. The SEM/EDS analysis revealed that the molten layer consists of a dispersion of particles over a matrix. Both the particles and the matrix were found to present a hybrid Al–Fe chemical composition. It can be inferred that the coupled effect of the pressure and the temperature at the interface promoted the formation of intermetallic phases [3].

As illustrated in Fig. 2b, the interface of the A welds was continuous. In addition, new material pockets are observed to be uniformly intercalated with the highly deformed base material, indicating that no continuous melting occurred. From the SEM/EDS analysis, it was observed that the new material regions also present a hybrid Al–Fe composition.

Localised hardness measurements were conducted over the molten layer of the E welds. The values ranged between about 260 $HV_{0.2}$ and about 920 $HV_{0.2}$, which are well-above the values registered for

deformed base metals. These values agree-well with the hardness usually reported to Al–Fe intermetallic phases [4].

It can be concluded that continuous interfacial melting was prevented by using an explosive mixture with a lower detonation/collision point speed, which enabled to achieve better welding conditions. The detrimental effect of the intermetallic phases on the weld structure was found to go beyond their brittle nature. The physical properties of these phases were found to strongly influence the phenomena that govern the interfacial bonding.

(a)   (b)
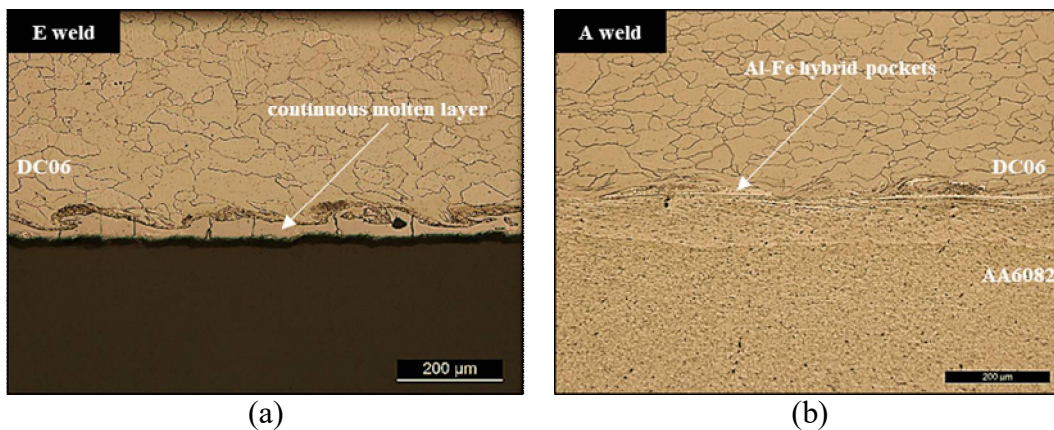
Fig. 2. Micrographs of the weld interface: (a) E weld; (b) A weld.

1. F. Findik, Recent developments in explosive welding, *Mater. Des.*, 2011, vol. 32, no. 3, pp. 1081–1093.
2. G. H. S. F. L. Carvalho, I. Galvão, R. Mendes, R. M. Leal, A. Loureiro, Influence of base material properties on copper and aluminium–copper explosive welds, *Sci. Technol. Weld. Joining*, 2018, in press.
3. G. H. S. F. L. Carvalho, R. Mendes, R. M. Leal, I. Galvão, A. Loureiro, Effect of the flyer material on the interface phenomena in aluminium and copper explosive welds, *Mater. Des.*, 2017, vol. 122, pp. 172–183.
4. M. J. Rathod, M. Kutsuna, Joining of aluminum alloy 5052 and low-carbon steel by laser roll welding, *Weld. J.*, 2004, vol. 83, pp. 16S–26S.

G. H. S. F. L. Carvalho et al.

SHOCK SYNTHESIS OF FEW-LAYER GRAPHENE AND NITROGEN-DOPED GRAPHENE MATERIALS

P. Chen[1], C. Xu[1], H. Yin[1], X. Gao[1], Q. Zhou[1], and L. Qu[2]

[1] State Key Laboratory of Explosion Science and Technology, Beijing Institute of Technology, Beijing 100081, China
[2] Key Laboratory of Cluster Science, Ministry of Education of China, School of Chemistry, Beijing Institute of Technology, Beijing 100081, China

e-mail: pwchen@bit.edu.cn

Shock wave action combining shock-induced chemical reaction will cause a series of changes of material physical and chemical properties [1, 2]. In this study, few layer graphene and nitrogen-doped graphene materials were prepared through the reaction of calcium carbonate and magnesium induced by shock wave. The recovered samples were characterized using various techniques such as transmission electron microscopy, scanning electron microscopy (Fig. 1), Raman spectroscopy and X-ray photoelectron spectroscopy. The shock synthesis of graphene materials required a balance between the growth rate of graphene materials and the formation rate of carbon atoms. The pressure and temperature were two important factors affecting the synthesis of graphene materials.

Similarly, few layer graphene nanosheets were successful synthesized by reduction of CO_2 with calcium hydride under detonation-driven flyer impact loading. A scheme of shock synthesis of graphene material from CO_2 is illustrated in Fig. 2. Furthermore, by adding ammonium nitrate to the reaction system, nitrogen-doped graphene materials could also be prepared through this one-step shock-wave treatment. In addition, the nitrogen-doped graphene was demonstrated to act as a metal-free electrode with an efficient electrocatalytic activity toward oxygen reduction reaction in alkaline

solution (Fig. 3), the measurement procedure is described elsewhere [3].

In conclusion, shock wave technique provides a novel and simple route to transform CO_2 or carbonate into useful graphene materials. Significantly, the formation of highly valued form of carbon directly from CO_2 may provide a new pathway to mitigate this greenhouse gas.
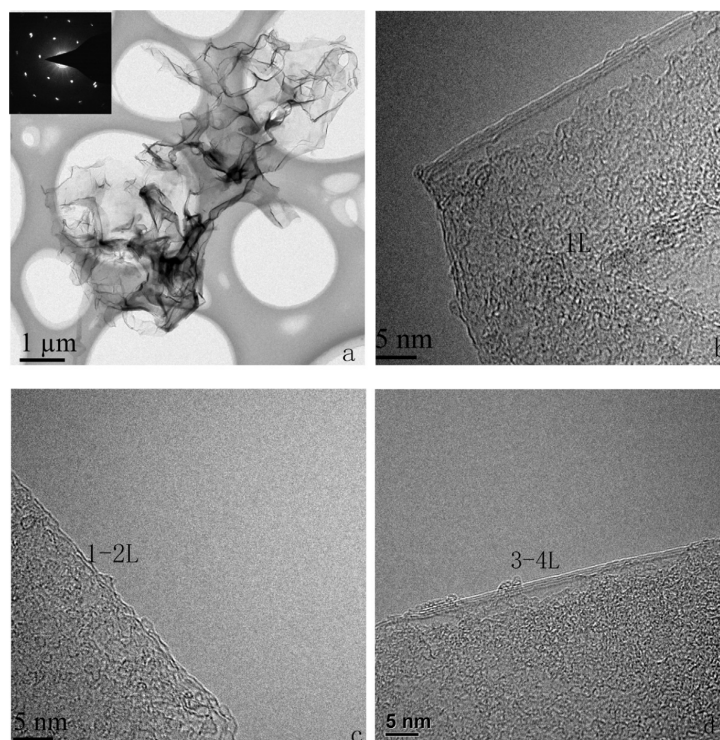
Fig. 1. TEM images of (a) typical films. The inset of (a) shows SEAD pattern. HRTEM images of (b) monolayer, (c) double layer, and (d) three to four layers.
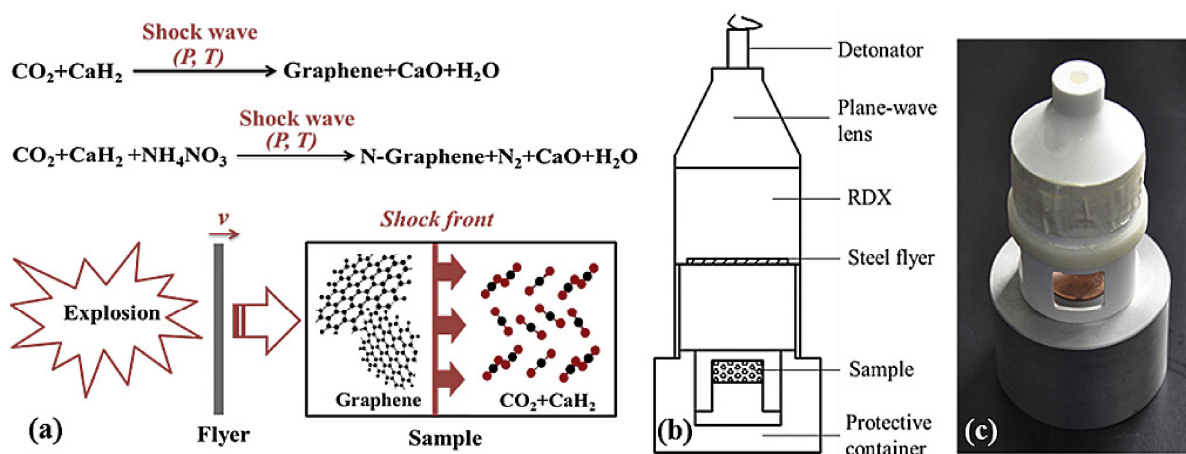
Fig. 2. Schematic representations: (a) Shock wave process for the synthesis of graphene material from dry ice. (b) Diagram of shock-loading apparatus. (c) Photo of real experimental setups.

P. Chen et al..
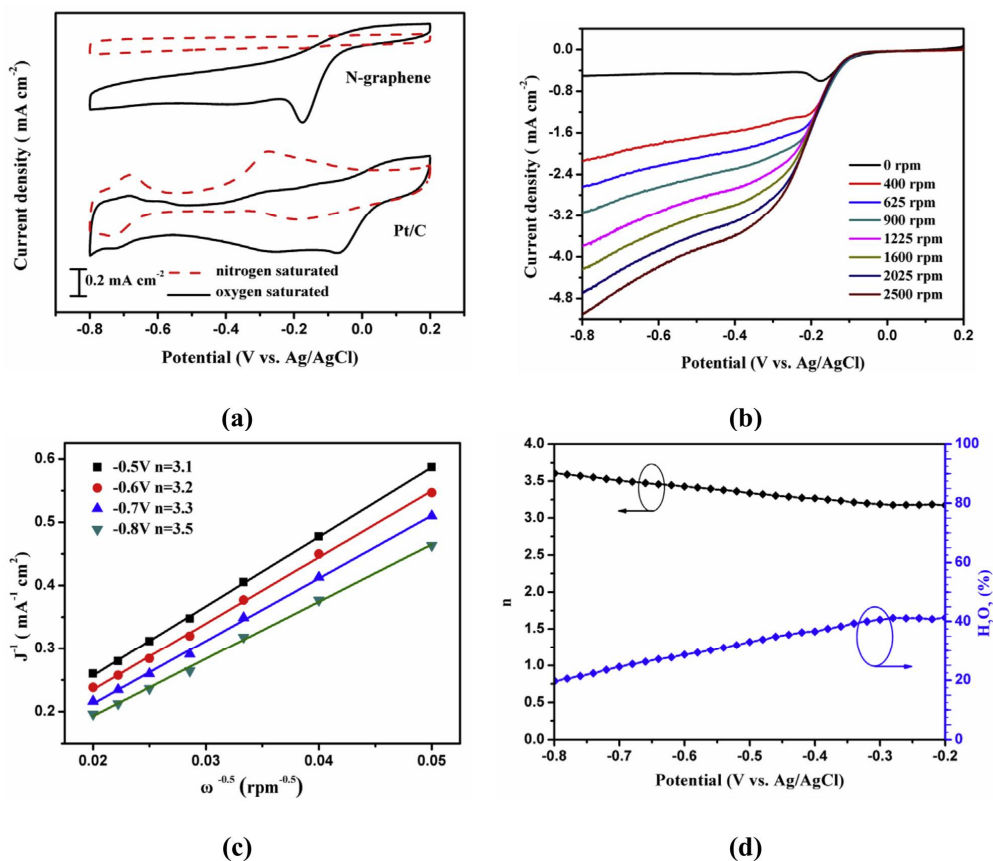
Fig. 3. ORR performance of shock synthesized N-graphene and commercial Pt/C in 0.1 M KOH solution. (a) CV curves at a scan rate of 10 mV s^{-1}. (b) LSV curves of the N-graphene at different rotating speeds. (c) The Koutecky–Levich plots derived from LSV curves at different potentials from –0.2 to –0.8 V. (d) HO$_2^-$ production and the corresponding n derived from RRED measurement.

1. N. N. Thadhani, Shock-induced chemical reactions and synthesis of materials, *Prog. Mater. Sci.*, 1993, vol. 37, pp. 117–226.
2. J. J. Liu, Y. N. Bai, P. W. Chen, N. F. Cui, H. Yin, Reaction synthesis of TiSi$_2$ and Ti$_5$Si$_3$ by ball-milling and shock loading and their photocatalysis activities, *J. Alloys Comp.*, 2013, vol. 555, pp. 375–380.
3. Y. Zhao, C. Hu, L. Song, L. Wang, G. Shi, L. Dai, L. T. Qu, Functional graphene nanomesh foam, *Energy Environ. Sci.*, 2014, vol. 7, pp. 1913–1918.

EXPLOSIVE HARDENING AND ITS APPLICATION IN PRODUCTION OF RAILROAD SWITCH FROGS

A. A. Deribas[1], A. A. Shtertser[2]*, and E. E. Zubkov[3]

[1] Joint Institute for High Temperatures, Russian Academy of Sciences, ul. Izhorskaya 13 Bld. 2, Moscow, 125412 Russia
[2] Lavrent'ev Institute of Hydrodynamics, Siberian Branch, Russian Academy of Sciences, pr. Lavrent'eva 15, Novosibirsk, 630090 Russia
[3] JSC Novosibirsk Railroad Switch Plant, ul. Aksenova 7, Novosibirsk, 630025 Russia

*e-mail: asterzer@mail.ru

The first patent on explosive hardening (EH) of manganese steel was issued in 1955 [1]. In 1960 the works on EH began in Novosibirsk at the Lavrent'ev Institute of Hydrodynamics. It was found that strong shock waves generated by explosion can heat the substance up to the melting point, induce phase transitions, change microstructure and improve the mechanical properties, such as hardness, plasticity and strength [2]. In the most commonly used EH method, the high explosive layer is laid directly on the hardened material. In this case, high explosives with detonation velocity of more than 7 km/s are used, and these are the plasticized explosives mostly. Possibilities of EH can be expanded by use of less brisant high explosives and intermediate porous layer between the explosive charge and hardened material [3]. This method is based on the effect of amplification of the shock wave generated in a treated material when the interlayer thickness is small, so that the primary shock wave arising in a porous interlayer does not fade on a distance between the explosive charge and the hardened sample. Figure 1 shows the hardness change with depth in manganese steel for different explosives and using two methods of hardening, direct and via the sand layer. Explosives used in experiments and their properties are listed in Table 1.

Explosive	Density ρ_e, g/cm^3	Detonation velocity D, km/s	Detonation pressure P, GPa
PE GP-87	1.6	7.2	21.0
RDX	1.0	6.2	10.0
Amatol	1.0	4.2	5.0
PE LVV-11-1	1.42	7.4	19.4

Note: PE – plasticized explosive

Evidently, powdery amatol and RDX charges with the thickness of 40 and 20 mm, respectively, and with an intermediate layer of dry sand ensure the same hardness on the sample surface as 9 mm thick plasticized explosive GP-87 (see Fig. 1). It was found that maximal hardening effect is achieved when the thickness of sand layer is 0.25 – 0.50 of the explosive charge thickness for powdery amatol and RDX. Thus, we can see, that not only high explosives with high density and detonation velocity but low-density powdery explosives having a detonation velocity substantially less than 7 km/s are suitable for EH.
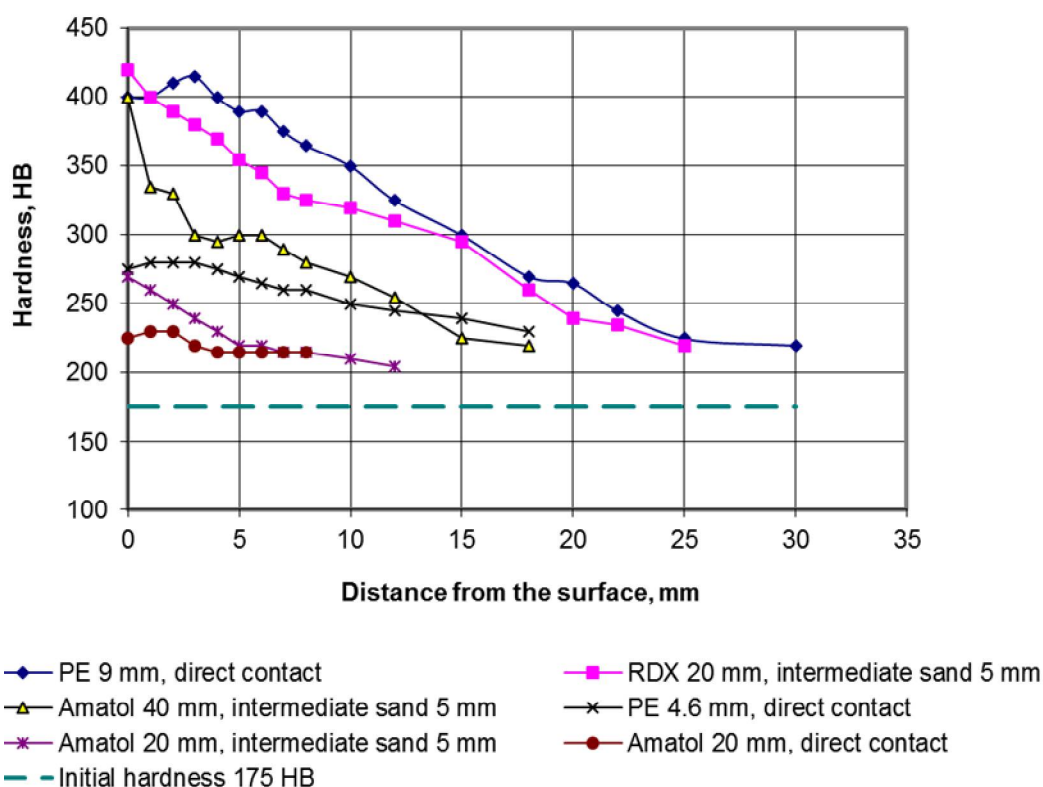
Fig. 1. Dependence of hardness on distance from the surface in explosively hardened manganese steel. PE: plasticized explosive GP-87.

The first steps to the full-scale industrial application of EH were made in 1960s when Administration of Novosibirsk Railroad Switch Plant has applied to Lavrent'ev Institute of Hydrodynamics with the problem of increasing of the service life of the railroad switch frog (Fig. 2). The most wear places are on the frog guardrails and frog core (Fig. 2b). At this, the wear of the frog core is usually 5–6 times greater than that of the railroad switch as a whole. During a dozen of years, Lavrent'ev Institute of Hydrodynamics and Ural Branch of All-Russian Institute of Railway Transport conducted the research works, developed the technology, designed and manufactured explosion chambers and performed the service tests of hardened frogs. It has been proven that EH increases the lifetime of frogs by 20–30%. Finally, in 1979 the special shop for explosive hardening of switch frogs has started working in Novosibirsk Railroad Switch Plant. In the first years, the production rate was 1–2 thousand of hardened items per year. Presently, the production volume of Novosibirsk Railroad Switch Plant is 10–12 thousand hardened pieces per year. Since 1979, the hardening shop has produced more than 350 thousand switch frogs. Now more than 90% of produced R65 frogs (grades 11/1 and 1/9) are explosively hardened.
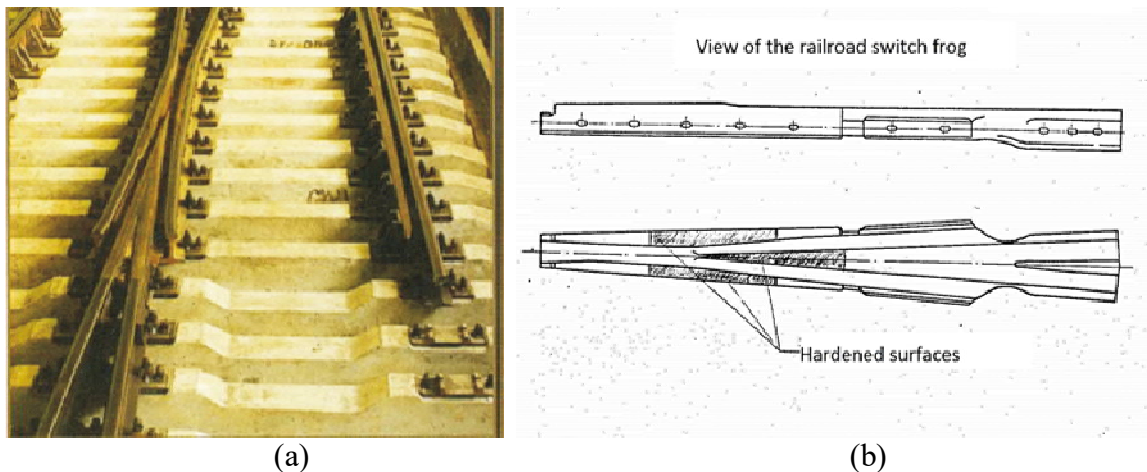
Fig. 2. (a) Railroad switch frog on the railway track and (b) surfaces for hardening on the frog guardrails and frog core wedge.

Some elements of explosion chambers were improved during their exploitation (chamber cover truck, working table, air vent valve, rail track) in order to increase the productivity. However, the main chamber parts (body and cover) withstood about 120 thousand explosions in every chamber and currently operate successfully.

A. A. Deribas et al.

EH process includes the use of PE LVV-11-1 produced by Novosibirsk Plant of Artificial Fibers in the form of a tape with a thickness of 4 mm and a width of 50 mm. Characteristics of LVV-11-1 are given in Table 1. For the hardening of guardrails explosive charge with a thickness of 16 mm is formed on the treated surface (4 layers of LVV-11-1 tape), whereas the core wedge is hardened with 16 mm thick PE charge (3 layers of LVV-11-1 tape). EH increases the surface hardness from 200 *HB* to 350–380 *HB*, the depth of a hardened material is 30–35 mm. This prevents the initial crushing of the frog core and guardrails during operation therefore its lifetime grows.

Important to note is that EH of a cast high-manganese steel G13L (Hadfield steel) is useful when the initial plasticity of material $\delta >$ 30%. This is due to a substantial decrease in δ after hardening. It is necessary to avoid the loss of plasticity and, as a result, cracking and chipping of metal during the frog operation. The degree of hardening can be increased using the second explosive loading and the values of more than 380 *HB* are achievable. However, according to the above reasons, the re-loading is possible only when steel has a great plasticity reserve.

1. N. A. McLeod, Method of hardening manganese steel, *US Patent No. 2703297,* Patented March 1, 1955.
2. A. A. Deribas, *Physics of hardening and explosive welding*, Novosibirsk: Nauka, 1980 (in Russian).
3. A. A. Shtertser, A. A. Deribas, I. N. Gavril'ev, N. A. Kostyukov, The method for increase metal hardness by explosion, *RF Patent No. 1309404*, Patented May 20, 1997.

INITIATION AND COMBUSTION OF MECHANOACTIVATED MIXTURES OF ALUMINUM AND COPPER OXIDE

A. Yu. Dolgoborodov[1,2,3], B. D. Yankovskii[1], V. G. Kirilenko[2], A. N. Streletskii[2,3], S. Yu. Anan'ev[1,3], I. V. Kolbanev[2], and G. A. Vorob'eva[2]

[1] Join Institute for High Temperature, Russian Academy of Sciences, ul. Izhorskaya 13 Bld. 2, Moscow, Russia
[2] Semenov Institute of Chemical Physics, Russian Academy of Sciences, ul. Kosygina 4, Moscow, Russia
[3] Moscow Institute of Physics and Technology, Dolgoprudny, Russia

e-mail: aldol@ihed.ras.ru

Thermite mixtures based on metals and solid oxidants allow to obtain a significant exothermic effect during combustion (up to 8 kJ/g), while the burning rate of mixtures of micron powders usually does not exceed several tens of mm/s, which limits the field of their application. This is due to the fact that the rate of propagation of chemical reactions in solid mixtures is determined primarily by the effective contact surface of the reactants. To increase this surface, various methods are used: ultrasonic mixing of nanosized powders, electrochemical deposition of submicron metal-oxidizer layers, etc. [1]. One of the relatively new methods for obtaining fast-burning thermite compounds is the preliminary mechanochemical activation of mixtures of micron-sized particles in energy-intensive ball mills. At the same time, the components are shredded and mixed at the submicron and nano levels, and new defects in the crystal structure are formed, which makes it possible to increase the rate of chemical reaction on the surface of the reagents and, accordingly, we get a way to control the processes of energy release during combustion and shock wave action. In Russia, the method of mechanoactivation of solid oxidant-metal fuel mixtures has been actively used since the

A. Yu. Dolgoborodov et al.

beginning of the 2000s [2–5], and the resulting materials are called mechanically ectivated energetic composites (MAECs).

Among the variety of thermite mixtures, special attention is drawn to the composition of Al + CuO, which makes it possible to obtain one of the highest exothermic effects per unit volume (more than 20 kJ/g). In this paper, new research results on the initiation and burning of MAEC Al/CuO based on micron and nanosized powders using the mechanoactivation are presented.

As the initial components, micron and nanosized powders were used: industrial pyrotechnic powder Al PP-2L (flake $50 \div 100$ μm × $2 \div 5$ μm), CuO ($20 \div 50$ μm), nanosized nAl (Alex $100 \div 200$ nm) and nCuO ($50 \div 80$ nm). Al weight content was from 18 to 25%. Mixing and activation were carried out in the vibration mill of the Aronov design or in an Activator-2sl planetary mill with steel drums and balls. A rough estimate of the energy intensity of the two types of mills based on the growth of the specific surface area of the test material (MoO_3) $J = 9.7$ W/g for Ativator-2sl at a total power and $J = 3.7$ W/g for the Aronov mill. Weight load of powders was 10–25 g, the mass of balls was 200–300 g. Hexane was added to reduce frictional heating. The starting powders and MAEC were analyzed by X-ray diffraction, electron microscopy and thermo-gravimetric analysis. Image analysis shows that as a result of activation, the obtained material were a polydisperse mixture of fairly large conglomerates of flat fragments of Al particles ($\sim 1–10$ μm) with submicron CuO particles (see Fig. 1a). The products of high-speed burning of MAEC Al/CuO are shown in Fig. 1b. There are 10-μm spherical Al_2O_3 particles consisting of stuck submicron particles. Cu is in the form of large smeared drops on the surface of Al_2O_3 or in the form of nanosized particles condensed from the gas phase.

A number of the dependences of the combustion parameters on the activation dose D_a were determined in experiments: ignition temperature by hot surface, brightness temperature of burning products, burning rate in cylindrical channels and electrical resistivity in cloud of products. The dynamics of the expansion of products in free space during electric spark and shock wave initiation was analyzed.

The burning rate was measured in plastic and glass tubes (diameter of 4–10 mm) by recording of product emission by light fiber or high-

speed photography. The porosity of charges was 60–70%. The initiation was carried out by heating the NiCr wire or by an electric spark. The spark energy was regulated by changing the current amplitude in the range of 1.5–50.0 mJ at duration of the current pulse of 1.2 μs. Experimental setup with electric spark initiation and individual frames at different sparks energies are shown in Fig. 2. Brightness temperature of products was measured by four-channel pyrometer.
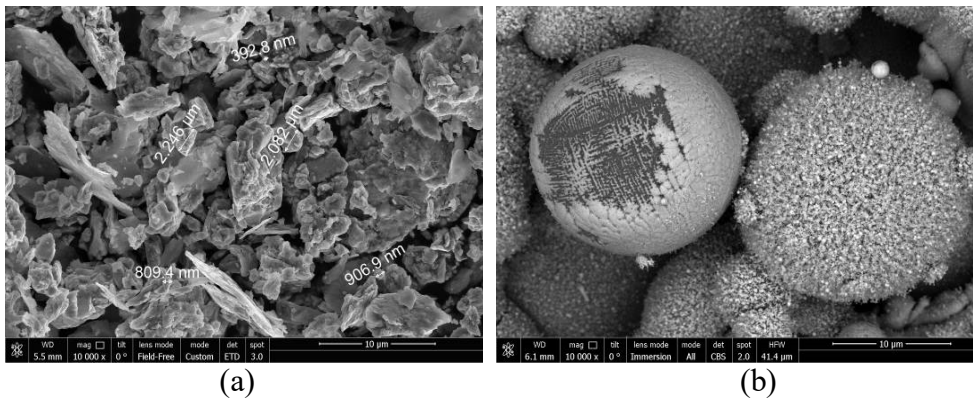
Fig. 1. SEM images of MAEC Al/CuO, (a) t_a = 8 min and (b) burning products (light - Cu, gray - Al_2O_3).
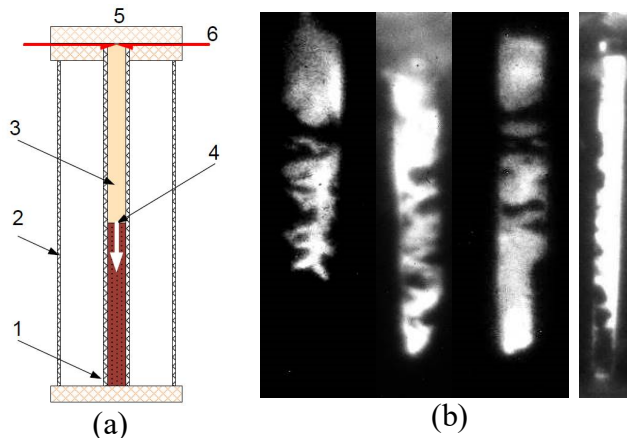
Fig. 2. (a) Schematic of experimental setup: *1* dark part of glass tube (no combustion), *2* glass vessel with water, *3* light part of tube (combustion), *4* boundary between dark and light parts of tube, *5* spark gap, *6* electrodes. (b) The photos of inhomogeneities of the luminescence at different spark energy.

Depending on D_a and initiation method, the measured burning rate varies from 10 to 700 m/s and the product temperature is in the range of 2000–3700 K. In case of low-energy electric spark (< 20.0 mJ), the combustion has a pronounced heterogeneous character. Photo

registration shows that zones of bright glow of hot products alternate with dark zones. As the spark energy increases, the uniformity of the glow increases. The highest reactivity, burning rate and temperature of products for MAEC Al/CuO were obtained at $D_a = 1.8 \div 2$ kJ/g. With increasing D_a there is a partial reaction of the reagents in the activation process.

In the case of shock-wave initiation of compositions in a semi-enclosed volume, the main process of energy release proceeds in the flow of products dispersed in the unloading wave. The initial flow rate of the products is more than 800 m/s. The maximum brightness temperature in the cloud of partially ionized products reaches 3700 K, the resistivity is about 107 Ohm·mm^2/m. In general, the results of the work have shown the promise of preliminary mechanochemical activation for the production of fast-burning thermite compositions of Al/CuO. The use of the original nanoscale components is inadvisable, since it does not give appreciable advantages. The reactivity of thermite mixtures based on CuO can be controlled by the addition of metals having catalytic action.

1. V. E. Zarko, A. A. Gromov, *Energetic Nanomaterials: Synthesis, Characterization, and Application*, Elsevier, 2016.
2. Yu. Dolgoborodov, M. F. Gogulya, M. N. Makhov, et al. Detonation-like phenomena in Al/S mixture, *Proc. Twenty-Ninth Intern. Pyrotechnics Seminar*, 2002, pp. 557–563.
3. Yu. Dolgoborodov, M. N. Makhov, I. V. Kolbanev, A. N. Streletskii, Mechanically activated pyrotechnic composition, *RF Patent No. 2235085*, 2004.
4. Yu. Dolgoborodov, Mechanically activated oxidizer–fuel energetic composites, *Comb. Explos. Shock Waves*, 2015, vol. 51, no. 1, pp. 86–99.
5. N. Streletskii, M. V. Sivak, A. Yu Dolgoborodov, Nature of high reactivity of metal/solid oxidizer nanocomposites prepared by mechanoactivation: A review, *J. Mater. Sci.*, 2017, vol. 52, pp. 11810–11825.

EXPLOSIVE LABORATORY INSTALLATION FOR CYLINDRICAL COMPRESSION

S. V. Dudin, V. A. Sosikov, and S. I. Torunov

Institute of Problems of Chemical Physics, Russian Academy of Sciences, Chernogolovka, Moscow, 142432 Russia

e-mail: dudinsv@ficp.ac.ru

The investigation of the cylindrical compression of various materials, as well as the action of strong convergent shock waves, is of interest both from the point of view of the practical use of these phenomena and to solve certain problems of theoretical physics. Such problems include 1) the problem of the formation and development of a cylindrical detonation wave [1–3] with multipoint initiation, 2) cylindrical compression of tubes, 3) the development of inhomogeneities in liquids under the action of converging cylindrical shock waves, 4) ejection of fine particles and plasma from a cylindrical surface upon the emergence of a strong shock wave, 5) the problem of initiating of thermonuclear fusion upon compression of a plasma in a magnetic field. Full-scale experiments, where a cylindrical detonation wave is formed, are quite expensive and laborious. In addition, they require a large amount of high-energy explosive. And this, in turn, entails the need for explosive experiments on testing areas.

A compact laboratory installation in which a cylindrical detonation wave is formed by the method of multi-point initiation is developed at IPCP RAS. The weight of the charge used is less than 1 kg in TNT equivalent. The appearance of the device is shown in Fig. 1. The upper part shows the front view of the device; the bottom, the side view. To form a cylindrical detonation wave, 12 to 48 initiation points are used (*1* in Fig. 1). The main charge in the form of a ring is made of an explosive (*2*). The collar (*3*) is between the charge and the initiation points. It is designed to dampen the interaction of detonation

waves from neighboring initiation points. In the central part, the test material (*4*) is in a thin-walled metal liner (*5*). All points are initiated simultaneously from the detonator (*6*), which is located at the bottom of the unit.
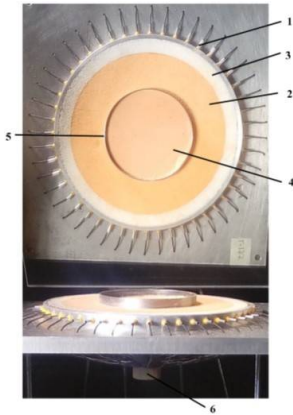
Fig. 1. Laboratory installation.

Fig. 2. The appearance of the camera NANOGATE-4BP.

One of the methods used to monitor the operation of devices and visualize the processes of cylindrical compression is high-speed photography. For this purpose, the domestic camera "NANOGATE-4BP" (Fig. 2) is used.

The main characteristics of the camera:
- Number of electron-optical channels in chamber – 4;
- The spectral range of the photocathode sensitivity is 380–800 nm;
- Working diameter of the photocathode is 18 mm;
- The duration of the gating pulse is from 10 ns to 20 µs;
- The temporal instability (jitter) of the trigger of the camera is less than 0.2 ns;
- Spatial resolution for all strobe-pulse durations is of 30 pairs of lines per mm;
- Resolution 1380*1024 pixels;
- The experiments were performed using a Nikon 70-300 mm f/4.5-5.6G lens ED-IF AF-S VR Zoom-Nikkor.

With the help of this complex, which includes an explosive laboratory installation and a high-speed Nanogate-4BP camera, the following experimental investigations have been carried out:
- formation of a cylindrical detonation wave by the method of multipoint initiation (Fig. 3) [4–6];
- compression of a thin-walled metal liner [7];

- the output of a strong shock wave on a free cylindrical surface, ejection of microparticles and plasma [8];

- initiation of condensed and liquid explosives by a cylindrical shock wave (Fig. 4).
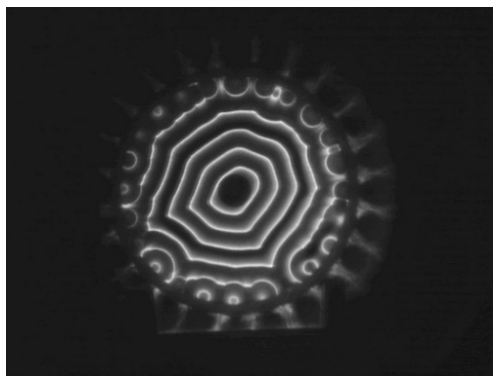
Fig. 3. The formation of a cylindrical detonation wave by the method of multipoint initiation (successive positions of the wave front with an interval of 2 μs).

| 41 μs | 49 μs |
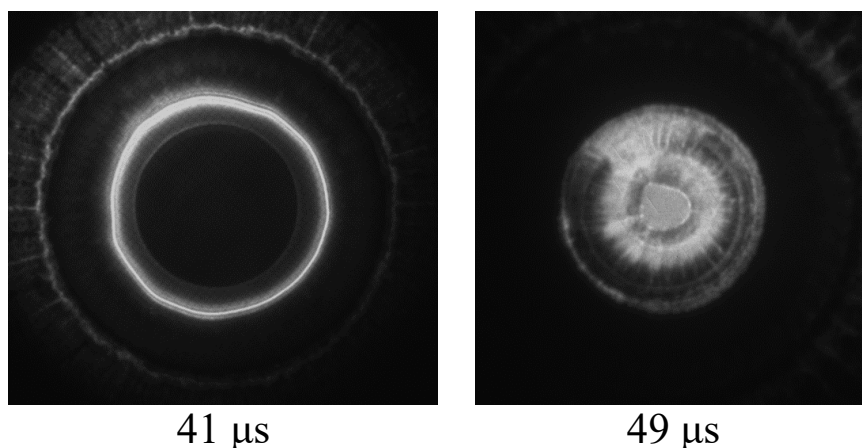
Fig. 4. Initiation of a liquid explosive by a cylindrical shock wave. 41 microseconds – shock wave approach to the cuvette with liquid explosive, 49 microseconds – detonation wave in liquid explosive.

1. Y. B. Zeldovich, Parity nonconservation in electron scattering and in other effects in the first order of the weak interaction coupling constant, *Zh. Eksp. Teor. Fiz.*, 1959, vol. 36, p. 964.

S. V. Dudin et al.

2. L. Al'tshuler, S. Kormer, A. Bakanova, A. Petrunin, A. Funtikov, A. Gubkin, Irregular conditions of oblique collision of shock waves in solid bodies, *Zh. Eksp. Teor. Fiz.*, 1962, vol. 41.
3. L. Guerri, A. Taroni, Computation of the flow behind converging detonation wave in cylindrical or spherical geometry, *Euratom. Rep. "Eur 1848e,"* 1964.
4. S. V. Dudin, V. A. Sosikov, S. I. Torunov, Experimental investigation of cylindrical detonation wave, *J. Phys. Conf. Ser.*, 2016, vol. 774, p. 012074.
5. A. V. Shutov, V. G. Sultanov, S. V. Dudin, Mathematical modeling of converging detonation waves at multipoint initiation, *J. Phys. Conf. Ser.*, 2016, vol. 774, no. 1, p. 012075.
6. S. V. Dudin, V. A. Sosikov, S. I. Torunov, Formation features of cylindrical detonation wave at multipoint initiation, *J. Phys. Conf. Ser.*, 2018, vol. 946, p. 012057.
7. S. V. Dudin, V. A. Sosikov, S. I. Torunov, The output of a shock wave on the inner surface of a cylindrical liner, *J. Phys. Conf. Ser.*, 2018 (in press).
8. M. I. Kulish, S. V. Dudin, Microparticles and plasma stream registration during cylinder compression of a metal liner, *J. Phys. Conf. Ser.*, 2018 (in press).

THE MECHANISM OF DETONATION NANODIAMONDS GRAPHITISATION UNDER HEATING AND IRRADIATION

V. P. Efremov and E. I. Zakatilova

Joint Institute for High Temperatures, Russian Academic of Sciences, ul. Izhorskaya 13 Bld. 2, Moscow, 125412 Russia.

e-mail: ei.zakatilova@mail.ru

Crystal structure (detonation nanodiamond) is formed in the detonation products upon utilization of high explosives on the carbon base with negative oxygen balance. Both nano and micro diamonds can form in the detonation products of the same explosive depending on the explosion condition.

At this time, the application of this substance is difficult. This is due to a heterogeneous particle structure of detonation nanodiamond, which affects its properties. According to the literature data, there is a scatter, and sometimes even a contradiction in the values of the nanodiamond properties. For example, the initial temperature of the graphitisation of detonation nanodiamond particles is in a wide range from 670°C [1] to 980°C [2]. However, this scatter is not observed for micro and bulk diamonds. The properties of detonation microdiamonds are close to those of a bulk diamond.

The stability of detonation nanodiamonds to various energetic influence is in the focus present physical investigations [3–5]. In [3], the influence of irradiation by heavy ions on the structure of single-crystal diamond has been studied. Conversion of diamond phase into amorphous carbon in the ion track occurs when the critical damage threshold is exceeded [3]. The critical damage threshold is decreased when nanodiamond is irradiated by fast heavy ions [4]. Based on the results of numerical simulation, it was determined that the formation of amorphous track in the nanoparticle center with a size of 5 nm occurs upon irradiation of nanodiamond by heavy ions. The complete

transition of diamond particle into amorphous phase occurred below this size [4]. Determination of critical size of nanoparticles, in which there is a two-phase diamond and graphite, under irradiation will allow to create material with unique properties. Before the critical threshold of damage in nanodiamonds point defects are formed. As a result of heat treatment of irradiated samples, Wigner energy is released and the crystal structure of the material is restored [5]. Upon annealing of nanodiamonds irradiated with fast neutrons, the Wigner energy was 237 J/g, while the Wigner energy of irradiated graphite was only 9.5 J/g [5]. Thus, the mechanism of graphitization of the diamond phase upon irradiation depends on the type of energy release.

To fabricate the target for irradiation, we conducted a study of the thermal stability of detonation nanodiamonds during ordinary heating. The synchronous thermal analysis, Raman spectroscopy, X-ray diffraction analysis and scanning electron microscopy were used to study samples after heat treatment.

The heat treatment of detonation nanodiamond powder was carried out in corundum crucible with a closed lid at atmospheric pressure from room temperature to 1500°C at rates of up to 2 and 10°C/min in a dynamic argon atmosphere. The investigation of stored sample by the X-ray diffraction analysis (Fig. 1) showed a decrease in the fraction of diamond phase with increasing final processing temperature [6]. There is a difference in the diffraction patterns of detonation nanodiamonds from micro and bulk diamonds. In particular, the main diffraction peak from the base plane (111) is much wider for nanodiamond than that for micro- and bulk diamond. The effect of the rate of heat treatment on the size parameters of the powder particles was also revealed. At a rate of 10°C/min, spherical conglomerates of particles with a size of about 30–40 nm (Fig. 2b) predominated in the sample. In the case of heating with a rate of 2°C/min, planar carbon structures were found in the sample and the size of the spherical particles was about 6–7 nm (Fig. 2c). It is established that even under normal thermal loading the range of the start and finish of graphitization is unusually large (from 800 to 1500°C).

The results of the thermal stability of nanodiamond allowed us to recommend the temperature for the preparation of a target from a mixture of chromium + nanodiamonds, which was subsequently used

as a source of material for coating steel parts (Fig. 3). Sputtering was carried out at the Petrovsky Scientific Center FUGAS, JSC. This processing of details led to a hardening of the surface and an increase in the working life. After investigation of coating, whole nanodiamonds were found in the substance. The production of chromium + nanodiamonds mixture at the temperature of 680°C does not lead to an annihilation of the nanodiamond. When the mixture is impacted on the steel surface to be coated, the pressure rises above the yield strength of chromium, which leads to plastic deformation of particles with micron size. At the same time, nanodiamonds are not destroyed. Thus, under the conditions of ion-plasma deposition, powder nanoparticles undergo no structural and phase changes.
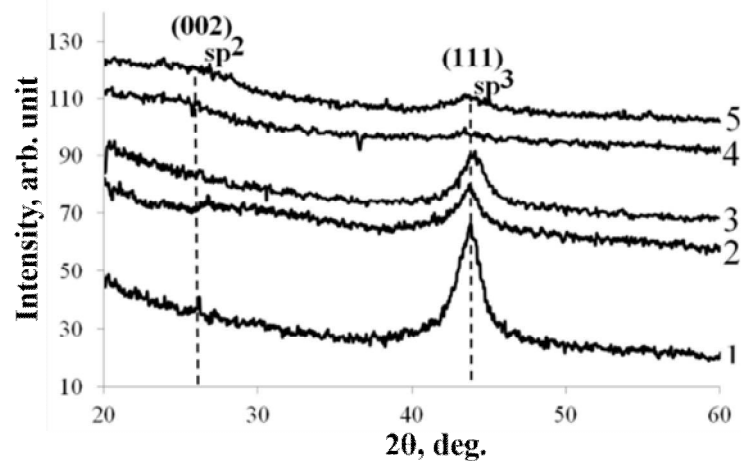
Fig. 1. X-ray diffraction patterns of the powder sample of detonation nanodiamond (*1*) in the initial state and after heat treatment at (*2*) *T* = 600°C and rate of 10°C/min; (*3*) *T* = 1000°C and rate of 10°C/min; (*4*) *T* = 1500°C and rate of 10°C/min; and (*5*) *T* = 1500°C and rate of 2°C/min.

(a)   (b)   (c)
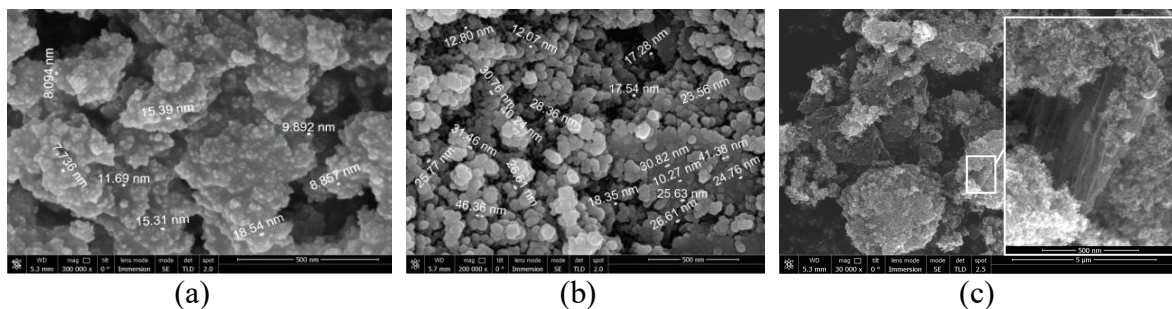
Fig. 2. Microstructure of nanodiamond powder: (a) before heat treatment; (b) after heat treatment at *T* = 1500°C and rate of 10°C/min; (c) after heat treatment at *T* = 1500˚C and rate of 2˚C/min.

V. P. Efremov and E. I. Zakatilova

Fig. 3. (*1*) Sample-witnesses and (*2*) stock model with a protective coating including detonation nanodiamonds. Sputtering was carried out at Petrovsky Scientific Center FUGAS, JSC.

1. N. S. Xu, J. Chen, S. Z. Deng, Effect of heat treatment on the properties of nano-diamond under oxygen and argon ambient, *Diam. Relat. Mater.,* 2002, vol. 11, pp. 249–256.
2. V. A. Popov, A. V. Egorov, S. V. Savilov, V. V. Lunin, A. N. Kirichenko, V. N. Denisov, V. D. Blank, O. M. Vyaselev, and T. B. Sagalova, Features of the transformation of detonation nanodiamonds into onionlike carbon nanoparticles, *J. Surf. Invest.. X-ray, Synchrotron Neutron Tech.,* 2013, vol. 7, no. 6, pp. 1034–1043.
3. D. P. Hickey, K. S. Jones, R. G. Elliman, Amorphization and graphitization of single-crystal diamond — A transmission electron microscopy study, *Diam. Relat. Mater.,* 2009, vol. 18, pp. 1353–1359.
4. F. Valencia, J. D. Mella, R. I. Gonzalez, M. Kiwi, E. M. Bringa, Confinement effects in irradiation of nanocrystalline diamond, *Carbon,* 2015, vol. 93, pp. 458–464.
5. F. Cataldo, G. Angelini, Z. Révay, E. Ōsawa, T. Braun, Wigner energy of nanodiamond bombarded with neutrons or irradiated with γ radiation, *Fuller. Nanotub. Carbon Nanostruct.,* 2014, vol. 22, pp. 861–865.
6. V. P. Efremov, E. I. Zakatilova, The analysis of thermal stability of detonation nanodiamond, *J. Phys. Conf. Ser.,* 2016, no. 774, 012014.

GROWTH OF DEFECTS OF DISCONTINUITY OF BIMETALLIC STEEL-TO-TITANIUM PLATE BILLET JOINT DURING MANUFACTURING EQUIPMENT AND ITS OPERATION

A. M. Fedorov, I. A. Schastlivaya, V. A. Mezhonov, and D. E. Oderyshev

NRC "Kurchatov Institute" − Central Research Institute of Structural Materials "Prometey", St. Petersburg, Russia

e-mail: mail@crism.ru

The paper presents the results of NRC "Kurchatov Institute" − CRISM "Prometey" on the study of change in the area of defects of discontinuity of bimetallic steel-to-titanium plate billet joint during technological operations in manufacturing equipment and its operation. They are as follows:

   - growth of a defect of bimetallic plate billet discontinuity under cyclic bending load;

   - growth of a defect in the assembly of tube and tube plate under cyclic loading along the tube axis;

   - growth of a defect during hot rolling.

INVESTIGATION OF STRUCTURE FORMATION AT GAS DYNAMIC COLD SPRAY OF ALUMINUM–ZINC POWDER

S. V. Ganin[1], O. G. Zotov[1], A. I. Shamshurin[1], V. A. Markov[2], and V. A. Sokolova[2]

[1] Peter the Great Polytechnic University,
St. Petersburg, 195251 Russia
[2] Kirov St. Petersburg State Forest-Technical University,
St. Petersburg, 194021 Russia

e-mail: S.V.Ganin@gmail.com

Gas dynamic cold spray of metal surfaces is a process of formation of metal coatings during impact of particles of plastic metals, which are accelerated in a supersonic gas jet to velocities up to some hundreds meters per second, with the substrate at temperatures lower than melting point of these materials. Upon impact of unmelted metal particles with the substrate, particles undergo plastic deformation and the kinetic energy of the particles is converted into heat and, partially, into bonding energy with the substrate, ensuring the formation of a continuous layer of densely packed metal particles [1, 2]. Such technology is used to restore a worn-down surface and to increase wear resistance due to hardening of surface layers.

In the present work, we studied the structure of the coating layer after cold spray of powder A-20-11 produced by the Obninsk Center for Powder Spraying using a DIMET-405 device. Powder A-20-11 is a mixture containing 50% aluminum powder, 25% zinc powder and 25% corundum with a particle size of 20–50 μm. Spraying was carried out at temperatures of 300 and 500°C under a working gas (air) pressure of 10 atm. The studies of the microstructure of samples cut out from the coating layer were carried out using a Tescan MIRA3 electronic scanning microscope.

The results of local chemical analysis showed that the structure of the surface layers is multiphase. The bright structural component in Figs. 1 and 2 is zinc, and the dark one is aluminum. SE images show clearly difference between the phases of pure aluminum and the volumetric inclusions of oxide Al_2O_3. The analysis of the structure shows that zinc being deposited melts, forming a solid matrix with inclusions of aluminum and corundum (Al_2O_3) particles. It is interesting to note that the structure of the coating at a spraying temperature of 300°C, which is below the melting point of zinc (419 °C), is similar to the structure of the coating sprayed at 500°C, when zinc particles are deposited in the molten state. This indicates that the deformation heating of particles during impart with the substrate uniquely exceeds 150°C.
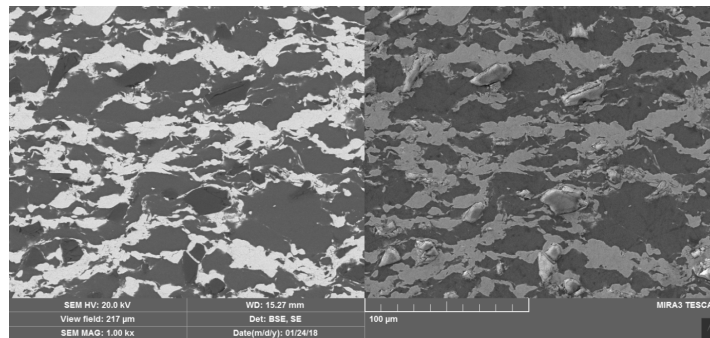
Fig. 1. SEM images of the coating layer sprayed at 300°C (BSE and SE regimes).
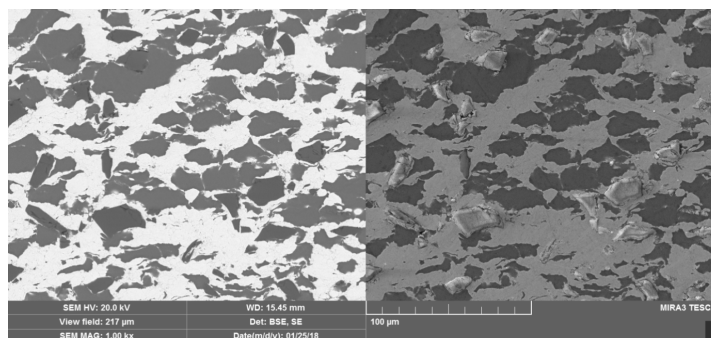
Fig. 2. SEM images of the coating layer sprayed at 500°C (BSE and SE regimes).

1. A. P. Alkhimov, V. F. Kosarev, S. V. Klinkov, V. M. Fomin, *Cold Gas-Dynamic Spraying. Theory and Practice*, Moscow: Fizmatlit, 2010 (in Russian).
2. A. P. Alkhimov, V. F. Kosarev, A. N. Papurin, *Cold Gas-Dynamic Spraying Method*, The joint report of physicists of the American Institute of Physics, 1991, pp. 1047–1049.

B. Godibadze et al.

DEVELOPMENT OF SUPERCONDUCTIVE MgB$_2$ HYBRID COMPOSITES AND INVESTIGATION THEIR STRUCTURE/PROPERTY RELATIONSHIP

B. Godibadze[1], A. Peikrishvili[2,3], T. Gegechkori[3], and G. Mamniashvili[3]

[1] Tsulukidze Mining Institute, Tbilisi, 0186 Georgia
[2] Tavadze Institute of Metallurgy and Materials Science, Tbilisi, 0186 Georgia
[3] Javakhishvili Tbilisi State Univerity, Tbilisi, 0179 Georgia

e-mail: bgodibadze@gmail.com

We applied the original hot shock-assisted consolidation method combining a high temperature with the two-stage explosive process without any further sintering, which produced superconducting materials with high density and integrity. The consolidation of MgB$_2$ billets was made at temperatures above the melting point of Mg up to 1000°C in partially liquid condition of Mg–2B blend powders. The influence of isotope B composition on critical temperature and superconductive properties was evaluated as well as the first successful application of this method for production of hybrid power transmission lines for simultaneous transport of hydrogen and electric energy was demonstrated.

The novelty of proposed nonconventional approach relies on the fact that the consolidation of the samples from coarse (10–15 μm) Mg–2B blend powders was performed in two stages. The explosive predensification of the powders was made at room temperature. In some cases, before dynamic predensification the loading of precursors into the containers was performed by static means or by vibro densification. In all cases, the second stage was done by the hot explosive compaction (HEC) at 1000°C with an intensity of loading of about 5 GPa. Cylindrical compaction geometry was used in all of the HEC experiments. Existing data of the application of shock wave

consolidation technology to fabricate high dense MgB$_2$ billets with higher T_c temperature practically gave the same results and limit of T_c = 40K still is maximal. Additionally as published data show, sintering processes after the shock wave compression are highly recommended providing full transformation of consolidating blend phases into the MgB$_2$ composites. Taking into account the mentioned and diffraction analysis results, we may be sure that after HEC of Mg–2B precursors, based on chemical reactions under shock wave front a full transformation of starting elements into the two-phase composition from MgB$_2$ and MgO takes place. The observation of eutectic colonies in the microstructure confirms the fact of melting/crystallization processes behind of shock wave front.

The liquid phase during HEC of Mg–B precursors at 1000°C provides the formation of MgB$_2$ phase over the entire bulk of billets with maximal T_c = 38.5 K. The type of applied B powder effects on the final result of superconductive characteristics of MgB$_2$ and in the case of amorphous B precursors better results are fixed (38.5 K against 37.5 K). The purity of precursors is important factor and existing of oxygen in the form of oxidized phases in precursors leads to a decrease in T_c and non-uniformity of HEC billets. The isotopic modification of starting boron powders is important too and the application of ^{10}B isotope in starting Mg–2B precursors provides higher critical temperature in formed MgB$_2$ composites.
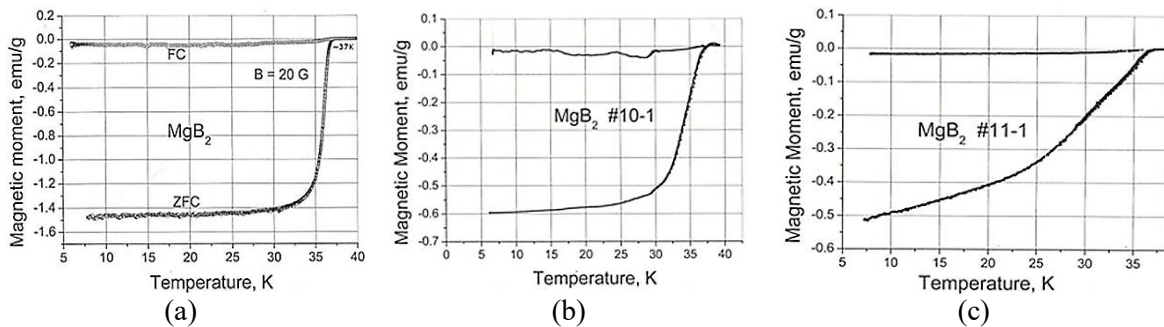
Fig. 1. Magnetic moment-temperature dependences measured in zero-field-cooled (ZFC) and field-cooled (FC) modes, showing the superconducting transition depending on container material and type of boron precursors. (a) HEC in steel container at 1000°C; (b) HEC in copper container with ^{10}B isotope; (c) HEC in copper container with ^{11}B isotope.

B. Godibadze et al.

INVESTIGATION OF STRENGTH OF MATERIALS OBTAINED BY ELECTRIC PULSE CONSOLIDATION OF POWDERS

V. Yu. Goltsev[1,2], E. G. Grigor'ev[2], N. A. Gribov[1], L. A. Degadnikova[1], A. V. Osintsev[1], and A. S. Plotnikov[1,2]

[1] National Research Nuclear University MEPhI, Moscow, 115409 Russia
[2] Merzhanov Institute of Structural Macrokinetics and Materials Science, Russian Academy of Sciences, Chernogolovka, Moscow, 142432 Russia

e-mail: gvy587@gmail.com

The safety of the operation of the critical structural elements is based on taking into account all the factors of force action, studying the patterns of damage accumulation and mechanisms of the development of cracks in the material, and determining the mechanical properties of the material. The modern test equipment allows to carry out tests in a complex with effective methods of visualization of destruction process of samples, which are based on the use of an optical method of digital image correlation. The optical video system determines the displacement of points on an object's surface or structural element under load relative to the initial position. The process of shooting and processing of photos are controlled from the computer by special software. The mathematical apparatus of the system is based on the digital image correlation methods (often referred to as DIC), by means of which the deformation of points of the sample surface is determined from the measured displacements. The advantage of the method lies in the fact that it is successfully applied to the study of the process of destruction of small-sized samples manufactured by the method of electric pulse consolidation.

Experiments were carried out at the NRNU MEPhI with the help of a testing machine and three-dimensional digital optical system Vic-

3D. Examples of the use of the DIC method during testing of small-sized disk samples of cast iron and graphite as model brittle materials, which are destroyed according to the "Brazilian test", are given. In addition, the effect of the sample size on resistance to destruction was investigated. The dependence of the strength of the tested materials on the degree of brittleness of the material was evaluated according to the formula recommended by the ASTM standard. The correction of the ASTM standard formula is proposed taking into account the character of the strain diagram of the sample loaded according to the "Brazilian test". The possibility of determination of the strength of materials obtained by electric pulse consolidation of powders is demonstrated. The processes and stages of destruction of test samples with different geometry and different types of loading were investigated. The test method of samples simulating nuclear fuel and obtained by sintering has been worked out using DIC method. Testing of models of fuel samples is carried out according to the scheme of "Brazilian test". The difference between fuel samples and solid disks is in the presence of a central hole in them. Calculation by the finite element method was used to compare the problems of the diametric compression of the disk sample with a central hole and without it. The dimensions of disks were assumed to be the same (a thickness of 4 mm, a diameter of 7.2 mm). The diameter of the central hole in one of the disks was 1.1 mm. The first and third principal and maximum shear stresses in both samples are compared. It is shown that the stress distribution in the loading zone for disk with hole and without it is close. Picture of stress for disk with hole is similar to a picture for disk without hole with perturbations introduced by the hub in the form of holes. The tensile stresses in the diameter plane of the hole are about five times higher than those in the solid disk. The destruction of both types of discs in the experiment occurs along a vertical diameter. The destruction of solid disk starts from contact zone and spreads to the center. In the disk with hole, a crack originates on the contour of the central hole at the intersection points with vertical diameter and propagates along this diameter until the sample is completely separated. The fracture stress for both types of samples is different. Samples of UO_2 fuel discs have been tested using the DIC method. Results of tests of samples of fuel and graphite as the fracture character and the level of strength showed good conformity. The

influence of modes of high-voltage electric pulse pressure on the structural and mechanical properties of the compact WNF 7–3 (90W–7Ni–3Fe) was investigated. It was shown that with increasing voltage of a high-voltage discharge, the tensile strength increases. The optimal mode of action was determined, at which the maximum level of strength and plasticity of the sintered material is ensured.

SHS METALLURGY OF CAST OXIDE MATERIALS

V. A. Gorshkov and P. A. Miloserdov

Merzhanov Institute of Structural Macrokinetics and Materials Science, Russian Academy of Sciences, Chernogolovka, Moscow, 142432 Russia

e-mail: gorsh@ism.ac.ru

In ISMAN, investigations of synthesis of cast oxide and oxynitride ceramics have been recently performed in the combustion regime via the SHS route [1–3]. This approach allows us to produce nitrogen-containing or oxide–oxide compounds and materials in the liquid (cast) state using thermite-type highly exothermic mixtures.

Oxynitride ceramics. In the present work, we attempted to synthesize cast aluminum oxynitrides by the following overall reaction schemes:

$$Fe_2O_3 + Al + AlN \rightarrow Al–O–N + FeAl \quad (1)$$
$$MoO_3 + Al + AlN \rightarrow Al–O–N + MoAl \quad (2)$$
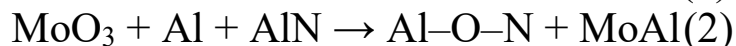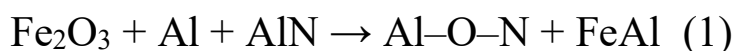
In the first case, Fe_2O_3/Al/AlN compositions added with AlN and Si_3N_4 can burn at the additive content no more than 50 wt %. In this region, after the initiation process, a combustion front formed propagates over the mixture. The combustion front velocity is determined by the content of additives. In the vicinity of the combustion limit, it is equal to 0.1–0.2 cm/s. At the AlN and Si_3N_4 content no more than 10 wt %, the combustion process yields cast products consisting of individual metallic and ceramic layers.

XRD analysis of the final cast oxynitride ceramics shows that the following main phases $Al_{2.81}O_{3.56}N_{0.44}$, $Al_8O_3N_6$, $Al_9O_3N_7$, and $Al_{2.78}O_{3.65}N_{0.35}$ can be synthesized depending on the experimental conditions. Optimization of synthesis conditions can contribute to the formation of a cast single-phase aluminum oxynitride $Al_{2.78}O_{3.65}N_{0.35}$.

For the second reaction, molybdenum (VI) oxide, aluminum nitride, and aluminum were used as raw materials. Optimal conditions

for obtaining the most stable phase Al_5O_6N from MoO_3/Al/AlN green mixture were determined. Green mixture (mass of 100 and 3000 g) was burned in quartz or graphite forms (d = 20–100 mm, mixture height was 50–250 mm) in SHS-reactors (3, 5 and 20 L in volume) under nitrogen initial pressure of 5 MPa. Since the combustion temperature in all experiments exceeded melting points of the products (Mo_xAl_y and Al_5O_6N), the process of separation took place. The combustion product was separated into two layers: Mo_xAl_y and Al_5O_6N. Al_5O_6N ingot (upper layer) was comminuted into powder with a grain size of to 150 μm and sintered by spark plasma sintering (SPS). In the experiments, the following optimal conditions of sintering were determined: T_s = 1850°C, a holding time of 10 min, a heating rate of 100°C/s, a cooling rate of 50°C/s, an external pressure of 40 MPa. Under these conditions, we prepared aluminum oxinitrides with a density of 3.61±0.01 g/cm^3, an average microhardness of 18.2±0.1 GPa, and a bending strength of 261±13 MPa.

Their phase composition corresponded to the initial powder composition. The results of the work show that initial pressure and ratio of components (α) are the main parameters affecting the microstructure and phase composition of the product. Optimal conditions were determined for SPS where high-strength compact ceramics with specified microstructure and phase composition of initial powders can be produced.

Oxide ceramics. We studied highly exothermic mixtures of chromium and aluminum oxides with zirconium oxide. Using thermodynamic calculations (Thermo program) and experiments carried out in the SHS-reactor under gas pressure, we determined the optimal conditions of synthesis and compositions of green mixtures to produce cast oxide materials with specified composition.

Materials based on corundum and chromium oxide are widely used in aerospace power engineering, microelectronics, and special ceramics and glasses. Zirconium oxide introduced into the solid solution of corundum crystallizes as a separate phase. Such composition seems promising for production of hard and crack-resistant ceramics. Previously, we reported on fabrication of cast Al_2O_3–Cr_2O_3 solid solutions by using the method of SHS metallurgy.

In this work, we explored the metallothermic SHS of Al_2O_3–Cr_2O_3–ZrO_2 cast materials through the following reaction route:

$$(CrO_3/Cr_2O_3/Al) + \alpha ZrO_2 \rightarrow CrAl + Al_2O_3–ZrO_2$$
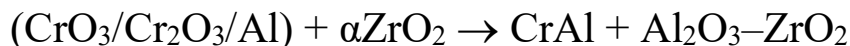
Preliminary thermodynamics calculations showed a rise in adiabatic combustion temperature (T_{ad}) from 3870 to 3370 K with increasing α (from 0 to 29 % wt). T_{ad} is seen to be above the melting point of products and starting reagents. With increasing α, the concentration of metallic phase decreased while that of ZrO_2 and oxide phase, increased.

Combustion was carried out in closed reactors (3, 20, and 30 L in volume) under inert atmosphere (Ar or N_2). Visual observation and video records showed stabilization of combustion front in 3–5 mm apart from the point of ignition. An increase in α led to a decrease in burning velocity U and combustion temperature T. Pressure increment ΔP remained constant for $\alpha < 5$ and then gradually declined. The output of the oxide phase exceeds the thermodynamically calculated one due to the presence of unreacted Cr_2O_3 in the oxide ingot.

In case of small charge (20 g), the product was found to contain considerable amount of CrAl that had no enough time to drift into the metallic ingot. To improve phase segregation, we used larger green samples (up to 1500 g) and raised T by increasing a fraction of heat-generating ingredient mixture Cr_2O_3 + Al.

1. V. A. Gorshkov, A. G. Tarasov. V. I. Yukhvid, Autowave synthesis of cast aluminum oxynitrides with a high nitrogen content, *Russ. J. Phys. Chem. B*, 2010, vol. 4, no. 2, pp. 304–307.
2. S. L. Silyakov, V. A. Gorshkov, V. I. Yukhvid, T. I. Ignat'eva, Effect of nitride additives (AlN and Si_3N_4) on the combustion of Fe_2O_3/Al mixtures and the formation of the chemical composition of the combustion products, *Russ. J. Phys. Chem. B*, 2013, vol. 7, no. 4, pp. 433–436.
3. V.A Gorshkov, P.A. Miloserdov, V.I. Yukhvid. Autowave synthesis of cast oxide ceramics Al_2O_3–$Cr_2O_3 \times ZrO_2$. *Inorg. Mater.: Appl. Res.*, 2016, vol. 7, no. 6, pp. 791–795.

INNOVATIVE SOLUTION IN THE AREA OF MANUFACTURING MULTILAYERED COMPOSITE MATERIALS BY EXPLOSION WELDING FOR THE ATOMIC, CHEMICAL, OIL AND GAS INDUSTRY

V. A. Grachev[1], A. E. Rozen[2], A. V. Dub[3], Yu. P. Perelygin[2], I. A. Safonov[3,4], A. E. Korneev[4], I. L. Kharina[4], S. Yu. Kireev[2], A. A. Rozen[2,5], and N. N. Ratsuk[3]

[1] Frumkin Institute of Physical Chemistry and Electrochemistry, Russian Academy of Sciences, Moscow, 119071 Russia
[2] Penza State University, Penza, 440026 Russia
[3] National University of Science and Technology MISIS, Moscow, 119049 Russia
[4] RF State Research Centre JSC RPA CNIITMASH, Moscow, 115088 Russia
[5] ROMET Ltd (Skolkovo Innovation Center), Moscow, 143026 Russia

e-mail: aerozen@bk.ru

On a global scale corrosion losses amount to 4–6% of the national income in the developed countries. The losses related to failure of a structure, process shutdown, depressurization of an equipment, cause greater economic and ecological detriment. For this reason, the methods of corrosion prevention need to be improved and new corrosion resistant materials and products need to be developed. The problem of corrosion resistance is especially acute for the atomic, chemical, energy, oil and gas industry. The using of traditional high-alloy steels with an increased chrome and nickel content, first, considerably increases the cost of such materials. Second, it provokes intensive growth of corrosion pits (pitting), the depth of which may reach up to 10 mm per year. One of the ways to solve this problem is using a new class of multilayered composite materials (MCMs) with an internal protector that was created by the group of authors. Preliminary results from the laboratory studies show the possibility of multiple increasing in a resource in comparison with traditional

materials. The main methods of manufacturing MCMs with an internal protector are considered. These include pack rolling, explosion welding (EXW), combination of explosion welding and rolling (EXW + R), arc welding, electroslag welding, gas dynamic spraying, thermal spraying, electroplating and additive layer-by-layer manufacturing. Advantages, disadvantages, limitations on the use and cost of these technologies are considered. EXW and combinative technology (EXW + R) are most efficient and cost-effective methods of producing MCMs. In the area of nuclear power, the creation of systems of the pressure head and controlled special sewerage of the complex of protective cameras (CPC) made of MCMs with an internal protector are carried out by the Institute of Nuclear Materials, State Research Center RPA CNIITMASH, Penza State University, ROMET Ltd. The use of MCM will lead to an increase in a serviceable life of radioactive waste treatment systems by 12 times. The entire range of works is planned (the development of design documentation, approval in the State Atomic Energy Corporation ROSATOM and the Federal Environmental, Industrial and Nuclear Supervision Service of Russia). Complete replacement of CPC is intended. The highest losses from corrosion occur in the chemical industry. The equipment is operated in alkalis and acids, in environments with a high content of halides and in a wide range of temperatures and pressures. The possibility was established when using MCM with an internal protector to reduce the stops for current and capital repairs by 11 and 8 times, respectively. The resource of operation of a wide range of technological equipment is determined. In connection with the development of new fields and the extraction of gas and oil from greater depths, the corrosive activity of oilfields environments increases. Therefore, operating time of production tubing (assembled from oil-well tubing) has significantly decreased. The main cause of premature failure is corrosion-mechanical destruction caused by increased aggressiveness of the extracted fluid. It is established that seamless pipes can be produced of MCMs with an inner protector, the service life of which can be increased by 10 times or more. It is shown that the corrosion resistance of composite material is in one segment with tantalum and platinum, and in the price segment — at the level of traditional chromium-nickel stainless steels. Its consumer value can be multiplied.

PULSED HIGH-VOLTAGE WELDING OF MAGNETIC CORES FROM MAGNETICALLY SOFT ALLOY

E. G. Grigor'ev[1], V. Yu. Goltsev[2], V. S. Kashirin[2], A. V. Osintsev[2], K. Yu. Ochkov[2], A. S. Plotnikov[1,2], and A. V. Yudin[2]

[1] Merzhanov Institute of Structural Macrokinetics and Materials Science, Russian Academy of Sciences, Chernogolovka, Moscow, 142432 Russia
[2] National Research Nuclear University MEPhI, Moscow, 115409 Russia

e-mail: eugengrig@mail.ru

This research analyses the influence of the parameters of high-voltage electric pulse welding on the microstructure of weld seams and mechanical parameters of samples. Special tooling was developed for the process of high-voltage electric pulse welding, allowing welding of ring samples. The method of determination of mechanical characteristics of toroidal samples was developed. The influence of parameters of high-voltage electric pulse welding, such as current density and applied pressure, on the microstructure of a weld seam and density of a weld joint is established. The study of magnetic parameters of samples is conducted.

The high-voltage pulse welding method uses special high-voltage process equipment, which allows providing controlled pulse electric power impact on the joined parts. This equipment has been designed and created in the interdepartmental laboratory of advanced technologies for creation of new materials for implementing advanced electric pulse technologies of development of new materials and products made them with unique structure and properties unattainable by other methods. A more detailed description of the equipment can be found in [1–3]. The objective of this paper is to investigate the influence of technological parameters of the high-voltage electric pulse welding (current pulse amplitude and applied pressure) on the joint efficiency of the elements in the reference samples, to compare

the characteristics of magnetic circuits made of thin rings of soft magnetic alloy 49K2FA with characteristics of the glued magnetic cores.

The study of magnetic properties of the samples showed that with this method of joining rings into the magnetic core there is no deterioration of the magnetic characteristics of the material. E.g. for the sample produced by two pulses with an amplitude of 4.0 kV, the following magnetic characteristics were obtained: B = 2.26 T, H_c = 50 A/m, μ = 15000 G/Oe.

The method of bend testing of annular samples produced by pulsed high-voltage resistance welding of a packet of thin annular sheets made of 49K2FA alloy is described. The ring is loaded with a compressive force applied to the plane of the ring. The results of tests of four annular samples with the simultaneous application of the method of digital correlation of the images for recording the displacement field and visualizing the strain fields in the loaded object are presented. The test results indicate that the samples separate into individual elements prior to failure with the loss of stability in the stage of elastoplastic loading. The possibilities of reaching a relatively high level of strength and resistance to delamination in the elastic loading stage are indicated. The problem of bending of the ring is solved by the finite element method using an ANSYS program. It is shown that the experimental results and numerical analysis data are in good agreement.

1. E. G. Grigoryev, V. N. Bazanov, Electric current pulse welding of titanium VT1-0 with stainless steel 12X18H10T, *Moscow State University of Education J.: Natural Sciences*, 2008, no. 2, pp. 84–88.
2. E. G. Grigoryev, V. N. Bazanov, Electric current pulse welding of titanium with 18–10 stainless steel, *Adv. Mater. Res.*, 2010, vols. 83–86, pp. 1251–1253.
3. E. G. Grigoryev, Welding of titanium with stainless steel by high-voltage electric-current pulse, *Proceedings of the 2011 International Conference on Powder Metallurgy and Particulate Materials*, 2011, pp. 642–646.

E. G. Grigor'ev et al.

EXPLOSION WELDING OF Al + Cu BIMETALLIC JOINTS FOR ELECTRICAL CONTACTS

R. D. Kapustin, I. V. Denisov, and I. V. Saikov

Merzhanov Institute of Structural Macrokinetics and Materials Science, Russian Academy of Sciences, Chernogolovka, Moscow, 142432 Russia

e-mail: kapustin-roman@mail.ru

The manufacture of aluminum + copper electrically conducting bimetallic materials for electrical contacts and adapters by explosion welding was investigated.

Materials for electric contacts for the production of adapters should have high electrical and heat conductivity and low and stable contact resistance. The electrical contacts of bimetallic adapters are based on copper and aluminum. Explosion welding differs from other methods of production of bimetals in that the joint forms as a result of high-speed collision of the metals and the acceleration and displacement of the welded elements take place under the effect of the expanding explosion products.

Explosion welding is accompanied by the heating of welded surfaces with impact-compressed gases formed in the gap between the welded materials. The strength of the joint in explosion welding is higher than that of the individual components of the bimetal.

The production of the copper + aluminum bimetallic adapters by explosion welding is characterized by the fact that no liquid phase forms at the joint boundary. This minimizes the formation of intermetallic compounds and, consequently, results in sufficiently high shear and bending strength and high electrical conductivity of the produced bimetal. This is the result of using a low-speed explosive based on the mixture of microporous ammonium nitrate and oil fuel (ANFO). However, this explosive may damage the surface of the

cladding layer, leaving 1–2-mm indentations equal to the diameter of the granules of ammonium nitrate.

The aim of the present work is the development of a method of producing an Al + Cu bimetal with no surface defects and intermetallic compounds in the welded joint using an explosive substance based on microporous ammonium nitrate with diesel fuel. The following sheets were used in experiments to produce bimetallic adapters: copper sheets (grade M1, 2 × 150 × 300 mm) and aluminum sheets (grade AD1, 2 × 150 × 300 mm).

The explosive used in the experiments was a mixture of microporous ammonium nitrate with oil fuel (ANFO) with a volume ratio of 96:4. The surface of the cladding layer (copper) was protected against mechanical damage by detonation products using a following damping layer:

– bituminous mastic with a thickness of 1.5 mm;
– milled ammonium nitrate with the thickness of 2 mm.

After explosion welding, the experimental procedure included the heat treatment of the produced bimetal in a muffle furnace (heating to a temperature of 200°C, holding for 1 h) to relieve the internal stresses. The heat treatment conditions were selected to avoid the formation of intermetallic phases in the Al + Cu joint at the given temperature.

The following conclusions can be made based on the experimental results:

(1) The explosion welding parameters using the ANFO in producing the electrically conducting M1 + AD1 bimetallic material with a large area, resulting in the absence of the intermetallic compounds at the interface, were determined.

(2) The results show that the presence of the damping layer with a thickness smaller than 1.5 mm protects the cladding layer against the mechanical damage by the products of detonation of explosive substance consisting of ANFO.

(3) The experimental results also show that the strength characteristics of the welded joint in the bimetal are similar to the properties of the initial material (aluminum); the results show that the specific electrical conductivity of the M1 + AD1 bimetal without heat treatment is higher than that of the identical bimetal after heat treatment and of aluminum.

MATHEMATICAL MODELING OF NON-STATIONARY HEAT PROCESSES DURING FREE SHS COMPRESSION OF MATERIALS

S. V. Karpov[1], A. M. Stolin[2], L. S. Stelmakh[2], and A. O. Glebov[1]

[1] Tambov State Technical University, Tambov, 392000 Russia
[2] Merzhanov Institute of Structural Macrokinetics and Materials Science, Russian Academy of Sciences, Chernogolovka, Moscow, 142432 Russia

e-mail: karpov.sv@mail.tstu.ru

The development of self-propagating high temperature synthesis (SHS) is related to research of possibilities of formation of combustion products [1]. The general regularities of formation of SHS-materials have not been sufficiently studied that is rather important upon development of efficient methods for manufacturing products with complex shape. For the examination of ability to formation of some common class of materials, free SHS compression method was proposed [2]. It is the compaction and formation of material under high temperatures (10^3 K) and external pressure (10–100 MPa) in conditions of uniaxial compression.

Experimental study showed that the method despite its simplicity allow to obtain macro layered gradient materials, platens and plates as well as to apply the coatings on metal surfaces. The advantage of the method is the use of the most favorable stress state and high-temperature shear plastic deformation condition that promotes healing of macro cracks and pores in deformed material.

The method of free SHS compression is promising, therefore, it deserves a detailed research on the base of mathematical modeling. That approach is especially important for the SHS processes distinguished by rigid conditions. The purpose of research is development of thermal models for quantitative and qualitative description of non-stationary heat exchange of hot powder materials

during the free SHS-compression as well as offering recommendations for optimization of thermal processes.

The cylindrical sample located on a cylindrical plate of given height was considered as a computational geometric model. In some particular cases, the heater of a squared section of a predefined power was located in a plate. Pressing of material was performed after its combustion and following exposure with the help of cylindrical plunger moved downward with a constant specified speed. Therefore, the task was formulated in a cylindrical coordinate system.

For the modeling of moving combustion front it is suggested to realize a partition of a sample to n elementary cylinders. First, order boundary conditions (combustion temperature) were set on boundaries of elementary cylinders. Thus, during combustion front passage appropriate boundaries of layers are "ignited". Thereby a serial combustion of material layers is imitated. Partition of a sample on cylinders was implemented according to recommendations of [3] to provide a passage of combustion wave within the time range of 0.2–0.5 s.

The process of free SHS compression of hot powder materials included stages of combustion of initial mixture and exposure. It should be noted that these stages took place without plunger of a press. The following stage of compression of material assumes direct contact between plunger and material. Special boundary condition of thin thermally resistive layer was applied for taking into account that peculiarities during non-stationary heat processes.

Vertical boundary speed of material V_r during the time is an important topic. The value of V_r can be specified experimentally or analytically. The first approach is described in [4] and based on an assumption of linear dependence between height of material and its density during the constant speed of plunger. In this paper, the values of V_r were found experimentally (Fig. 1).

The finite element method is accepted for theoretical analysis of the forming processes. From the basics of mechanics of continua, it is known that there are different ways of representation of moving particles of matter according to different reference frame. In this paper, an arbitrary Lagrangian–Eulerian formulation [5] is used for modeling large plastic deformations of free SHS compression. By

using of this approach the finite element mesh nodes are moving by specified path that provides possibility of continuous mesh rebuild.

Temperature curves (°C) of different layers of sample, plate and plunger during combustion (0–9 s), exposure (9–10 s), pressing (10–12.5 s), and cooling (12.5–17.5 s) are shown in Fig. 2.

Numerical simulation showed that the use of heating plates provides compensation for heat loss of material. Temperature gradients in the bulk of material at any stage of SHS are decreased. Therefore, the use of heating plates for SHS management is a promising direction.
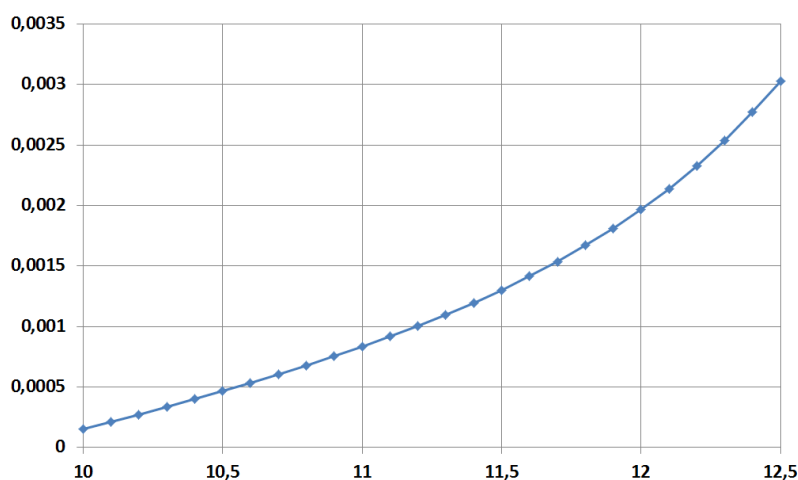
Fig. 1. Experimental time dependence of the vertical boundary speed.
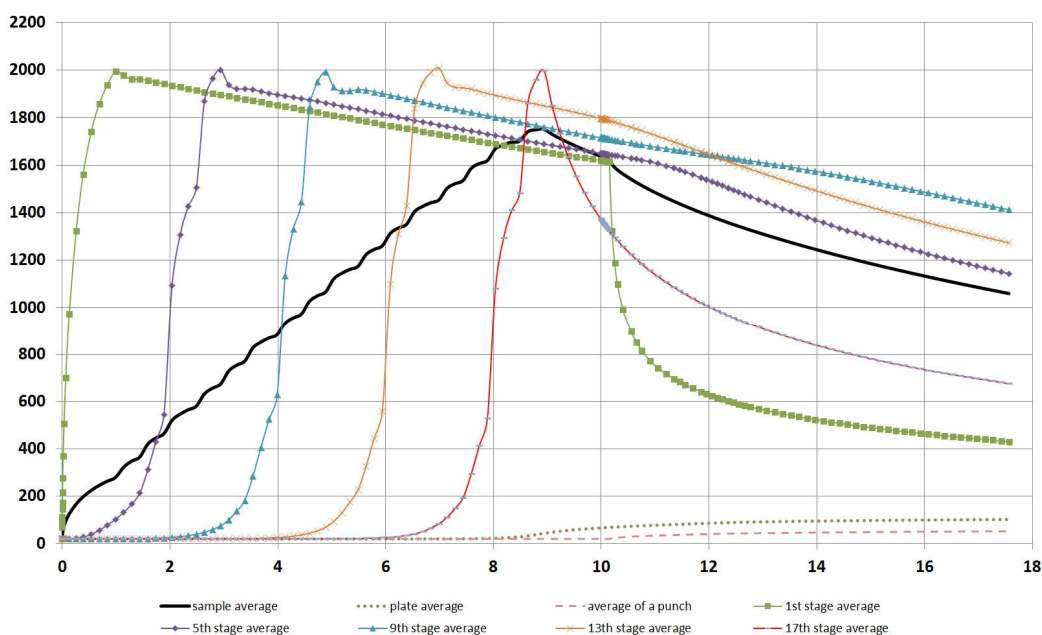
Fig. 2. Calculated temperatures (°C) of material layers, plate and plunger.

1. P. M. Bazhin, A. M. Stolin, V. V. Sarantsev, Study of the formability of composite nanoceramics, *Vopr. Sovrem. Nauki i Prak.: Universitet im. V.I. Vernadskogo*, 2012, no. 43, pp. 51–56 (in Russia).
2. A. M. Stolin, V. V. Kozlov, A. V. Kalugin, Processes of forming products of combustion by the method of free SHS-compression, *Dokl. Akad. Nauk.,* 1999, vol. 366, no. 2, pp. 225–227.
3. A. P. Amosov, A. F. Fedotov, Finite-element plane model of thermal conditions in self-propagating high-temperature synthesis of blanks in a friable shell, *J. Eng. Phys. Thermophys*, 2001, vol. 74, no. 5, pp. 160–166.
4. S. V. Karpov, et al. Mathematical modeling of material pressing with regard to its compaction, *Virtual modeling, prototyping and industrial design*. Tambov, 2017. P. 560–565 (in Russia).
5. P. V. Borovik, D. A. Usatyuk, *New approaches to mathematical modeling of technological processes of pressure treatment*, Alchevsk, 2011 (in Russia).

BASIC MODELS OF VOLUME SYNTHESIS OF Ti-BASED COMPOSITES

A. G. Knyazeva[1,2]

[1] Institute of Strength Physics and Materials Science, Siberian Branch, Russian Academy of Sciences, Tomsk, 634055 Russia
[2] Tomsk Polytechnic University, Tomsk, 634050 Russia

e-mail: anna-knyazeva@mail.ru

The volume synthesis or the synthesis in the explosion mode obeys some preference in comparison with the mode of layerwise combustion, since there is the most homogenization of synthesized product in a first situation and it is possible to control the process by means of the change in the thermal contact conditions of the reacting system with the environment and with the heater. This process can be controllable when the initial mixture composition is varied, inert particles are used as admixtures; the heating rate and the heating way are changed; external mechanical loading is applied [1–5].

In the case of thermal explosion mode, the reactions happen in the volume homogeneously or not very homogeneously and are accompanied by high heat release that diminishes due to inert admixtures or due to non-stoichiometrical initial composition. The final composition of the synthesis product turns out irreversible and depends on numerous factors. The reagent dispersion, admixture presence, initial porosity, heating way, pressing size and geometry, and etc. belong to important factors. To develop the models allowing to predict the irreversible composition of the synthesis product the various synthesis conditions were analyzed and a series of basic models was suggested taking into account the staging of the conversion. The titanium-based composites synthesized from non-stoichiometric mixtures Ti (+Al) + C, B, Si with titanium excess were chosen for investigation.

(1) The simplest model [6] corresponds to the pressing of small size when temperature distribution absents. In this approximation correspondingly to classical notions, it is assumed that only one reaction takes a place in these systems with formation of final products TiC, TiB$_2$, and Ti$_5$Si$_3$ that corresponds to summary reaction scheme

$$\text{Reagent} \rightarrow \text{Product}$$
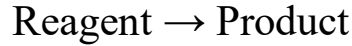
In contrast to classical works, we believe that the melting is observed in some temperature interval between the solidus and liquidus temperatures, where the liquid phase part changes with some kinetical law. The pressing heating is carried out by radiant heat from vacuum chamber walls (from the heater). The cheating rate is controlled by heater temperature T_W and by the rate of this temperature change to some given value. The law of porosity change is given also.

(2) When the staging of chemical conversion is taken into account, the mathematical model is added by kinetical equations corresponding to reaction scheme. For example, in the system Ti + C following reactions [7] are possible

$$\text{Ti} + \text{C} \rightarrow \text{TiC}; \ 2\text{Ti} + \text{C} \rightarrow \text{Ti}_2\text{C}; \ \text{Ti} + \text{TiC} \rightarrow \text{Ti}_2\text{C};$$
$$\text{Ti}_2\text{C} \rightarrow \text{TiC} + \text{Ti}; \ \text{Ti} + 2\text{C} \rightarrow \text{TiC}_2 ; \ \text{TiC} + \text{Ti}_2\text{C} \rightarrow \text{Ti}_3\text{C}_2;$$
$$\text{Ti} + \text{C} + \text{Ti}_2\text{C} \rightarrow \text{Ti}_3\text{C}_2; \ \text{TiC}_2 + \text{Ti} \rightarrow 2\text{TiC}; \ \text{Ti}_3\text{C}_2 \rightarrow \text{Ti}_2\text{C} + \text{Ti}.$$
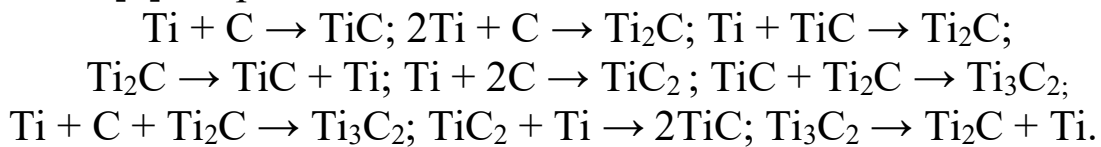
Aluminum addition complicates the reaction scheme.

As a rule, the residual oxygen presets in the chamber or in the powder mixture, hence the composite synthesis is accompanied by oxide phase formation. As a result, the irreversible composition is obtained and it can change during disintegration (when composite powders are made) and during following sintering in the labor vacuum chamber, on the surface of solid substrate or in the melting pool where the composite powder is supplied in the technologies of surface treatment or three-dimensional objects creation with laser or electron beam energy application. Taking into account the temperature distribution along the pressing thickness, it allows analyzing the role of not uniform heating or not uniforming initial composition in the dynamics of the synthesis. However, non-stoichiometric composition does not guarantee the explosion mode for the synthesis.

(3) Composite synthesis can be carried out in closed volume or in the container with walls of finite thickness. On the one hand, the walls

demand the additional heat for the heating to given temperature; on the other hand, the walls store the heat supporting the synthesis when the external heating is ceased or chemical heat release is not enough for reaction accomplishment. In this case, closed reactor walls exchange the heat with the heater immediately. Kinetical part of the problem is similar to previous one. The dynamics of this process is illustrated in [8] for the system Al, Fe_2O_3, Fe, Cr, and Ni. The explicit accounting the inert admixtures in the reacting composition leads to the specific degenerate mode appearance [9]. The features appear in the Ti-based system also.

(4) The combination of the heating with the mechanical loading, for example, at the conditions of HIP (hot isostatic pressing) or SPS (spark plasma sintering), allows obtaining high-density product with special properties. The dynamics of the synthesis depends in this case on a more number of parameters. Mathematical model takes into account the different ways of the heating, including Joule heating in the volume, the plunger heating, the heating through reactor walls, and symmetrical and non-symmetrical conditions of the loading. The synthesis mode depends additionally on geometrical parameters of the reactor. Various modifications of the model were described in [10–12]. Similar conditions can lead to irreversible composition of the product. However, powders obtaining in this case is a problem.

1. V. V. Barzikin, Thermal explosion under linear heating, *Combust. Explos. Shock Waves*, 1973, vol. 9, no. 1, pp. 29–42; DOI: 10.1007/BF00740358.
2. A. G. Merzhanov, B. G. Barzikin, V. G. Abramov, Theory of thermal explosion: from Semenov to our days, *Chimich. Fiz.* [*Chem. Phys.*], 1996, vol. 15, no. 6, pp. 3–44. (in Russian).
3. V. V. Evstigneev, E. V. Smirnov, A. V. Afanasev, et al. Dynamical thermal explosion in mechanically activated pow-der mixtures, *Polzunovskiy Vestinik* [*The bulletin of Polzunov*], 2007, no. 4, pp.162–167 (in Russian).

4. E. A. Levashov, A. S. Mukasyan, A. S. Rogachev, D. V. Shtansky, Self-propagating high-temperature synthesis of advanced materials and coatings, *Int. Mater. Rev.*, 2017, vol. 62, no. 4, pp. 203–239.

5. A. M. Stolin, A. G. Merzhanov, Critical conditions of thermal explosion in the presence of chemical and mechanical heat sources, *Combust. Explos. Shock Waves*, 1971, vol. 7, no. 4, pp. 431–437.

6. Y. Kukta, A. G. Knyazeva, Modeling of composite synthesis at the conditions of controlled thermal explosion, *AIP Conf. Proc.*, 2017, vol. 1909, P. 020113; DOI.org/10.1063/1.5013794.

7. A. G. Knyazeva, E. N. Korosteleva, O. N. Kryukova, G. A. Pribytkov, Yu. A. Chumakov, Physical regularities of titanium-based composite powder synthesis for additive manufacturing technologies, *Russ. Inter. J. Ind.. Eng.*, 2017, vol. 5, no. 4, pp. 3–13 (in Russian).

8. A. G. Knyazeva, N. Travitzky, Modeling of exothermic synthesis of composite with oxide inclusions, *MATEC Web Conf.*, 2017, vol. 115, pp. 04004; DOI: 10.1051/matecconf/201711504004.

9. A. G. Knyazeva, A. A. Chashchina, Numerical study of the problem of thermal ignition in a thick-walled container, *Combust. Explos. Shock Waves*, vol. 40, no. 4, pp. 432–437.

10. S. N. Sorokova, A. G. Knyazeva, Modeling of intermetallide synthesis on the substrate of cylindrical form, *Phys. Mesomech.*, 2009, vol. 12, no. 5, pp. 77–90.

11. A. G. Knyazeva, S. N. Sorokova, Modelling of powder consolidation using electro heating assisted by mechanical loading, *J. Phys. Conf. Ser.,* 2017, vol. 790, no. 1, 012012; DOI:10.1088/1742-6596/790/1/012012.

12. A. G. Knyazeva, S. P. Buyakova, Mathematical model of three-layer composite synthesis during hot isostatic pressing, *AIP Conf. Proc.*, 2016, vol. 1783, 020092.

MONOCLINIC BORON CARBIDE FROM SHS

S. V. Konovalikhin[1], V. I. Ponomarev[1], D. Yu. Kovalev[1], and S. A. Guda[2]

[1] Merzhanov Institute of Structural Macrokinetics and Materials Science, Russian Academy of Sciences, Chernogolovka, Moscow, 142432 Russia
[2] Southern Federal University, Rostov-on-Done, 344090 Russia

e-mail: ksv17@ism.ac.ru

Boron carbide is a suitable material for many high performance applications such as nuclear industry, armor for personnel and vehicle safety, rocket propellant, etc. [1–3]. The methods of boron carbide synthesis are carbothermic reduction, synthesis from elements, vapour phase reactions, hot isostatic pressure, spark plasma sintering, etc. [2, 4]. The most widely accepted crystal structure of boron carbide is hexagonal (sp. gr. $R\bar{3}m$ no. 166). Figure 1 shows the crystal structure of hexagonal boron carbide.

Boron carbide prepared by SHS of stoichiometric mixture of B_2O_3, Mg, and C has been studied. It has been established that boron carbide crystals are hexagonal [5–7] and monoclinic (table, Figs. 2, 3) [8, 9]. Monoclinic boron carbide crystals were discovered for the first time. Among other synthesis methods, no monoclinic boron carbide crystals is found.

According to the X-ray diffraction data, hexagonal and monoclinic crystals of boron carbide have almost the same structures (Figs. 1–3) [9]. They differ by the icosahedron structure. There is no 3-fold axis in monoclinic crystal. The distortions in icosahedron structures lead to the appearance of reflections, which should be extinguished in hexagonal crystals. However, the differences are apparent only upon X-ray diffraction study of single crystals. Therefore, the X-ray diffraction patterns of monoclinic and hexagonal crystals are the same (Fig. 4).
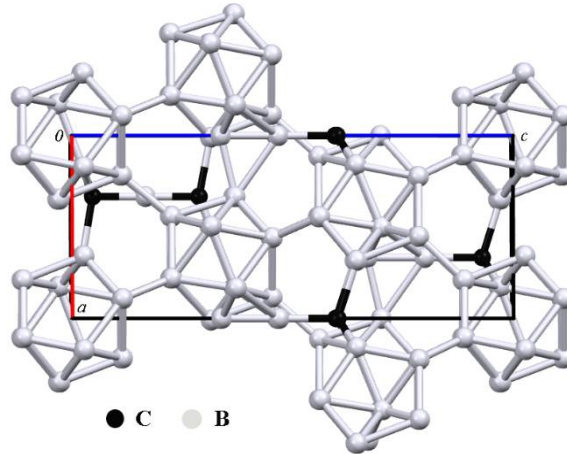
Fig. 1. Crystal structure of hexagonal boron carbide.

Parameters of monoclinic and hexagonal boron carbide prepared by SHS.

Parameters	1	2	3	4	5
Ref	[7]	[8]	[9]	[6]	[6]
Composition	$B_{11.4}C_{3.6}$	$B_{12}C_3$	$B_{12.7}C_{2.3}$	$B_{13}C_2$	$B_{12}C_3$
a, Å	5.594(1)	8.668(1)	8.746(1)	5.623(1)	5.604(1)
b, Å	5.594(1)	5.162(1)	5.625(1)	5.623(1)	5.604(1)
c, Å	11.977(2)	5.596(2)	13.592(2)	12.255(2)	12.079(1)
α, deg	90	90	90	90	90
β, deg	90	90	94.38(1)	90	90
γ, deg	120	60.43(2)	90	120	120
V, Å³	324.5(2)	217.8(3)	666.7(3)	337.1(3)	328.5(1)
Space group	$R\bar{3}m$	$B2/m$	$C2/m$	$R\bar{3}m$	$R\bar{3}m$
n^*	141	94	282	141	141

n^* is the number of valence electrons in the unit cell.
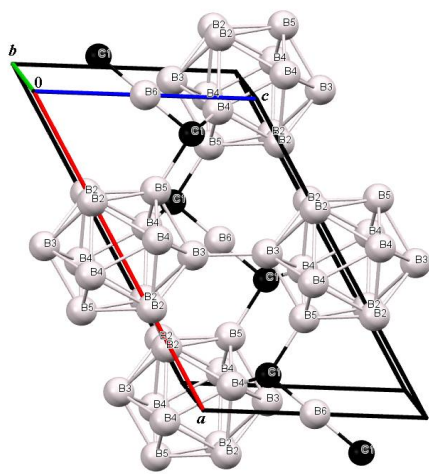
Fig. 2. Crystal structure of crystal *2*.
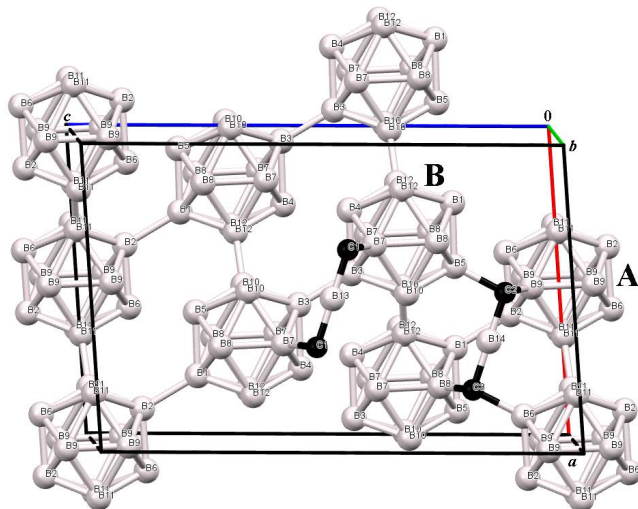
Fig. 3. Crystal structure of crystal *3*.
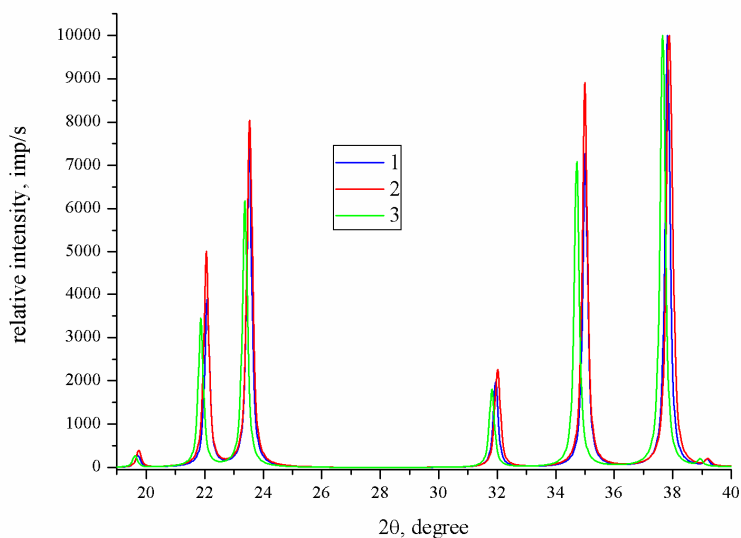
Fig.4. X-ray diffraction patterns of crystals *1–3*.

We used the density functional theory based on VASP to calculate the total energies (ε_{total}) of crystals *1–3*. We constructed a variety of 3 x 3 x 3 supercells. The aim of calculations was to compare ε_{total} of hexagonal and monoclinic crystals. The unit cells of crystals *1–3* have different numbers of atoms. Therefore, a ratio of ε_{total}/n is used for comparison. It has been found that ε_{total} of crystals *1–3* are the same and equal to 51.9, 51.9 and 52.0 kcal/mol, respectively.

Monoclinic crystal was prepared by SHS method. The SHS method is characterized by high (~ 100 deg/s) rates of the cooling of the melt. It is possible that thermodynamically unstable intermediate structures were formed and retained. The other methods of synthesis have smaller cooling rates (~ 100 deg/h) [4]. Under such conditions, the thermodynamic unstable structures were transformed.

Thus, monoclinic boron carbide crystals prepared by SHS are first discovered. The formation of monoclinic boron carbide crystals can be caused by the condition of reaction.

1. F. Thevenot, Boron Carbide − a Comprehensive Review, *J. Eur. Ceram. Soc.*, 1990, vol. 6, no. 1, pp. 205−225.
2. V. Domnich, S. Reynaud, R. A. Haber, M. Chhowalla, Boron Carbide: Structure, Properties, and Stability under Stress, *J. Am. Ceram. Soc.*, 2011, vol. 94, no.11, pp. 3605−3628.
3. H. Werheit, Boron carbide: Consistency of components, lattice parameters, fine structure and chemical composition makes the

complex structure reasonable, *Solid State Sciences*, 2016, vol. 60, pp. 45.

4. A. K. Suri, C. Subramanian, J. K. Sonber, T. S. R. Ch. Murthy, Synthesis and consolidation of boron carbide: a review, *Intern. Mat. Reviews,* 2010, vol. 55, no. 1, pp.4−40.

5. V. I. Ponomarev, I. D. Kovalev, S. V. Konovalikhin, V. I. Vershinnikov, Ordering of carbon in boron carbide, *Crystallography*, 2013, vol. 58, no. 3, pp. 420−425 [in Russia].

6. I. D. Kovalev, V. I. Ponomarev, V. I. Vershinnikov, S. V. Konovalikhin, SHS-produced boron carbide: special features of crystal structure, *Int. J. Self-Propag. High-Temp. Synth.*, 2012, vol. 21, no. 2, pp. 134–138.

7. S. V. Konovalikhin, V. I. Ponomarev, Carbon in Boron Carbide: The Crystal Structure of $B_{11.4}C_{3.6}$, *Rus. J. Inorg. Chem.*, 2009, vol. 54, no. 2, pp. 197–203.

8. A. S. Shteinberg, V. A. Raduchev, V. V. Denisevich, V. I. Ponomarev, S. S. Mamyan, I. A. Kanayev, Boron Carbide Single Crystal Growing Using Direct High-Frequency Melting in Cold Vessel, *Dokl. Akad. Nauk. SSSR*, 1991, vol. 317, no. 2, pp. 370–374.

9. S. V. Konovalikhin, V. I. Ponomarev, G. V. Shilov, I. D. Kovalev, Monoclinic boron carbide crystals, *Russ. J. Struct. Chem.*, 2017, vol. 58, no. 8, pp.1694–1700.

THE INFLUENCE OF THE HEAT LOAD ON THE MICROSTRUCTURE AND MECHANICAL PROPERTIES OF CHOSEN NIOBIUM-CLAD STEELS AND NICKEL ALLOYS OBTAINED BY EXPLOSIVE WELDING

R. Kosturek[1,*], M. Wachowski[1], L. Śnieżek[1], and A. Gałka[2]

[1] Military University of Technology, Faculty of Mechanical Engineering
[2] EXPLOMET High-Energy Techniques Works

*e-mail: robert.kosturek@wat.edu.pl

This study presents the results of the research on the effects of the heat treatment and utilization in high temperature on chosen niobium-clad plates. During this research, niobium plates have been successfully explosively welded with three different alloys: stainless high-temperature steel, non-alloy steel and inconel alloy. The ANFO-base explosive material used in the explosive welding process had detonation velocity about 2200 m/s. The obtained bimetal plates have been subjected to the different types of the heat treatment: stress-relief annealing ($610°C/2$ h) and normalizing ($910°C/40$ min). In order to examine the influence of the heat treatments on the properties of the obtained joints the mechanical testing and microstructure analysis have been performed. Additionally, the properties of niobium/inconel alloy and niobium/stainless high-temperature steel have been examined in the state after utilization ($400°C/200$ h). The microstructure of the joints has been investigated using scanning electron microscope. The quality of joint was established in the peel test. It has been stated that obtained joints have characteristic wavy shape and low participation of the melted zones. The examples of the images of niobium–steel joint interface (left) and melted zone (right) are shown below (Fig. 1).
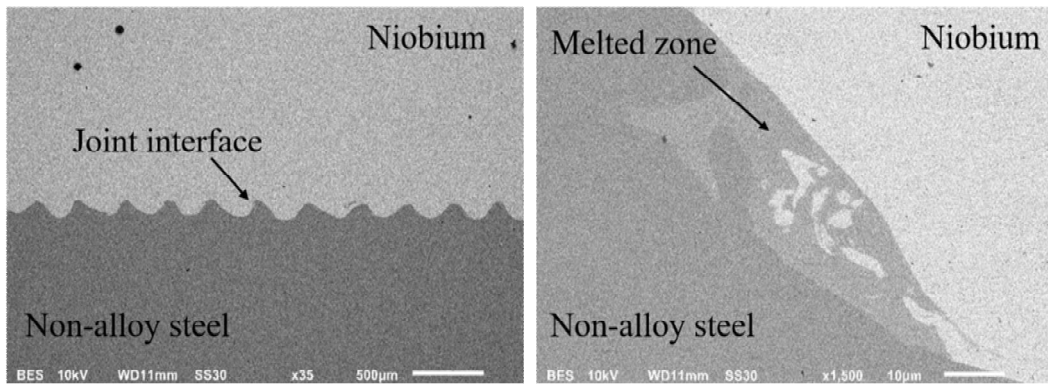
Fig. 1. Niobium–steel joint interface and the melted zone.

The very important aspect of this research was to identify the reason of the huge decrease in the strength of niobium–inconel alloy joint after utilization ($400°C$ / 200 h). The results of the peel test indicate as the effect of the utilization the peel strength of niobium–inconel alloy joint decreases by about 70% (as-welded state: 320 MPa, after utilization: 98 MPa). The images of niobium–inconel alloy joint interface after utilization are shown below (Fig. 2).
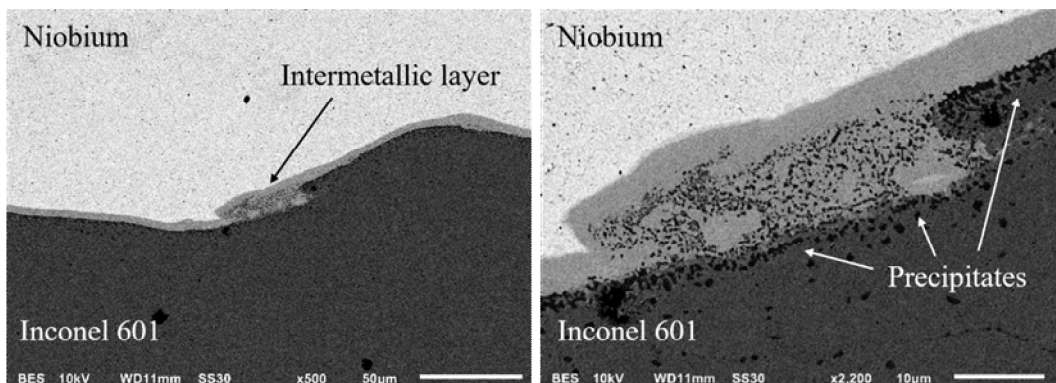
Fig. 2. Niobium–inconel joint interface after utilization.

The analysis of the chemical composition shows the present of the intermetallic phases and chromium-rich precipitates in the joint zone. The results of the line scan of chemical elements (left) and the elemental mapping (right) are shown below (Fig. 3).

It has been stated that heat load-activated changes have been caused by diffusion of niobium, nickel and iron through the joint interface. The precipitates and intermetallic phases have been defined as the main reason of the decrease in the strength of the niobium–inconel alloy joint. All types of the joints subjected to the heat treatment in this investigation was similarly analyzed in terms of changes in their chemical composition (diffusion, precipitates,

intermetallic phases). The obtained results have allowed to describe accurately the relations between changes in the joint microstructure and its mechanical properties (peel strength). The heat treatment of the niobium-clad plates could have negative influence on the quality of joint, especially in the case of the bond with nickel-rich alloys, due to tendency for intermetallic phase formation between niobium and nickel.
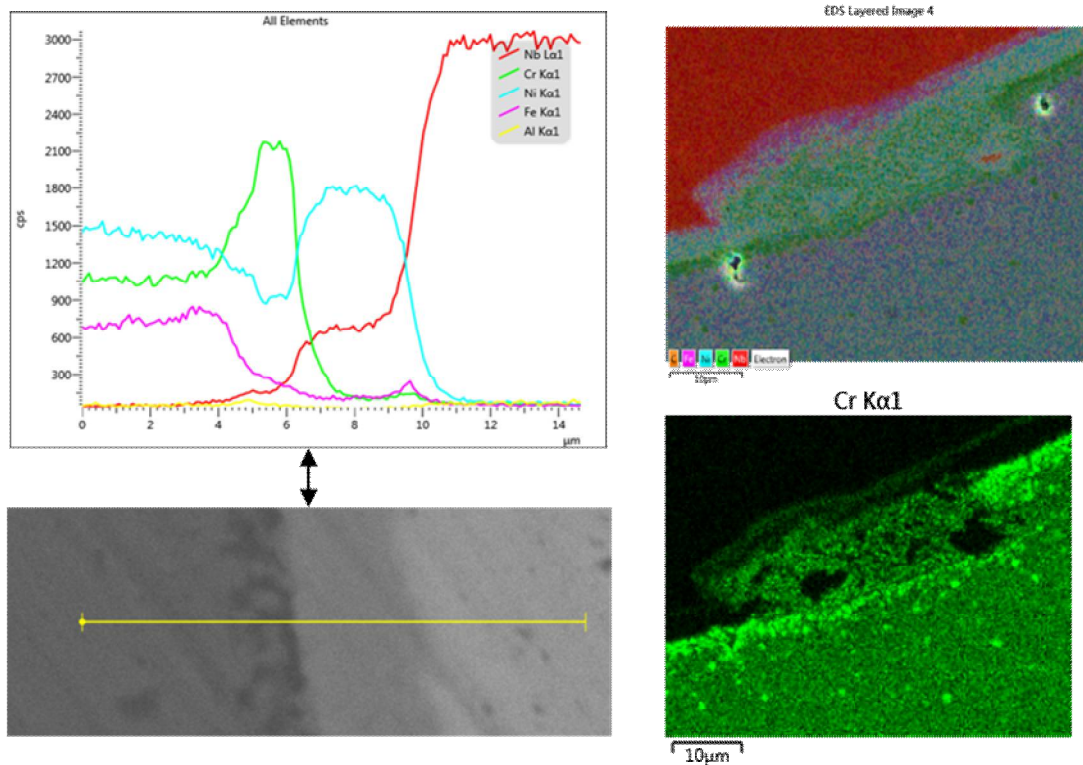
Fig. 3. The results of the analysis of the chemical composition of niobium–inconel joint interface after utilization.

DIAGNOSTICS OF SHS: TIME RESOLVED X-RAY DIFFRACTION METHOD

D. Yu. Kovalev and V. I. Ponomarev

Merzhanov Institute of Structural Macrokinetics and Materials Science, Russian Academy of Sciences, Chernogolovka, Moscow, 142432 Russia

e-mail: kovalev@ism.ac.ru

Study of the structure- and phase formation of materials during chemical reactions requires effective diagnostic methods that allow understanding the materials transformation. Creating of a sensitive high-speed X-ray detector is a fundamental step in developing of diffraction methods for dynamics of fast transformations in materials during chemical reactions. Time resolved X-ray diffraction (TRXRD) is a unique experimental method for study the evolution of the crystal structure during the process of phase transitions. The idea of the method consists in the registration sequence patterns with minimum time exposure from material in the process of its transformation, i.e. diffraction cinema. The method allows to receive in controllable conditions of experiment with complete information not only about changes in phase composition, presence of intermediate products in high-temperature combustion front and in a prehearing zone, but also to study influence of separate parameters (pressure, temperature, impurity) on the combustion process. This study presents the latest results obtained using the TRXRD.

TRXRD Study of Magnesium Diboride Obtained by SHS [1]. TRXRD was used to study the dynamics of phase formation in magnesium diboride during self-propagating high temperature synthesis (SHS) in the thermal explosion mode (Fig. 1). The MgB_2 phase was emerged without the formation of intermediate compounds. The effect of the heating rate on the formation mechanism of the MgB_2 phase was established. The presence of oxygen impurities has a

significant impact on the kinetics and formation mechanism of MgB_2. If the heating rate exceeds 150 deg/min, the oxide coating is not formed around the magnesium particles, which results in the solid-phase reaction $Mg + 2B = MgB_2$ through a reactive diffusion mechanism. Moreover, the self-ignition temperature of the mixture is lower than the melting point for magnesium. Mechanical activation of the mixture leads to variations in the kinetics of MgB_2 formation, significantly increases the period of simultaneous existence of Mg and MgB_2, and reduces the temperature at which the reaction occurs.
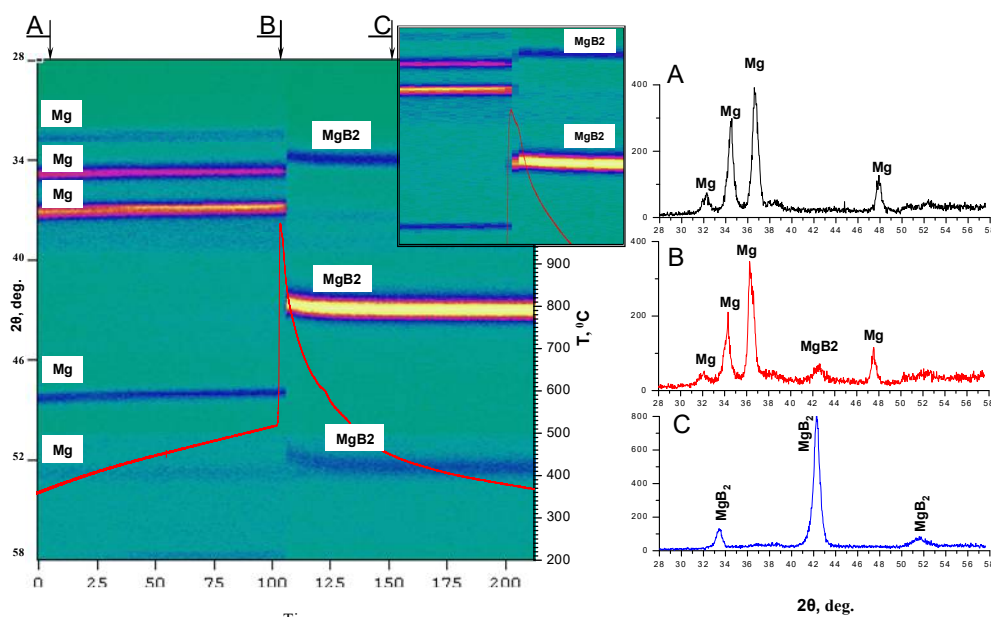
Fig. 1 Diffraction pattern and thermogram of the Mg + 2B mixture obtained in the ball mill and heated in the helium medium at the rate of ~ 150 deg/min.

TRXRD Study of Thermochemical Conversion of Iron Oxide [2]. Thermochemical conversion of compounds of transition metals with formation of high-porous composite material, comprising nanosized particles of these metals can occur in the flameless combustion wave of energy-rich materials with the polymeric system ballast. The distinctive features of this process are the absence of a flame, low combustion temperature (250–400°C) and propagation velocity (0.05–1.0 mm/s) of the combustion wave. We investigated the phase formation in mixture of iron oxide (III) - hexogen in a nitrogen atmosphere. TRXRD method showed that the process of reduction of iron oxide (III) in the wave of flameless combustion occurs in stage-by-stage manner (Fig. 2). The lines of the initial components

disappeared when the combustion front reaches the detection area. We may observe the appearance of line of (200) FeO. Lines of the FeO phase are recorded during 15 seconds and then disappear. At the same time, the nucleation and growth of the intensity of the Fe_3O_4 phase lines of (220), (311), and (400) are observed. The analysis of the diffraction patterns reveals that the formation of the final product occurs through the intermediate phase FeO to the final Fe_3O_4 phase. The process occurs entirely in the solid phase without amorphization of structure. Size of the coherent domain of Fe_3O_4 is 5–7 nm. Thus, as a result of the flameless combustion of mixtures containing the iron precursor I, a high-porous polymer matrix filled with particles of nanosized iron compounds is formed.
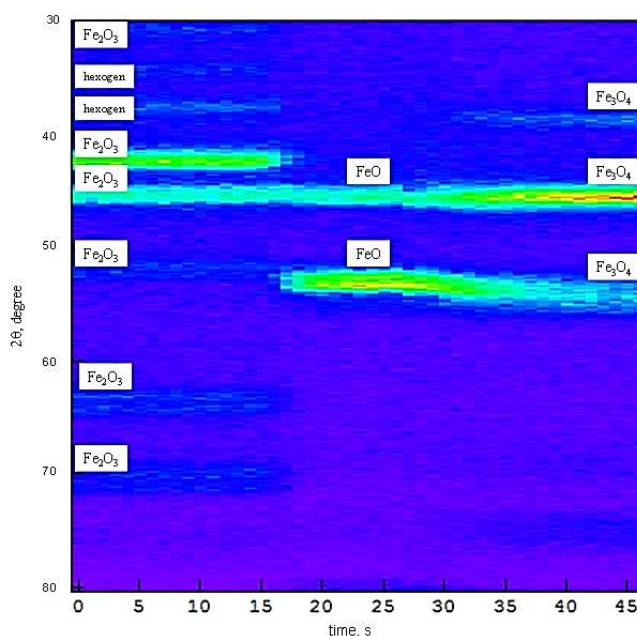
Fig. 2. Diffraction pattern of the combustion process of mixture Fe_2O_3 – hexogen.

Exothermic Self-Sustained Waves with Amorphous Nickel [3]. We investigated the self-propagating exothermic waves associated with crystallization of Ni from the amorphous precursor. TRXRD data indicate that amorphous nickel crystallizes in the temperature range of 170–210°C. The results (Fig. 3a) show that at v = 120 K/min, long range order begins to develop at a temperature of 170°C, which is in a good agreement with DSC data. Figures 3b and 3c show several XRD patterns acquired at different stages of crystallization and kinetics of intensity for Ni (111) diffraction peak. These results show that crystallization completes at 210°C, which corresponds to T_m

D. Yu. Kovalev and V. I. Ponomarev

determined by DSC. The results of DSC and TRXRD analysis allow to suggest that the exothermic crystallization of Ni takes place between ~ 170° and 210°C during external heating conditions with characteristic time scale on the order of few seconds. Self-diffusion of α-Ni atoms is the rate-limiting stage for crystallization. Utilization of amorphous metal as a reactant significantly increases the rate of solid-state reactions. For example, in reactive intermetallic forming systems, such as Ni + Al, the self-sustaining reaction propagation velocity with α-Ni is twice higher than that with crystalline Ni of the same morphology.
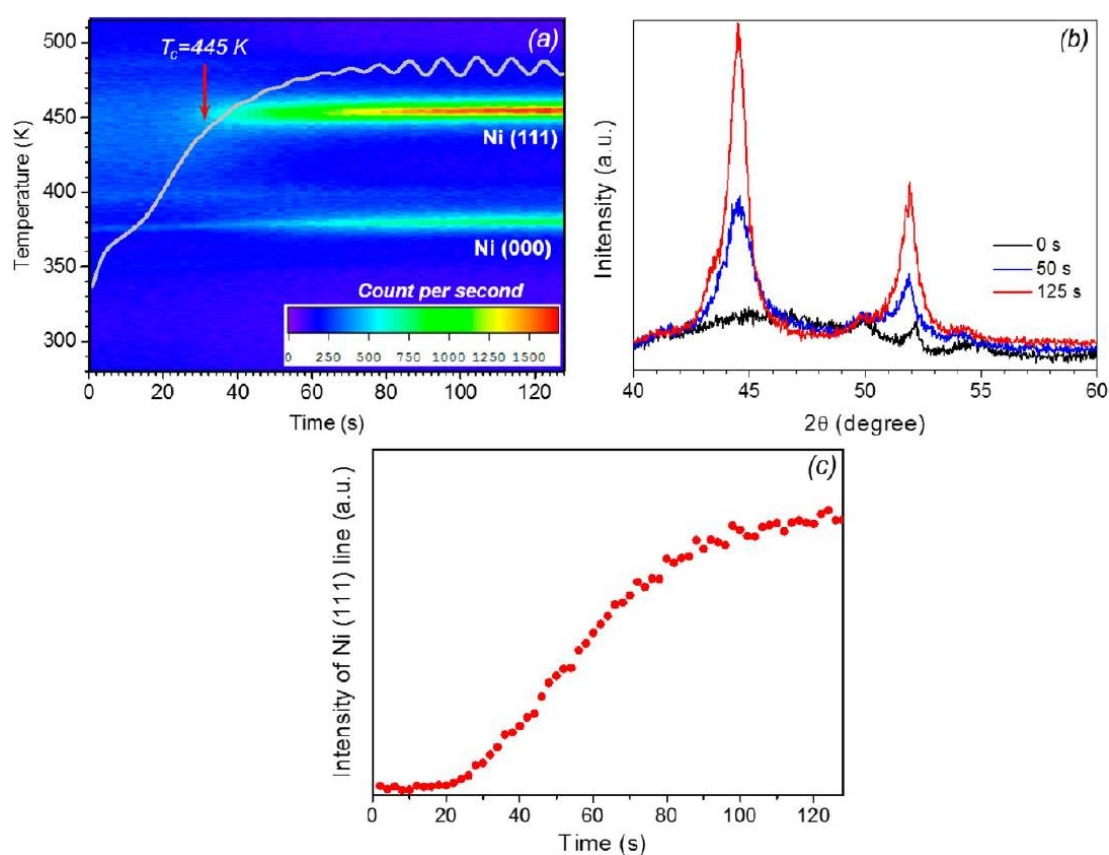
Fig. 3 TRXRD during crystallization of Ni from the amorphous precursor: (a) dynamic of crystallization, (b) selected diffraction patterns, and (c) kinetics of crystallization.

Completed to date, TRXRD studies have shown high informative value method to determine the mechanism of structural and chemical transformations.

dual-use technologies in interests of national safety. Basic researches of processes of burning and explosion.

1. D. Yu. Kovalev, A. Yu. Potanin, E. A. Levashov, N. F. Shkodich, Phase formation dynamics upon thermal explosion synthesis of magnesium diboride, *Ceram. Inter.*, 2016, vol. 42, no. 2, Part B, pp. 2951–2959.
2. Yu. M. Mikhailov, V. V. Aleshin, D. Yu. Kovalev, Thermochemical conversion of Iron Oxide in a wave of flameless combustion, *XX Mendeleev Congress on general and applied chemistry*, Ekaterinburg: Ural Branch of the Russian Academy of Sciences, 2016.
3. K. V. Manukyan, C. E. Shuck, M. J. Cherukara, S. Rouvimov, D. Yu. Kovalev, A. Strachan, A. S. Mukasyan, Exothermic self-sustained waves with amorphous nickel, *J. Phys. Chem. C*, 2016, vol. 120, no. 10, pp. 5827–5838.

D. Yu. Kovalev and V. I. Ponomarev

NUMERIC SIMULATIONS OF THE STEEL–ALUMINIUM TRANSISTION JOINT UNDER MONOTONIC LOADING

M. Kowalski[1], M. Böhm[1], and A. Kurek[2]

[1] Faculty of Mechanical Engineering, Department of Mechanics and Machine Design, Opole University of Technology
[2] High Energy Techniques Works EXPLOMET Gałka, Szulc

e-mail: m.kowalski@po.opole.pl

Increasing requirements for engineering constructions drive improvements of machine and equipment parameters in terms of safety, efficiency and economic criteria. Numerous factors influence the overall shape of construction assumptions, including important aspects related to the broadly understood protection of the natural environment. New recommendations and industry standards are possible to meet by application of composites and modern methods of joining construction materials. One of the technologies allowing the production of the composite materials with universal properties is explosive welding [1–3]. In the process of joining of materials, the energy of detonation of explosives is used to perform the bonding. To obtain a solid connection between the materials strictly defined parameters of charges must be preserved. Explosive technologies are currently used in the process of production of elements of process and energy apparatus. The progressive development of explosive welding technologies causes a constant increase of the multilayer materials application scope. An example is the shipbuilding industry, where multilayer components are used as transition joints. In case of this join type, which contains weld joints and explosively welded interfaces, the prediction of construction behaviour under different loading cases is very important. Identification and simulation of transition joints behaviour is also significant from the perspective of the fatigue phenomena. In the specialist literature there are many studies on the microstructural and strength properties of cladded materials, however,

there are no publications about nonlinear strength simulations of the transition joints [4–7]. Transition joint investigated in presented paper consisted of the following layers: aluminium alloys 5083 and 1050, titanium Grade 1, steel Grade D (Fig. 1).
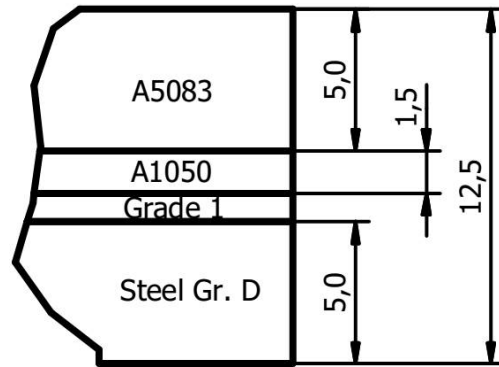
Fig. 1. Composite configuration.

Transition joint after web members welding is presented in Fig. 2.

Fig. 2. Transition joint.

Material properties used in simulation process were obtained by tension tests performed for specimens cut out from the material plates used in explosive welding process. Tests were carried with extensometer (Fig. 3).

Strains and stresses registered during tests were the sources of material properties in finite element method material data. FEM analysis results were presented in form of contour lines. An example stress distribution in the interface layer between Steel Gr. D and titanium Grade 1 were presented in Fig. 4.
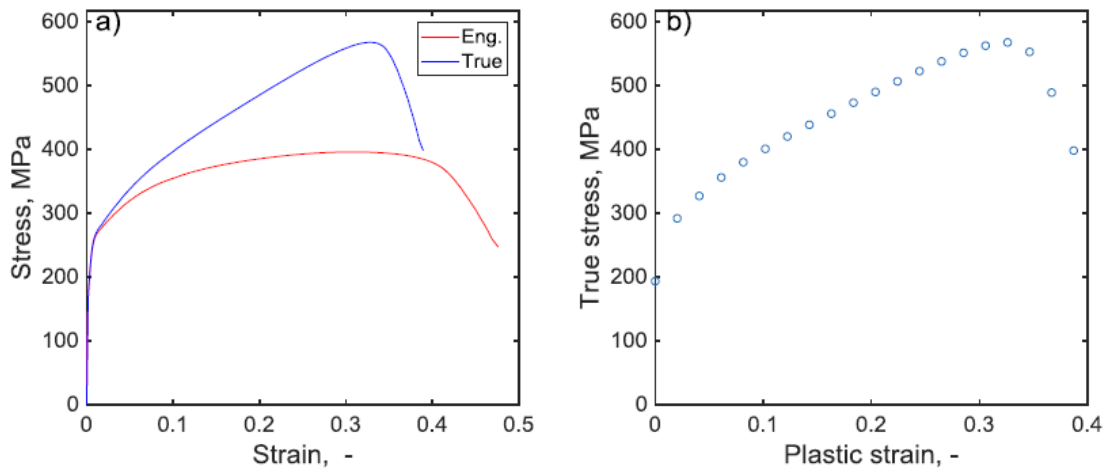
Fig. 3. Example tension test results of titanium Grade 1,
(a) engineering vs true stress, (b) plastic strain vs true stress.
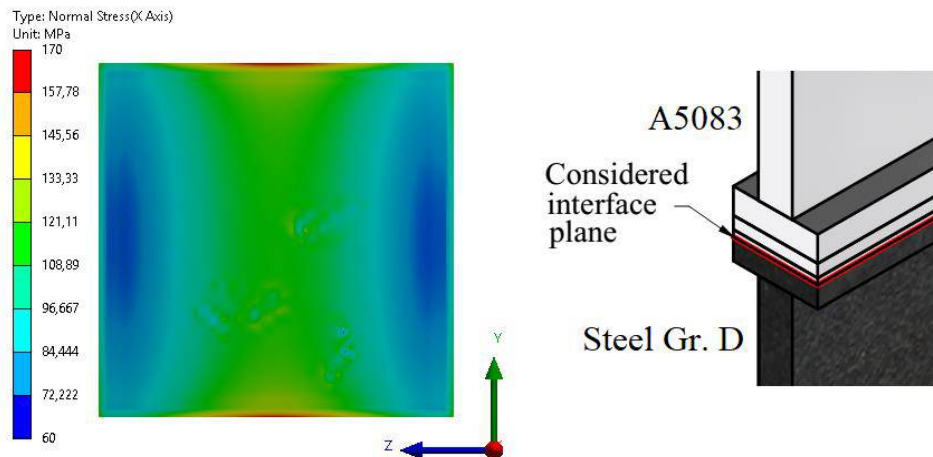
Fig. 4. Normal stress under tension in interface layer (steel S235JR + N–titanium Grade 1).

Simulated tests conditions coincided with the requirements of ABS shipbuilding industry standards [8]. Standard recommendation requires strength tests in the form of monotonic tensile test, shear test, and delamination test. Publication presents the results of the FEM calculation and comparison between experimental and calculation data.

1. S. A. A. Akbari-Mousavi, L. M. Barrett, S. T. S. Al-Hassani, Explosive welding of metal plates, *J. Mater. Process. Tech.*, 2008, vol. 202, pp. 224–239.
2. L. Čižek, D. Ostroushko, Z. Szulc, R. Molak, M. Pramowski, Properties of sandwich metals joined by explosive cladding method, *Arch. Mater. Sci. Eng.*, 2010, vol. 43, pp. 21–29.

3. F. Findik, Recent developments in explosive welding, *Materials & Design,* 2011, vol. 32, pp. 1081–1093.
4. R. Kacar, M. Acarer, An investigation on the explosive cladding of 316L stainless steel-din-P355GH steel, *J. Mater. Process. Tech*., 2004, vol. 152, pp. 91–96.
5. M. Kowalski, Identification of fatigue and mechanical characteristics of explosively welded stee–titanium composite, *Frattura ed Integrità Strutturale*, 2017, vol. 42, pp. 85–92.
6. H. Paul, L. Lityńska-Dobrzyńska, M. Miszczyk, M. Prażmowski, Microstructure and phase transformations near the bonding zone of al/cu clad manufactured by explosive welding, *Arch. Metall. Mater*., 2012, vol. 57, iss. 4, pp. 1151–1162.
7. Y. Wang, H. G. Beom, M. Sun, S. Lin, Numerical simulation of explosive welding using the material point method, *Inter. J. Impact Eng*., 2011, vol. 38, pp. 51–60.
8. ABS Rules for materials and welding–aluminum and fiber reinforced plastics (frp), American Bureau of Shipping, Huston, 2017.

THE UNSTEADY CELLULAR MODES OF FILTRATION COMBUSTION

P. M. Krishenik[1], S. V. Kostin[1], N. I. Ozerkovskaya[1], and K. G. Shkadinskii[2]

[1] Merzhanov Institute of Structural Macrokinetics and Materials Science, Russian Academy of Sciences, Chernogolovka, Russia
[2] Institute of Problems of Chemical Physics, Russian Academy of Sciences, Chernogolovka, Russia

e-mail: petr@ism.ac.ru

The possibility of structuring of the thermal diffusion flame was demonstrated by Ya. B. Zel'dovich as long ago as 1944 [1]. In recent years, increased attention has been drawn to research of the structure of the combustion front of heterogeneous reactive compositions. Regardless of the effect of initial perturbations, the exothermic conversion of such systems can be accompanied by the spontaneous formation of regular structures, the symmetry of which should differ from the symmetry of initial perturbations.

The structuring of the infiltration front in the combustion of metal powders in the mode of natural gas infiltration was first theoretically and experimentally investigated in [2, 3], where the wave infiltration modes of the combustion of porous media were analyzed and the dynamics of initiation of cellular wave structures was investigated.

The aim of the present study is to determine the boundaries of existence of the steady and unsteady modes of propagation of the infiltration front. The focus is on establishing the macrokinetic laws of combustion propagation in the parametric domain where a planar combustion front is unstable and cellular pulsating combustion waves arise and propagate. Examining the evolution of the structure of a cell within a pulsation period makes it possible to establish how the parameters of heat and mass transfer and chemical reactions are related to the possibility and stability of combustion in porous media.

The reported results on the nonlinear dynamics of formation and propagation of a cellular pulsating combustion demonstrate a new approach to studying nonlinear effects in the wave propagation of an exothermic reaction in chemically active media. From a practical point of view, analysis of the combustion of the proposed model systems enables to determine optimal conditions of the infiltration combustion of porous media for obtaining synthesis products. The main result of the study is to establish the laws of the pulsating movement of cells and the disclosure of the physical mechanisms of the formation and propagation of a structured front from the modern theory of combustion.

When a planar infiltration combustion front loses its stability, it breaks into individual cells, which propagate in the self-sustaining pulsation mode. A combustion cell has an intricate internal structure and a complex propagation dynamics, both being associated with the characteristics of the chemical interaction of the multicomponent reactive gas with the condensed reagent. During the process of combustion in the self-regulatory regime, the conditions of mass and heat transfer may vary, causing the cells to change the direction of movement. The self-oscillatory propagation of a cellular front is associated with the thermal instability of the infiltration combustion of porous media. The pattern of the development of cellular combustion instability is determined by the physicochemical and geometric characteristics of the burning sample, processes of infiltration transport, and heat loss power into the environment. The maximum frequency of oscillations of the front corresponds to the minimum cross-sectional dimensions of the cells. The failure of the self-oscillatory combustion of the cells occurs during a depression period, when chemical interaction proceeds at a low temperature.

The existence of the cellular combustion mode and its manifestations are of interest from the standpoint of safety. This mode sets in under conditions where the one-dimensional analysis excludes the possibility of burning. This means that the domain of conditions providing combustion can be expended due to the onset of the self-sustained propagation of hotspots highly exothermic condensed systems with a relatively slow infiltration transport reactive gas.

1. Ya. B. Zel'dovich, *Theory of combustion and detonation of gases,* Moscow: Akad. Nauk SSSR, 1944 (in Russian).
2. N. I. Ozerkovskaya, A. N. Firsov, K. G. Shkadinskii, Emergence of spatial structures during filtration combustion, *Combust., Explos., Shock Waves*, 2010, vol. 46, no 5, pp. 515–522.
3. S. V. Kostin, P. M. Krishenik, N. I. Ozerkovskaya, A. n. firsov, k. g. shkadinskii, cellular filtration Combustion of Porous Layers, *Combust., Explos., Shock Waves*, 2012, vol. 48, no 1, pp. 1–9.

THE FORMATION OF COATINGS USING SYNTHESIZED MODIFYING POWDERS AND THE ENERGY OF ELECTRON BEAM

O. N. Kryukova[1] and A. G. Knyazeva[1,2]

[1] Institute of Strength Physics and Materials Science, Siberian Branch of the Russian Academy of Sciences, Tomsk, 634055 Russia
[2] Tomsk Polytechnic University, Tomsk, 634050 Russia

e-mail: okruk@ispms.tsc.ru

Currently there is an increased interest in additive manufacturing. Additive manufacturing is perspective technologies of products by means of gradual build-up of layers. The processes based on powders using (selective laser melting and sintering, electron-beam technologies of melting and sintering) present a large part of additive manufacturing. Technologies differ in the way of powder supply, the level of input energy, the application of external physical fields and the accompanying physical phenomena [1, 2]. In recent years, there has been an interest in the developing of composite powder materials for various applications (aerospace, medicine, etc.).

The development and use of composite materials is one of the main trends in the evolution of modern material science and engineering. Composites consist of a matrix and the reinforcing elements distributed in it and exhibit qualitatively new properties. For applications in electron-beam additive technologies, composites with metallic matrices (conductive electric current) are of interest [3, 4].

Mathematical modeling makes it possible to study nonequilibrium phenomena accompanying the synthesis of composite powders and the layer-by-layer formation of products, as well as the regularities of the formation of properties whereas mode change of synthesis and fusion.

This work presents two-dimensional model of modification of the surface of the steel billet and the formation of coatings using synthesized modifying powders and electron beam energy. The

mathematical model takes into account the melting and shrinkage of the powder layer, the change in porosity and phase composition. Modifying powder is a matrix based on titanium (or titanium with aluminum additives) with reinforcing elements of carbon, boron or silicon compounds (C, B, Si) with titanium and aluminum. In the nonequilibrium conditions of composite synthesis, the formation of intermetallic Ti and Al phases, as well as various carbides, borides or silicides of titanium, is possible in the matrix. It is possible the presence of the residual oxygen, which leads to the formation of oxides of titanium and aluminum. Powder of nonequilibrium composition is used for coating, surface modification or for growing 3D objects.

Mathematical model of coating is realized numerically. It takes into account the flow of powder into the melt forming behind the moving electron beam or onto a hard surface. The model and the algorithm are similar to ones in [5, 6]. Calculations show that multiphase coatings form during processing. The phase composition of the coating can be controlled by changing the composition of the initial powders and processing parameters, which is also studied numerically. The effective properties of the coating are evaluated for the quasi-stationary stage, which is quickly established for each passage of the electron beam. As a result, the phase composition of the surface layer and the effective properties are calculated depending on the technological conditions. For other systems, similar models are described in [7, 8].

The mathematical model allows choosing the technological parameters that provide a minimum porosity and a suitable surface relief.

1. X. Gong, T. Anderson, K. Chou, Review on powder-based electron-beam additive manufacturing technology, *Manufacturing Rev.*, 2014, vol. 1, no. 2; DOI: 10.1051/mfreview/2014001.
2. T. DebRoy, H. L. Wei, J. S. Zuback, T. Mukheriee, J. W. Elmer, J. O. Milewski, A. M. Beese, A. Wilson-Heid, A. De, W. Zhang, Additive manufacturing of metallic components–Process, structure and properties, *Prog. Mat. Sci.*, 2018, vol. 92, pp. 112–22.

3. L. E. Murr, Metallurgy of additive manufacturing: Examples from electron beam melting, *Addit. Manufact.*, 2015, vol. 5, pp. 40–53.

4. L. E. Murr, E. Martinez, K. N. Amato, S. M. Gaytan, J. Hernandez, D. A. Ramirez, P. W. Shindo, F. Medina, R. B. Wicker, Fabrication of metal and alloy components by additive manufacturing: examples of 3d materials science, *J. Mater. Res. Technol.*, 2012, vol. 1, no. 1, pp. 42–54

5. A. G. Knyazeva, I. L.Pobol, A. I. Gordienko, V. N. Demidov, O. N. Kryukova, I. G. Oleschuk, Simulation of thermophysical and physico-chemical processes occurring at coating formation in electron-beam technologies of surface modification of metallic materials, *Phys. Mesomech.*, 2007, vol. 10, pp. 207–220.

6. O. N. Kryukova, A. G. Knyazeva, Critical phenomena in particle dissolution in the melt during electron-beam surfacing, *J. Appl. Mech. Tech. Phys.*, 2007, vol. 48, no 1. pp. 109–118.

7. A. G. Knyazeva, O. N. Kryukova, Modeling of controlled synthesis of intermetallic coatings, *J. Phys. Conf. Ser.*, 2017, vol. 899. P 072001.

8. O. N. Kryukova, K. A. Kolesnikova, N. K. Gal'chenko, Numerical and experimental study of electron-beam coatings with modifying particles FeB and FeTi, *IOP Conf. Ser. Mater. Sci. Eng.*, 2016, vol. 140, 012011.

ON THE APPLICATIONS OF PHOTONIC DOPPLER VELOCIMETRY

M. Künzel[1, 2] and P. Nesvadba[2]

[1] Institute of Energetic Materials, University of Pardubice , Faculty of Chemical Technology, Studentska 95, Pardubice, 53210 Czech Republic
[2] OZM Research, s.r.o., Bliznovice 32, Hrochuv Tynec, 53862 Czech Republic

e-mail: kunzel@ozm.cz

Photonic Doppler velocimetry (PDV) had been developed before 2005 in the USA [1]. Since that time PDV has gained a lot of attention and its usage has spread within several countries including, China, France, Russia, United Kingdom, and Czechia. The PDV allows measuring velocity profiles (velocity-time dependencies) of moving objects with high time resolution of up to 5 ns and accuracy of the measured velocity of about 0.1–0.5% [2].

In recent years various uses of PDV had been tested and evaluated at the Institute of Energetic Materials, University of Pardubice. Three different PDV instruments had been employed in testing of the PDV abilities: single channel prototype PDV, four-channel custom made PDV and at the end, commercial four-channel Optimex-PDV (OZM Research). The voltage signals were recorded using a high bandwidth Tektronix oscilloscope. The oscilloscope records were analyzed using short-time Fourier transform (STFT) with a Hamming window. The use of PDV for selected applications is reviewed in this contribution.

The falling hammer behaviour was observed at the moment of impact on a high explosive sample. PDV probe recorded velocity of the hammer directly before the moment of impact on the sample which exhibits as a short velocity drop to a zero value. Various types of reflected hammer velocity profiles were obtained for different

explosives and depending on type of the explosive and mechanism of its initiation.

A large blasting chamber was loaded with high explosive charge placed in its center. The PDV allowed to measure velocity of the chamber wall as it was accelerated by shock waves generated by the explosion. Ringing of the wall continued until the end of recording time window. Displacement was obtained by integrating the velocity profile for the most intensive pair of peaks. The maximum displacement agreed well with preliminary numerical model predictions.

A concrete slab 0.3 m thick was subjected to detonation of a high explosive charge of 25 kg of TNT placed 0.5 m above. A large spall fracture occurred on the soffit of the slab and the spalled material was accelerated towards a PDV probe which was able to capture the spall movement including its early stages. The resulting velocity profile provides input data for numerical modelling of blast response of the material [3].

Explosion welding allows to weld practically any combination of metallic materials with excellent joint quality. However, parameters of the explosive and spatial relations of all the parts must be adjusted correctly. The probe placed against the cladder plate allows to determine the whole velocity profile of the plate including its terminal velocity at which the impact with the base plate occurs. The PDV proved to be applicable even in a full scale open field explosion welding [4].
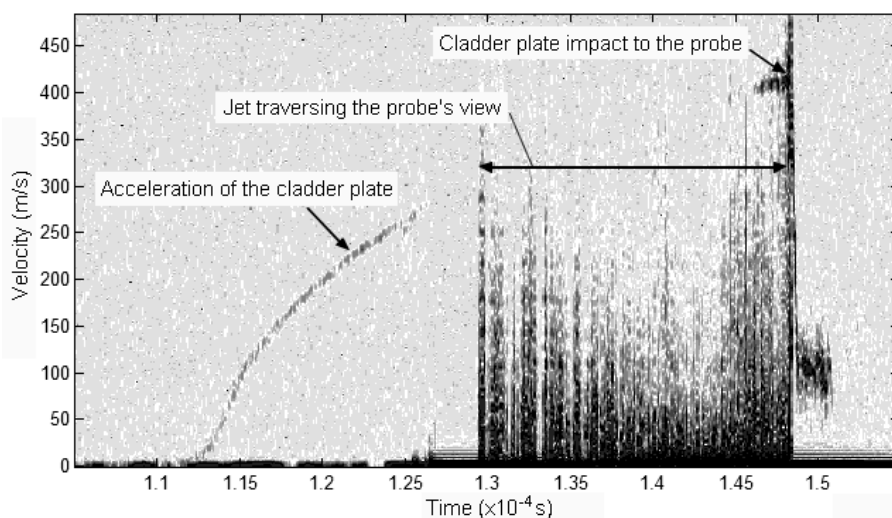
Fig. 1. Cladder plate velocity profile obtained in a full scale welding operation.

Cylinder expansion test is a classical procedure, which has been used since 60' for determination of metal acceleration ability of explosives. An explosive charge is confined in a copper tube and expansion of the explosively accelerated tube walls is recorded in time. The PDV instrumentation is superior compared to the outdated methods of wall expansion tracking by electric contact pins or streak cameras in view of accuracy, resolution and simplicity of operation [5, 6].

One of the methods for determination of pressure profiles in the detonation waves is the impedance window method. A layer of transparent material such as polymethylmethacrylate with a thin aluminium layer at the interface is attached to the explosive charge and the interface velocity is recorded by the PDV. The particle velocity profile of the interface may subsequently be converted to the pressure profile using impedance matching technique and the Chapman-Jouguet (CJ) detonation pressure of the explosive can be determined [7].

Another way to obtain detonation zone parameters is a measurement of initial velocity of explosively accelerated thin metal disc. The velocity steps caused by shock reverberations in the disc can also be used to determine expansion path of the detonation products (isentrope) which is an important information for numerical modelling of blast loading processes. The limiting velocity at the rear part of the profile corresponds to the energy transferred to the flyer from the detonation products – the acceleration ability of the explosive [8].

1. T. Strand, D. R. Goosman, C. Martinez, T. L. Whitworth, W. W. Kuhlow, Compact system for high-speed velocimetry using heterodyne techniques, *Rev. Sci. Instrum.,* 2006, vol. 77, pp. 083108; doi: 10.1063/1.2336749.
2. D. H. Dolan, Accuracy and precision in photonic Doppler velocimetry, *Rev. Sci. Instrum.,* 2010, vol. 81, pp. 05390; doi: 10.1063/1.3429257.
3. M. Künzel, M. Foglar, J. Pachman, Photonic Doppler velocimetry instrumentation in real scale concrete slab blast loading experiments with an attempt to measure the influence of the type of concrete on the debris velocity, In proc. *Design and Analysis of Protective Structures* (DAPS), Singapore: 2015.

4. J. Kucera, A. C. Anastacio, P. Nesvadba, M. Künzel, J. Selesovsky, J. Pachman, Experimental determination of acceleration of explosively driven metal by photonic Doppler velocimetry in the process of explosive welding, *Prop., Explos. Pyrotech.*, 2018, [accepted for publication].

5. C. G. Rumchik, R. Nep, G. C. Butler, B. Breaux, C. M. Lindsay, The miniaturization and reproducibility of the cylinder expansion test, In proc. *AIP Conference Proceedings*, 2012, vol. 1426, pp. 450; doi: 10.1063/1.3686315.

6. M. Künzel, J. Selesovsky, J. Pachman, First attempts in cylinder expansion testing, In proc. *New Trends in Research of Energetic Materials* (NTREM), Pardubice, Czechia, 2017.

7. J. Pachman, M. Künzel, O. Němec, J. Majzlik, A comparison of methods for detonation pressure measurement, *Shock Waves*, 2018, [published online]; doi: 10.1007/s00193-017-0761-5.

8. K. T. Lorenz, E. L. Lee, R. Chambers, A simple and rapid evaluation of explosive performance - the disc acceleration experiment, *Propellants, Explos, Pyrotech.*, 2015, vol. 40, no. 1, pp. 95–108; doi:10.1002/prep.201400081.

APPLICATION OF THE VANADIUM BARRIER LAYER IN STEEL–TITANIUM BIMETAL IN HIGH TEMPERATURE CONDITIONS

V. V. Kurilkin[1], I. V. Saikov[1], A. Yu. Malakhov[1], and A. A. Berdychenko[2]

[1] Merzhanov Institute of Structural Macrokinetics and Materials Science, Russian Academy of Sciences, Chernogolovka, 142432 Russia
[2] Polzunov Altai State Technical University, Barnaul, 656038 Russia

e-mail: revan.84@mail.ru

An actual problem in the creation of bimetallic compositions is the tendency of their components to the formation of intermetallic compounds which considerably reduce mechanical and operational properties of bimetals. An example of such materials is steel–titanium bimetal. An effective solution to this problem is the use of a barrier layer that separates the basic materials from each other excluding their mutual diffusion [1]. The effectiveness of the application of the vanadium barrier layer in order to prevent the formation and growth of intermetallic compounds in the weld zone of the stainless steel + titanium grade 1 bimetal is investigated. The bimetal samples were heated to temperatures of 600, 700, 800, and 900°C, holding for 1, 3, 5, and 10 h.

Heating of samples to 600°C at all holding times and holding for 1 h at 700°C did not lead to a significant change in the structure of the welded joint and to the appearance of diffusion and intermetallic layers. The first diffusion layer, which arose as a result of the diffusion of titanium into vanadium, was found in samples subjected to heating to 700°C for 3 h. The thickness of the layer is 3 μm and the titanium content in it is 2–3% (at). An increase in the holding time to 10 h leads to an increase in the thickness of the interlayer to 9±1 μm and in the titanium content to 73±13% (at). Such a high content of

titanium in the interlayer indicates a change in the direction of diffusion. The prevailing process was the diffusion of vanadium into titanium. The heating at 800 and 900°C activated the diffusion process at the interface between titanium and vanadium. The appearance of the diffusion layer was noted already after 1 h. An increase in the holding time to 10 hours favors an increase in the thickness of the diffusion layer between the materials (Fig. 1).

Diffusion processes at the boundary between vanadium and steel are excited at 900°C. The diffusion layer between titanium and vanadium has approximately the same thickness along the length of the boundary. The interlayer at the boundary between vanadium and steel is formed as a result of the diffusion of carbon and iron along the intergranular boundaries of vanadium. The penetration depth of carbon and iron in vanadium is up to 7–10 µm. A decarburized zone with a depth of 11–12 µm is formed in the steel, and cracks are generated along this interface at a distance of 1–8 µm. Further increase in the holding time leads to the development of cracks and partial destruction of the compound.
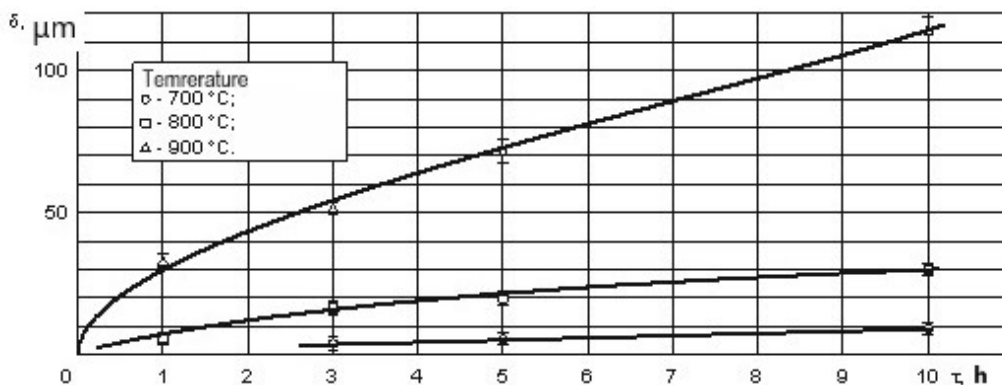
Fig. 1. Kinetics of growth of the thickness of the diffusion layer at the titanium–vanadium interface (δ) depending on the heating temperature and the holding time (τ)

As a result of studies, it has been proved that the vanadium barrier layer at high temperatures reliably prevents the mutual diffusion between steel and titanium, excluding, thus, the formation of intermetallic compounds at the interface.

The explosive welding experiments were carried out in Bitrub International Ltd. This work was performed by using the set of modern scientific instruments available for multiple access at ISMAN.

V. V. Kurilkin et al.

FORMATION OF Ti–Al₃Ti MULTILAYER COMPOSITES WITH TETRAGONAL AND CUBIC STRUCTURES OF INTERMETALLIC BY EXPLOSIVE WELDING AND SUBSEQUENT ANNEALING

D. V. Lazurenko[1], V. I. Mali[2], A. A. Kashimbetova[1], M. A. Esikov[2], I. A. Bataev[1], A. Stark[3], and F. Pyczak[3]

[1] Novosibirsk State Technical University, pr. K. Marksa 20, Novosibirsk, 630073 Russia

[2] Lavrent'ev Institute of Hydrodynamics, Siberian Branch, Russian Academy of Sciences, pr. Lavrent'eva 15, Novosibirsk, 630090 Russia

[3] Helmholtz Zentrum Geesthacht, Max-Planck-Straße 1, Geesthacht, 21502 Germany

e-mail: pavlyukova_87@mail.ru

Recently Ti–Al₃Ti composites are in the focus of attention of many researchers. These materials possess the number of outstanding properties such as high specific stiffness, which is twice higher than that of steel, and specific hardness similar to that of ceramics [1]. Also, multilayer materials with intermetallic component demonstrate high fracture toughness and ballistic properties [2]. However, their plasticity is still low. It is explained by high brittleness of Al₃Ti compound [3]. Titanium trialuminide has tetragonal $D0_{22}$ structure which can be formed by stacking two cubic $L1_2$ lattices with formation of periodic antiphase boundaries. $D0_{22}$ can be characterized as the distorted long-periodic cubic structure. The dislocation mobility in this structure is very low and the predominant deformation mechanism is twinning. To improve the plasticity of this tetragonal structure, it is reasonable to transform it to cubic, which can be realized by alloying [4]. In this study we consider the possibility to transform the structure of Al₃Ti acting as a component of Ti–Al₃Ti composite produced by explosive welding and subsequent annealing

[5] and discuss the particularities of intermetallic formation in binary and ternary systems. To modify Al_3Ti structure, copper was used. Forty-layered Al–Ti and five-layered Al–Ti–Cu composites were fabricated by explosive welding at the Lavrent'ev Institute of Hydrodynamics and subjected to heating up to 100 hours. The annealing temperature of the binary composite was equal to $640^{\circ}C$. The choice of the heating temperature of Al–Ti–Cu composite was made based on the results of synchrotron measurements carried out at German Electron Synchrotron (Deutsches Elektronen-Synchrotron – DESY) in the High Energy Materials Science Beamline (P07) operated by Helmholtz-Zentrum Geesthacht [6]. It was found that Al_3Ti with the cubic structure forms through the series of the reactions with participation of binary Al–Ti and Al–Cu compounds. It was demonstrated that fracture toughness of ternary composite was high as compared to binary one due to a higher plasticity of the intermetallic with cubic lattice.

1. K. S. Vecchio, Synthetic multifunctional metallic-intermetallic laminate composites, *JOM*, 2005, vol. 57, iss. 3, pp. 25–31.
2. A. Rohatgi, D. J. Harach, K. S. Vecchio, K. P. Harvey, Resistance-curve and fracture behavior of Ti–Al_3Ti metallic-intermetallic laminate (MIL) composites, *Acta Mater.,* 2003, vol. 51, iss. 10, pp. 2933–2957
3. G. Sauthoff, *Intermetallics*, Weinheim: VCH, 1995.
4. R. A. Varin, Intermetallics: Crystal Structures, in *Encyclopedia of Materials: Science and Technology*, Elsevier Science Ltd., 2001, pp. 4177–4181.
5. D. V. Lazurenko, I. A. Bataev, V. I. Mali, A. A. Bataev, I. N. Maliutina, V. S. Lozhkin, M. A. Esikov, A. M. J. Jorge, Explosively welded multilayer Ti–Al composites: Structure and transformation during heat treatment, *Mater. Design.*, 2016, vol. 102, pp. 122–130.
6. N. Schell, A. King, F. Beckmann, T. Fischer, M. Müller, A. Schreyer, The high energy materials science beamline (HEMS) at PETRA III, in *Materials Science Forum*, 2014, pp. 57–61.

INITIATION OF THERMAL EXPLOSION IN Ni/Al REACTION MULTILAYER FOILS BY ELECTRIC CURRENT PULSE

I. Lendiel, P. Shlonskii, and A. Cherkachin

E.O. Paton Electric Welding Institute of NAS of Ukraine, ul. Kazimira Malevicha 11, Kyiv, 03150 Ukraine

e-mail: lend_el@ukr.net

A self-sustaining exothermic synthesis reaction in a reaction multilayer foil (RMF), which consists of intermetallic-forming elements, can be initiated by local heating leading to the formation of a self-propagating high-temperature synthesis (SHS) front or as a result of self-ignition of the entire volume of the RMF (thermal explosion), when it is heated to a certain temperature with a certain speed [1, 2]. Exothermic reaction in the thermal explosion (TE) mode provides a high intensity of heat formation as compared to the SHS mode. The realization of the exothermic synthesis process in the RMF with a high intensity of heat generation can be of practical interest when using RMF as a heating source for local heating of materials that contact with RMF [3, 4]. For the practical application of this approach, it is important to study the various possibilities for initiating the TE in the RMF. Earlier it was shown that the TE in RMF can be achieved, for example, by heating a foil with an infrared pulse or a pulse of microwave radiation [3, 4].

In this work, it is considered to initiate the TE by passing an electric current pulse through RMF using the example of Ni/Al RMF.

To initiate the TE by passing a current pulse through the RMF, a special setup was used, which is available in E.O. Paton Electric Welding Institute (Fig. 1). It consists of capacitor battery C_0 (16.08 μF), inductance L_0 (1788 nH), active resistance R_0 (0,092 Ω), controlled air discharger (CAD), Rogowski coil RC, and high-voltage source (not shown on the diagram).
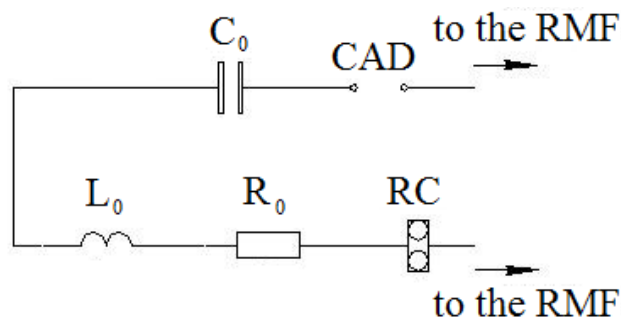
Fig. 1. Electrical diagram of the setup for the TE implementation of the RMF.

Condenser C_0 was charged from a high voltage source up to the required voltage. After that, a trigger pulse was applied to the CAD, which led to the discharge of the capacitor directly on the RMF, whereby the TE was initiated. As a result of the initiation of TE in the RMF, a bright flash and dispersion of the foil into fragments was observed. X-ray studies of the powder formed as a result of the TE showed that NiAl intermetallic was formed in the foil.

For study of the influence of energy parameters on the dispersion of intermetallic particles, the RMF was clamped between two plates of polymethylmethacrylate (PMMA) with dimensions of $20 \times 10 \times 5$ mm (Fig. 2a). The transparency of PMMA makes it possible to investigate the macrostructure of the reaction foil, to determine the size and distribution of intermetallic particles in the frontal plane (Fig. 2). The investigations were carried out at 13.5, 18, 26.2, and 28.1 kA pulses with a duration of 17 μs.

The obtained data show that in the entire range of current pulses, it is possible to initiate the TE in the RMF, which is accompanied by intense heat generation in the form of infrared radiation and dispersion of the foil. The analysis of the obtained results showed that the degree of crushing of the foil is determined primarily by the magnitude of the electric current: as the current pulse increases, the dispersion of the particles of the resulting intermetallic compound decreases.

The possibilities of the practical application of the TE in the RMF initiated by the current pulse are being discussed.

I. Lendiel et al.
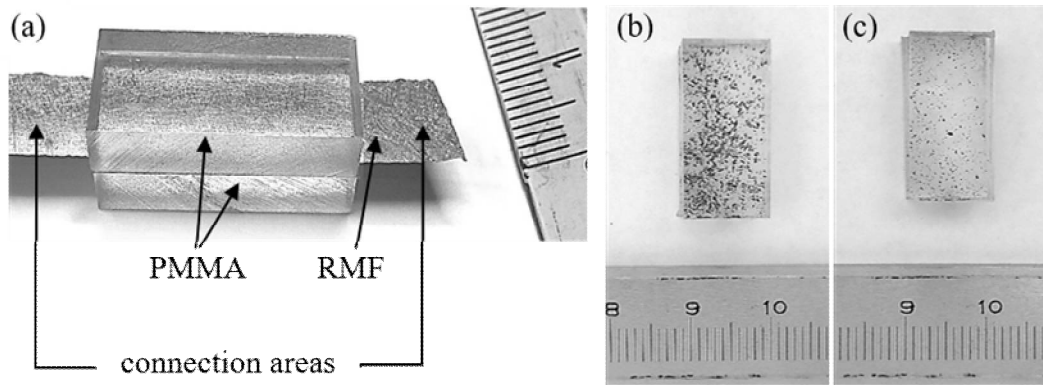
Fig. 2. (a) Scheme of investigated sample. Macrostructure of PMMA plates, which was obtained as a result of the initiation of the TE by pulses of a different current: (b) 13.5 kA and (c) 28.1 kA (front image).

1. E. Besnoin, S. Cerutti, O. Knio, T. P. Weihs, Effect of reactant and product melting on self-propagating reactions in multilayer foils, *J. Appl. Phys.*, 2002, vol. 92, no. 9. pp. 5474–5481.
2. A. G Gasparyan, A. S. Shteinberg, Macrokinetics and thermal explosion in mixtures of Ni and Al powders, *Phys. Combust. Explos.*, 1988, vol. 24, no. 3, pp. 67–74.
3. T. Zakusylo, T. Melnichenko, A. Ustinov, I. Lendiel, D. Kuzmenko, Joining of thermoplastics using Ni/Al reactive multilayer foil, *9th international conference of young scientists on welding and related technologies*, 2017, Kyiv, pp. 131–136.
4. A. I. Ustinov, D. N. Kuzmenko, M. V. Kravchuk, Ya. D. Korol, Initiation of thermal explosion in Ti/Al nanofoils, *Int. J. Self-Propag. High-Temp. Synth.*, 2015, vol. 24, no. 2, pp. 72–77.

CHARACTERIZATION OF TEMPERATURE EXCURSION IN EXPLOSIVE STEEL–COPPER BONDS

S. Liu[1], V. Petr[1], J. Banker[2], and C. Prothe[3]

[1] Advanced Explosive Processing Research Group (AXPRO), Colorado School of Mines, Golden, Colorado 80401, U.S.A.
[2] Retired, Dynamic Materials Corporation, Boulder, Colorado 80301, U.S.A.
[3] NobelClad, Boulder, Colorado 80301, U.S.A.

e-mail: sliu@mines.edu

Due to the rapid and dynamic nature of explosive welding (EXW), it is very difficult to measure physical properties during the process. Initial detonation behavior, shock wave propagation as well as temperature evolution throughout the explosive welding process are essential information desired for complete modeling and understanding of the process and final product characteristics. The main objective of this work was to determining the evolution of interface temperature between the base and flyer plates during the EXW process. Knowledge of interfacial temperature excursion would lead to proper selection and safe design of explosive welded couples. On a broader scale, the information could also allow for better process design with optimized explosives and improved interface bonding between the base and flyer plates.

To determine the bond interface temperatures, four tracer materials with different melting temperatures were inserted between the copper flyer and steel base plates for experimentation. These materials were in either foil or powder form. Some of the tracers required adhesive bonding to fix them onto the base plates. The four tracers were Pb–Sn solder (wires), Al (foils), Fe/S (powders), and W (rods)/Ti (foils). They were selected according to their system melting temperatures, from around 180ºC to over 3400ºC. The tracers were placed in and across from the direction of wave propagation. The layout of the

tracers also attempted to minimize the disruption caused by the presence of the tracers. After explosive bonding occurred, X-ray radiography were performed on the bonded plates. Density differences between the different tracer materials and the base and flyer plates showed evidence of porosity, melting, and fragments (in the case of tungsten). The samples were cross-sectioned, ground, polished and etched, and examined following standard metallographic techniques. Light optical and electron microscopy with energy dispersive spectroscopy (EDS) were used to characterize phase changes and mixing of molten materials.

Localized melting was observed in the solder, aluminum, tungsten, and titanium tracers. In the case of solder, porosity was also present, indicating vaporization of the solder alloy. Vaporization can be expected because of the low melting and boiling temperatures of Pb and Sn. At the copper-solder interface, a wavy interface was observed which confirms the propagation of the shock wave and that solder was initially bonded to the flyer plate by explosive bonding. Trapped iron and copper particles substantiated the establishment of an explosive jet. Rapid temperature excursion caused subsequent melting and vaporization of the solder material.

The 1xxx series Al foil was not clearly distinguishable from radiography because of the low density of Al. Light optical micrographs clearly showed the presence of a wavy interface, which is the characteristic of an explosive bond. Alloying between Cu and Al did occur along the interface. There was clear evidence of melting and the presence of porosity indicated vaporization. When Ti–6Al–4V tracers were used, a relatively thick explosive bond region was present. On the copper side, however, cracking and decohesion were observed. Solidification cracking appeared to occur across the thermomechanically mixed regions.

The most interesting findings were related to tungsten. Because of the high strength and low ductility, the tungsten rod shattered into small pieces during explosive bonding. By identifying the direction of the shock wave, on the backside (spalling side) of several tungsten particles, evidence of melting was observed. Fine, nodular structure on the surface of tungsten fragments that were dendrite tips were visible, indicating that temperature excursion could be locally high to exceed the melting temperature of tungsten. Jet consisted of material from the

base and flyer plate interacted with the tungsten to form the final materials in the pockets at the interface.

Thermodynamic calculations estimated that the bulk local maximum in the copper/steel system was located between 1538°C and 2595°C. In locations where jet interaction occurred, temperature exceeding the melting temperature of tungsten was reached. Thermodynamics and energy calculations must be used to estimate temperature as material properties and energy/temperature relations vary in each material system and the applied energy or amount of explosive used in the system.

INFLUENCE OF EXPLOSIVE CHARGE DENSITY AND SIZE OF PRILLS ON THE VELOCITY OF DETONATION OF ANFO EXPLOSIVES

S. Liu[1], V. Petr[1], J. Banker[2], and C. Prothe[3]

[1] Advanced Explosive Processing Research Group (AXPRO), Colorado School of Mines, Golden, Colorado 80401, U.S.A.
[2] Retired, Dynamic Materials Corporation, Boulder, Colorado 80301, U.S.A.
[3] NobelClad, Boulder, Colorado 80301, USA.

e-mail: vpetr@mines.edu

The mixture of ammonium nitrate and fuel oil (ANFO) is a highly non-ideal, heterogeneous explosive that is used in the explosive cladding industry. Ammonium Nitrate (AN) (NH_4NO_3) is produced by neutralizing nitric acid (HNO_3) with ammonia (NH_3). Ammonium nitrate plants in the United States produce about nine (9) million tons of ammonium nitrate, and approximately 15 to 20 percent of this amount is used for explosives. Prills can be produced in either high or low-density form this depends on the concentration of the AN. High-density (HD) prills are typically used as fertilizer and low-density (LD) prills are used as explosives. LD prills, in the range of 1.29 specific gravity, are formed from a 95.0 to 97.5 percent ammonium nitrate solution, and HD prills, in the range of 1.65 specific gravity, are formed from a 99.5 to 99.8 percent ammonium nitrate solution.

In early 2013, a research program at the Advanced Explosives Processing Research Group (AXPRO) at Colorado School of Mines (CSM) was established to determine if it would be more economical for the mining industry to use HD prills instead of LD prills. This paper presents a comparison between HD and LD prill performance as explosives, using the evaluation of velocity of detonation of ANFO charges confined in steel test cylinders. The LD prills used to conduct testing were 840 kg/m³ spherical explosive-grade prills, approximately

2.4 mm in diameter, manufactured by Dyno Nobel. The HD prills were 1,050 kg/m^3 industrial-grade miniature prills, approximately 1.0 mm in diameter, and manufactured by Agrium. Experimental testing that characterized the physical properties of each explosive, including loading density, shelf life, and fuel oil content, was conducted to understand the effect of AN characteristics on the velocity of detonation.

It was found that the HD pills had a strong influence on the detonation velocities of ANFO. In the case of LD ANFO samples which were prepared with AN that had the when tested the lower detonation velocity (3.85 km/s) was observed when the smallest particle diameter (0.35 mm) was used. This LD ANFO value corresponded to 75% of the ideal detonation velocity, which was theoretically predicted by the CHEETAH ideal detonation computer code. The 60 days aging (shelf life) showed the change of the detonation velocities of ANFO and the reaction of ANFO was not influenced fuel oil contents 6% LD pills and 3% for HD prills during the storage period.

EVALUATION OF MECHANICAL PROPERTIES AND CORROSION RESISTANCE OF EXPLOCLAD MULTILAYER MATERIALS

I. S. Los'[1], S. Yu. Kireev[1], and A. V. Pryshchak[2]

[1] Penza State University, Penza, 440026 Russia
[2] Research and Design Institute of Radioelectronic Engineering, Zarechny, Penza, 442960 Russia

e-mail: silverelk@rambler.ru

The aim of this work is study of the bonding strength and corrosion resistance of multilayer metallic materials with internal protector [1, 2]. The objects of research were three-layer and four-layer materials. The destructive mechanical tests were carried out in accordance with GOST 10885–85. They involved shear test, bend test and impact strength test. The following layered materials have been studied: 12Kh18N10T steel (analog of AISI 321) + St3 (analog of A570) + 12Kh18N10T + St3, 08Kh18N10T (analog of AISI 321) + Steel 10 (analog of ASTM A-179) + 08Kh18N10T + 09G2S (analog of ASTM A-516 Grade 70), and 12Kh18N10T + Steel 10 + 12Kh18N10T. Before the shear test, the microanalysis of each interlayer boundary was carried out to evaluate molten zone sizes. Multilayer specimens with flat-top projection on interlayer boundary were tested after explosive welding (EXW) and after normalizing. Results of shear test are shown in Fig. 1. The bonding strength for each interlayer boundary exceeded the permissible minimum characteristic of 220 MPa in both series of tests.

The bend tests were performed for three-layer and four-layer materials with a thickness of 6.8 and 15.9 mm, respectively. The bending angle was 145 degree. No separation, cracks and other defects were detected.

The impact strength tests were carried out for basic materials of four-layer materials. Specimens with *U*-shaped concentrator were

tested at room temperature (20°C) and $T = -30$°C after explosive welding (EXW) and normalizing (EXW +N). Results of impact strength test were satisfactory (Fig. 2).

The original corrosion test procedures were developed. Welded joints and separable joints were used as tested specimens [3]. The tests were carried out in corrosive environments with different pH (from 1 to 11). The protective effect performance criterion was a ratio of mass corrosion index of protected layer to mass corrosion index of monometallic material. It was calculated that corrosion resistance of multilayer 12Kh18N10T + Steel 10 + 12Kh18N10T material was in excess of corrosion resistance of stainless steel 12Kh18N10T in FeCl$_3$ by more than 12 times.
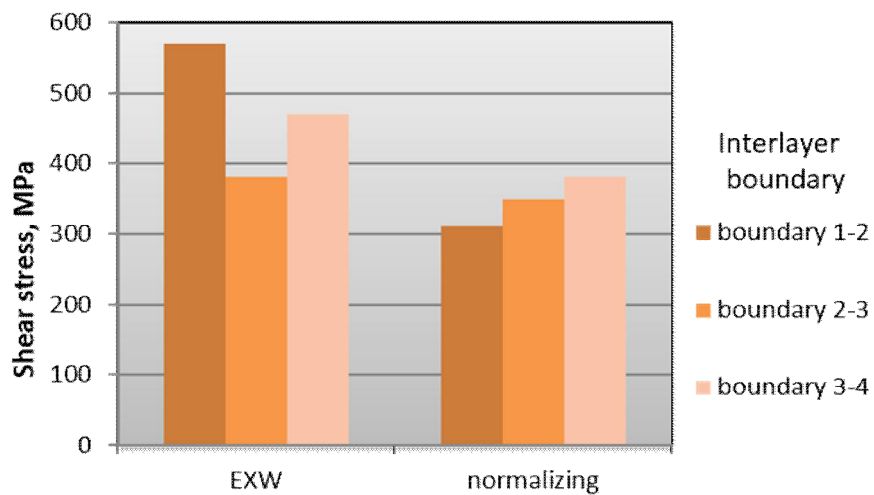
Fig. 1. Shear stress of four-layer 12Kh18N10T + St3 + 12Kh18N10T + St3 material.
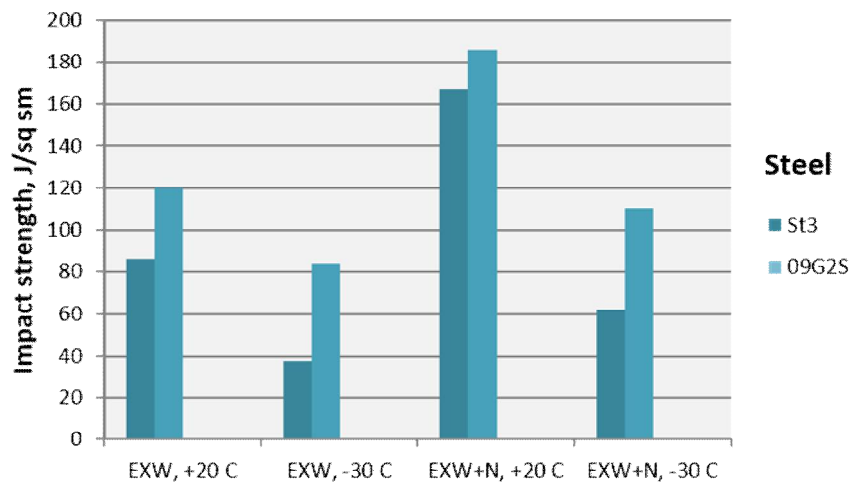
Fig. 2. Impact strength of basic materials at room temperature (20°C) and $T = -30$°C.

I. S. Los'et al.

1. A. E. Rozen, I. S. Los', L. B. Pervukhin, Yu. P. Perelygin, Yu. A. Gordopolov, G. V. Kirii, P. I. Abramov, S. G. Usatyi, D. B. Kryukov, O. L. Pervukhina, I. V. Denisov, A. A. Rozen, *Multilayer material with enhanced corrosion resistance and methods for preparing same*, Eurasian Patent 016878, 2012.
2. A. E. Rozen, c, Yu. P. Perelygin, S. Yu. Kireev, A new corrosion-resistant multilayer material, *Prot. Met. Phys. Chem. Surf.*, 2014, vol. 50, no. 7, pp. 856–859.
3. S. Yu. Kireev, I. S. Los', A. E. Rosen, Yu. P. Perelygin, Procedures for corrosion tests of multilayered metal material, *Korroziya: Materialy, Zashchita*, 2017, no. 8. pp. 42–47.

INTRODUCING DAICEL'S ACTIVITIES RELATED TO DETONATION NANODIAMONDS

T. Mahiko[1], Y. Hidaka[2], D. Ishimoto[2], Y. Kishino[2], T. Kouuchi[2], and T. Ina[1]

[1] Innovation Park, Daicel Corporation, 1239, Shinzaike, Aboshi-ku, Himeji, Hyogo 671-1283 Japan
[2] Harima Plant, Daicel Corporation, 805, Umaba, Ibogawa-cho, Tatsuno, Hyogo 671-1681 Japan

[1]e-mail: tm_mahiko@jp.daicel.com

Nanodiamonds (NDs) are expected to provide industrial advantages among various nano-carbon materials because of their unique properties. ND composite of various materials is expected to exert improvement in physical property and/or functionality. Daicel has been making efforts for integrated production of detonation nanodiamonds (DNDs) from detonation synthesis of NDs and development of ND products designed for various applications.

Among NDs made by various synthetic methods, we work with DNDs (Fig. 1) made from explosives [1]. Diamond structure is formed from carbon atoms in the explosive molecules at very high temperature and pressure generated by detonation of a mixture of TNT and RDX in a closed chamber. An advantage of this method is that it can produce NDs in larger quantities at lower cost than other ND production methods. To maximize these features, we made development of the detonation process to generate diamond structure of DNDs. As a result, we were able to increase dramatically the yield of ND obtained from raw explosives. In addition, our DNDs have characteristics such as a small particle size (4 to 6 nm), a narrow particle size distribution, a large specific surface area (> 300 g/cm^2), a high chemical stability, and capable of being mixed with various materials.

Now we have started operating a pilot-scale detonation chamber (Fig. 2) and a purification facility commensurate with the detonation capacity, both installed in Japan. We can provide various types of ND samples with a high industrial quality control.
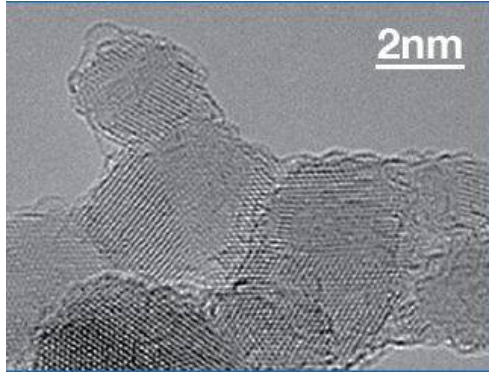
Fig. 1. TEM image of DNDs.

Fig. 2. Pilot-scale detonation chamber.

1. V. V. Danilenko, Specific Features of Synthesis of Detonation Diamonds, *Combust. Explos. Shock Waves,* 2005, vol. 41, no. 5, pp. 577–588.

EXPLOSIVE WELDING OF STAINLESS STEEL PIPE TO CARBON STEEL

A. Yu. Malakhov, I. V. Saikov, and I. V. Denisov

Merzhanov Institute of Structural Macrokinetics and Materials Science, Russian Academy of Sciences, Chernogolovka, Moscow, 142432 Russia

e-mail: sir.malahov2009@yandex.ru

The aim of this research is the study of the influence of explosive parameters and experimental schemes on the microstructure and properties of the welded interface and on the degree of transverse deformation. In this context, we carried out experiments on the explosive welding (EW) of pipes: outer layer was steel 37G2F (108 × 12 mm); inner (clad) layer was steel 08Kh18N10T (80 × 2 mm). The length of the pipes was 1 m. The experiments were carried out according to three developed schemes.

Schemes *1* and *2* assumed the filling of the inner cavity of the assembled pipes with an environment, which would reduce the degree of transverse deformation of the pipes during explosive cladding and prevent the destruction of the clad thin-walled layer. In the scheme *3*, an additional charge of explosives was used as a supporting element. The inner and outer charges were initiated by the layer of ammonite 6ZhV. As a result of experiments using schemes *1* and *2*, samples of bimetallic pipe billets with a length of 1 m were obtained. Scheme *3* failed to obtain a solid cylindrical billet. This is caused by the loss of synchronicity of anti-charges and, as a consequence, by the difference in pressures and throwing velocities of the inner and outer pipes.

Ultrasonic testing of the welded joint showed the presence of continuity defects at the butt ends of a two-layer pipe obtained according to the scheme *1* with a length of 50–60 mm. In the case of scheme *2*, the continuity defects were detected in the beginning and at the end of pipe with the length of up to 40 and 30 mm, respectively.

The places of incomplete penetration were found through the whole length of the pipe. Edge defects are caused by the scheme of centering to provide welding gap between the base billet and the clad billet.

To estimate the degree of deformation of the two-layer pipe billets produced by welding, the measurements of the outer diameter of the pipes along their full length and their out-of-roundness were carried out. As mentioned above, the initial outer diameter of the main thick-walled pipe was 108 mm. After the EW, it was 102 mm for the pipe with solid-liquid filler and 104 mm with filler in the form of steel rod. The investigation of the microstructure of the joint in longitudinal sections of the pipe obtained according to the scheme *1* showed no cracks and separations in the clad layer and base metal, and between the layers. The joint boundary through the whole length of the pipe has a wavy form with local regions of cast inclusions.

FEATURES OF HIGH-RATE DEFORMATION OF COPPER–TITANIUM RODS DURING EXPLOSION WELDING

A. Yu. Malakhov, I. V. Saikov, and P. A. Nikolaenko

Merzhanov Institute of Structural Macrokinetics and Materials Science, Russian Academy of Sciences, Chernogolovka, Moscow, 142432 Russia

e-mail: sir.malahov2009@yandex.ru

Explosive welding of long cylindrical products has a number of unresolved problems today. The main one is a sharp drop in the strength characteristics of the joint at a distance of more than 8–10 diameters, as well as in the deformation of the billet in the longitudinal and transverse directions. During explosive welding, shock waves pass through the welded materials. They, in turn, create elastic perturbations in the metal, which are capable to deform it. The degree of deformation significantly depends on the impact parameters, which in turn are calculated depending on the thickness of the throwing element and properties of the welded alloys. In the case of explosion welding of cylindrical products, there are significant problems in the calculation of welding regimes and development of additional equipment to reduce various kinds of deformation. This is because the process of throwing of a deformable element is much more complicated than that in the case of explosive welding of sheets.

The purpose of this paper was to determine experimentally the degree of longitudinal and transverse deformation of a titanium pipe VT1–0 during its explosion welding with a copper rod and to determine the effect of high-rate deformation on the elongation of the throwing pipe.

In the rod, a core was copper (16 mm in diameter (M1 brand)) and a shell was VT1–0 titanium alloy pipe 22 mm in diameter. The method of reference points and statistical processing of the results

revealed the dependence of the elongation of the titanium pipe (length of 1.5 m) on the detonation velocity D. Explosive welding of the copper rod with titanium pipe was performed according to three different regimes (different detonation velocities). It was found that the higher the detonation velocity, the smaller the elongation. At the velocity of more than 3.5–4.0 km/s, the titanium pipe becomes elongated. The greatest increase in the elongation of the pipe is observed over a length more than 800 mm from the beginning.

EXPLOSIVE WELDING OF METAL/Al AND PROCESS LIMITATIONS

R. Mendes[1], G. Sena[2], J. Ribeiro[1], A. Campos[1], and A. Loureiro[2]

[1] ADAI / LEDAP, DME, University of Coimbra, Rua Luis Reis Santos, Polo II, 3030-788 Coimbra, Portugal
[2] CEMMPRE, DME, University of Coimbra, Rua Luís Reis Santos, Polo II, 3030-788 Coimbra, Portugal

e-mail: ricardo.mendes@dem.uc.pt

Aluminum is one of the most used metals in engineering due to its unique characteristics. The use of combinations of aluminum and other metals like copper, stainless steel and carbon steel is growing considerably for electrical applications and transitions joints that need the combination of their respective properties with the low weight of aluminum [1, 2]. However, as the materials have very different physical properties like the melting temperature, welding these combinations by arc welding processes is very difficult. Thus, the joining between these materials usually achieves success through solid state welding processes like the explosion welding (EXW).

EXW is usually considered a solid-state welding process in which the detonation products of an explosive composition accelerate one of the materials to be welded against the other in order to promote a high-velocity oblique collision (see Fig. 1) that causes severe, but localized, plastic flow at the interacting surfaces.

Different explosives mixture can be used in order to reach the desired detonation velocity [3]. The high collision velocity, between 0.3 and 2 mm/µs, brings about pressures considerably greater than the strengths of any known material. This result in significant plastic deformation and the mixing of the surface layers of the materials to be bonded which can result in a linear or a wavy interface.
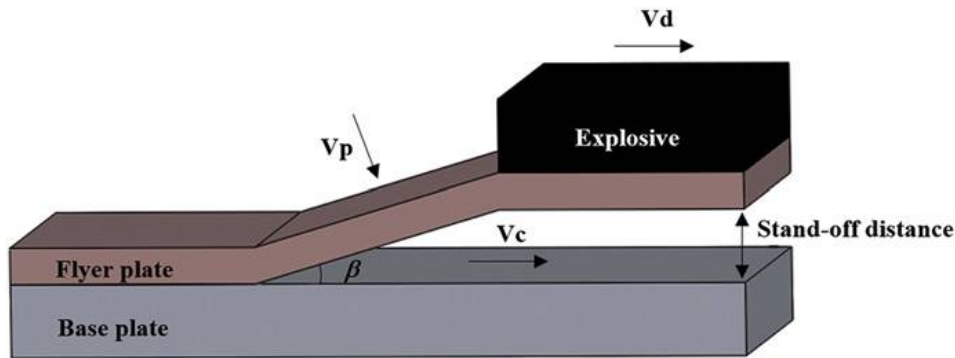
Fig. 1. Schematic representation of explosive welding process.

Physical properties like density; melting temperature and thermal conductivity play important role for the welding success. Welding metals having a similar density have a tendency to produce an interface having bigger waves. Despite the welding interface under low β–Vc show no wave in the joining zone [4] when the flyer is denser than the base plate and has a much higher melting temperature, it is possible that above a certain ratio, will prevent the formation of a wavy interface [2].

The objective of this work is to characterize some features regarding the weldability of aluminum alloys to other metals by EXW. Different welding parameters and explosive compositions for processing Al dissimilar welds were tested. For the Cu/Al [2, 5] and SS/Al systems the welds were performed on parallel configuration using ANFO and emulsion explosive (EE) with two different sensitizers, hollow glass microspheres (HGMS) and expanded polystyrene spheres (EPS) [3]. The effect of explosive to flyer mass ratio and the explosive compositions sensitized with different additives on the interface morphology and characteristics will be discussed.

While for the SS/Al was not possible to produce a successful welding, for Cu/Al a successful joining was possible. Despite presenting no waves or very small waves a higher wave amplitude was observed in welds produced with explosive compositions sensitized with EPS (Fig. 2). In turn, the dimension of the molten pockets was influenced by the explosive ratio, increasing in size with increases in the values of this parameter. The intermetallic content of these zones varied according to the sensitizer type.
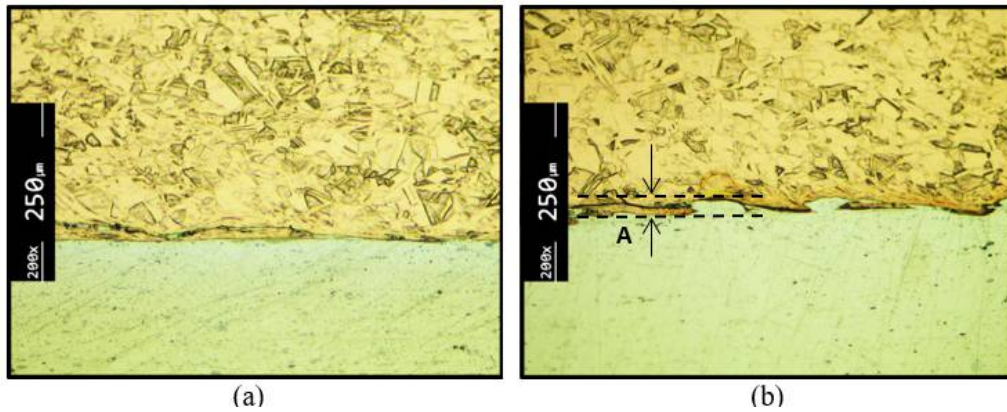
Fig. 2. Morphology of the weld interface produced with explosive composition sensitized with: (a) HGMS; (b) EPS.

The weldability window (plane of coordinates β–Vc) is a tool which shows the set of parameters that would increase the possibility to achieve a successful joining by EXW [4, 6]. However, there are cases in which despite using the parameters indicated by the weldability window, the plates separate after impact. Therefore, new approach must be considered to explain the unsuccessful welding.

As the EXW process is a high velocity collision process, a shock wave is generated in the flyer and base plate. The shock wave in flyer plate is reflected on the interface between the detonation products and flyer plate and attains again the interface between the two metals.

Considering the relative shock impedance of the flyer and base plate and comparing the time to solidify the melted pockets [7] formed during collision process with the time needed for the shock wave travelling inside the flyer attains again the interface of the materials, a second tool can be used to complement the weldability window approach.

1. G. H. S. F. L. Carvalho, I. Galvão, R. Mendes, R. M. Leal, A. Loureiro, Influence of base material properties on copper and aluminium–copper explosive welds, *Sci. Technol. Weld. Join.*, 2017, (in press); doi:10.1080/13621718.2017.1417783.
2. G. H. S. F. L. Carvalho, R. Mendes, R. M. Leal, I. Galvão, A. Loureiro, Effect of the flyer material on the interface phenomena in aluminium and copper explosive welds, *Mater. Des.*, 2017, vol. 122, pp. 172–183; doi:10.1016/j.matdes.2017.02.087.
3. R. Mendes, J. Ribeiro, I. Plaksin, J. Campos, B. Tavares, Differences between the detonation behavior of emulsion

R. Mendes et al.

explosives sensitized with glass or with polymeric micro-balloons, *J. Phys. Conf. Ser.*, 2014, vol. 500, pp. 1–6; doi:10.1088/1742-6596/500/5/052030.

4. A. A. Deribas, I. D. Zakharenko, Surface effects with oblique collisions between metallic plates. *Combust. Explos. Shock Waves*, 1974, vol. 10, pp. 358–367; doi:10.1007/BF01463767.

5. M. M. Hoseini Athar, B. Tolaminejad, Weldability window and the effect of interface morphology on the properties of Al/Cu/Al laminated composites fabricated by explosive welding, *Mater. Des.*, 2015, vol. 86, pp. 516–525.

6. J. B. Ribeiro, R. Mendes, A. Loureiro, Review of the weldability window concept and equations for explosive welding, *J. Phys. Conf. Ser.*, 2014, vol. 500, 52038; doi:10.1088/1742-6596/500/5/052038.

7. I. D. Zakharenko, Critical conditions in detonation welding, *Fiz. Goreniya i Vzryva*, 1972, vol. 8, pp. 422–427.

INVESTIGATION OF THE CaCrO$_4$/TiO$_2$/Al/C SYSTEM FOR THE PRODUCTION OF TITANIUM–CHROMIUM CARBIDE BY THE SHS METALLURGY METHOD

P. A. Miloserdov, V. A. Gorshkov, V. I. Yukhvid, and O. M. Miloserdova

Merzhanov Institute of Structural Macrokinetics and Materials Science, Russian Academy of Sciences, Chernogolovka, Moscow, 142432 Russia

e-mail: yu_group@ism.ac.ru

The creation of new materials with a high level of properties and technologies for their production is a key problem for modern technology. In this paper, we study the possibility of obtaining carbide ceramics from mixtures based on calcium chromate CaCrO$_4$ by the SHS metallurgy method. Refractory chromium compounds Cr$_{23}$C$_6$, Cr$_7$C$_3$, and Cr$_3$C$_2$ possess useful properties for solving technical problems (high hardness, strength, and wear and corrosion resistance) and are widely used in practice to create protective coating. The solubility of Cr$_3$C$_2$ in TiC at 1700°C is 30%. At the chromium carbide content of 30%, the microhardness of titanium carbide (3000 kg/mm^2) increases to 4000 kg/mm^2 [1–3].

We studied two green mixtures. The overall reaction schemes can be represented in the form

$$CaCrO_4 + Al + nC = Cr_xC_y + Al_2O_3 + CaO \ (70\%) \quad (1)$$
$$TiO_2 + (70\% \ Al/30\% \ Ca) + C = TiC + Al_2O_3 + CaO \ (30\%) \quad (2)$$
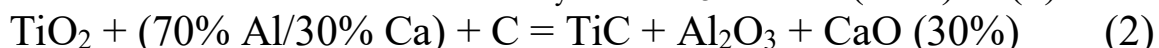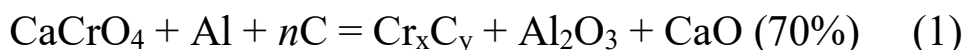
Thermodynamic analysis was carried out using a THERMO program. In system (1), the carbon content was varied to produce various chromium carbides: Cr$_{23}$C$_6$, Cr$_7$C$_3$ and Cr$_3$C$_2$. The analysis showed that the adiabatic temperature of the chemical transformation of the mixture (T_{ad}) exceeds 3000 K, and the products of the chemical

transformation of $CaCrO_4 + 2Al + nC$ mixture at this temperature consist of Cr–Al–C melts ("metallic" phase, the desired product) and Al_2O_3–CaO (oxide phase, slag product), as well as the gas mixture of metal vapors (Al, Cr, Ca), suboxide (Al_2O, Al_2O_2), and CO. An increase in the carbon content in the mixture (n) from 0 to 3.7% leads to a decrease in T_{ad} and weight fraction of the oxide phase, and to an increase in the content of the metallic and gas phases (Fig. 1).
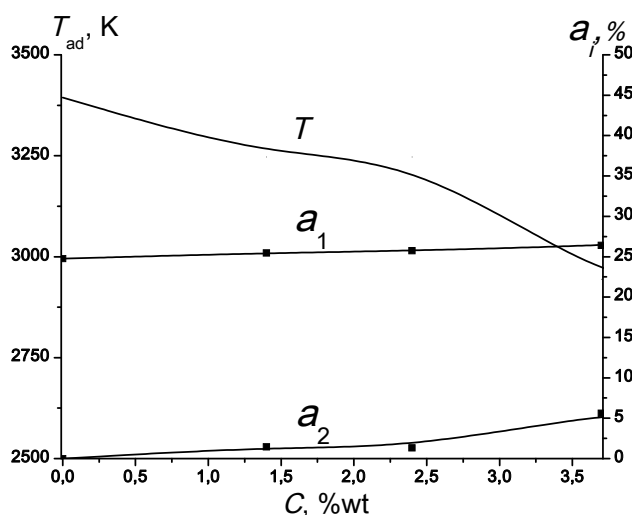
Fig. 1. Influence of the carbon content in the initial mixture on the calculated adiabatic temperature (T_{ad}) and mass fractions of metallic (a_1) and gaseous (a_3) chemical conversion products.

Experiments on this system showed that within the range $n = 0$–3.7%, the mixture retains the ability to burn. Combustion proceeds in the frontal mode with a constant velocity. Combustion products have a molded appearance and are easily divided into two layers: metal (target) and oxide (slag). As the carbon content in the initial mixture increases, the burning velocity and relative mass loss during combustion decrease, and the yield of the target product in the ingot increases (Fig. 2).

The results of the analysis show that the target products consist of different chromium carbides including MAX phase Cr_2AlC.
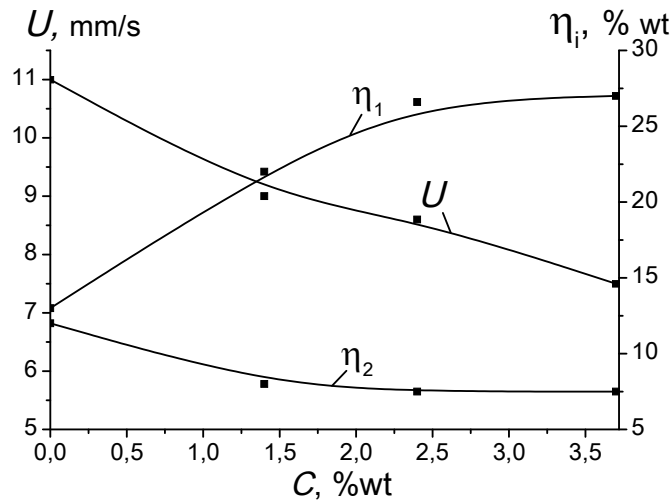
Fig. 2. Burning velosity U, yield of metallic phase η_1, and spread of combustion products (dispersion) η_2 as a function of n. $U = l/t$, where l is the height of the mixture, t is the time of burning; $\eta_1 = m/M_1$, $\eta_2 = [(M_1 - M_2)/M_1] \times 100\%$, M_1 is the mass of the initial mixture, M_2 is the mass of the final combustion products and m is the mass of the metal ingot.

The results of the thermodynamic analysis of mixtures, which were calculated from different ratios of mixtures (1) and (2) to produce titanium–chromium carbide, are shown in Fig. 3. It can be seen that an increase in the fraction of the mixture *2* (α) to 70% leads to a smooth decrease in the combustion temperature. Within the range $\alpha = 70-100\%$, the combustion temperature drops to 2600 K. The quantity of gaseous combustion products decreases to zero at $\alpha = 50\%$. The yield of the desired product (a_1) increases with increasing α. Experiments performed at $\alpha = 30\%$ indicate that the mixture burns, but there is no phase separation. To intensify the combustion process, a highly exothermic $CaO_2 + Al$ additive was added to the mixture, which led to the production of a cast product. XRD analysis shows that the product consists predominantly of the $Cr_xTi_{1-x}C$ phase (Fig. 4).
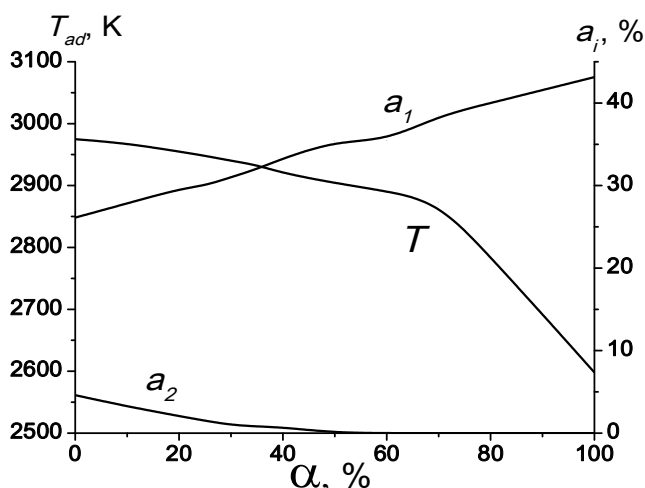
Fig. 3. Effect of α on the calculated adiabatic temperature (T_{ad}), mass fractions of metallic (a_1) and gaseous (a_2) chemical conversion products. $\alpha = (M_2/(M_1 + M_2)) \times 100\%$, where M_1 is the mass of the mixture (1), M_2 is the mass of the mixture (2).
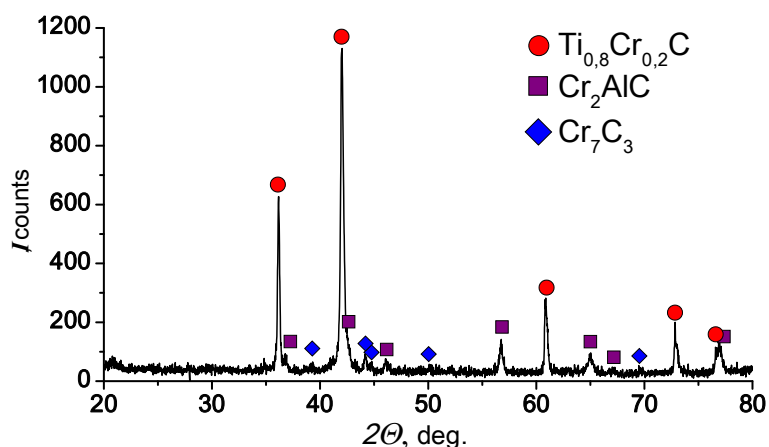
Fig. 4. XRD pattern of the product obtained at α = 30%.

1. R. Kiffer, F. Benezovskij, *Solid materials,* Moscow: Metallurgiya 1968 (in Russian).
2. V. V. Rudneva, G. V. Galevskij, Investigation of the corrosion resistance of nanopowders of refractory borides and carbides in solutions of electrolytes, *Izv. Vuzov. Tsvetnaya metallurgiya*, 2007, no. 2, pp. 67–70 (in Russian).
3. V. V. Rudneva, G. V. Galevsky, Thermooxidative stability of nanopowders of refractory carbides and borides, *Izv. Vuzov. Chernaya Metallurgiya*, 2007, no. 4, pp. 20–24 (in Russian).

SINTERING BEHAVIOR OF ZrC–TiC–MoSi$_2$ CERAMIC COMPOSITE

T. Minasyan[1], S. Aydinyan[1], L. Liu[1], S. Cygan[2], and I. Hussainova[1]

[1] Tallinn University of Technology, Ehitajate 5, 19180 Tallinn, Estonia
[2] Institute of Advanced Manufacturing technology, Wrocławska 37, 30-011 Kraków, Poland

e-mail: sofiya.aydinyan@gmail.com

Zirconium carbide (ZrC) belongs to a class of ultra-high temperature ceramics and is used as a candidate material for cutting tools, wear-resistance components and nuclear reactor core materials where its high temperature stability, room temperature hardness, low neutron cross-section, and high Young modulus are considered especially useful. However, scope of possible applications of ZrC expected to be significantly expanded due to the improving of densification behavior, high temperature hardness, sinterability and fracture toughness [1, 2]. TiC reinforcing ability was investigated on hardness and fracture toughness of 98% relative density samples produced by hot isostatic pressing (HIP) and high-pressure high-temperature (HPHT) sintering [3,4]. However further studies are needed to achieve full densification of ZrC with improved physicomechanical characteristics. In the present study, high-pressure high-temperature (HPHT) sintering was used as an innovative approach for the sintering of refractory carbides in the presence of molybdenum disilicide as toughening agent.

Commercially available ZrC powder underwent ball milling with TiC and MoSi$_2$ for 2 h in a stainless steel mill using 4:1 wt % ball to powder ratio. The densification process was carried out using the Bridgman-type toroidal apparatus - HPHT SPS technique. Under the influence of a simultaneous action of pressure (6–7.7 GPa) and temperature (1800–1950ºC) the sintering process occurred much faster

than in the case of conventional sintering. A typical duration of sintering process with HPHT method in the studied system lasts 40 s, which contributes to the grain growth limitation. Generally, due to the different thermodynamic conditions of the manufacturing process the materials obtained with HPHT method are characterized by full density, isotropy of properties and sometimes by a completely different phase composition in relation to the conventionally sintered materials. Due to the extended plastic deformation range at ultra-high pressure after the process materials will be characterized by improved mechanical properties (Young modulus, microhardness, etc.).

The bulk densities of the sintered samples were measured by Archimedes' technique using distilled water medium showing high density near to theoretical one. The hardness was determined by the Vickers indentation method applying load of 98.1 N (10 kg) and a dwell time of 10 s using an INDENTEC hardness testing machine. The comparison of microhardness results of the ZrC–TiC (18.6 GPa) and ZrC–TiC–$MoSi_2$ (22.4 GPa) systems showed that it significantly increases by the addition of molybdenum disilicide, conditioned by enhanced density of the samples.

Taking into consideration the phase transformation processes during the sintering process high temperature X-ray diffraction analysis was performed in the ZrC–TiC–$MoSi_2$ system in a temperature range from 20 to 1200°C (Fig. 1). Oxidation starts at 800°C leading to the formation of different modifications of zirconia and titanium, while molybdenum disilicide was stable in the whole studied temperature interval. SEM/EDS analyses indicate the good sinterability of composite, as well as homogeneous distribution of TiC and $MoSi_2$ phases through the ZrC particles.
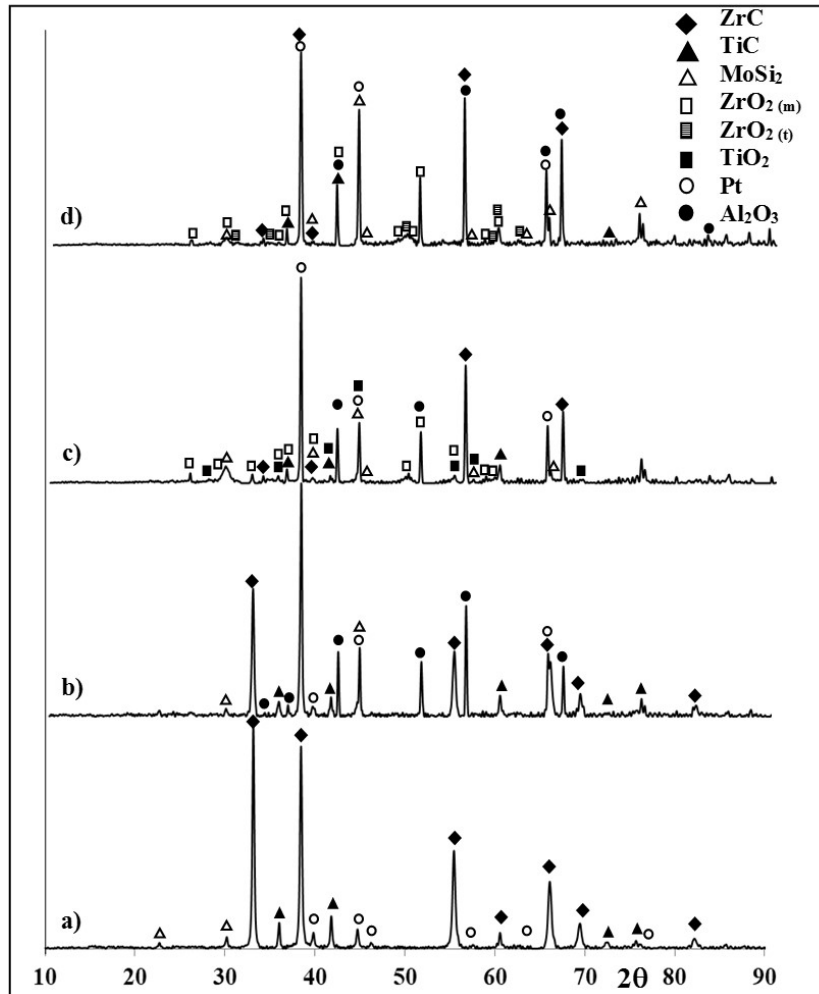
Fig. 1. XRD patterns of the sintered ZrC–TiC–MoSi$_2$ composite: (a) 20°C, (b) 600°C, (c) 800°C, (d) 1000°C.

1. L. Feng, L. Seahoon, L. Heesoo, Nano-sized zirconium carbide powder: Synthesis and densification using a spark plasma sintering apparatus, *Int. J. Ref. Met. & Hard Mater.*, 2017, vol. 64, pp. 98–105.

2. Ch. Nachiappan, L. Rangaraj, C. Divakar, V. Jayaram, Synthesis and densification of monolithic zirconium carbide by reactive hot pressing, *J. Amer. Cer. Soc.*, 2010, vol. 93, no. 5, pp. 1341–1346.

3. M. Umalas, I. Hussainova, V. Reedo, D.-L. Young, E. Cura, S.-P. Hannula, R. Lõhmus, A. Lõhmus, Combined sol–gel and carbothermal synthesis of ZrC–TiC powders for composites, *Mater. Chem. Phys.*, 2015, vol. 153, pp. 301–306.

4. D.-L. Yung, S. Cygan, M. Antonov, L. Jaworska, I. Hussainova, Ultra high-pressure spark plasma sintered ZrC–Mo and ZrC–TiC composites, *Int. J. Ref. Met. & Hard Mater.*, 2016, vol. 61, pp. 201–206.

T. Minasyan et al.

SYNTHESIS AND CONSOLIDATION OF Mo–Cu COMPOSITE NANOPOWDER

T. Minasyan[1,3], H. Kirakosyan[1], S. Aydinyan[1,3], L. Liu[3], I. Hussainova[3,4], and S. Kharatyan[1,2]

[1] Laboratory of Kinetics of SHS Processes, Nalbandyan Institute of Chemical Physics NAS RA, 5/2, P. Sevak Str., Yerevan, 0014 Armenia

[2] Department of Inorganic and Analytical Chemistry, Yerevan State University, A. Manoogian Str., Yerevan, 0025 Armenia

[3] Department of Mechanical and Industrial Engineering, Tallinn University of Technology, Ehitajate tee, Tallinn, 19086 Estonia

[4] ITMO University, Kronverkskii 49, St. Petersburg, 197101 Russia

e-mail: tatminas@gmail.com

The technological development often requires materials of tailorable properties, such as pseudo-alloys of copper and molybdenum, which mechanical and thermo-electrical properties are highly influenced by percentage of the compounds and fabrication methods. The Mo–Cu materials combine the properties of both metals leading to the optimization of alloy properties, such as high thermal and electrical conductivity, fatigue resistance, low and alterable thermal expansion coefficient, low weight, nonmagnetic and excellent high-temperature behavior [1, 2]. In view of these features, they find their main applications as welding electrodes, microwave carriers, optical and power packages, heat sinks, micro electrical hybrids and butterfly packages for telecom systems.

Here we report the preparation of Mo–Cu composite materials by self-propagating high temperature synthesis (SHS) or combustion synthesis (CS) method using copper molybdate and Mg/C combined reducer as precursors. For the consolidation of composite powder, the spark plasma sintering (SPS) technique was exploited. Copper molybdate was prepared by two pathways: calcination of MoO_3 and

CuO powders mixture in air at 700°C for 3 hours (CuMoO$_4$(I)) and chemical co-precipitation of molybdenum and copper water soluble salts (CuMoO$_4$(II)).

Thermodynamic calculations were performed to reveal the possibility of combustion in the CuMoO$_4$ (I and II)–yMg–xC system, as well as to estimate the adiabatic combustion temperature and the equilibrium quantities of possible products. Based on the thermodynamic calculation the combustion reactions were performed with a relatively low amount of magnesium ($y = 1.2$ mol for CuMoO$_4$(I) and $y = 1.5$ mol for CuMoO$_4$(II)) for the complete reduction of copper molybdates at moderate conditions.

The optimum composition of mixtures was found by changing the amount of carbon in the initial mixture. The combustion peculiarities of the CuMoO$_4$(I)–1.2Mg–xC and CuMoO$_4$(II)–1.5Mg–xC systems were investigated in the wide range of carbon amount up to 3 moles. As a result, the mixtures of CuMoO$_4$(I)–1.2Mg–2.2C and CuMoO$_4$(II)–1.5Mg–1.6C were found as optimum for complete reduction of both the metals. Following the synthesis the acid leaching was performed to get rid of byproduct magnesia. SEM analysis indicate that M–Cu nanosized (50–100 nm) composites with spherical particles of narrow size distribution (Fig. 1a, 1b) were obtained.
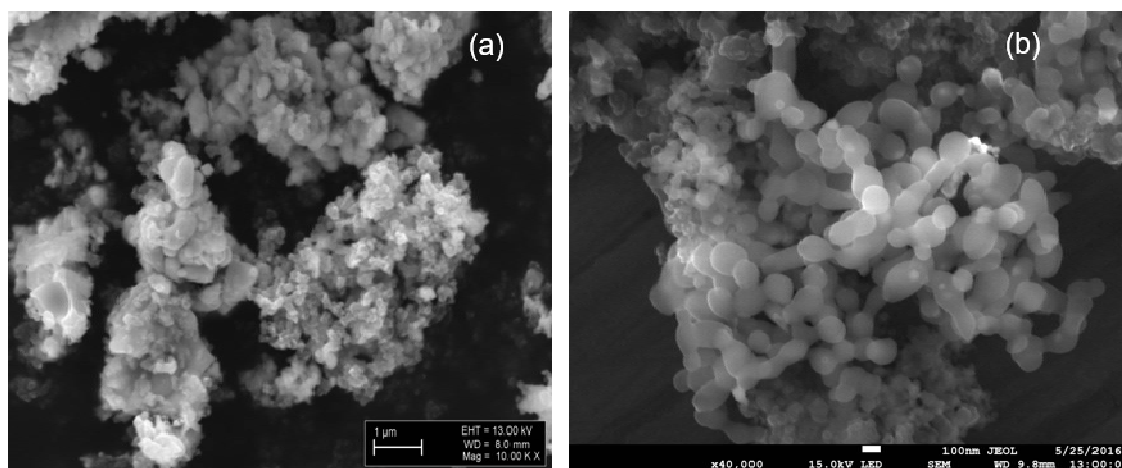
Fig. 1 SEM micrographs of (a) Cu–Mo (I) and (b) Cu–Mo (II) powders.

Interruption of the combustion process in bulk copper wedge was performed to evaluate the interaction mechanism based on the phase and microstructural composition of the samples taken from various sections of the wedge. The copper wedge experiments revealed that

the multi-stage interactions at the combustion of $CuMoO_4$–Mg–C systems start with a low caloric carbothermic reaction without preliminary salt decomposition and continue by a high-caloric magnesiothermic reduction.

After characterization, Mo–Cu composite was subjected to SPS in a temperature range from 950 to 1050°C. As expected, a longer dwelling time results in grain coarsening and, consequently, decrease in hardness. Based on parametric studies, the optimum temperature for compaction was chosen 1000°C applied during 3 min. Cu–Mo compact samples showed improved density and enhanced microhardness values (3.11–3.21 GPa).

1. S. V. Aydinyan, H. V Kirakosyan, S. L. Kharatyan, Cu–Mo composite powders obtained by combustion-coreduction process, *Int. J. Ref. Met. & Hard. Mater.,* 2016, vol. 54, pp. 455–463.
2. S. N. Alam, Synthesis and characterization of W–Cu nanocomposites developed by mechanical alloying, *Mater. Sci. Eng*: *A,* 2006, vol. 433, no. 1–2, pp. 161–168.

PHENOMENA OF WELDING FOR SIMILAR AND DISSIMILAR MATERIALS IN THE OBLIQUE COLLISION

A. Mori[1], S. Tanaka[2], and K. Hokamoto[2]

[1] Mechanical Engineering, Sojo University, 4-22-1 Ikeda, Nishi-ku, Kumamoto, 860-0082 Japan
[2] Institute of Pulsed Power Science, Kumamoto University, 2-39-1 Kurokami, Chuo-ku, Kumamoto, 860-8555 Japan

e-mail: makihisa@mec.sojo-u.ac.jp

In the explosive welding technique, the collision angle and collision velocity are the important parameters to achieve the good welding. It is known well that a metal jet and the interfacial waves, which are the characteristic phenomena in explosive welding, are generated when the collision angle and the velocity are in the suitable range. To know the parameters and the collision conditions, the optical observation and the numerical simulation for the oblique collision using a powder gun were done by authors [1]. In this investigation, the results of the optical observations and the numerical analysis for similar and dissimilar material combinations were reported.

A pure copper disc and a magnesium disc (AZ31) (32 mm-diameter) were used for material combination. Figure 1 shows the experimental results for dissimilar material combination when the copper and the AZ31 disc were used as the target and the projectile disc, respectively. And 10 mm-thick copper plate was set behind the projectile plate to control the impact velocity. As shown in Fig. 1, metal jet was observed clearly in the similar and dissimilar metals. However, the welding could not be achieved in the magnesium alloy used.
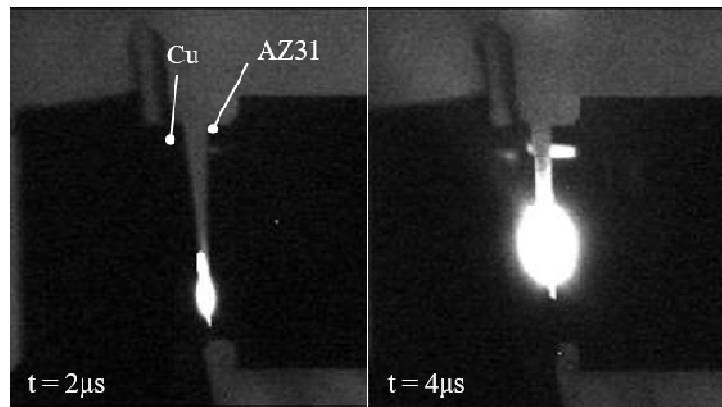
Fig. 1. Framing photographs of the oblique collision for copper and magnesium alloy combination (The collision velocity: 464 m/s; the collision angle: 7 deg.).

In Fig. 2, the example of the numerical simulations was shown in the condition of Fig.1. The generation of metal jet and the small wavy interface was simulated by using SPH solver in AUTODYN-2D. From this numerical result, the metal jet consists the magnesium alloy only and the temperature in the collided interface of AZ31 was increased at 3000~3500 K. And many oblique lines (like shear bands) could be observed in this combinations. The amount of kinetic energy loss calculated by the equation in [2] was 3.342 MJ/m^2. It was thought that the hard-brittle reaction layer was generated and the separation was occurred along the interface of Cu-magnesium alloy for high kinetic energy conditions. Then, to decrease the kinetic energy loss, the method to make a dent in a diaphragm was applied. As a result of this method, the welding of similar and dissimilar metal for magnesium alloy was achieved as shown in Fig. 3.
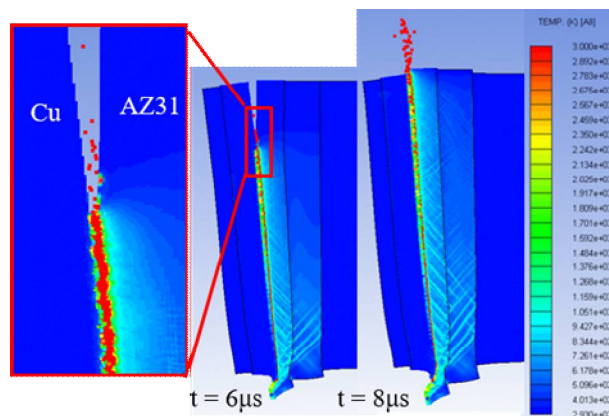
Fig. 2. Temperature contour simulated by AUTODYN-2D (5mm-Cu and 7mm-AZ31, with 10mm-thick Cu disc, V_p = 464 m/s, α = 7°).
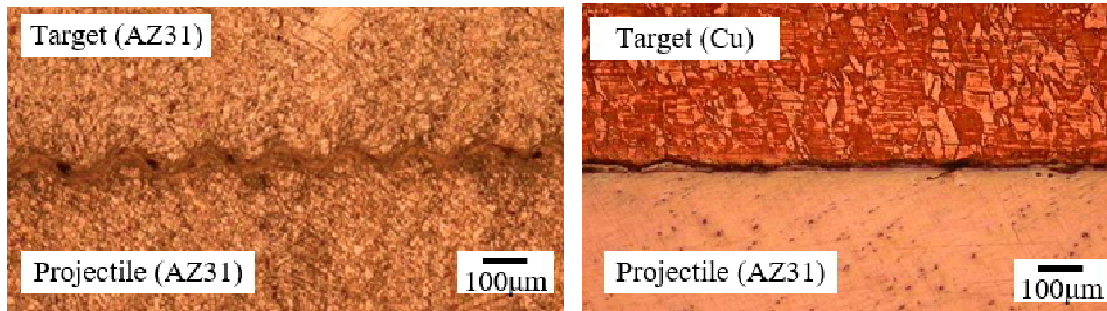
Fig. 3. Welded interface of similar (AZ31–AZ31; Left) and dissimilar (AZ31–Cu; Right) combination.

1. A. Mori, S. Tanaka, K. Hokamoto, Optical observation of metal jet generated by high speed inclined collision, *Proc. SPIE 10328,* 2017, 103281Q.
2. P. Manikandan, K. Hokamoto, A.A. Deribas, K. Raghukandan, R. Tomoshige, Explosive Welding of Titanium/Stainless Steel by Controlling Energetic Conditions, *Mater. Trans.*, 2006, vol. 47, no. 8, pp. 2049–2055.

THE INFLUENCE OF SEVERE PLASTIC DEFORMATION ON THE PROPERTIES OF METALS AND ALLOYS

R. R. Mulyukov

Institute for Metals Superplasticity Problems, Russian Academy of Sciences, Ufa, 450001 Russia

e-mail: radik@imsp.ru

Severe plastic deformation methods such as high-pressure torsion, equal channel angular pressing and multiple isothermal forging are used to convert coarse-grained metals and alloys into ultrafine-grained (UFG) and nanostructured (NS) materials. The features of these materials are their mechanical and physical properties. There is observed a decrease in the elastic modulus, polymorphic transformation temperature, magnetic transformation temperature, saturation magnetization and electron work function. The values of the yield stress, strength, amplitude-independent internal stress, specific isobaric heat capacity, specific electrical resistivity, diffusion coefficient and ion induced electron emission increase. Furthermore, the extraordinary superplasticity characteristics are observed. The presence of nonequilibrium grain boundaries in nanostructured materials can lead not only to quantitative changes but also to qualitative ones in the behavior of metals and alloys.

Examples of practical application of ultrafine-grained and nanostructured materials produced by severe plastic deformation are also presented.

DETERMINATION OF THE LEVEL OF THE STRESSED-DEFORMED CONDITION OF BIMETALS PRODUCED BY EXPLOSION WELDING USING METAL MAGNETIC MEMORY METHOD

D. V. Nonyak[1], O. L. Pervukhina[1], and L. B. Pervukhin[2]

[1] Merzhanov Institute of Structural Macrokinetics and Materials Science, Russian Academy of Sciences, Chernogolovka, Moscow, 142432 Russia
[2] Bardin Research Institute for Ferrous Metallurgy, Moscow, 105005 Russia

e-mail: nonyak@bk.ru

Bimetals obtained by explosion welding are firmly connected layers, combining different physical and mechanical properties of the initial materials. As a rule, large-sized products used in corrosive mediums are produced of these materials. The welding zone in the bimetal is the interface where the materials are in the stress-stain state after the explosion loading, heat treatment, further technological redistribution.

According to the literature on the study of the structure of the joint and the properties of sheet bimetals obtained by explosion welding on the basis of structural steel, stainless steels, nonferrous metals and alloys, it has been found that if the bimetal underwent incorrect heat treatment and was deformed, defects, cracks and fractures coming from the welding zone can possibly appear in the process of making items from it [1]. When residual stresses were measured on individual samples of metal pairs using the destructive methods, a high level of residual stresses close to the yield point was found right in the welding zone. After the heat treatment of bimetals, the level of residual stresses, the structure and strength of the joint changes [2]. In the process of using products made of bimetals, when they are heated to operating temperatures and then cooled, the stress-strain state also changes. This can lead to the structural changes due to diffusion

processes and, as a consequence, to changes in the properties and durability of the product. Nowadays, there are no published studies on the complex effect of the mentioned factors on the evolution of the stress-strain state in the process of production of bimetal and items made of it. Thus, the study of the stress-strain state at all stages of creating material and equipment of it is a relevant task.

The strategy of determining the level of the stress-strain state of the welding zone of bimetals by the non-destructive method of magnetic memory of metals will be presented in this research. The complex of studies of materials with different magnetic properties made it possible to reveal the regularities of the influence of shock wave loads and technological redistribution (heat treatment, plastic deformation) on the properties of material magnetization and the distribution of potentially dangerous stress concentration zones. Comparison of the results of mechanical tests, studies of the structure and continuity of the joint made it possible to establish their evolution and their connection with the level of stresses in obtaining bimetal and the following technological alterations.

Complex studies of the connection of the stress-strain state, structural changes and parameters of the technological process will make it possible to create materials with an optimal combination of residual stresses, structure and properties of the joint due to the formation of these parameters in the process of production of the bimetal that will increase the structural strength and durability of the bimetal equipment produced by explosion welding.

Experimental studies of the stress-strain state of bimetal at all stages of production are carried out on the equipment and production facilities of Bitrum International LLC.

1. L. B. Pervukhin, V. A. Maltsev, Yu. A. Konon, B. D. Tsemahovich, A. D. Chudnovsky, Distribution of internal stresses in bimetal steel 22K+08X18N10T, obtained by explosion welding, *Met. Sci. Heat Treat.*, 1975, no. 11, pp. 28–32.
2. Yu. A. Konon, L. B. Pervukhin, A. D. Chudnovsky, *Welding by explosion*, M.: Mashinostroenie, 1987.

STUDY OF TECHNOLOGICAL PARAMETERS IN Ti–Cr–C–STEEL, Ti–B, Ti–B–Me SYSTEMS FOR OBTAINING PRODUCTS BY SHS–ELECTRICAL ROLLING

G. Oniashvili, Z. Aslamazashvili, T. Namicheishvili, G. Tavadze, Z. Melashvili, A. Tutberidze, and G. Zakharov

Tavadze Institute of Metallurgy and Materials Science, Tbilisi, 0186 Georgia

e-mail: oniash@gtu.ge

In the paper the innovation technology of self-propagating high-temperature synthesis (SHS)–electrical rolling (ER) is proposed. For realizing the process, it is mandatory and sufficient that initial components after initiation by thermal pulse could interaction with the heat emission, which ensures the self-propagation of synthesis front in lieu of heat transfer over the entire sample.

By using the electrical contacts, electric energy is delivered in the heart of deformation area with the use of electric contact and the heat generated in the initial section of deformation heart initiates the SHS process. As a result, the front of synthesis is created, which starts to move with certain speed in the sample located in container. At a certain time, the rolls instantly start to rotate with a set rate to ensure the synchronization of velocity of rolling and synthesis front displacement along the material. The synthesized product in hot plastic condition is delivered to the rolls in the nonstop regime in the deformation zone, simultaneously, providing the current in deformation zone in order to compensate the energy loses. As a result of using the innovation SHS–ER technology we produce required metal-ceramic product of any length (Fig. 1).
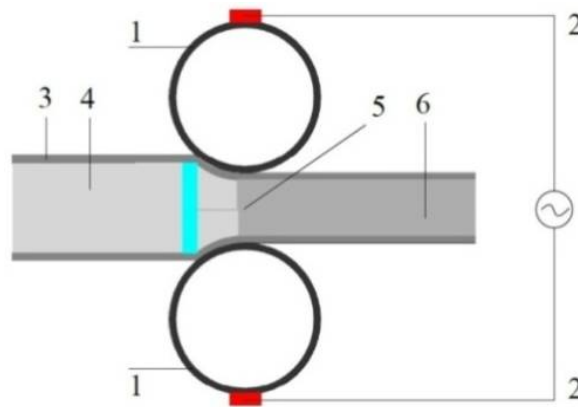
Fig. 1. Production of composite material by SHS – electrical rolling; *1* rolls, *2* heating electric contacts, *3* container, *4* briquette of chasm, *5* synthesis (combustion) front, *6* rolled sample.

In Ti–Cr–C–Steel, Ti–B and Ti–B–*Me* systems, the high quality (imporosity or low porosity < 2%) of materials and product directly depends on the liquid phase content immediately after the passing of synthesis front in the sample. The high content of the liquid phase provides the higher quality of material. The content of the liquid phase depends on the synthesis parameters: speed and temperature of synthesis. The higher are the speed and temperature of synthesis, the higher is the liquid phase content.

For obtaining high-quality rolled samples, in addition to the synthesis parameters, it is also important to define technological so-called compaction parameters and their optimal values. These parameters (time, pressure and temperature) depend on the parameters of synthesis and are determined experimentally. These parameters are as follows: time of delay from initiation of synthesis to the starting of rolling τ_d; rolling time τ_r; initial rolling pressure P_i; rolling pressure P_r; current for the compensation of heat losses I; rolling velocity V_r and synthesis velocity V_s. These described parameters were defined. The optimal values of the parameters, which provide the maximum density, hardness and strength, were defined using mathematical statistics.

INVESTIGATION OF THE INFLUENCE OF SHOCK ACTIVATION ON MAIN PROPERTIES OF PIEZOELECTRIC CERAMICS

Ch. G. Pak, A. V. Pryshchak, and G. A. Koshkin

Penza State University, ul. Krasnaya 40, Penza, 440026 Russia

e-mail: metal@pnzgu.ru

The apparatus for transformation of mechanical vibrations and stresses into electrical signal is based on devices incorporating materials possessing piezoelectric properties. Piezoelectric effect is a concentration of surplus electrical charge with opposite polarity on opposite surfaces of crystal under the applied mechanical stress. This effect occurs due to deformations of stressed crystal lattice that leads to the change in the dipole momentum of domains, which comprise the microstructure of material. The most widely used class of piezoelectric materials for industrial application is a piezoelectric ceramics of different types.

The goal of present work is to investigate the influence of shock activation on electrical and mechanical properties of piezoelectric ceramics of the lead zirconate titanate (PZT) family. To achieve the main goal, the following intermediate tasks were defined: (a) to develop a principal scheme of shock activation process; (b) to determine optimal parameters of high explosive (HE) charge; (c) to investigate electrical and mechanical properties of materials produced with activated powders.

Basic scheme of shock activation process is presented in Fig. 1. The used scheme is typical of shock activation of ceramic powders.
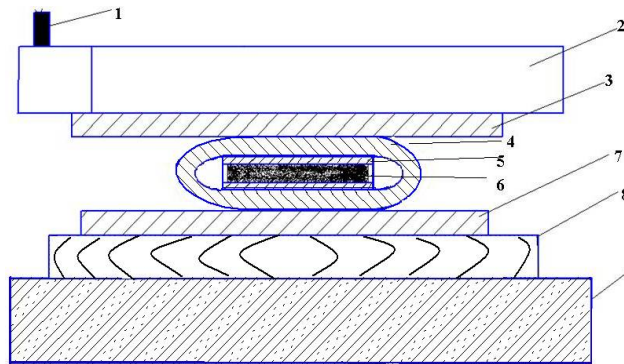
Fig. 1. Schematic of shock activation process: *1* electric detonator; *2* explosive container; *3* flyer plate; *4* tube; *5* container; *6* powder ; *7* base plate; *8* woodchip board; *9* soil.

Upon determination of parameters of HE charge, in addition to geometrical properties, the assembly parameters of the initial powder system were also taken into account. Shock activation was applied for already synthesized PZT powders with different compositions. Main controlled input parameters of powder are particle size, their surface morphology, and mechanical properties (strength, microhardness, density).

After the shock activation, green compacts were ground using a planetary mill with stabilized zirconia balls. Powders were mixed with a temporary organic binder and pressed under a pressure of 75–100 MPa. Compacts were sintered in lead-rich environment to avoid deviations from stoichiometric composition. Sintered samples were cut into disks and coated with metal of opposite faces. Then, metallized samples were subjected to polarization for stabilizing their electrical and mechanical properties. Piezoelectric modulus d_{33}, permittivity ε, tangent of dielectric losses tan δ, Q factor, and bending strength σ of obtained samples were determined.

1. B. Jaffe, *Piezoelectric ceramics*, Elsevier, 2012, vol. 3.
2. J. L. Jordan, N. T. Naresh, Effect of shock-activation on post-shock reaction snthesis of ternary ceramics, *AIP Conference Proceedings*, 2002, vol. 620, no. 1.
3. A. E. Rozen, *Development of scientific basis of technological process of explosive pressure, structure formation and properties of ferroelectric ceramic materials*, Doctor of technical sciences thesis, Volgograd, 1999 (in Russian).

OBTAINING CLOSE-CUT-FRACTION SPHERICAL MICROPOWDERS OF HEAT-RESISTANT ALLOY BASED ON NICKEL MONOALUMINIDE

E. I. Patsera[1], V. V. Kurbatkina[1], E. A. Levashov[1], Yu. Yu. Kaplanskii[1], and A. V. Samokhin[2]

[1] National University of Science and Technology MISIS, Moscow, 119049 Russia
[2] Baikov Institute of Metallurgy and Materials Science, Moscow, 119334 Russia

e-mail: Patsera_yevgeniy@mail.ru

Adoption of additive technologies (AT) by Russian enterprises is a trend in production modernization at the modern stage of development. Use of spherical powders, which have high values of fluidity and loose bulk density as well as a definite granulometric composition, is a peculiarity of manufacturing articles and parts through AT. Developers of alloys and materials for articles with complicated shapes show the largest interest in AT, because it is in this field that the potential of tough-to-machine alloys, such as intermetallic-based alloys, can be fulfilled. Nickel monoaluminide (NiAl), which possesses a unique complex of physico-mechanical properties, is a promising basic material for creation of heat-resistant alloys of new generation able to supplant nickel superalloys. However, its practically zero viscosity of failure at room temperature as well as its insufficient strength and low resistance to creep at a temperature of more than 700°C prevent the industrial application of NiAl-based alloys. The strength characteristics of NiAl can be enhanced by selecting an optimal alloying system that would make it possible to strengthen NiAl with refractory metals such as Cr, Co, Mo, Ti, Hf, etc.

This research has been aimed at development of an effective way of obtaining close-cut-fraction micropowders from new heat-resistant

alloys based on nickel aluminide in order to make geometrically complicated vital parts of airspace machinery using additive production technologies.

The promising NiAl–Cr–Co–Hf CompoNiAl M5–3 alloy composition [1] was chosen in order to obtain close-cut-fraction micropowders from materials of the new generation for additive technologies. Elemental synthesis with addition of the functional additive NaCl was used as a way of obtaining powders from heat-resistant alloy based on nickel aluminide (CompoNiAl M5–3 composition). According to the results of researches conducted earlier, it has been established that addition of sodium chloride (NaCl) to Ni+Al mixture decreases the heat release, temperature and speed of combustion during the elemental synthesis process.

Influence of the initial temperature on the temperature and speed of combustion of the composition with the salt has been researched in the work. The combustion temperature of CompoNiAl M5–3 + 10% NaCl mixture is 1380º C, which is lower than the melting temperature of nickel. As the initial temperature grows, the combustion speed increases, but the temperature remains practically constant, which is characteristic of intermetallic systems with a melting component.

The stages of the phase formation in the combustion wave have been studied through the stopped combustion front method. By analyzing the stages of the reactions that take place during the synthesis of CompoNiAl + 10% NaCl composition, it can be concluded that dissolution of nickel in aluminum melt is the driving force of the synthesis process. At the same time, NiAl, as opposed to the NiAl + 10% NaCl system studied earlier, forms not from the melt, but in the aftercombustion zone as a result of diffusive processes.

The research of the kinetics and stages of the reactions in the CompoNiAl M5–3 + 10% NaCl mixtures has shown that in order to synthesize alloy of the specified composition, it is necessary to use mechanical activation (MA) aimed at decreasing the scale of its heterogeneity and enhancing the reactive capacity of the mixture. The powders of refractory chromium and hafnium metals used in the work are polydisperse, and the big particles do not have enough time to dissolve completely during the synthesis, which leads to inhomogeneity of the chemical and phase composition of the synthesized products.

The optimal mode of the MA was researched using planetary mills Pulverisette 5/2 (Fritsch, Germany), MPP-1 (Technics and Technology of Disintegration, Russia) and Activator-4M (Activator, Russia). The centrifugal acceleration was 22, 28, and 150 g, respectively. The reaction mixture of specified composition was activated at equal parameters: a balls-material ratio of 10:1 and a drum filling coefficient $\varphi = 0.55$. The comparative researches of the structure and distribution of components in the MA mixtures and synthesized samples have shown that the treatment of the initial mixture in the Activator-4M for 12 min is the optimal mode. Experimental researches of grinding the synthesized CompoNiAl M5–3 composition alloy samples obtained through the elemental synthesis and washing them from the salt have been conducted. The optimal mode of the disintegration that ensures the maximal output of the 20–45 μm fraction has been found. Powders of this fraction have been tested when researching into the spheroidization process in an electroarc plasmatron reactor.

The plasmatic treatment was the most effective when using the electroarc plasmatron with a nozzle of 38 mm and mixture of plasma-forming gases Ar with H_2 (up to 17 v/v %). The degree of spheroidization of the particles treated in this mode reaches 98%. The research results have been used for obtaining close-cut-fraction spherical micropowders of heat-resistant alloy based on nickel monoaluminide with a multi-level hierarchic structure that contains nanodisperse emanations of the excess phase formed through the SHS method from the elemental powders in one stage.

1. A. A. Zaitsev, Z. A. Sentyurina, E. A. Levashov, Y. S. Pogozhev, V. N. Sanin, P. A. Loginov, M. I. Petrzhik, Structure and properties of NiAl–Cr(Co,Hf) alloys prepared by centrifugal SHS casting. Part 1: Room temperature investigations, *Mater. Sci. Eng. A*, 2017, vol. 690, pp. 463–472; doi:10.1016/j.msea.2016.09.075.

E. I. Patsera et al.

SYNTHESIS OF SUPERREFRACTORY SOLID SOLUTIONS BASED ON BORIDES OF ZIRCONIUM, HAFNIUM AND TANTALUM

E. I. Patsera[1], V. V. Kurbatkina[1], E. A. Levashov[1], and N. A. Kochetov[2]

[1] National University of Science and Technology MISIS, Moscow, 119049 Russia
[2] Institute of Structural Macrokinetics and Materials Science, Russian Academy of Sciences, Chernogolovka, Moscow, 142432 Russia

e-mail: patsera_yevgeniy@mail.ru

Composites based on diborides of tantalum, hafnium and zirconium are promising materials for operation at temperatures higher than 2000ºC. The combination high thermal conductivity and low coefficient of thermal expansion of these materials creates prerequisites for their high resistance to a thermal shock, which is extremely important for materials applied in airspace technologies.

Self-propagating high-temperature synthesis (SHS), which permits synthesizing unique composites [1, 2], is a method for obtaining refractory materials. That is why the aim of the work was to research into the possibility of obtaining superrefractory materials based on solid solutions of zirconium diboride, hafnium diboride and tantalum diboride through the SHS method.

The adiabatic temperature was calculated by THERMO software, which amounted to 3323 K for the $Zr + 27.7\%$ Ta $+ 16.4\%$ B ($ZrB_2 + 20\%$ TaB_2) composition (hereinafter 1) and 3222 K for the $Zr + 48.7\%$ Ta $+ 14.5\%$ B ($ZrB_2 + 40\%$ TaB_2) composition (hereinafter 2). At that temperature, the initial regents and intermediate products can melt in the Zr–Ta–B system, and the process will take place with less kinetic impediments. The results of the calculation of the adiabatic temperature of combustion of the Hf–Ta–B mixtures showed that T_{ad} equals 3522 K for the Hf–18.03% Ta–10.78% B (80% $HfB_2 + 20\%$

TaB_2) composition (hereinafter *3*) and 3372 K for the Hf–47.69% Ta– 12.03% B (60% HfB_2 + 40% TaB_2) composition (hereinafter *4*). At a temperature of 3522 K, the initial reagents of the first composition as well as the intermediate borides of tantalum and hafnium will melt, and in the case of the second composition, at 3372 K, boron (T_{melt} = 2350 K) and hafnium (T_{melt} = 2505 K) will melt.

The attempts to measure the speed and temperature of combustion of the composition mixture *1* at different initial temperatures (T_0) were unsuccessful. However, when the mixture was diluted by 10% of the end product (Zr,Ta)B_2, the combustion speed amounted to 13.4 mm/s and the temperature was 3451 K. The combustion temperature (T_c) of the mixture *2* was 2686 K at T_0 = 293 K. It has been shown that the dependence of the combustion speed on T_0 is linear: as T_0 grows from 293 K to 823 K, the speed increases from 5 mm/s to 23.4 mm/s. However, at T_0 higher than 293 K, the combustion temperature could not be measured, since it exceeded operating temperature of thermocouple. A spin mechanism of the combustion, which evidences the limiting role of vapor mass transport of the reagents and its influence on the combustion mechanism, is a peculiarity of this system.

Combustion temperature T_c of mixtures has also been measured in the Hf–Ta–B system at various T_0 from 297 to 673 K. The combustion process could not be initiated in composition mixture *3* at room temperature. This is due to formation of a stronger, in comparison with zirconium, oxide film on the hafnium particles; the film seems to be destroyed only when heated up to 413 K. The measured T_c values proved to be lower than the calculated ones by 700 K. At T_0 of more than 413 K, the combustion temperature of both compositions feebly depends on T_0 and amounted to 2550 K, and taking into account the measurement error, it may be considered invariable. This can be related to formation of a large amount of the melt. For the composition *4*, a bend was observed on the dependence $T_c(T_0)$ at T_0 = 413 K. Formation of tantalum boride at a temperature lower than the melting point of boron is a peculiarity of this system, which is possible with the participation of vapor mass transport of the reagents. Hafnium diboride forms from the melt after the boron has melted.

Using the stopped combustion front (SCF) method — quenching in a copper wedge and further EDS analysis of characteristic zones of the

combustion wave in the SCF sample — the following phenomenological scheme of the structure formation in the Zr–Ta–B combustion wave has been proposed (Fig. 1) [3].
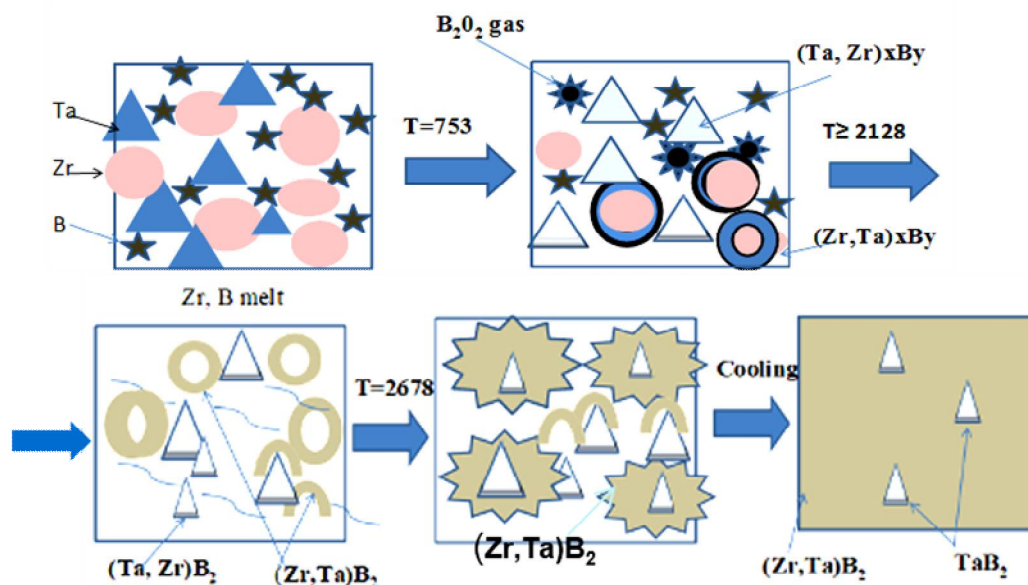
Fig. 1. The scheme of the structure formation in the combustion wave of the Zr–Ta–B mixture.

The research of the samples with the SCF in the Hf–Ta–B mixtures has permitted making an assumption about the behavior of the reactions in the combustion wave. Initially, volatile suboxide B_2O_2 forms in the warm-up zone at the temperature of 750 K; the suboxide is chemosorbed on the surface of the tantalum and hafnium particles with the formation of tantalum boride and hafnium boride. When the temperature reaches 2153 K at the places where the HfB particles contact the solid solution β-Hf with a boron content of 13 at % (≤ 0.8 mass %), the eutectic reaction HfB + β-Hf → L takes place and the melt appears. The boron melts at 2365 K, and the first crystals of HfB_2 appear almost at the same time. Then, the hafnium melts (2505 K) and starts to interact actively with the boron. The high combustion temperature results in large thermal losses into the environment, and there is practically no aftercombustion zone on the SCF sample. That is why the final composition of the products formed in the combustion zone changes feebly if cooled fast.

Using the unpressurized SHS technology, sinters were obtained and then ground into powder with a grain size less than 10 μm. If composition *1* is charged, single-phase solid solution $(Zr,Ta)B_2$ is the

synthesis product; and if composition *2* is charged, the synthesis product is two-phase composition that contains approximately 80% of $(Zr,Ta)B_2$ and 20% of TaB_2. The products of the synthesis from the mixtures *3* calculated to form $HfB_2 + 20\%\ TaB_2$ contain solid solution $(Hf,Ta)B_2$ (61%), HfB_2 (33%), and HfB (6%). No independent TaB_2 phase has been found. The composition of the synthesis products from the mixtures *4* calculated to form 60% HfB_2–40% TaB_2 is more complex and contains 4 phases: 45% of $(Hf,Ta)B_2$; 25% of HfB_2; 19% of $(Ta,Hf)B_2$, and 11% of TaB_2.

Thus, the possibility of obtaining solid solutions based on borides of zirconium $(Zr,Ta)B_2$, hafnium $(Hf,Ta)B_2$ and tantalum $(Ta,Hf)B_2$ has been shown. Boride ceramics based on $(Zr,Ta)B_2$ and $(Hf,Ta)B_2$ with record hardness values of 70 GPa, elastic modulus of 594 GPa and elastic recovery of 96% has been obtained from submicron powders through the hot pressing technology and SPS. The thermal conductivity coefficient of the $(Zr,Ta)B_2$ solid solution amounted to 35–42 W/m·K, which is higher than that of TaB_2 but lower than the thermal conductivity of ZrB_2. The $(Zr,Ta)B_2$ samples were tested for fire resistance at the temperature of 2900–3000ºC. It has been established that the oxidized surface of the samples partially melts, and the forming melt heals the cracks and decreases the catalytic activity.

1. E. A. Levashov, A. S. Mukasyan, A. S. Rogachev, D. V. Shtansky, Self-propagating high-temperature synthesis of advanced materials and coatings, *Inter. Mater. Rev.*, 2017, iss. 4, vol. 62, pp. 203–239.
2. I. Borovinskaya, A. Gromov, E. Levashov, Yu. Maksimov, A. Mukasyan, A. Rogachev, *Concise Encyclopedia of Combustion Synthesis: History, Theory, Technology, and Products*, Eds I, Elsevier, 2017.
3. V. V. Kurbatkina, E. I. Patsera, E. A. Levashov, A. N. Timofeev, Self-propagating high-temperature synthesis of refractory boride ceramics $(Zr,Ta)B_2$ with superior properties, *J. Eur. Ceram. Soc.*, 2018, vol. 38, pp. 1118–1127.

INFLUENCE OF MECHANICAL ACTIVATION PARAMETERS ON MA-SHS OF TaC-BASED SINGLE-PHASE SUPER-REFRACTORY SOLID SOLUTIONS

E. I. Patsera[1], V. V. Kurbatkina[1], E. A. Levashov[1] , S. A. Vorotilo[1], and N. A. Kochetov[2]

[1] National University of Science and Technology MISIS, SHS Research & Education Center MISIS-ISMAN, Moscow, 119049 Russia
[2] Merzhanov Institute of Structural Macrokinetics and Materials Science, Russian Academy of Sciences, Chernogolovka, Moscow, 142432 Russia

e-mail: patsera_yevgeniy@mail.ru

Carbides HfC, TaC, and ZrC possess high melting temperatures, corrosion resistance, hardness and resistance to ablation. Usually, solid solutions are characterized by increased hardness and thermal stability as compared to the constituting elements. However, the extraordinary high melting temperature of the aforementioned carbides hinders the production of single-phase solid solutions of refractory carbides by the conventional powder metallurgy techniques. Therefore, the possibility of production of solid solutions of refractory carbides by the self-propagating high-temperature synthesis (SHS) was investigated in this work. The influence of the regime of mechanical activation on the phase composition and structure of initial reagents and synthesized products in the systems Ta–Zr–C and Ta–Hf–C was demonstrated.

Mechanical activation was performed in AIR-0.015 and Aktivator-2S planetary ball mills. The following parameters of the treatment of reaction mixtures were investigated: duration, ball to mixture weight ratio, rotational speed, the sequence of the component's loading in the mill's jars, the atmosphere of activation. The heat release during the combustion was measured using the rapid combustion calorimeter.

Powders of carbide solid solutions were produced by the ball milling of combustion products. Phase composition was investigated by XRD analysis. Microstructure and chemical composition of the specimens were investigated using SEM and EDS.

During the mechanical activation, Ta particles are deformed and form scales. Smaller particles of C and Zr penetrate into the Ta scales. Consequently, agglomerated granules with the size of 200–300 µm are formed. An increase in the MA duration leads to an increase in the microdeformation of the crystal lattice of Ta and to a decrease in its coherent domains (CDs), signifying the increase in the stored energy. Investigation of the influence of the atmosphere of MA (air, vacuum, argon) demonstrated that in the case of MA in the air, the combustion products consist of single-phase solid solution (Ta,Zr)C with a minor (< 3%) admixture of ZrO_2. In the case of MA in an oxygen-free atmosphere (argon, vacuum), three phases were formed: TaC, ZrC, and (Ta,Zr)C. An optimal regime of MA-SHS was devised, ensuring the synthesis of ZrO_2-free single phase solid solution (Ta,Zr)C with a lattice parameter $a = 0.4488$ nm, corresponding to the 15 at % of ZrC in the solid solution.

MA of reaction mixtures Ta–Hf–C was conducted in the planetary ball mill with a varied rotational speed. The increase in the rotational speed by 3.5 times led to a decrease in CSA by an order of magnitude as well as an increase in deformation of the crystal lattice of Ta by 1.5–2 times. Experimental investigations demonstrated that the reaction mixture activated at 678 rotations per minute (rpm) could not be ignited at temperatures T_0 less than 550 K. However, after the MA at 900 rpm, the mixtures could be ignited at room temperature. The differentiated MA led to the increase in the content of oxides in the combustion products. Single-phase solid solution (Ta,Hf)C with HfO_2 content less than 1% was produced. The (Ta,Hf)C solution was characterized by the crystal lattice parameter $a = 0.4487$ nm, corresponding to 18.0 at % HfC in the solution.

E. I. Patsera et al.

INTERFACIAL REACTIONS DURING ANNEALING OF EXPLOSIVELY WELDED SHEETS

H. Paul[1,*], M. M. Miszczyk[1], M. Prażmowski[2], A. Gałka[3], Z. Szulc[3], P. Bobrowski[1], and Ł. Maj[1]

[1] Institute of Metallurgy and Materials Science, Polish Academy of Sciences, Krakow, Poland
[2] Opole University of Technology, Faculty of Mechanics, Opole, Poland
[3] ZTW Explomet, Opole, Poland

e-mail: h.paul@imim.pl

Layered products are often used in industry for structure application. Their production is justified not only by the economical factors but also by the necessity to fulfil particular functional requirements. It is usually sufficient to apply a thin layer of a material, of high strength or anti-corrosive properties to meet the operation requirements. One of the ways is the fabrication of high strength multi-layer composites, in which the base material is separated by thin layers consisting of phases of a very high hardness.

The hard phases occurrence can be initiated by the element diffusion during heating from the adjacent (parent metals) layers. However, the key factor, which determines the occurrence of effective diffusion processes is the quality of permanent joining of metals. Due to properties, the size of the basic components and usually the high differences in the melting points of joined metals explosive welding (EXW) is, at present, the only efficient way of joining the plates into the assembled material [1]. Since the structure of the joint of explosively welded clads can be easily 'modified' in further thermal treatment operations by creating layers composed of intermetallic phases. (The main drawback of the intermetallic in various metals compositions is their high hardness and brittleness). This opens the possibility to fabricate materials of a laminar structure and

significantly improved properties. Various composites reinforced with intermetallic are usually suggested for industrial applications, e.g. as a structural armour materials which are specially designed to exhibit high material strength and resistance to ballistic impacts. However, many physical and chemical aspects of the phase transformations during heating/annealing occurring in areas near-the-interface, remain strongly unrecognized.
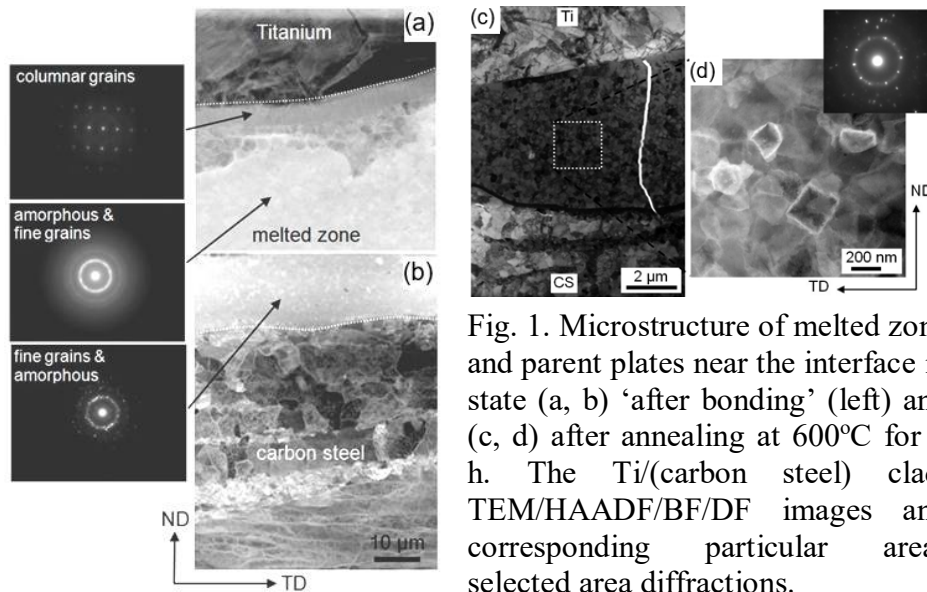
Fig. 1. Microstructure of melted zone and parent plates near the interface in state (a, b) 'after bonding' (left) and (c, d) after annealing at 600ºC for 1 h. The Ti/(carbon steel) clad. TEM/HAADF/BF/DF images and corresponding particular areas selected area diffractions.

The clad systems, which have been studied in the present work, comprise: AA2519/AA1050/Ti(Gr5), Ti(Gr1)/(Cu or AA1050), AA1050/Cu, (stainless or carbon steel)/Zr700 and Ta/(carbon steel) metals compositions. EXW to clad manufacturing was performed by High Energy Technologies Works 'Explomet' (Opole, Poland) using charges from the ANFO group. The clads were obtained by means of the constant stand-off explosive cladding technique. A detonator was located in the middle of the shorter edge of the flyer plate. Then the samples cut-off from explosively welded bi-, tri- or multi-layered metallic clads were annealed at different temperatures (depending on melting points of joined metals) for times ranged between 1 and 1000 h. For microstructure investigations, the interfacial layers were analysed using transmission (TEM) and scanning (SEM) electron microscopy. Nanoscale observations of the selected areas were carried out employing FEI Technai Super TWIN G^2 FEG (200 kV) microscope equipped with a high-angle annular dark field scanning/transmission detector (HAADF/STEM) and an energy

dispersive X-ray (EDX) microanalysis system. The structure observations combined with advanced EDX micro-/nano- scale chemical composition analyses were focused on the distribution of elements in areas near the interface. Mesoscale analyses were carried by SEM with the use of an FEI Quanta 3D equipped with **a** backscattered electrons (BSE) detector. Investigations of the reaction products formed at the cladding interface were carried out using point, line and mapping energy dispersive X-ray (EDX) analyses.

Various types of changes were observed in layers near the interface of EXW clads due to applied annealing conditions [2, 3]. In the case of low temperature annealing (and for short annealing times), e.g. before the technological operations of straitening, the essential changes were only observed inside the melted zones. Since annealing temperatures were higher than the one defining the glass temperature transition of given alloy, then the transformation of amorphous phases into fine grained one was observed. In these cases none of the microstructural changes were observed inside severely deformed layers of joined plates in areas near the interface, as presented in Fig. 1 for Ti/(carbon steel) clad. Similar behavior was observed inside the melted zones of (carbon or stainless steel)/Zr700, Ti(Gr5)/AA2519, Ti(Gr1)/AA1050 and Ti(Gr1)/Cu metals compositions. The diffusion processes across the interface are dominant for high (and very high) annealing temperatures (as compared to the melting points of joined materials) and for longer annealing times. In all analysed cases of metal compositions, the appearance of new phases and/or the disappearance, growth or transformation of the existing ones was observed. The phases formed during annealing always have the character of continuous diffusion layer(s). It was observed that chemical composition of phases can be predicted based on the 'classical' phase equilibrium diagrams. Moreover, the sequence of phases occurrence is strictly related to the distance from the parent plates, as presented in Fig. 2 for Al/Cu metals composition.

It is concluded that application of the SEM (including in-situ heating in SEM) and TEM for investigations of the microstructure and the chemical composition changes near the interface of EXW sheets allowed to explain the mechanism of good reliable bonding formation of such materials. Both the amorphous phases and the nano-crystallites were identified near the interface in 'after bonding state'.

During annealing the diffusion of elements across the interface induce strong changes inside melted zones and those resulting from the elements migration across the interface.
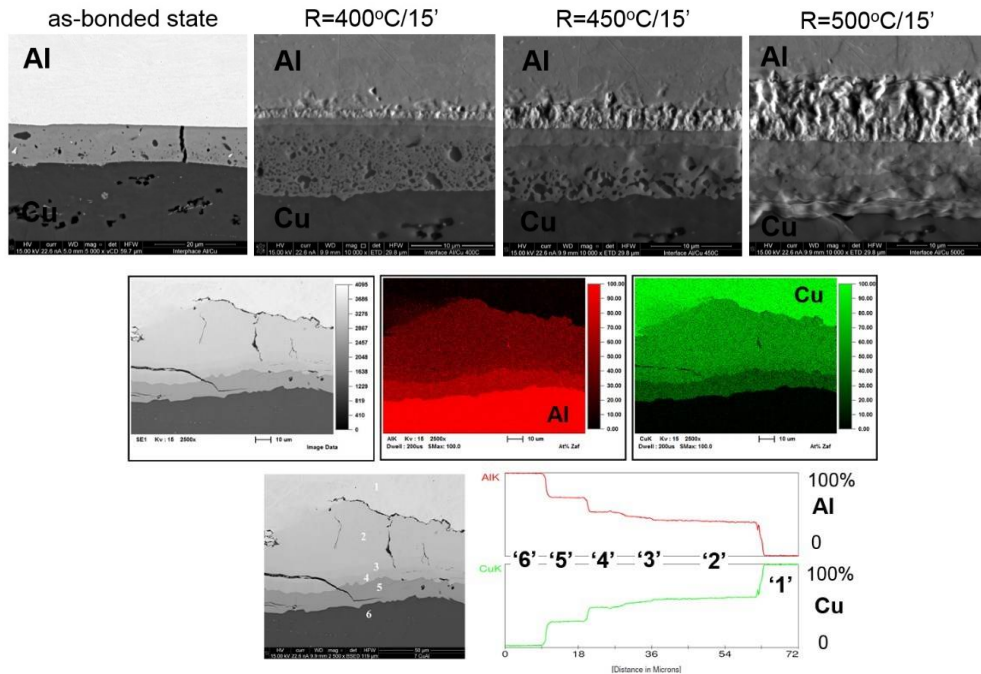
Fig. 2. Chemical composition changes near the interface of EXW Al/Cu clad observed in sample annealed at temperatures ranged between 400°C and 500°C for 15 min (for each interval). SEM in-situ heating and SEM/EDX chemical composition measurements for sample annealed at 500°C.

1. T. Z. Blazynski, *Explosive Welding, Forming and Compaction,* New York: Applied Science Publishers LTD, 1983.
2. W. Skuza, *Wieloskalowa charakterystyka połączeń w platerach Ti/Cu spajanych metodą wybuchową*, PhD thesis, IMMS PAS Krakow, 2016, ISBN: 978-83-60768-34-1 (*in polish*).
3. D. M. Fronczek, *Microstructural and kinetic characterization of the phenomena occurring at the clad's interfaces manufactured by explosive welding*, PhD thesis, IMMS PAS Krakow, 2017, ISBN: 978-83-60768-37-2.

H. Paul et al.

LIQUID PHASE SHOCK WAVE CONSOLIDATION OF NANOSTRUCTURED Ta–Ag COMPOSITES

A. B. Peikrishvili[1,3], E. Sh. Chagelishvili[2], B. A. Godibadze[2], G. I. Mamniashvili[3], L. I. Qurdadze[3], and A. A. Dgebuadze[2]

[1] Tavadze Institute of Metallurgy and Materials Science, Tbilisi, 0186 Georgia
[2] Tsulukidze Mining Institute, Tbilisi, 0186 Georgia
[3] Javakhishvili Tbilisi State University, Tbilisi, 0168 Georgia

e-mail: apeikrishvilii@yahoo.com

The different compositions of Ta–Ag blends of powders were consolidated near and above of the melting point of silver using two stage cylindrical geometry of loading. In order to prevent deformation and to maintain consolidated billets with correct geometry the precursors first were consolidated at room temperatures to increase their density and to prevent the strong shrinkage during the second stage loading at high temperatures. There were consolidated Ta–Ag compositions under the different intensity of loading. The pure ammonium nitrate and the mixture with saltpeter (50/50) were mainly used during the experiments to consolidate precursors under the intensity of loading of 10 and 5, respectively. The temperature of consolidation during the second stage loading were changed under and above of melting point of silver up to 1000°C.

As there was established the application of too high temperatures above of melting point of silver and consolidation at $1000–1100^{0}$C leads to formation of thermal stresses behind of shock wave front during the cooling processing. The cracking may be observed in whole volume of obtained samples. The decrease in the loading temperature and consolidation of Ta–Ag precursors near 950°C essentially reduces the cooling rate of hot billets and prevents the cracking in whole volume of consolidated samples.

As investigation showed the low intensity of loading with increased pulse duration is more effective for Ta–Ag compositions providing obtaining samples with higher value of hardness. The mentioned may be observed only for compositions with high content of tantalum and may be explained by their strong plastic deformation. With increasing silver content the difference in hardness value for both cases of loading practically becomes the same (Table 1).

The investigation of macro- and microstructures of samples showed that consolidation of Ta–Ag precursors near to melting point of silver provides obtaining of high dense billets without cracking and uniform distribution of consisting phases.

Figure 1 represents the macro- and microstructure of different Ta–Ag composites obtained after consolidation at 950°C.

Table 1. The distribution of hardness for different Ta–Ag composites consolidated at 950°C with different intensity of loading.

Composition	Hardness HV kg/mm^2 Loading under 10 GPa	Hardness HV kg/mm^2 Loading under 5 GPa
Ta–10% Ag	456	680
Ta–20% Ag	408	510
Ta–40% Ag	288	278
Ta–60% Ag	169	172
Ta–80% Ag	89	91
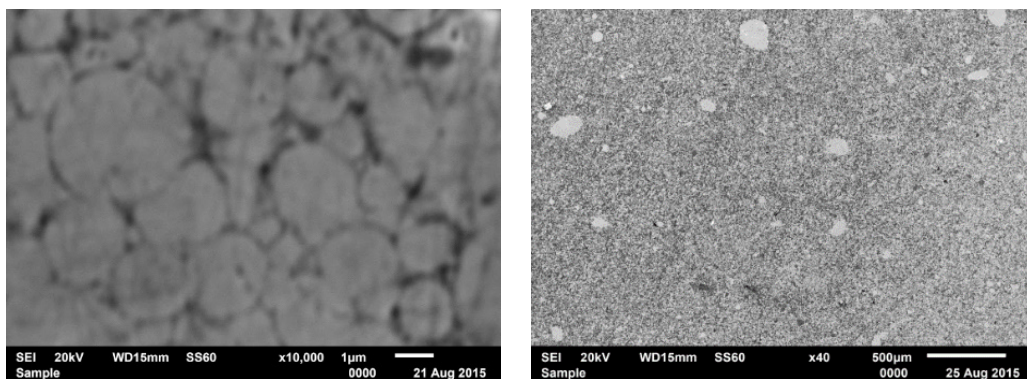
Fig.1. Macro- and microstructures of liquid phase shock wave consolidated Ta–Ag composites obtained near to 1000°C with intensity of loading under 10 GPa.

SHOCK ASSISTED LIQUID-PHASE CONSOLIDATION OF Ta(Nb,V)–Al COMPOSITES

A. B. Peikrishvili[1,4], L. J. Kecskes[2], G. F. Tavadze[1], B. A. Godibadze[3], and E. Sh. Chagelishvili[3]

[1] Tavadze Institute of Metallurgy and Materials Science, Tbilisi, 0186 Georgia
[2] Matsys, Inc., Sterling, Virginia, USA
[3] Tsulukidze Mining Institute, Tbilisi, 0186 Georgia
[4] Javakhishvili Tbilisi State University, Tbilisi, 0168 Georgia

e-mail: apeikrishvili@yahoo.com

The main purpose of the work presented herein is to combine hot explosive consolidation technology (HEC) with Self-Propagating High-Temperature Syntheses processes (SHS) to obtain Ta–Al, Nb–Al, or V–Al high-density cylindrical billets with perfect structure and improved properties.

In the first stage of the investigation, experiments were carried out to pre-densify the precursors at room temperatures using explosive consolidation to obtain billets with increased density and to activate particle surfaces for further sintering processes. In the second stage of the investigation, the same experiments were repeated; however, the consolidations were conducted at hot conditions below and above the SHS reaction temperatures of the preliminary compacted blends of these composite materials. The loading intensity in all cases was under 10GPa. The temperature for the second stage of consolidation in the hot condition was under 950°C. The heating time before loading was under 30 minutes.

It was established that the initiation of SHS process and a complete reaction in the Ta–Al powder composites starts at around 940°C. In order to fabricate billets at or near the theoretical density with a nearly perfect structure, correct cylindrical geometry, and to prevent cracking, it was necessary to load explosively the billets prior to

reaching 940°C. Consolidation of the billets above 940°C led to cracking throughout the entire volume of the HEC billet. Subsequent X-ray diffraction investigation of the fabricated Ta–Al, Nb–Al, or V–Al samples shows that the initiation of SHS reaction behind of shock wave front directly depended on preheating temperature. Full synthesis (i.e., 100% conversion to tantalum aluminide products) in the Ta–Al reaction mixture with formation of various product phases becomes possible only after consolidation at or above 940°C. In contrast, investigation of the Nb–Al and V–Al reaction mixtures after the two-stage HEC process showed that obtaining fully reacted samples with the formation of their respective aluminides was practically impossible under the same loading conditions. After the SHS reaction, for the Nb–Al and V–Al precursors, increasing the temperature during loading and consolidation always led to cracking in the entire volume of the resultant billets. This may be explained by considering the density differences between the reaction mixtures. In in contrast to the lower density of Nb or V, the density of Ta (almost twice) provides an impetus for the formation of a higher intensity shock wave during the consolidation of the Ta–Al blend of powders, resulting in the full synthesis and formation of tantalum aluminides in the entire volume of the HEC billets (Fig. 1). The type of intermetallic compounds was found to depend on the ratio of the precursor elements in the starting composition.

The aforementioned observations, other features of the structure-property-processing relationships for the consolidated Ta–Al and Nb–Al based composites, depending on the loading conditions used, as well as the set-up and operation of the HEC device will be presented and discussed.
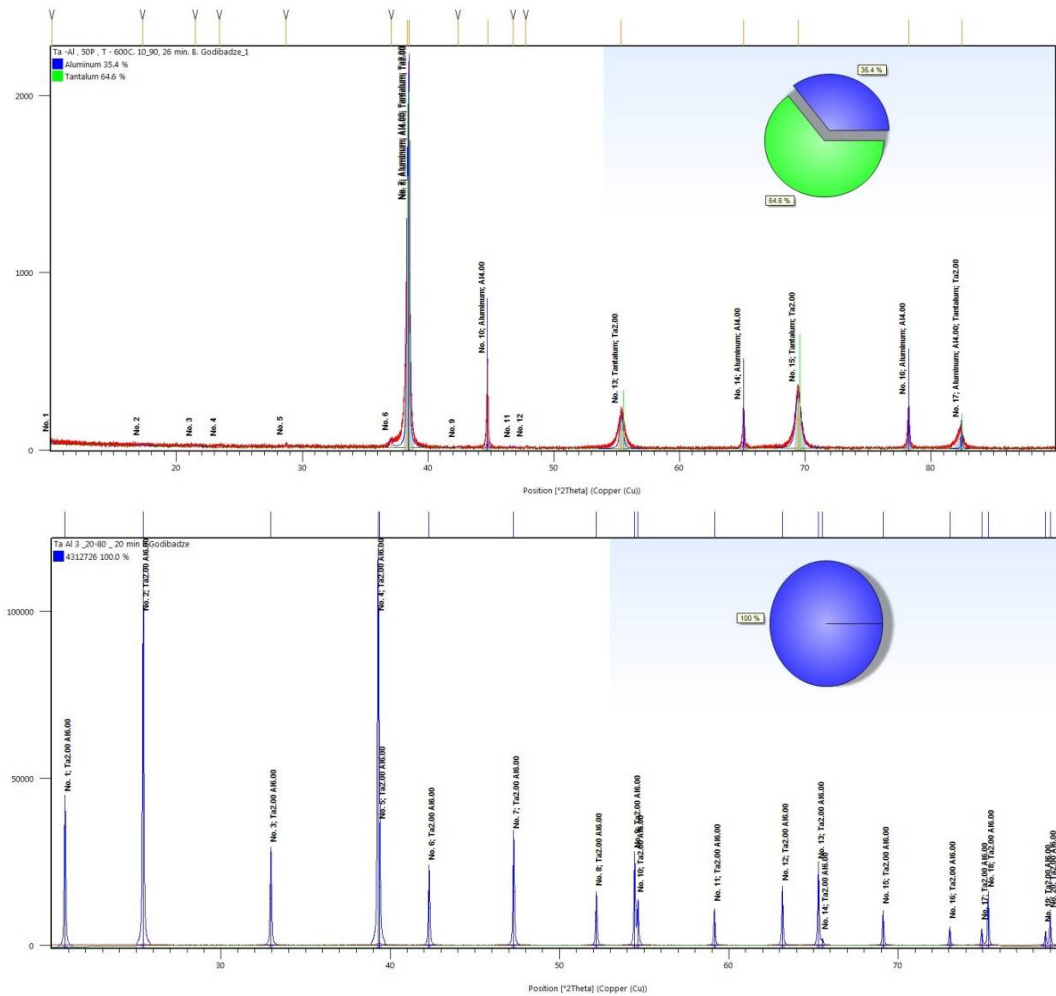
Fig. 1. X-ray diffractograms of Ta–Al reaction mixtures after HEC at 600°C and 950°C shows the synthesis, full (100%) conversion, and formation of tantalum aluminides at or above 950°C only.

HOT SHOCK WAVE CONSOLIDATION OF NANOSTRUCTURED TUNGSTEN BASED COMPOSITES

A. B. Peikrishvili[1,4], L. J. Kecskes[2], G. F. Tavadze[1], B. A. Godibadze[3], E. Sh. Chagelishvili[3], and G. Sh. Oniashvili[1]

[1] Tavadze Institute of Metallurgy and Materials Science, Tbilisi, 0186 Georgia,
[2] Matsys, Inc., Sterling, VA, USA.
[3] Tsulukidze Mining Institute, Tbilisi, 0186, Georgia
[4] Javakhishvili Tbilisi State University, Tbilisi, 0168, Georgia

e-mail: apeikrishvilii@yahoo.com

Using Hot Explosive Consolidation (HEC) technology, we have fabricated and consolidated different composites of blended W–Ag, W–Cu, and W–Ta powders based on a nanoscale W powder to obtain bulk nanostructured billets to near theoretical densities. Two nanoscale W powders and one nanoscale Ta were used. The W powders had grain sizes of 100 and 150 nm, respectively; the Ta powder had a grain size of 80nm. The Ag and Cu powders with grain sizes of around 5 μm were used to prepare the starting blend of precursor powders. The heating temperature during the processing ranged from below to above the melting point of Ag and Cu up to 1100°C. The HEC loading intensity was under 10GPa. Our investigations showed that the use of powder blends based on nanostructured W followed by their explosive consolidation near the melting point of Cu or Ag preserved the nanoscale of the W grains and enabled the fabrication of full density cylindrical billets without notable coarsening of the grain size. The consolidated samples showed good integrity and improved physical and mechanical properties; see Tables 1 and 2 for the hardness of the samples.

Table 1. Hardness distribution of the consolidated W–Ag samples.

Compacted Composite	Compaction Temperature [°C]	Loading Gr.	Vickers Microhardness [kg/mm^2]
W–5% Ag	1000	50	331.5
W–10% Ag	940	50	248.5
W–10% Ag	1050	50	208.20
W–50% Ag	1050	50	47.5

Table 2. Hardness distribution of the consolidated W–Ta samples.

Compacted Composite	Compaction Temperature [°C]	Loading Gr.	Vickers Microhardness [kg/mm^2]
W–20%Ta (100nm/80nm)	1080	50	825.02
W–40%Ta (100nm/80nm)	1080	50	713.2
W–20%Ta (150nm/80nm)	1050	50	787.5
W–40%Ta (150nm/80nm)	1050	50	710.9

The structure and characteristics of the obtained samples depended on the phase content, distribution of phases, and processing parameters used during the explosive synthesis and consolidation. For the case of the nanostructured W–Ta composites we found that it was important to have a definite matching of the constituent particle sizes to prevent the cracking in the HEC billets to provide in obtaining samples without visible structural defects (see Figs. 1, 2).

(a) (b) (c) (d)
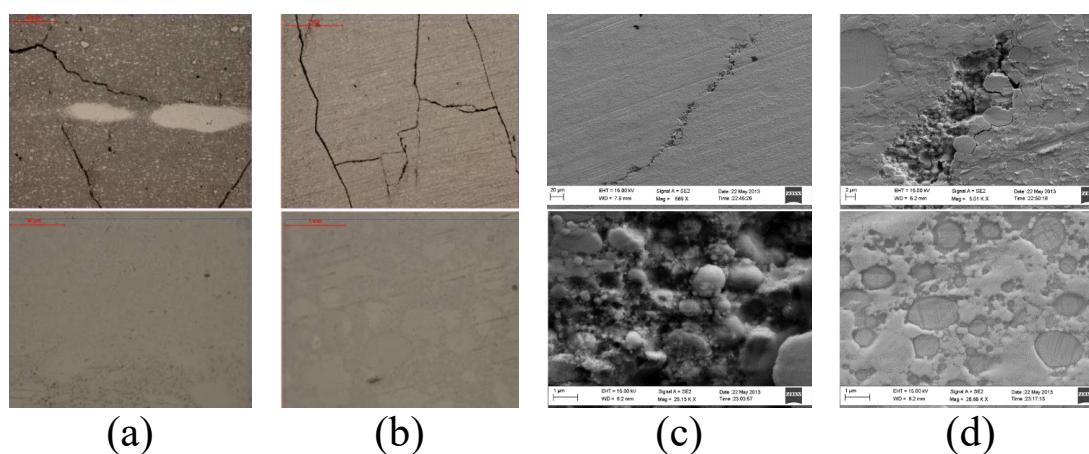
Fig. 1. The macro- and microstructures of the consolidated nanostructured W–(20–40)%Ta composites. (a) and (c) W–20%Ta; (b) and (d) W–40%Ta. The grain sizes of W and Ta are 150 and 80 nm, respectively.

(a)　　　　　　　　(b)　　　　　　　　(c)　　　　　　　　(d)
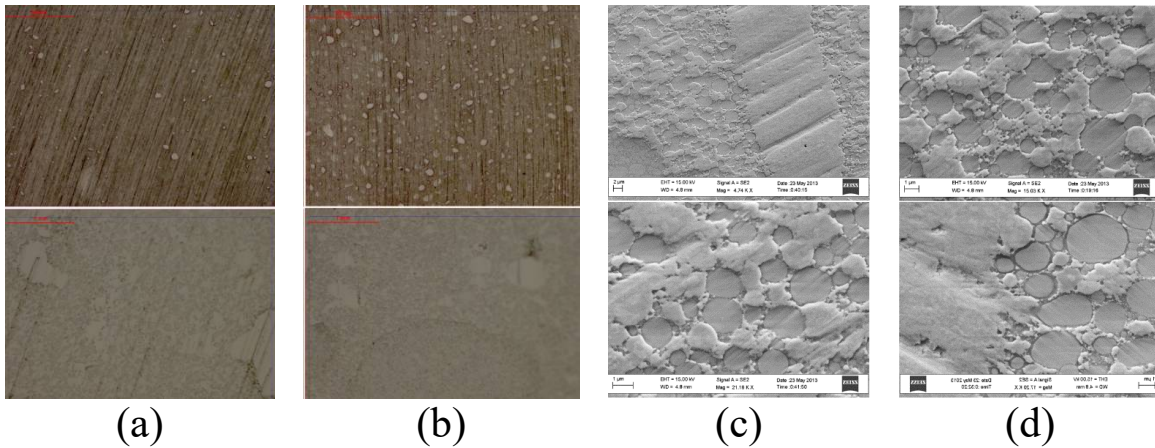
Fig. 2. The macro- and microstructure of the consolidated nanostructured W–(20–40)%Ta composites. (a) and (c) W–20%Ta; (b) and (d) W–40% Ta. The grain sizes of W and Ta are 100 and 80 nm, respectively.

Additionally, we observed that the electrical properties (i.e., resistance and dependence of the susceptibility) of the consolidated W–Cu (Ag) composites were dependent upon the phase content and the density of the consolidated samples. We will present and discuss the processing of the precursors and the fabrication of these nanostructured W based composites, including a detailed description of the HEC technique.

INFLUENCE OF THERMAL PROCESSING ON STRUCTURAL CHANGES OF STEEL + TITANIUM BIMETAL OBTAINED BY EXPLOSIVE WELDING IN ARGON MEDIUM

O. L. Pervukhina

Merzhanov Institute of Structural Macrokinetics and Materials Science, Russian Academy of Sciences, Chernogolovka, Moscow, 142432 Russia

e-mail: opervukhina@mail.ru

Local areas of incomplete fusion in steel + titanium bimetal, the appearance of which is caused by the formation of air pockets in the welding gap, after heat treatment were studied. These areas were compared with defect-free bimetal samples cut out from different sections of large-sized sheet after heat treatment. The object of the study was a 09G2S/VT1–0 bimetal sheet (30 × 1860 × 3280 mm) welded by explosion in a protective gas (argon) environment. The quality of the joint was determined using ultrasonic testing over the entire sheet length (along the direction of detonation). The zone with noise detected was considered as a defective area.

Results of pull-off tests showed that the strength of the joint in different regions of the large-sized sheet is 302–424 MPa; in the defective area, is less than 100 MPa.

Heat treatment of samples involved annealing at 550°C for different durations (1, 2, 3, 6, and 12 h) followed by air cooling. The studies of the welded joint structure and composition of inclusions were conducted using optical and scanning electron microscopy. The average thickness of the molten metal layer (δ) at the interface of layers was calculated as a ratio of the total area of cast inclusions to the length of the measured section.

It has been revealed that the bimetallic sheet is characterized by the stable structure along the entire length. The structure of the welded

joint exhibits the wavy character with the same wave parameters and individual cast TiFe inclusions. However, the wave formation in the defective area is disturbed. At the joint interface, a continuous interlayer consisting of TiFe, $TiFe_2$, and Ti_2Fe intermetallics is formed.

As shown in Fig. 1, the heat treatment leads to an increase in δ. The sizes of inclusions depend on the holding time and environment in the welding gap (argon or air). For high-quality welded zones, the thickness varies insignificantly along the sheet length. Cracks and pores are within the inclusions even after 12-h annealing. In the defective zone, the thickness δ increases sharply after annealing for 3 h. Growth rate of δ corresponds to the data on the kinetics of growth of intermetallic layers upon welding between steel and titanium in air.
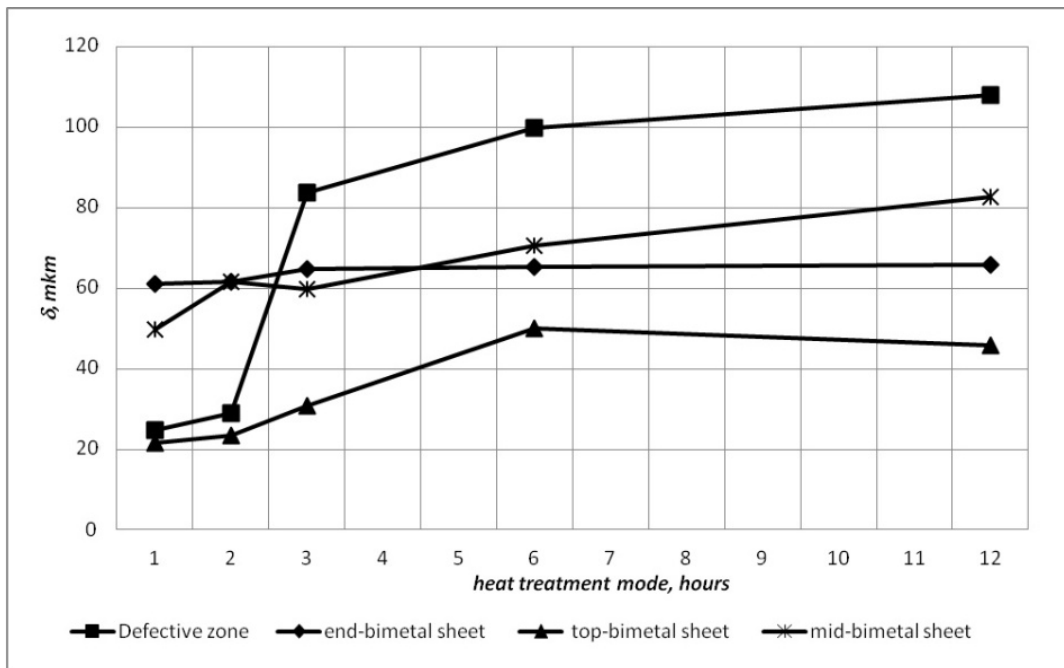
Fig. 1. Average thickness of intermetallic inclusions at the steel–titanium interface as a function of annealing time ($T = 550°C$).

INVESTIGATION OF INITIATION OF Zn + S STOICHIOMETRIC MIXTURE BY PULSE IMPACT

E. V. Petrov, **I. V. Saikov**, **and G. R. Saikova**

Merzhanov Institute of Structural Macrokinetics and Materials Science, Russian Academy of Sciences, Chernogolovka, Moscow, 142432 Russia

e-mail: petrow-ewgeni@mail.ru

Creation of new materials with unique properties and their investigation under extreme conditions at high pressures is one of the urgent tasks of modern science. Such processes are pulse impacts such as shock-wave compaction [1] and synthesis initiated by exploding wire [2].

The exothermic system of zinc and sulfur was chosen as an object of study. It reacts with the formation of predominantly condensed reaction products and satisfies a necessary and sufficient thermodynamic criterion for detonation ability [3].

Shock-wave compaction of powder mixture in a cylindrical recovery fixture occurred using a detonation wave providing an all-round uniform compression of the recovery fixture with powder. The synthesis initiated by exploding wire was carried out in a steel cylindrical reactor. The electric pulse was applied to two isolated contacts, which exploded the wire and initiated the reaction in the powder mixture. Sampling of the final product for the study was carried out from various zones along the length of the recovery fixture and reactor.

XRD analysis of products obtained in the recovery fixture and in the reactor showed that in both cases the main product is hexagonal zinc sulfide. However, zinc sulfide in the reactor can be formed in two modifications: hexagonal and cubic. The simultaneous presence of these two phases in the product formed during reaction between Zn and S powders indicates the crystallization at temperatures above or

near the phase transition temperature. The SEM study showed that the zinc sulfide product resulting upon implementation of two types of experiments corresponds to hexagonal ZnS.

Thus, the studies carried out indicate that the synthesis in a Zn + S stoichiometric mixture is possible both upon shock-wave compression of the recovery fixture and upon initiation in the reactor using exploding wire. The resulting products have the same hexagonal structure.

1. V. D. Rogozin, *Explosive processing of powder materials*, Volgograd: Polytechnic, 2002 (in Russian).
2. V. S. Trofimov, E. V. Petrov, On detonation in Zn–S blends, *Int. J. of Self-Propag. High-Temp. Synth.*, 2014, vol. 23, no. 4, pp. 187–191.
3. Yu. A. Gordopolov, V. S. Trofimov, A. G. Merzhanov, On the possibility of gas-free detonation of condensed systems, *Dokl. Akad. Nauk*, 1995, vol. 341, no. 3, pp. 327–329.

FORMATION OF GRADIENT STRUCTURES OF FUNCTIONAL COATINGS AFTER THE IMPACT OF HIGH-SPEED PARTICLES FLOW

E. V. Petrov and V. S. Trofimov

Merzhanov Institute of Structural Macrokinetics and Materials Science, Russian Academy of Sciences, Chernogolovka, Moscow, 142432 Russia

e-mail: petrow-ewgeni@mail.ru

The main objective of hardening technologies is to ensure the self-organization of surface phenomena with the consequent formation of structures of functional surface layers of various materials or gradient structures and the control of properties of these structures under a variety of physical high-temperature and force impacts. At the same time, the key element in the self-organization of surface phenomena is the stable formation of the layer of certain thickness with given structure or phase composition. An important issue is related to the processes of the structural formation of the layer.

In this paper, we investigated the processes of the formation of gradient structures of functional coatings obtained by using the technology of the flow impact of solid refractory particles accelerated by directional explosion based on the effect of superdeep penetration.

When experiments, the shock wave and the products of the explosion accelerate the dispersed tungsten powder with a particle size of 10–16 μm and, along with it, affect the investigated cylindrical sample with a diameter of 24 mm and a height of 40 mm. Tungsten particles were detected by SEM at a depth of ~ 13 mm from the surface of impact, which exceeds the initial size of the tungsten particle (14 μm) by 930 times.

Figure 1 shows the SEM image of the structure of steel along with relevant EDS data. The cellular structure of austenite with a grid of tungsten carbide and inclusions of tungsten particles was found

(Fig. 1). An evaluation of the nature of the structure formation processes shows that in accordance with the Fe–W phase diagram, the temperature in functional layers with a honeycomb austenite structure exceeds a temperature of 1060°C, which corresponds to the peritectoid reaction. The polymorphic transformation of iron with the formation of austenite and the dissolution of tungsten carbide in austenite proceed at this temperature. During cooling, the austenite solution is supersaturated by tungsten and stabilized. Upon further cooling, the structure of the stabilized supercooled austenite is formed, and the excess of tungsten is precipitated as tungsten carbide at the boundaries of austenitic grains weakly alloyed with tungsten (Fig. 1).

Thus, during the surface treatment of steel U8 samples by the flow of tungsten powder particles accelerated by the energy of the explosion, a cellular supercooled austenite with the tungsten carbide grid along the grain boundaries is formed in the structure of steel, which is identical to the structure of a cast high-speed steel with a complex carbide eutectic resembling ledeburite located along the grain boundaries of austenite.
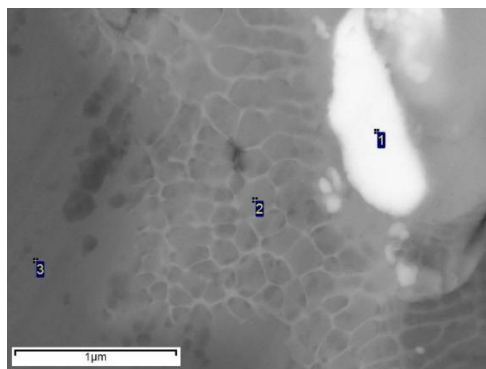
Area	C	Fe	W
1	24.17	12.95	62.89
2	26.79	59.90	62.89
3	25.01	74.99	–

Fig. 1. SEM image of steel reinforced by the flow of tungsten particles accelerated by the energy of the explosion and respective EDS data (wt %).

E. V. Petrov and V. S. Trofimov

SHS OF ADVANCED HEAT-RESISTANT CERAMICS IN THE Me^{IV}(–Me^{VI})–Si–B(C) SYSTEM

A. Yu. Potanin[1]*, I. V. Yatsuk[1], S. Vorotilo[1], Yu. S. Pogozhev[1], D. Yu. Kovalev[2], and E. A. Levashov[1]

[1] National University of Science and Technology MISIS, Moscow, 119049 Russia
[2] Merzhanov Institute of Structural Macrokinetics and Materials Science, Russian Academy of Sciences, Chernogolovka, Moscow, 142432 Russia

*e-mail: a.potanin@inbox.ru

The key research problem associated with development of the next-generation space transportation systems is to find novel materials that would be resistant to oxidation at temperatures above 2000°C and to exposure to high-enthalpy gas flow containing abrasive particles. These materials show a high promise for use in supersonic transport [1] with sharp wing and fairing edges, as well as in spacecrafts within the nozzle throat in solid-fuel engine systems.

The promising materials include hard and refractory materials based on zirconium boride ZrB_2 that have the melting point more than 3000°C and are characterized by high strength, fracture resistance, wear resistance, and thermal stability. An important advantage of ZrB_2-based composites is high thermal conductivity ensuring rapid heat transfer away from the contact surface with a flow of oxygen-rich gas.

Alloying of ZrB_2 and silicon-containing compounds, such as SiC, $MoSi_2$, $ZrSi_2$ [3–5], gives rise to a protective borosilicate glass layer upon oxidation. Formation of B_2O_3 contributes to efficient healing of microcracks and pores that inevitably emerge in the protective layer during its operation.

High-temperature composite ceramics based on refractory-metal borides and silicides are fabricated using hot pressing and spark

plasma sintering techniques [3–5]. SHS enabling production of high-purity refractory compounds and various combinations thereof is an alternative method [6].

This study focuses on the kinetics and mechanism of combustion and on stages of chemical transformations in the Zr–B–Si, Zr–B–Si–C, Mo–Si–B, and Mo–Hf–Si–B mixtures in the combustion wave. The staging of structural phase transformations was studied by dynamic X-ray diffraction (DXRD) analysis and combustion front quenching (CFQ) performed in a bulk copper wedge. The characteristic regions of the combustion front were assessed using electron microscopy and micro-X-ray spectrometry analysis.

Figure 1 shows the characteristic dynamic X-ray diffraction patterns of combustion of the Zr–B–Si–C mixture with composition calculated so as to obtain 75% ZrB_2–25% SiC. Primary ZrB_2 grains crystallize from the eutectic Zr–Si melt supersaturated with boron. Silicon carbide SiC also crystallizes from the melt with a latency of no longer than 0.5 s.
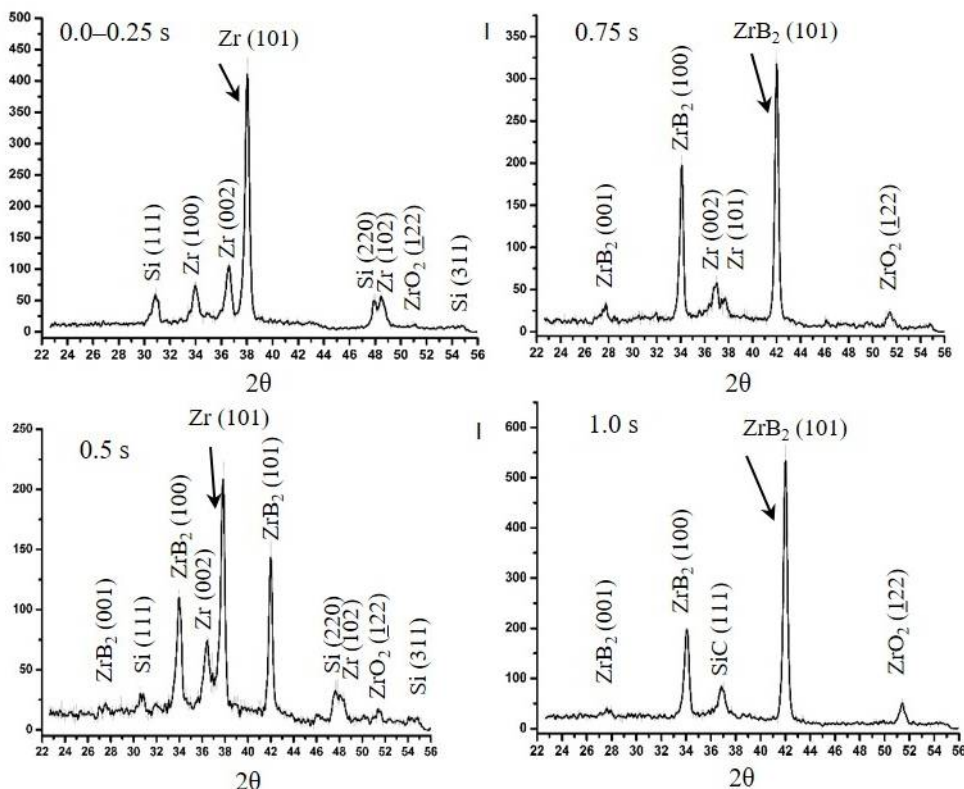
Fig. 1. Selective series of the DXRD patterns of combustion of the Zr–B–Si–C mixture with composition calculated as to obtain 75%ZrB_2–25% SiC.

According to the results of comprehensive studies (DXRD and CFQ) of combustion in the Mo–Hf–Si–B mixtures, we suggest the following mechanism of structural phase transitions in the combustion wave. HfB_2 is initially formed in the heat-up zone via the mechanism of solid-phase interaction involving the gas-transport reaction [7]. Figure 2 shows the microstructure of the quenched combustion front containing submicron sized HfB_2 grains. After Si melted, its melt spreads over the surface of Mo, Hf, and B particles. $MoSi_2$ grains are formed due to reactionary diffusion of Si into Mo at the film/melt interface [8]. Diffusion counterflow of Mo and Hf atoms saturates the Si melt until primary boride crystals MoB and HfB_2 are precipitated. The final product includes the $MoSi_2$, MoB, and HfB_2 phases.
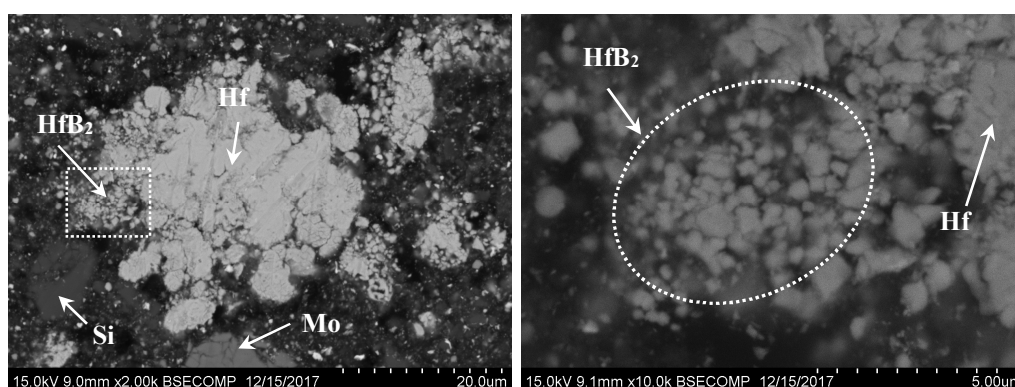
Fig. 2. Microstructure of the quenched combustion front of the Mo–Hf–B–Si mixture in the warm-up zone.

The resulting ceramic composites show promise in designing thermo-strained parts not only as constructional materials but also to design an efficient system for protecting carbon–carbon composite materials (CCCMs) against high-temperature gas-phase corrosion and erosion. An effective method to protect heat-loaded products is the formation on the surface of heterogeneous protective coatings, for example, by slurry deposition (surfacing or impregnation) using powder precursor.

1. A. Paul, D. D. Jayaseelan, S. Venugopal, E. Zapata-Solvas, J. Binner, B. Vaidhyanathan, A. Heaton, P. Brown, W. E. Lee, UHTC composite for hypersonic applications, *Am. Ceram. Soc. Bull.*, 2012, vol. 91, no. 1, pp. 22–29.
2. E. Wuchina, E. Opila, M. Opeka, W. Fahrenholtz, I. Talmy, UHTCs: Ultra-high temperature ceramic materials for extreme environment applications, *Electrochem. Soc. Interface*, 2007, pp. 30–36.
3. D. Sciti, S. Guicciardi, A. Bellosi, Properties of a pressureless-sintered ZrB_2–$MoSi_2$ ceramic composite, *J. Am. Ceram. Soc.*, 2006, vol. 89, no. 7, pp. 2320–2322.
4. S. Q. Guo, K. Yutaka, N. Toshiyuki, T. Hidehiko, Pressureless sintering and physical properties of ZrB_2-based composites with $ZrSi_2$ additive, *Scripta Mater.*, 2008, vol. 58, pp. 579–582.
5. W. W. Wu, G. J. Zhang, Y. M. Kan, P. L. Wang, K. Vanmeensel, J. Vleugels, O. V. Biest, Synthesis and microstructural features of ZrB_2–SiC-based composites by reactive spark plasma sintering and reactive hot pressing, *Scripta Mater.*, 2007, vol. 57, no. 4, pp. 317–320.
6. E. A. Levashov, A. S. Mukasyan, A. S. Rogachev, D. V. Shtansky, Self-propagating high-temperature synthesis of advanced materials and coatings, *Int. Mater. Rev.*, 2017, vol. 62, no. 4, pp. 203–239.
7. V. V. Kurbatkina, E. I. Patsera, E. A. Levashov, A. N. Timofeev, Self-propagating high-temperature synthesis of refractory boride ceramics $(Zr,Ta)B_2$ with superior properties, *J. Eur. Ceram. Soc.*, 2018, vol. 38, pp. 1118–1127.
8. E. A. Levashov, Yu. S. Pogozhev, A. Yu. Potanin, N. A. Kochetov, D. Yu. Kovalev, N. V. Shvyndina, T. A. Sviridova, Self-propagating high-temperature synthesis of advanced ceramics in the Mo–Si–B system: Kinetics and mechanism of combustion and structure formation, *Ceram. Int.*, 2014, vol. 40, pp. 6541–6552.

APPLICATION OF SHS FOR PRODUCTION OF ADVANCED Me$^{(IV–VI)}$–Si–B CERAMICS FOR PVD OF HIGH-TEMPERATURE PROTECTIVE COATINGS

A. Yu. Potanin*, I. V. Yatsuk, Ph. V. Kiryukhantsev-Korneev, Yu. S. Pogozhev, N. V. Shvindina, A. V. Novikov, and E. A. Levashov

National University of Science and Technology MISIS, Moscow, 119049 Russia

*e-mail: a.potanin@inbox.ru

This work is supposed to carry out experimental studies on obtaining high-temperature ceramic materials based on borides and silicides of transition refractory metals of the IV–VI groups of the periodic elements table by self-propagating high-temperature synthesis (SHS) technology [1]. Also, the mechanisms of the phase and structure formation, as well as the stages of reactions during the ceramics synthesis, in the Zr–B–Si, Zr–B–Si–C, Mo–Si–B, and Mo–Hf–Si–B systems were studied. The high-temperature ceramic experimental samples including target-cathodes were produced by forced SHS pressing technology. The coatings were deposited by magnetron sputtering. The complex material researches, which establish the relationship between the composition and the structure of ceramic materials, the parameters of sputtering and properties of coatings were carried out.

A wide range of composite target-cathodes based on ceramics and intermetallic compounds for magnetron sputtering of functional multicomponent nanostructured coatings (MNCs) can be obtained via forced SHS pressing technology [2–6]. Such kind of composite SHS targets possess a high relative density of up to 99.5%, homogeneous or gradient structures and high chemical purity along with necessary mechanical properties, thermal and electrical conductivities. During the magnetron sputtering with using of multicomponent composite

SHS-targets, the substance is transferred with a homogenous flow of metallic (Ti, Ta, Cr, Mo, Al, Zr, etc.) and non-metallic (Si, C, O, N) atoms and ions, since a target contains all the elements required for the formation of the coating. SHS-pressing technology allows obtaining disk and planar-extended segmented targets (Fig. 1), which can be used in both laboratory scale and industrial magnetron installations.

The results show that the temperature and velocity of combustion of compounds in the Zr–B–Si system have linear dependencies on the initial temperature (T_0). The stage of zirconium diboride and disilicide chemical reaction formation did not change with increasing in T_0. The calculated values of the effective activation energy of SHS process indicate the leading role of the reaction interaction between zirconium and boron and silicon in a melt. Evolution of chemical transformations in the combustion wave of the Zr–Si–B mixture was studied. First, the ZrB_2 crystals were formed through the Zr–Si melt, further the $ZrSi_2$ phase was appeared with a delay of 0.5 s, and unreacted Si was crystallized for 1 s later.

(a)   (b)
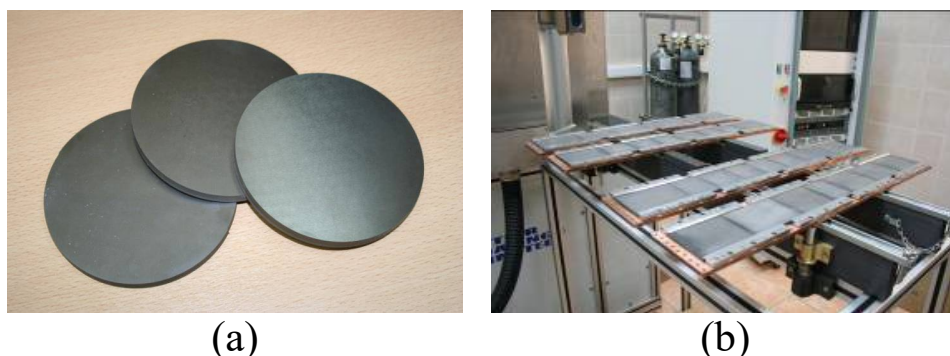
Fig. 1. Composite target obtained via forced SHS pressing technology: (a) disk and (b) planar-extended segmented.

The dense samples characterized by high hardness and low residual porosity were produced by forced SHS-pressing technology. Phase composition was investigated. It was established that the diboride ZrB_2 is a main phase. Phases $ZrSi_2$, Si and ZrB_{12} were contained depending on the initial mixture composition (Fig. 2). These compositions are advanced for high-temperature application in oxidizing condition owing to the formation of strong oxide films SiO_2–ZrO_2–B_2O_3 along with the complex oxide $ZrSiO_4$, which serve as an effective diffusion barrier and reduce the oxidation rate.

Hard Zr–Si–B–(N) films were deposited by magnetron sputtering of SHS-targets in Ar + N_2 (0, 10, 15, 25 and 100% N_2). The structure and chemical and phase composition of coatings deposited on different substrates have been studied using the methods of high resolution transmission and scanning electron microscopy, X-ray diffraction, X-ray photoelectron spectroscopy, Raman and infrared spectroscopy, energy-dispersive analysis, and glow discharge optical emission spectroscopy. Coatings were characterized in terms of their hardness, elastic modulus, elastic recovery, resistance to cyclic impact loading, friction coefficient, wear rate. Optical and electrical properties of films were also examined. To evaluate the short- and long-term oxidation resistance, diffusion-barrier properties, resistance to the thermo-cycling, and thermal stability, all coatings were annealed in air atmosphere at the temperature in the range of 1000–1500°C.
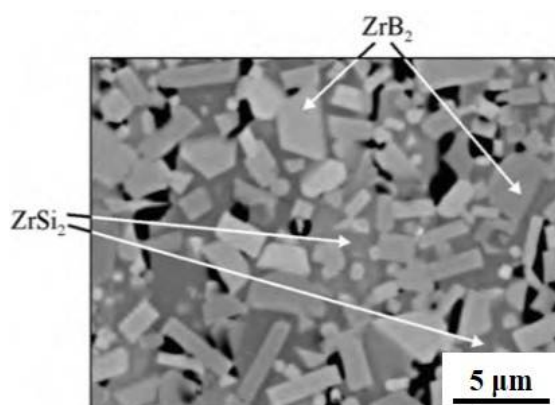
Fig. 2. Microstructure of compact SHS ceramic in the Zr–B–Si system.

It was concluded that the films deposited at low nitrogen partial pressure consist of nanocrystallites of hexagonal ZrB_2-phase with a size of 1–3 nm and amorphous regions. Nitrogen-rich films exhibit XRD-morphous structure. Specific optical properties were observed for these Zr–Si–B–(N) coatings. The refraction index, coefficients of transmittance and reflectance were measured for wavelength diapason from 200 to 2500 nm. The maximum hardness of 26 GPa, Young's modulus of 260 GPa, and elastic recovery of 60 % were determined for films deposited in Ar–15% N_2. Moreover, the nitrogen-rich coatings demonstrate high wear resistance in sliding and impact conditions, low friction coefficient of 0.2–0.4 in a wide temperature

range of 20–300°C. All films showed good oxidation resistance up to 1000°C. Maximal oxidation resistance of nitrogen-low Zr–Si–B–(N) films ($T_{ox} > 1400$°C) was achieved. High protective ability was explained by the formation of strong SiO_2 top-layer reinforced with ZrO_2 nanoparticles, which impedes penetration of oxygen into the depth of films.

1. E. A. Levashov, A. S. Mukasyan, A. S. Rogachev, D. V. Shtansky, Self-propagating high-temperature synthesis of advanced materials and coatings, *Int. Mater. Rev.*, 2017, vol. 62, no. 4, pp. 203–239.
2. E. A. Levashov, Yu. S. Pogozhev, A. Yu. Potanin, N. A. Kochetov, D. Yu. Kovalev, N. V. Shvyndina, T. A. Sviridova, Self-propagating high-temperature synthesis of advanced ceramics in the Mo–Si–B system: Kinetics and mechanism of combustion and structure formation, *Ceram. Int.*, 2014, vol. 40, pp. 6541–6552.
3. Yu. S. Pogozhev, E. A. Levashov, E. I. Zamulaeva, A. Yu. Potanin, A. Yu. Vlasova, A. V. Novikov, N. A. Kochetov, Combustion synthesis of multicomponent targets based on ceramics in the Cr–Al–Si–B system for PVD of heat-resistant thin films, *Galvanotechnik*, 2015, vol. 2, pp. 371–376.
4. Yu. S. Pogozhev, I. V. Iatsyuk, E. A. Levashov, A. V. Novikov, N. A. Kochetov, D. Yu. Kovalev, The kinetics and mechanism of combusted Zr–B–Si mixtures and the structural features of ceramics based on zirconium boride and silicide, *Ceram. Int.*, 2016, vol. 42, pp. 16758–16765.
5. E. A. Levashov, Yu. S. Pogozhev, A. S. Rogachev, N. A. Kochetov, D. V. Shtanskiy, Self-propagating high-temperature synthesis of composite targets based on titanium carbonitride, silicide and aluminide for ion-plasma deposition of multifunctional coatings, *Russ. J. Non-Ferrous Met.*, 2012, vol. 53, pp. 77–84.
6. A. F. Fedotov, A. P. Amosov, A. A. Ermoshkin, V. N. Lavro, S. I. Altukhov, E. I. Latukhin, D. M. Davydov, Composition, structure, and properties of SHS-compacted cathodes of the Ti–C–Al–Si system and vacuum-arc coatings obtained from them, *Russ. J. Non-Ferrous Met.*, 2014, vol. 55, pp. 477–484.

IMPORTANCE OF MORPHOLOGY OF POWDER IN EXPLOSIVE COMPACTION FOR PRODUCTION OF INTERMETALLIC ALLOYS

R. Prümmer and D. Kochsiek

EXTEC, 70619 Stuttgart, Germany

e-mail: rolf.prummer@iCloud.com

To improve the mechanical properties of alloys the microstructure has to be refined. Due to high pressure and rapid change of pressure and temperature during fabrication explosive consolidation is a good tool not only to obtain high-density compacts but also to improve the microstructure. To solve this task investigations are performed to produce intermetallic alloys TiAl and NiAl.

Explosive compaction (EC), hot explosive compaction (HEC) and their combination with SHS and shock wave synthesis are the means to achieve these goals. Starting materials are Al-, Ti- and Ni-powders. TiAl- and NiAl-powders are produced by mechanical alloying, using an attritor mill and from the melt by inert gas atomization. Also shock wave synthesis is undertaken starting from stoichiometric mixtures of Ti+Al-powders and Ni+Al-powders in order to produce TiAl- and NiAl-intermetallic alloys, respectively.

Explosive compaction and hot explosive compaction are performed with cylindrical samples. The arrangement is described in reference [1]. The powder is contained in a metallic tube which in turn is surrounded by a uniform layer of a proper explosive. The explosive consists of powdered explosives commercially obtainable. Their mixtures allow to adjust desired detonation velocities. Performance of hot explosive compaction is achieved by heating the capsule with contained metal powder inside an electric furnace up to 1000°C and subsequently dropping it into the hole of an explosive and the detonation initiated at the upper end and proceeding in axial direction, as described in [1]. Metallographic and X-ray diffraction

methods are the main tools to investigate the compacts. Tensile and in most case compressive samples serve for getting the mechanical properties. Electro spark erosion was used to obtain the samples from the compacts. Only samples with uniform consolidation over the cross section of cylindrical shape serve for this. How to obtain these is described in [1]. The best mechanical properties at room temperature are obtained from samples produced by the method of hot explosive compaction of mechanically alloyed powders both in case of TiAl and NiAl. The values obtained are exceeding room temperature values of TiAl- and NiAl-intermetallics hitherto known by more than 100%.

1. R. Prümmer, *Explosivverdichten pulvriger Substanzen*, Berlin: Springer Verlag, 1987, Russian translation: Mir Book Co, Moscow, 1990, Chinese translation: BaoTou, PRC, 1989.

R. Prümmer and D. Kochsiek

SCIENTIFIC BASIS OF CREATION OF NEW MATERIALS BY EXPLOSION WELDING TO PROVIDE SAFE HANDLING OF RADIOACTIVE WASTE

A. E. Rozen[1], A. V. Dub[2], G. V. Kozlov[1], S. I. Kamyshanskii[3], A. V. Khorin[1], I. A. Safonov[2, 4], A. A. Rozen[1], V. V. Mamontov[3], and E. F. Lezhneva[1]

[1] Penza State University, Penza, 440026 Russia
[2] National University of Science and Technology MISiS, Moscow, 119049 Russia
[3] Federal Research and Development Center Start Production Association, Zarechny, Penza, 442960 Russia
[4] JSC RPA CNIITMASH, Moscow, 115088 Russia

e-mail: aerozen@bk.ru

The radioactive waste (RW) management system includes activities for processing, conditioning, transportation, storage and final long-term isolation (disposal). The operating life of the main equipment used at various stages of RW management (vessels, devices, tanks, capacities, reactors, separators, pipelines, containers, transport packaging, etc.) does not exceed generally 40 years. In this regard, the creation of the new constructional materials providing structural stability, mechanical and isolating characteristics taking into account radiation, mechanical, chemical, thermal loadings and influences, which can arise at all stages of treatment of radioactive waste, is relevant.

High-strength cast iron with spheroidal graphite, which provides a good radiation protection due to graphite inclusions, is promising constructional material for radioactive waste of high and average degree of activity. Besides, this material has a complex of valuable physicomechanical properties: combination of high strength characteristics (from 400 to 900 MPa) and increased plasticity (up to 25%) with ferritic or austenitic structure.

The major limiting factor of its operational life is the resistance to corrosion. High-strength cast iron with spheroidal graphite, in particular, with austenitic structure from the point of view of traditional approaches of estimation of corrosion resistance for a large number of aggressive environments less than 0.1 g/(m^2·h) and a corrosion rate less than 0.12 mm/year belongs to the quite resistant class with a mass index of corrosion. Their operational life can reach 90 years. However, in the nuclear industry, where RW should be stored for thousands of years and more, these values no longer seem so reliable for the entire life cycle.

One way to solve the problem is an application of the new class of stratified composites (SC) with an internal protector, which are created by the group of authors. Preliminary results of laboratory researches indicate higher, by 10 times and more, corrosion resistance of these composites as compared to currently used. This technical solution is protected by the international patents in 11 countries [1, 2].

It is displayed that the most efficient method of production of such materials is the explosion welding, by which it is possible to produce sheet rolls with an area of up to 20 m^2 and more. Important technological issues (in particular, schemes of explosion welding of high-strength cast iron and precision thin-sheet SC with an internal protector) were solved. Data on such indexes of quality as strength properties of multilayer compositions, its plasticity, impact resistance, crack resistance, and corrosion destruction are obtained.

In the work, the theoretical approach combining a geometrical method of fractal dimension with the analysis of dynamic characteristics of interlaminar boundaries on the basis of physics of the high-speed processes was used. The offered approach allowed to carry out the system analysis of the structure defects and structure of interlaminar boundaries of composites and to vary parameters of external influence that has a scientific significance for obtaining multilayer structures with the operated characteristics.

The theoretical approach based on the functional and morphological methods of system analysis with application of elements of the graph theory is developed. It allowed to develop the scientific principles of creation of new architecture of a multilayer material, which has no analogs in the world. Using of this material

will greatly increase product operational life and will provide safe handling of RW at all stages of life cycle.

1. A. E. Rozen, I. S. Los', Yu. P. Perelygin, Multilayer material with enhanced corrosion resistance (variants) and methods for preparing same, *Eurasian Patent 016878*, June 30, 2012.
2. A. E. Rozen, I. S. Los', Yu. P. Perelygin, Multilayer material with enhanced corrosion resistance (variants) and methods for preparing same, *Patent 10-1300674 KIPO*, August 21, 2013.

STRUCTURING OF THE INTERLAYER BOUNDARIES DURING EXPLOSION WELDING OF LAYERED COMPOSITE MATERIALS AND MODELING OF WAVE FORMATION CONDITIONS

A. E. Rozen[1], Yu. P. Perelygin[1], S. G. Usatyi[1], A. V. Khorin[1], I. A. Safonov[2,3], O. N. Loginov[1], A. A. Rozen[1], and E. V. Zavartseva[1]

[1] Penza State University, Penza, 440026 Russia
[2] JSC RPA CNIITMASH, Moscow, 115088 Russia
[3] National University of Science and Technology MISiS, Moscow, 119049 Russia

e-mail: aerozen@bk.ru

Wide distribution of layered composite materials (LCMs) among other things is limited by difficulties linked with provision of equal strength conditions at all interlayer boundaries. This problem is especially topical for new LCM with an internal protector, the application of which in many industries in the medium term is able to reach several tens of thousands of square meters per year.

With the same gap, conditions of formation of interlayer boundaries between first and second plates, as well as between second and third ones will be different. Kinetic and energy differences at the interlayer boundaries vary as the new plates are brought into motion. Their total number can reach 4 upon receiving of LCM with one protector under one-sided effect of aggressive environment conditions and 14 upon receiving of LCM with two protectors under double-sided action of an aggressive environment. The paper will consider in detail the first version of the multilayered material structure.

As the condition of equal strength of all such interlayer boundaries identical conditions of plastic deformation during the passage of the shock wave may act. The reliability of this condition can be assessed by the interlayer boundaries profile matching (amplitude, wavelength

and its profile). If these characteristics are identical in different layers, then with high reliability it is possible to affirm an identity and their mechanical strength (peel, shear).

Under indicated boundary conditions, the possible adjustable parameters for explosion welding remain the height of the charge BB and the gap value at each interlayer boundary. Accordingly, the task of the process modeling is the determination of a limited number of factors: H_{BB} and h_1, h_2, h_3, providing a given amplitude value, wavelength, and also, a specific profile at each interlayer boundary. To assess the wave formation conditions, it was applied a mathematical modeling method using a LS-DYNA software product [1].

The following models of materials and equations of state were used in the calculation:

Explosive:
– material model – no. 9 (Wilkins–Geyrouh);
– equation of state – no. 2 (JWL).
Metal plate:
– material model – no. 15 (Johnson–Cook);
– equation of state – no. 4 (Mie–Grüneisen).
Finite element mesh characteristics used:
– amount of elements – 4795764;
– number of nodes – 5083509;
– maximum element size – 20 μm.
Features of the solution:
– the use of a multicomponent Lagrangian–Eulerian method;
– Lagrangian description of the projected plate motion;
– the use of Lagrangian–Euler coupling.

For the calculation, the following boundary conditions and assumptions were adopted:

– detonation wave propagation occurs uniformly along the entire length of the BB charge with a constant speed of 2100 m/s;

– stable wave formation at the interlayer boundary begins at a distance of 250 mm from the detonation point;

– conditions of wave formation at the interlayer boundaries of steel sheets remain stable up to a length of 6000 mm.

The obtained results indicate a good convergence of the calculated experimental values of the amplitude, wavelength, and shape factor,

including multilayered compositions. The modeling of the wave surface interlayer boundaries in the explosion welding of a three-layered material results are presented in Fig. 1. The deviation did not exceed 17%.
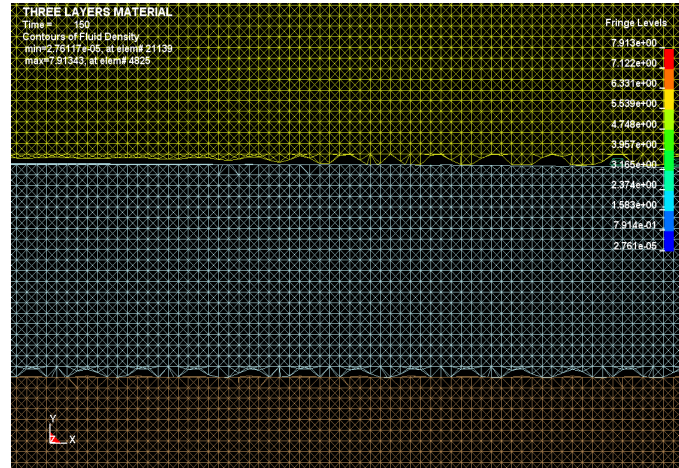

Fig. 1. The distribution of the wave surface at the interlayer boundaries in the calculated region.

The above calculation system allows to solve only direct problems, when the explosion welding original parameters was used to determine the wave pattern of the interlayer boundaries.

To solve the inverse problem, when it is necessary to use forming wave pattern characteristics for determination of explosion welding initial parameters, a direct search method was proposed. It consists in alternating one variable with a certain step, provided that the others remain constant. The search performs until the maximum or minimum of the objective function will be reached.

The calculated and experimental values indicate that the discrepancy between them does not exceed 17%. Wherein it managed to achieve the condition that the values of λ, *l*, and *K* in each layer differ from each other by no more than 8% (Fig. 2). The discrepancy between the basic values of the mechanical properties in each of the layers is also in the indicated limit.

The created calculation system for determining the basic parameters of explosion welding provides conditions of equal strength at all interlayer boundaries and can be proposed for a wide range of LCMs.
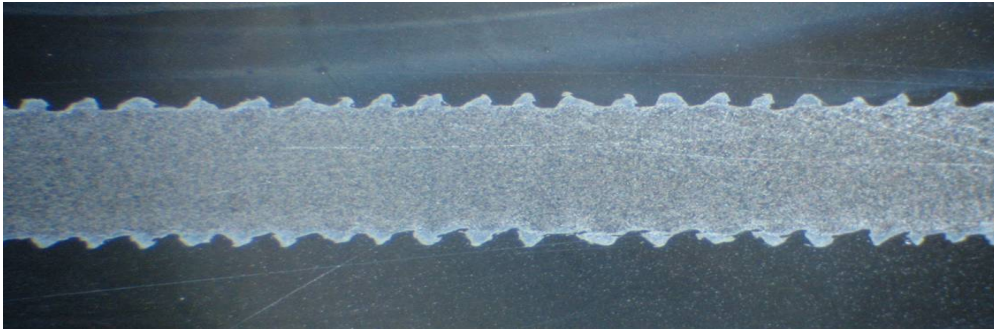
A. E. Rozen et al.

Fig. 2. Welded joint profile of a three-layer material after choosing the parameters of explosion welding according to the proposed calculation system.

1. A. E. Rozen, I. S. Los', A. Y. Muyzemnek, D. B. Kryukov, A. V. Chorin, I. V. Denisov, *Mathematical modeling of deformation and explosive processes occurring during explosion welding*, Bulletin of the Volgograd State Technical University. Explosion welding and properties of welded joints, 2006, i. 2, no. 9 (24), pp. 79–87.
2. A. E. Rozen, I. S. Los', L. B. Pervukhin, Y. P. Perelygin, S. G. Usatyi, D. B. Kryukov, A. A. Rozen, *Experience in the development and certification of multi-layer corrosion-resistant materials with "protector pitting-defence"*, News of higher educational institutions. The Volga region. Technical sciences, Penza: PSU Publishing House, 2014, no. 3, pp. 61–74.

INITIATION OF COMBUSTION OF METAL–TEFLON SYSTEMS WITH EXPLOSIVE ACTION

I. V. Saikov, M. I. Alymov, and S. G. Vadchenko

[1]Merzhanov Institute of Structural Macrokinetics and Materials Science, Russian Academy of Sciences, Chernogolovka, Moscow, 142432 Russia

e-mail: revan.84@mail.ru

The investigation is aimed at the study of features and conditions of initiation, reaction, and final phase formation in the energetic condensed metal–Teflon systems under shock wave loading. Thermodynamic calculations were carried out using a THERMO program [1]. Based on these calculations, 16 different mixtures were made. The adiabatic combustion temperatures, the composition and quantity of condensed products and the volume of gaseous products were calculated. To increase the combustion temperature, Teflon powder was used as one of the components. The calculations showed that the compositions provided a sufficiently wide range of adiabatic combustion temperatures from 1190°C for Cu–Al–C_2F_4 composition to 3280°C for Hf–B–C_2F_4. The compositions based on Ni–Al, Cu–Al and Nb–Al with Teflon differed in predominance of liquid phase in the products at relatively low combustion temperatures (1740ºC, 1190ºC and 1410ºC, respectively). The shock-wave loading of the samples was carried out in a multi-cell matrix by throwing a flyer. The acceleration of the flyer was carried out by detonation of the explosive. The detonation was initiated by an electric detonator located in the center along the assembly axis. Thus, the design of the recovery fixture provided the same loading conditions in all the cells. Ni–Al, Ni–Al–C_2F_4, Ti–B–C_2F_4, Hf–B–C_2F_4 systems reacted most completely. Thus, the systems based on metals (titanium and hafnium) with additives of boron and Teflon are the most promising ones to be used as a reaction material from the viewpoint of the achieved

synthesis temperature, initiation by shock-wave action and the reaction completeness [2, 3].

1. A. A. Shiryaev, Program for Thermodynamics Equilibrium Calculations "THERMO", 1998, www.ism.ac.ru/thermo/
2. I. V. Saikov, M. I. Alymov, S. G. Vadchenko, I. D. Kovalev, Investigation of shock-wave initiation in metal-teflon powder mixtures, *Lett. Mater.*, 2017, vol. 7, no. 4. pp. 465–468.
3. M. I. Alymov, S. G. Vadchenko, I. V. Saikov, I. D. Kovalev, Shock-wave treatment of tungsten/fluoropolymer powder compositions, *Inorg. Mater. Appl. Res.*, 2017, vol. 8, no. 2. p. 340–343.

RESIDUAL STRESSES IN BIMETAL PREPARED BY EXPLOSION WELDING

K. Saksl[1, 2], Š. Michalik[3], D. M. Fronczek[4], K. Šuľová[1, 5], M. Šuliková[2], A. Lachová[2], Z. Szulc[6], M. Fejerčák[1, 2], Z. Molčanová[1], and D. Daisenberger[3]

[1] Institute of Materials Research, Slovak Academy of Sciences, Watsonova 47, 040 01 Košice, Slovak Republic
[2] Faculty of Science, Institute of Physics, Pavol Jozef Šafárik University in Košice, Košice 041 80, Slovak Republic
[3] Diamond Light Source Ltd., Harwell Science and Innovation Campus, Didcot, Oxfordshire OX11 0DE, UK
[4] Institute of Metallurgy and Materials Science, Polish Academy of Sciences, 25 Reymonta St. 30-059 Cracow, Poland
[5] Faculty of Materials metallurgy and Recycling, Technical University of Košice, Letna 9, 042 00 Košice, Slovak Republic
[6] High Energy Technologies Works 'Explomet', 100H Oswiecimska St. 45-641 Opole, Poland

e-mail: ksaksl@saske.sk

Explosive welding is a method applied for joining of a wide variety of similar or fundamentally dissimilar materials that cannot be joined by any other welding or bonding technique. Under conditions of controlled explosion, two or more materials can be joined by pressure, generated by detonation of explosives placed on the top of a welded material. Impact on plates at their contact surfaces is governed by the laws of ideal fluid where shock wave with amplitude ranging from 10 to 100 GPa propagates through materials, causing strong deformation pronounced mainly at the bonded zone areas. Intensity of the impact substantially exceeds yield strength of basic materials, forming wavy interface often seen with spikes or jets of one material indented to another one. Such joining process, however, produces extraordinarily high residual stresses, stresses that exist in material independently of the presence of any external loads. Their presence may not be readily

apparent and so they may be overlooked or ignored during a process of engineering design. This, however, can cause great design risk because they can have profound impact on material strength, dimensional stability and fatigue life. Almost all manufacturing processes create residual stresses that can further develop during service life of the manufactured component. Several comparative, qualitative and quantitative methods for stress analysis are nowadays applied in engineering praxis. Among them X-ray diffraction is one of the most used and developed over the past 90 years. In this article we describe novel concept of two-dimensional X-ray diffraction (XRD^2) [1] and we demonstrate its applicability on determination of residual strains and stresses in a bimetallic duplex steel/ferrite steel system prepared by explosion welding, material originally designed for a geothermal applications. Our analysis is based on X-ray micro-diffraction experiments utilizing hard monochromatic X-rays focused down to micrometer size. In this way, bimetal in bulk form was analyzed and microstructural differences between the joined materials and their interface were determined.
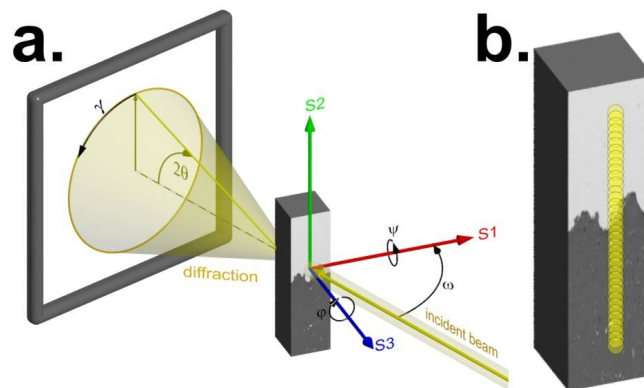

Fig. 1. (a) Orientation of laboratory diffraction and sample coordinate system S1, S2, S3. (b) The duplex steel/ferritic steel, yellow circles represents shot-by-shot scan along a straight path (length of 1.8 mm) with 10 μm step size by photon beam with an energy of 76.01keV focused down to 20 μm. The scan was done in direction from duplex steel (top) to ferritic steel (bottom).

1. O. R. Bergmann, G. R. Cowan, A. H. Holtzmann, Experimental evidence of jet formation during explosion cladding. *Trans. Metall. Soc. AIME.*, 1966, 236, pp. 646–653.
2. B. B. He, *Two-dimensional X-ray diffraction*, 1st ed. New Jersey: John Wiley & Sons, 2009.

REPROCESSING OF MILL SCALE WASTES BY SHS METALLURGY FOR PRODUCTION OF CAST FERROSILICON, FERROSILICO ALUMINUM AND FERROBORON

V. N. Sanin*, D. M. Ikornikov, D. E. Andreev, N. V. Sachkova, and V. I. Yukhvid

Merzhanov Institute of Structural Macrokinetics and Materials Science, Russian Academy of Sciences, Chernogolovka, Moscow, 142432 Russia

*e-mail: svn@ism.ac.ru

The metallurgical industry is one of the most massive material-forming industries. High amount of by-products in the form of mill scale sludge is generated every year in each section of steel making plants due to hot rolled metal processing at elevated temperatures. Mill scale, often called as scale, is the flaky surface consisting of the iron (II) oxide (FeO), iron(III) oxide (Fe_2O_3), and iron(II,III) oxide (Fe_3O_4, magnetite). It can be considered as a valuable metallurgical raw material for iron and steel making industry [1, 2]. The strict environmental regulations as well as the valuable metallic content cause the ability to recycle mill scales become an important issue. Currently, many metallurgical plants have accumulated large amounts of mill scale in the dumps, containing oils (4–12%) and moisture (4–18%). After the removal of oil and water, this material contains up to 70% of iron with the minimum amount of sulfur compounds and can be effectively used in both blast and steel smelting operations. The solution of this task is becoming more effective due to the world deficit and the constant growth of the cost of iron ore, as it allows to reduce raw materials dependence and improve the ecology. So, there has been a big tendency to recover the valuable iron content in the production process. Accordingly, the most used route to recycle the iron-contenting wastes, briquettes are charged into blast furnace due to

its reducing atmosphere or into the electric arc furnace (EAF) during the melting of stainless steel scrap [3]. These processes allow to process mill scale in the metal product, but the economic efficiency remains at a sufficiently low level.

The most effective approach is the use of energy efficient technologies and the expansion of nomenclature of the products obtained from the recycled scale. In this regard, the present study was conducted to evaluate the possibility, efficiency, and consequences of the reduction of mill scale in combustion mode. A promissory route to the production of cast ferroalloys with different compositions is using technique, which was called the SHS technology of high-temperature melts or the SHS metallurgy [4, 5]. This is an energy-saving technique due to the use of internal energy released in high-caloric combustion reactions. Early, the possibility of preparation on cast ceramic coatings inside metallic pipes was first demonstrated by reprocessing of mill scale [6].

In the work, the scales generated from steel making plants were collected and used for reparation of powder mixtures with the reducing agent (Al) and alloying additives (Si, B). The average particle size was 50–100 μm for the scale and less than 140 μm for aluminum (brand PA-4). The weight of the initial mixture for combustion was constant in all experiments (1200 g). Combustion was carried out in graphite molds 80 mm in diameter. The inner surface of the graphite molds was laminated with Al oxide (Al_2O_3) to ensure minimal reactive interaction between the form material and metal melt. Our previous studies have demonstrated that the SHS process carried out under high gravity conditions affords the best separation of the target product (ingot) from the slag (Al_2O_3) and convective mixing of all alloy components, which becomes especially important with an increase in the number and concentration of components in the alloys. Therefore, the synthesis of the as cast alloy under study was carried out in a centrifugal SHS setup [4]. The main data on the determination of optimal chemical and technological conditions for the production of cast ferroalloys in Fe–Si–Al, Fe–Si–Al (Cr, Mn), Fe–Si–Al–B systems will be presented at presentation. Figure 1 illustrates composition and the microstructure of SHS-produced as-cast ferroalloys by reprocessing of mill scale wastes.

	Al	Si	Mn	Fe
Sp. 1	4.3	23.2	0.6	71.9

(a)

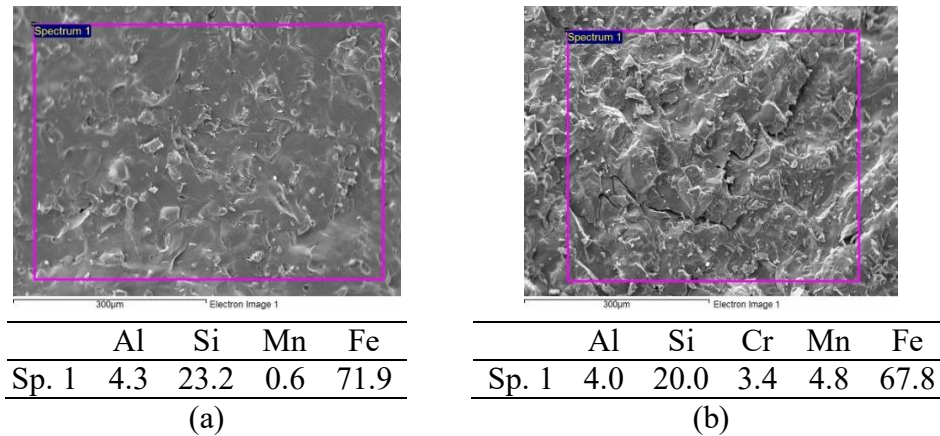|	Al	Si	Cr	Mn	Fe
Sp. 1	4.0	20.0	3.4	4.8	67.8

(b)

Fig. 1. SEN images and EDS results of synthesized cast ferroalloys (fracture): (a) Fe–Si–Al, (b) Fe–Si–Al (Cr, Mn).

The production of complex alloyed ferroalloys can be realized in combustion mode (SHS) for powder mixtures on the basis of scale. The process of obtaining high-alloy ferroalloys is completely energy independent, which makes it attractive for practical realization

1. V. I. Shatokha, O. O. Gogenko, S. M. Kripak, Utilising of the oiled rolling mills scale in iron ore sintering process, *Res. Cons. Recyc.*, 2011, vol. 55,, pp. 435–440.
2. D. Cartwright, J. Clayton, Recycling oily mill scale and dust by injection into the EAF, *Steel Times Int.*, 2000, vol. 24, pp. 42–43.
3. Q. Yang, N. Holmberg, B. Bjorkman, EAF smelting trials of briquettes at Avesta works of outokumpu stainless AB for recycling oily mill scale sludge from stainless steel production, *Steel Res. Int.*, 2009, vol. 80, pp. 422–428.
4. V. N. Sanin, D. M. Ikornikov, D. E. Andreev, V. I Yukhvid, Centrifugal SHS metallurgy of nickel aluminide based eutectic alloys, *Russ. J. Non-Ferr. Metall.*, 2014, vol. 55, pp. 613–619.
5. V. N. Sanin, V. I. Yukhvid, D. M. Ikornikov, D. E. Andreev, N. V. Sachkova, M. I. Alymov, SHS metallurgy of high-entropy transition metal alloys, *Dokl. Phys. Chem.*, 2016, vol. 470, pp. 145–149; doi:10.1134/S001250161610002X.
6. V. N. Sanin, D. E. Andreev, V. I. Yukhvid. Self-propagating high-temperature synthesis metallurgy of pipes with wear-resistant protective coating with the use of industrial wastes of metallurgy production, *Russ. J. Non-Ferr. Metall.*, 2013, vol. 54, no. 3, pp. 274–279.

SYNTHESIS OF CAST CoCrFeNiMn-BASED HIGH-ENTROPY ALLOYS AND COATINGS OF THEM BY CENTRIFUGAL METALLOTHERMIC SHS

V. N. Sanin[1]*, D. M. Ikornikov[1], D. E. Andreev[1], S. V. Zherebtsov[2], and V. I. Yukhvid[1]

[1] Merzhanov Institute of Structural Macrokinetics and Materials Science, Russian Academy of Sciences, Chernogolovka, Moscow, 142432 Russia.
[2] Belgorod National Research University, Belgorod, 308015 Russia

*e-mail: svn@ism.ac.ru

High-entropy alloys (HEAs) have recently emerged as a new class of advanced metallic materials promising for various applications [1, 2]. Their main feature is high complexity of chemical composition; according to original definition, HEAs should be composed at least five principal elements in close to equiatomic concentrations (5–35 at %) [3].

One of the promising classes of the HEAs, which attained particular attention, is fcc Co–Cr–Fe–Ni–Mn alloys. The alloys have unique mechanical properties: very high ductility at room temperature becomes even higher when the temperature decreases to the cryogenic interval. Although composition-structure-property relationships of the Co–Cr–Fe–Ni–Mn alloys are under extensive investigation, many aspects of behavior of these alloys have not received significant attention yet.

The problematic aspect is the production of HEAs with liquation free structure. Conventional casting processes for production of HEAs are the multistage vacuum-arc or induction remelting of extra-pure grade elements. To achieve the desired homogeneity, 4–6 remelts may be required depending on the composition and content of the alloying components. Therefore, the conventional metallurgical technologies are rather expensive and energy-consuming. The method referred as

the SHS-technology of high-temperature melts [4] or SHS-metallurgy [5] is a promissory route to produce cast HEAs. This is an energy-saving technique due to the use of internal energy released in high-caloric combustion reactions. Recently, the one was firstly demonstrated to prepare cast high-entropy transition metal alloys [6].

Powder mixtures of metal oxides (Co_3O_4, Cr_2O_3, Fe_2O_3, NiO, MnO_2) with metal reducer (Al) and pure C and ScF_3 as alloying elements were used as the starting components to produce the cast Co–Cr–Fe–Ni–Mn alloy. The procedure of fabrication of the SHS alloy and investigation have been described in detail in [6, 7]. Figure 1 illustrates the phase composition and microstructure of SHS-produced as-cast CoCrFeNiMn alloy without additives.

The XRD pattern and microstructure demonstrate the presence of single phase with fcc lattice. According to XRD, the fcc lattice parameter $a = 3.588$ nm. In addition, XRD and EBSD data show strong crystallographic texture typical of the cast materials. The alloy has a coarse-grained structure with a grain size of 250–400 μm. The grain boundaries are often curved and the shape of grains is irregular. No second phases were revealed by SEM and TEM.
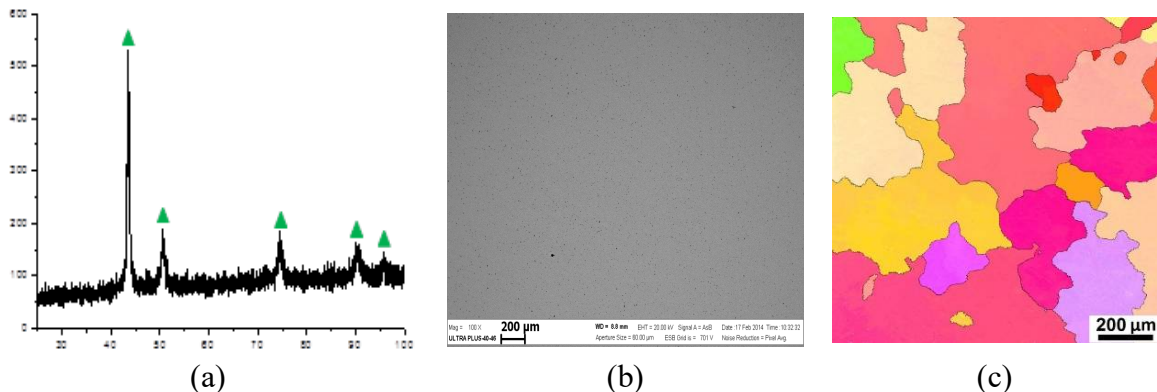

| (a) | (b) | (c) |

Fig. 1. Phase composition and microstructure of the as-cast CoCrFeNiMn alloy: (a) XRD pattern (▲ fcc (*Im3m*))*,* (b) SEM, (c) EBSD IPF map.

Alloyed components introduced into starting mixture of CoCrFeNiMn alloy also took part in the formation of chemical composition directly in the combustion wave. The alloying with up to 0.2 wt % C affects insignificantly the phase composition formation but leads to an increase in the hardness of the alloy. The same was observed upon alloying with Sc. The introduction of Al into the

V. N. Sanin et al.

composition of the alloy markedly reduces its density. At high Al concentrations, intermetallic NiAl phase is formed; a sharp decrease in the plasticity is observed.

In the work, we investigated the possibility of formation of the coating in-situ (SHS-coating) for HEAs on a metal substrate (Ti alloy) for the first time. Figure 2 shows the transition zone structure of the deposited coating layer/ Ti substrate. Analysis of the microstructure of the deposited layer revealed the presence of three zones (Fig, 2a) where the base material (Ti) gradient distributed over the height of the deposited layer. Figure 2b demonstrates the difference in the hardness of the substrate and coating, it is more than 3 times.

Thus, we can conclude on the prospects of the materials under investigation and the method of their production for the formation of volumetric materials and coating of them. The production of metallic composite materials based on the new principle of formation of polymetallic alloys can significantly expand the basis for the creation of new materials and facilitates the creation of new technological models.
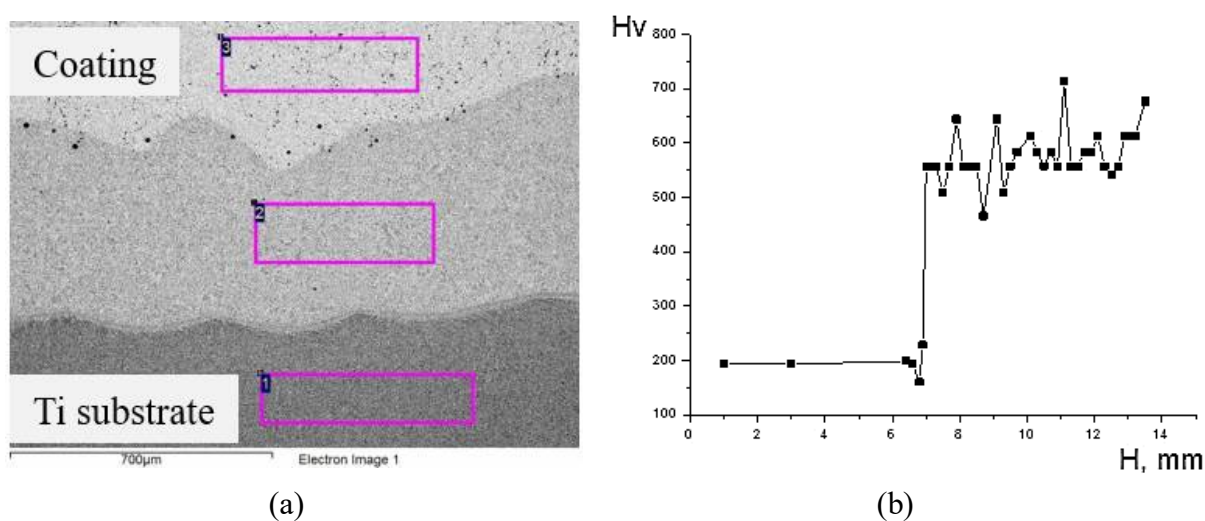

(a) (b)

Fig. 2. (a) Microstructure of the SHS surfacing and (b) dependence of microhardness on height of coating.

1. D. B. B. Miracle, O. N. N. Senkov, A critical review of high entropy alloys and related concepts, *Acta Mater.*, 2017, 122, pp. 448–511; DOI:10.1016/j.actamat.2016.08.081.

2. M. H. Tsai, J. W. Yeh, High-entropy alloys: A critical review, *Mater. Res. Lett.*, 2014, vol. 2, pp. 107–123; DOI:10.1080/21663831.2014.912690.

3. D. Miracle, J. Miller, O. Senkov, C. Woodward, M. Uchic, J. Tiley, Exploration and development of high entropy alloys for structural applications, *Entropy.*, 2014, vol. 16, pp. 494–525; DOI:10.3390/e16010494.

4. A. G. Merzhanov, Combustion processes that synthesize materials, *J. Mater. Process. Techol.*, 1996, vol. 56, pp. 222–241.

5. V. N. Sanin, D. M. Ikornikov, D. E. Andreev, V. I. Yukhvid, Centrifugal SHS metallurgy of nickel aluminide based eutectic alloys, *Russ. J. Non-Ferr. Metall.*, 2014, vol. 55, no. 6, pp. 613–619; DOI:10.3103/S1067821214060212.

6. V. N. Sanin, V. I. Yukhvid, D. M. Ikornikov, D. E. Andreev, N. V. Sachkova, M. I. Alymov, SHS metallurgy of high-entropy transition metal alloys, *Dokl. Phys. Chem.*, 2016, vol. 470, pp. 145–149; DOI:10.1134/S001250161610002X.

7. V. N. Sanin, D. M. Ikornikov, D. E. Andreev, N. V. Sachkova, V. I. Yukhvid, Synthesis of cast high entropy alloys with a low specific gravity by centrifugal metallothermic SHS-methods, *Adv. Mater. Tech.*, 2017, no. 3, pp. 24–33; DOI: 10.17277/amt.2017.03.pp.

PREPARATION OF 70Cu–30Fe ALLOY BY SHS METALLURGY AND SUBSEQUENT MECHANICAL HEAT TREATMENT

V. V. Sanin[1]*, M. R. Filonov[1], Yu. A. Anikin[1], D. M. Ikornikov[2], and V. I. Yukhvid[2]

[1] National University of Science and Technology MISiS, Moscow, 119049 Russia
[2] Institute of Structural Macrokinetics and Materials Science, Russian Academy of Sciences, Chernogolovka, Moscow, 142432 Russia

e-mail: sanin@misis.ru

Alloys with limited solibility in solids and liquids—such as Cu–Fe alloys—are difficult to fabricate by conventional methods [1]. These are normally produced by melting in microgravity, melting in crossed electromagnetic fields, mechanical intermixing of melts, mechanical alloying, and other techniques that are unprofitable and yield largely inhomogeneous products.

In this work, we fabricated 70Cu–30Fe alloys in a two-stage process involving: (a) metallothermic SHS of cast ingots under artifcial gravity and (b) subsequent pull-type forging at 850°C followed by cold drawing. The alloy under consideration may find its application in designing magnetically hard materials [2].

Combustion synthesis (stage a) was conducted in the centrifugal machine desribed elsewhere [3] for $n = a/g = 2$–50, where a is the centrigugal acceleration and g the acceleration of gravity. The main process parameters as a function of a/g are presented in Fig. 1.

As follows from Fig. 2, the SHS-produced alloy exhibits an heirarchical three-level structure. The first level (Figs. 2a, a') can be characterized by uniform distribution of Fe grains (10–30 μm in size) over the entire ingot volume. At the second level (Figs. 2b, b', b") we can discern the Cu particulates (0.5–4 μm) uniformly distributed within the Fe grains.
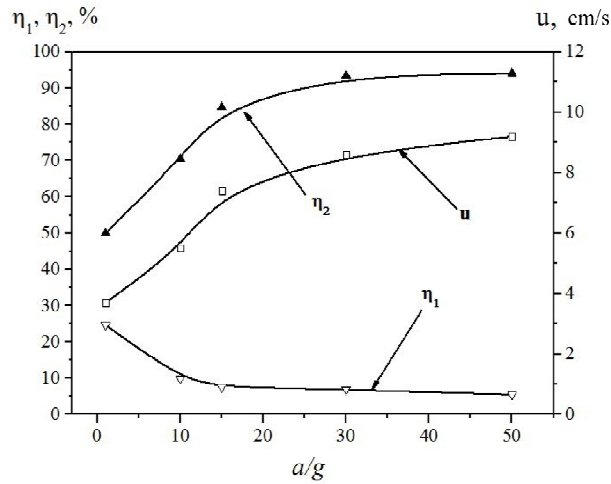
Fig. 1. Burning velocity *u*, material loss η_1, and yield of cast alloy η_2 as a function of *a*/*g*.
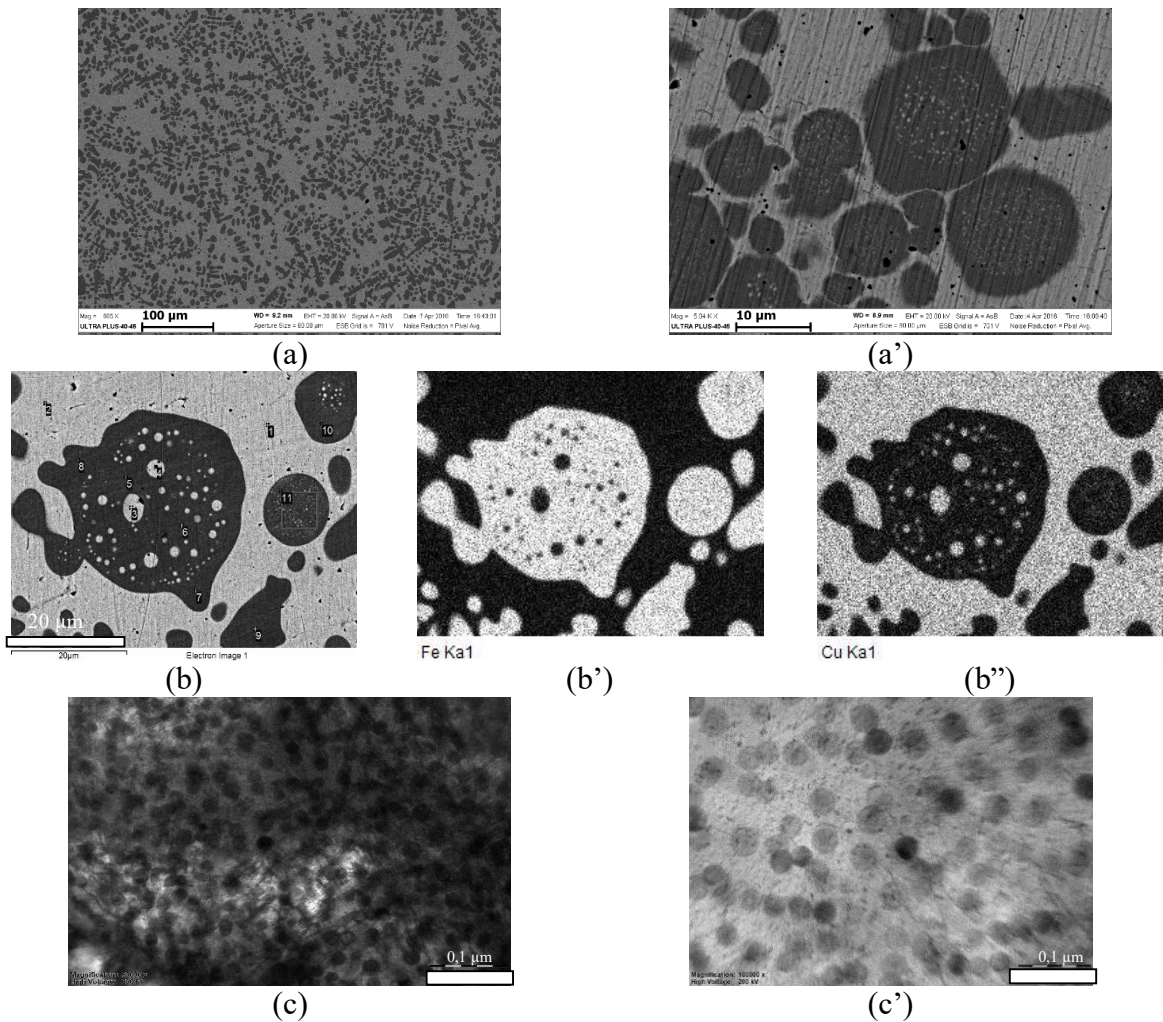

Fig. 2. TEM/EDS results for SHS-produced 70Cu–30Fe alloy.

At still larger magnification (Figs. 2c, c'), we can discern the third structural level, that is, the submicron Fe particles (20–25 nm) uniformly distributed within the Cu matrix. Such a structure can be

explained by specific conditions of SHS metallurgy. A high combustion temperature (above 2500 K) ensures the elevated solubility of Cu in Fe. Then, at the stage of crystallization, ever decreasing temperature facilitates the precipitation of Cu in the form of fine particles.

At stage *b*, SHS-produced ingots were heated in furnace to 850°C and subjected to pull-type forging to obtain 10-mm rods (their structure is shown in Fig. 3a) and then to cold drawing ($v = 4.5$ m/s, separation between draw plates of 0.2 mm) to obtain a wire with a diameter of 4.5 mm ($\varepsilon = 67\%$, Fig. 3b) or 3 mm ($\varepsilon = 86\%$, Fig. 3c).

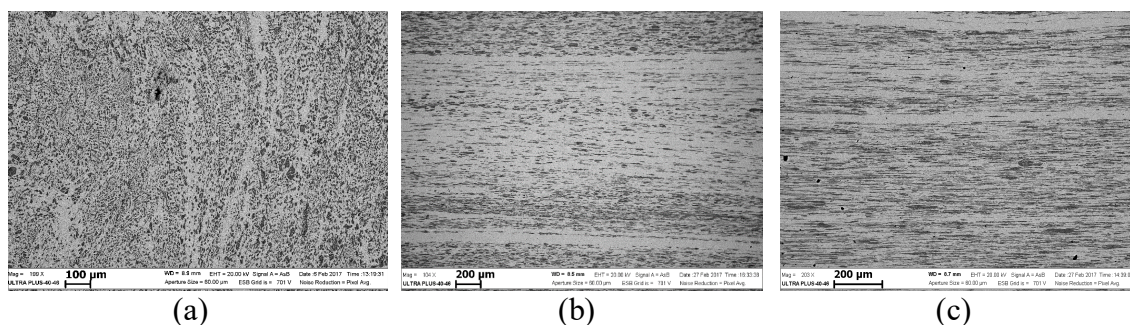(a)   (b)   (c)

Fig. 3. Microstructure of material cross section after (a) pull-type forging and cold drawing to (b) $\varepsilon = 67$ and (c) $\varepsilon = 86\%$.

Thermomechanical processing of SHS-produced Cu–Fe alloys can be readily used to regulate their structure and to fabricate bulk materials with longitudinally oriented structural constituents, which opens up new horizons for designing magnetic materials based on the systems with limited solubility.

1. Yu. S. Avraamov, A. D. Shalyapiun, *Alloys with limited solubility in the liquid phase*, Moscow: Interkontakt Nauka, 2002 (in Russ.).
2. M. El. Ghannami, C. Gómez-Polo, G. Rivero, A. Hernando, *Europhys. Lett.*, 1994, vol. 26, pp. 701–706.
3. V. N. Sanin, D. M. Ikornikov, D. E. Andreev, V. I. Yukhvid, Centrifugal SHS metallurgy of nickel aluminide based eutectic alloys, *Russ. J. Non-Ferr. Met.*, 2014, vol. 55, pp. 613–619.

NiAl-BASED ALLOY BY SHS METALURGY AND SUBSEQUENT REMELTING AND CASTING IN STEEL PIPE

V. V. Sanin[1]*, M. R. Filonov[1], E. A. Levashov[1], Yu. S. Pogozhev[1], V. I. Yukhvid[2], and D. M. Ikornikov[2]

[1] National University of Science and Technology MISiS, Moscow, 119049 Russia
[2] Merzhanov Institute of Structural Macrokinetics and Materials Science, Russian Academy of Sciences, Chernogolovka, Moscow, 142432 Russia

*e-mail: sanin@misis.ru

High-alloyed Ni, Co, or Fe presently are base alloys when developing many materials operated in extreme conditions (high temperatures and loads) used in such industries as aircraft and marine engine building, rocket and space vehicle technology, special techniques, technologies for creating nuclear power plants, etc. A significant number of works in this area is aimed at solving problems concerned with the development of new alloys with an increased level of physicochemical characteristics and technologies for their production. Particular attention is paid to alloys based on equiatomic nickel aluminide, which have unique combinations of chemical, physical, and operational properties: high melting point (1640^0C), chemical stability, low density, high heat and corrosion resistance. Despite the above advantages, these alloys have not yet been implemented on a large-scale, which is due to their lack of manufacturability, low ductility and strength at room temperature.

Common production technologies for such materials often do not allow achieving the required set of properties and, in addition, are complex, multi-step, energy-intensive. The combination of such factors does not allow for the commercial launch of these materials. One of the efficient directions in solving the problem of guaranteed

increase product quality of these materials while reducing the energy and material manufacture-related costs is the development of a comprehensive technology for the production of NiAl-based cast materials.

The present paper suggests a complex technology for the production of blend billets based on nickel aluminide, which includes: (*1*) synthesis of cast charge materials (SCCM) with a regulated chemical composition by centrifugal self-propagating high-temperature casting method [1], (*2*) one-stage metallurgical processing (induction remelting under vacuum or inert medium) of synthesized SHS materials (SCCM) with subsequent pouring into ingots to form blend billets of s set geometry. Initially, a set of experiments was performed to optimize the synthesis conditions for a multicomponent intermetallic alloy. The analysis of the samples in the investigated range of (*g*) values showed that the mass of the ingots of the alloy synthesized at 50–150 *g* (± 5 *g*) was close to the calculated (~ 98 mass %), and its loss (spread) in the combustion process did not exceed 1.5% by weight. All samples obtained at the given overload had a cast shape, and a clear separation into 2 layers was observed: the target alloy and the oxide layer (Al_2O_3). It is evident that residual porosity was not detected on the transverse cleavage of the ingot under the condition of synthesis of more than 50 *g* (Fig. 1).

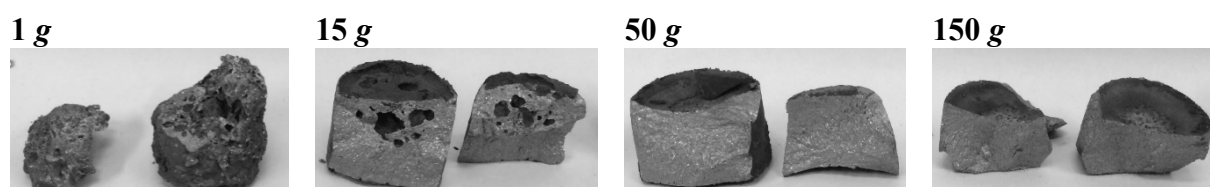**1 *g***　　　　**15 *g***　　　　**50 *g***　　　　**150 *g***

Fig. 1. Overall view of samples obtained with various overloads (*g*) after transverse cleavage.

During the next stage of the research, a remelting of the previously synthesized SCCM in a high-temperature viscometer VIC-VRM was performed to find the exact melting point of the investigated alloy, which equaled to 1570°C. Melting was carried out in an Ar atmosphere with an excess pressure of 0.3 atm. The next stage was vacuum induction remelting (VIR) of the obtained SHS-alloy blanks and pipe-casting followed by crystallization and preservation of this alloy in this cylindrical form. Based on the data obtained in earlier studies of these alloys [2], the main task was to study the required

diameter of the cylindrical crystallizer, as well as its composition. A series of melting and casting in various diameters and compositions of steels was carried out. The optimum variant was a cylindrical crystallizer made of steel grade 10 with a wall thickness of 6 mm. Figure 2a shows the resulting long-length sample. There is no chemical interaction of NiAl-based alloy with in the inner part of the pipe wall. The alloy is retained in the pipe only due to the coefficient of thermal expansion (CTE) and mechanical interaction by means of incisions (previously shown on the inner part of the pipe) (Fig. 2b).

(a)   (b)   (c)
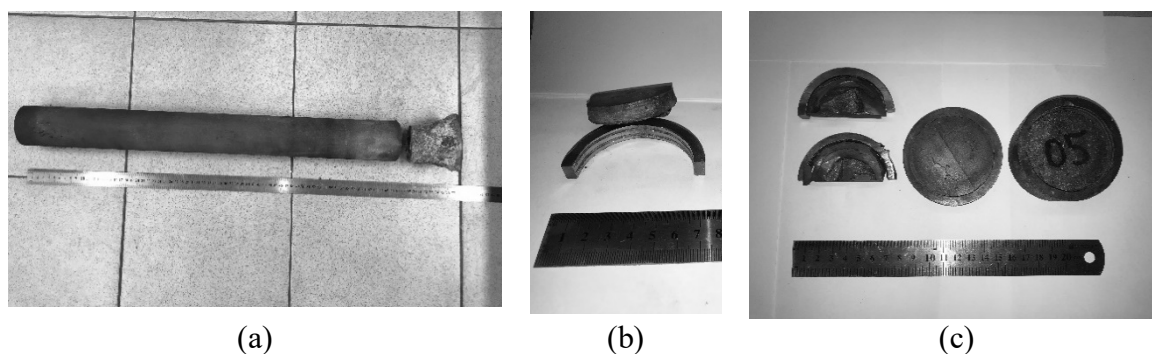
Fig. 2. (a) The resulting NiAl-alloy in the tube, (b, c) cut of NiAl-alloy.

After casting and crystallization, the pipe walls do not melt. Figure 2c shows samples taken from the base, middle and upper parts of the long-length sample. Thus, it is the possibility of subsequent turning on the entire surface.

Thus, a one-piece long-dimensional ($L = 600$ mm) cylindrical sample ($d = 70$ mm) was obtained from the NiAl-based alloy for subsequent plasma centrifugal sputtering and obtaining spherical pellets based on Fe + NiAl alloy with improved performance.

1. V.N. Sanin., D.M. Ikornikov, D.E Andreev., V.I. Yukhvid, Centrifugal SHS metallurgy of nickel aluminide based eutectic alloys, *Russ. J. Non-Ferr. Met.*, 2014, vol. 55, no. 6, pp. 613–619.
2. V.V. Sanin, Yu. A. Anikin, V. I. Yukhvid, and M. R. Filonov. Structural Heredity of Alloys Produced by Centrifugal SHS: Influence of Remelting Temperature, *Int. J. Self-Propag. High-Temp. Synth.*, 2015, vol. 24, no. 4, pp. 210–214.

CHEMICAL REACTIONS, EoS-CALCULATIONS AND MECHANICAL BEHAVIOR OF SHOCKED POROUS TUNGSTEN CARBIDE IN THE MBAR-RANGE

T. Schlothauer[1*], C. Schimpf[2], G. Heide[3], and E. Kroke[1]

[1] Institute of Inorganic Chemistry, Technical University Bergakademie Freiberg, Leipziger Strasse 29, Freiberg D-09596, Germany
[2] Institute of Materials Science, Technical University Bergakademie Freiberg, Gustav-Zeuner-Strasse 5, Freiberg D-09596, Germany
[3] Institute of Mineralogy, Technical University Bergakademie Freiberg, Brennhausgasse 14, Freiberg D-09596, Germany

[*]e-mail: thomas.schlothauer@mineral.tu-freiberg.de

The shock compaction of hard brittle materials for industrial use is linked with large problems. Few examples for undesirable behavior are cracking of the samples, chemical reactions in the powders and often a sample loss at higher pressures [1]. These facts make investigations with plane wave geometries extremely difficult. To overcome these problems different methods were tested, e.g. buffer plates for diamond compaction [2], preheating of the samples as shown for silicon nitride [3] and for tungsten bearing alloys [4], explosive liquid phase sintering [5] and thick walled hollow cylinder [6]. For the shock compaction of tungsten carbide, two properties of this material cause problems: its high hardness and its high density, resulting in an extremely high impedance. Since the behavior of this brittle material under shock influence is not well understood [7], shock recovery experiments under pressures above 100 GPa (calculated pressures) are required to get better insights into the properties of these interesting materials.

For the following experiments to recover WC-samples after shock treatment at calculated pressures $P > 100$ GPa, the impedance corrected sample recovery system with passive plane wave generator,

which has been developed at the Freiberg High Pressure Research Center (FHP), was used [8].

In this setup, every sample loss by the recovery capsule is impossible, thus, for all problems the reason for all kinds of material failure (jetting, sample blow out) is the sample itself. The general scheme of the used apparatus is shown in Fig. 1. For the following experiments material parameters, required for EoS-calculations (e.g. density, melting point, sound velocity, Gueneisen parameter) from literature data were taken into account [7–12]. For the experiments described as follows, sample masses of 1840–1880 g (plastinated RDX) and flyer plate masses from 114 to 148 g were used. The sample recovery capsule and flyer plates were made from stainless Cr–Ni steel.
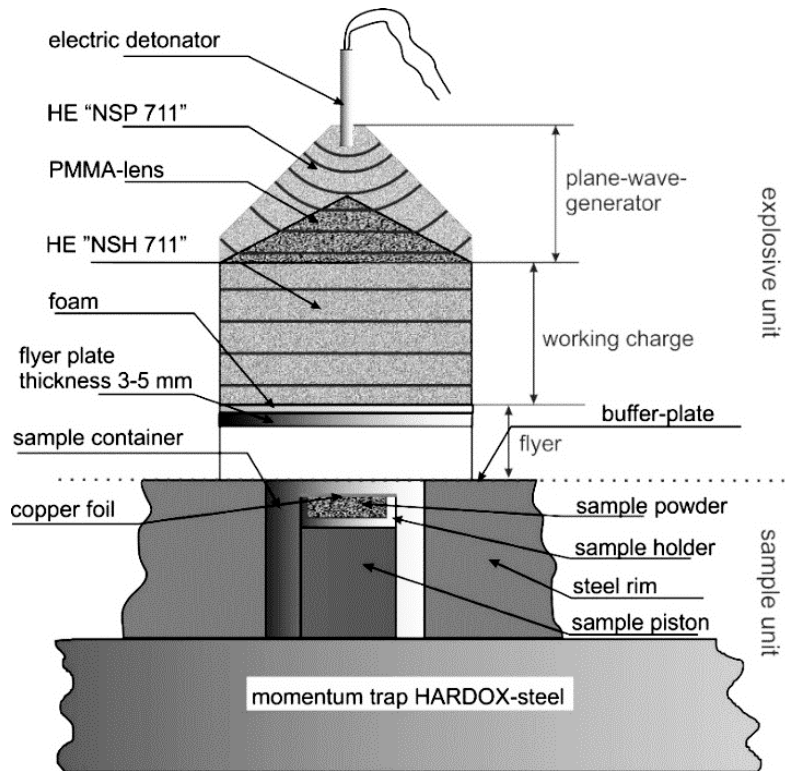
Fig. 1. General setup of the standard device used for shock wave treatment at TU Bergakademie Freiberg.

The EoS-parameters in the sample were calculated with self developed MatLab-codes [8] using the basic data for tungsten carbide under low and high pressure shock treatment [7, 10]. Important results are given in Fig. 2. It is shown that a calculated pressure of approximately 160 GPa was reached (Fig. 2a). But the determination of the true experimental pressure is much more difficult. As shown in

[13], in the case of plane collision experiments a higher impedance in direction of the incident shock must be strictly avoided. Otherwise undesired effects like shock reflections against this incoming shock will occur. This may result in a pressure reduction in the sample with its high impedance, which is not clearly predictable. This concerns especially experiments under using of thinner flyer plates (sample thickness of 5 mm, flyer plate thickness of 4 mm).
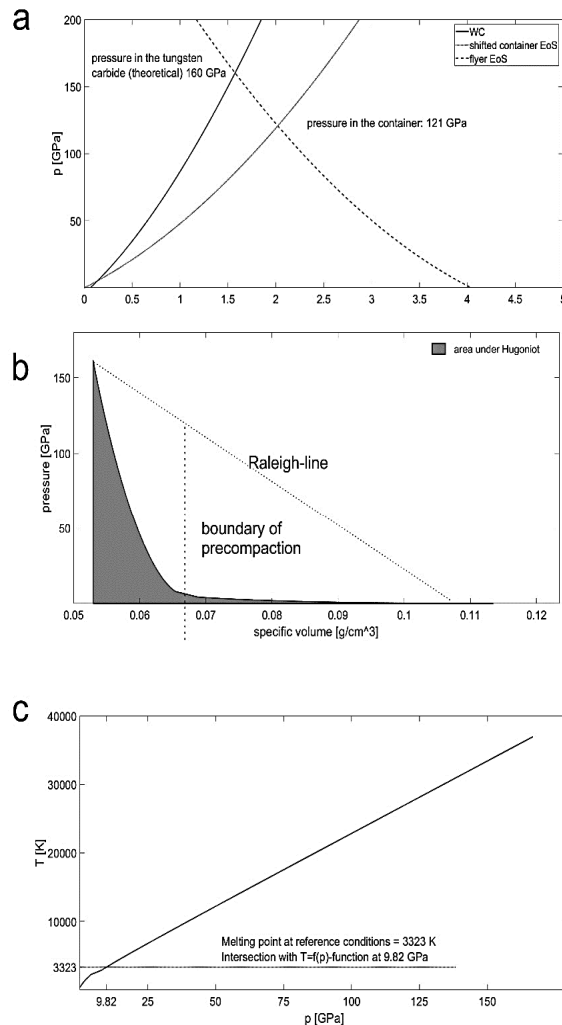

Fig. 2. Few graphical EoS-representations for the tungsten carbide: (a) $P = f(U_\mathrm{p})$ plot for the flyer and container together with the predensified WC (EoS-data in [10]); (b) $P = f(V_0 - V)$ plot with precompaction of the sample (initial porosity $k = 2.0$) and compression of the sample up to peak pressures. Precomapction EoS-data in [7], high-pressure data in [10]; (c) $T = f(P)$ plot with the melting point under 1 bar. Data were calculated with a heat capacity c_P of 0.1814 J/(K·g) [11]; melting point in [9].

After shock experiments, the samples were analyzed using SEM and XRD in the case of powdered samples. The SEM images show very large structural variations (Fig. 3a) from completely densified tungsten carbide over a partially densification to melting effects and chemical reactions. Near the sample holder the sample shows clear indications of melting, so-called cast structures (Fig. 3b) [14]. In central areas of the sample, the WC grains show only partial compaction with free intergranular spaces (Fig. 3c). The denser structures as shown in Fig. 3a are often characterized by sharp edged WC grains, but in this case the intergranular spaces are filled by a mass with a lighter colour in the SEM (Fig. 3d). This phase was later identified using XRD as W_2C (ditungstenmonocarbide). A similar effect was described earlier in [15]. In few cases it is possible to identify single WC grains with partial decomposition into the also hexagonal phase ditungstenmonocarbide W_2C (Fig. 3e). Additionally on few places the starting material WC completely reacted and is fully replaced by W_2C, which shows indications of melting processes (vacuoles) and additionally the typical needle-like internal structure (Fig. 3f). The XRD analysis (results are not shown due to limited space) gives a composition of 88 vol % WC and 12 vol % W_2C.

For this reason the real experimental pressure in the experiments described here may differ strongly from the calculated ones, as shown in Fig. 3a. The decay of monotungstenmonocarbide into ditungstenmonocarbide follows the reaction:

$$2\,WC \rightarrow W_2C + C$$
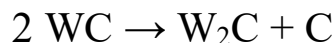
Because this reaction takes places under elevated pressures, the free carbon as a reaction product must be detectable as diamond using XRD.

In the case of only poorly compacted samples obtained in other similar experiments, diamond values up to 6 wt % were detected together with large amounts of graphite. This graphite is a decay product of diamond under the extremely high temperatures after the shock experiment, wich results from the large compression from an initial porosity of 2.0 to the fully densified state (Fig. 2b) together with the very low heat capacity of tungsten carbide (0.1814 J/(K·g) [11].

The behavior of the sample provides data about the real pressures and exceeds the threshold pressure of diamond formation. The shock

temperature must be higher than the melting point of W_2C under pressure (the filled intergranular spaces indicate a melting under pressure along the loading path) and simultaneously higher than the melting point of WC along the release path, here it is assumed as melting point under standard pressure. This is shown in Fig. 2c. Under low pressure conditions the melting points of both phases are similar [9].
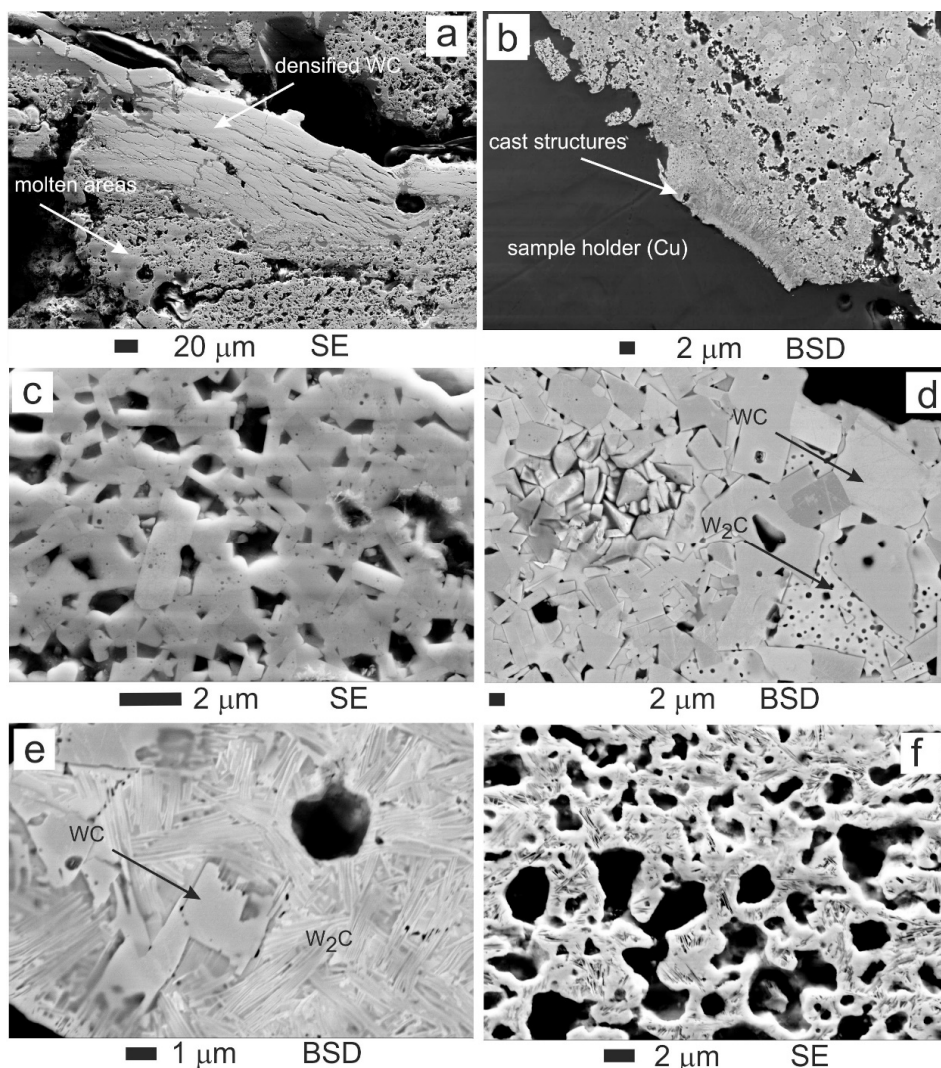

Fig. 3. SEM images of shocked tungsten carbide (WC), enlargement at scale, SE-secondary electron picture, BSD-back scattering detector: (a) structural overview with different degrees of compaction and partial melting; (b) rim of the sample (black-sample holder) with cast structures, indicating former molten WC; (c) partially compacted WC grains with empty spaces between them; (d) sintered WC body with former molten W_2C in the intergranular spaces; (e) decay of WC into W_2C with needle-like internal structure; (f) former molten W_2C with vacuoles.

Vogler et al. [10] measured the compression of WC up to more than 6 Mbar ($P = f(V_0 - V)$) together with calculated values after the p-λ model [16]. At this elevated pressure the measured values show a strongly reduced density as compared to the prediction. Taken into account the experimental results as given here one reason for this lower density may be the decay of WC into W_2C under melting and the formation of diamond with a lower density as compared to both carbides. In this case calculations for solid WC are no longer valid.

For future research, this kind of recovery experiments concerning refractory carbides may open new interesting possibilities to obtain novel composites with interesting but still unknown properties.

1. D. E. Grady, Dynamic properties of ceramic materials *SAND-94-3266*, 1995, 53 p., Sandia National Labs., Albuquerque, NM, Albucuerque, https://www.osti.gov/scitech/biblio/72964.
2. K. I. Kondo, S. Sawai, Fabricating nanocristalline diamond ceramics by a shock compaction method, *J. Am. Ceram. Soc*, 1990, vol. 73. no. 7, pp. 1983–1991.
3. K. I. Kondo, S. Soga, A. Sawaoka, M. Araki, Shock compaction of silicon carbide powder, *J. Mat. Sci.*, 1985, vol. 20, no. 3, pp. 1033–1048, doi:10.1007/BF00585748.
4. F. D. S. Marquis, A. Mahajan, A. B. Mamalis, Shock synthesis and densification of tungsten based heavy alloys, *J. Mat. Proces. Techn.*, 2004, vol. 161, 1–2, pp. 113–120.
5. R. Pruemmer, Explosive compaction of powders, principle and prospects, *Materialwissenschaft und Werkstofftechnik*, 1989, vol. 20, no, 12, pp. 410–415; doi:10.1002/mawe.19890201213.
6. V. F. Nesterenko, *Dynamics of heterogeneous materials*, *High pressure shock compression of condensed matter*, New York: Springer, 2001, vol. 10, 510 p.
7. T. J. Vogler, J. W. Gluth, D. E. Grady, C. A. Hall, *Dynamic compaction of tungsten carbide powder*, SAND2005-1510, Albuquerque, New Mexico 87185 and Livermore, California 94550, 2005.
8. T. Schlothauer, Aufbau des Schockwellenlabors im Lehr- und Forschungsbergwerk „Reiche Zeche" der TU Bergakademie Freiberg und die Entwicklung von dynamischen

Höchstdrucksynthesemethoden, PhD-thesis, Institut für Mineralogie, TU Bergakademie Freiberg, Freiberg.

9. D. P. Dandekar, Shock equation of state and dynamic strength of tungsten carbide, in *AIP Conference Proceedings: 12th APS Topical Conference*, *AIP Conference Proceedings*, edited by M. D. Furnish et al., 2002, pp.783–786.

10. T. J. Vogler, S. Root, M. D. Knudson, W. D. Reinhart, *High-pressure shock behavior of WC and Ta2O5 powders,* SAND2011-6770, Albuquerque, New Mexico 87185 and Livermore, California 94550, 2011.

11. R. J. L. Andon, J. F. Martin, K. C. Mills, T. R. Jenkins, Heat capacity and entropy of tungsten carbide, *J. Chem. Thermodyn.*, 1975, vol. 7, no. 11, pp. 1079–1084; doi:10.1016/0021-9614(75)90241-4.

12. R. R. Reeber, K. Wang, Thermophysical properties of α-tungsten carbide, *J. Amer. Ceram. Soc.*, 1999, vol. 82, no. 1, pp. 129–135; doi:10.1111/j.1151-2916.1999.tb01732.x.

13. P. S. DeCarli, M. A. Meyers, *Design of uniaxial strain shock recovery experiments*, in Shock Waves and High Strain-Rate Phenomena in Metals: Concepts and Applications, edited by M. A. Meyers and L. E. Murr, Plenum Press, New York, 1981, pp. 341–373.

14. H. J. Shin, J. K. An, S. H. Park, D. N. Lee, The effect of texture on ridging of ferritic stainless steel, *Acta Mater.*, 2003, vol. 51, no. 16, pp. 4693–4706; doi:10.1016/S1359-6454(03)00187-3.

15. G. A. Adadurov, O. N. Breusov, A. N. Dremin, V. F. Tatsii, Effect of shock waves on refractory compounds, *Sov. Powder Metall. Met. Ceram.*, 1971, vol. 10, no. 11, pp. 859–861; doi:10.1007/BF00793994.

16. D. E. Grady, N. A. Winfree, G. I. Kerley, L. T. Wilson, L. D. Kuhns, Computational modeling and wave propagation in media with inelastic deforming microstructure, *J. Phys. IV France*, 2000, 10(PR9), Pr9-15-Pr9-20; doi:10.1051/jp4:2000903.

REGULARITIES OF SYNTHESIS OF NICKEL-BONDED TITANIUM CARBIDE FROM DIFFERENT TITANIUM GRADES

B. S. Seplyarskii, R. A.Kochetkov, and T. G. Lisina

Merzhanov Institute of Structural Macrokinetics and Materials Science, Russian Academy of Sciences, Chernogolovka, 142432 Russia

e-mail: numenor@list.ru

Titanium carbide-based materials with a metallic binder have a wide range of applications due to their hardness, wear resistance and plasticity. Long-term experience in studying SHS processes has shown that the grade of initial reagents can significantly affect the patterns of combustion and phase composition of products obtained. The present work studies the regularities of synthesis of nickel-bonded titanium carbide from powdered and granulated charge of PTM and PTM-1 grades of titanium in a co-flow of inert and active gas.

The experimental setup and method of preparation of granules and diluted mixtures are described in [1]. The particles of titanium powders of different grades had the same chemical composition but differed in shape and size. The PTM-1 titanium particles had a planar shape with less developed surface and their size was about 1.5 times greater. The specific surface area of the PTM-1 titanium powder determined using a Sorbi-M specific surface meter was 0.35 m^2/g (0.59 m^2/g for PTM grade titanium). The particle size distribution was determined on a MicroSizer-201 particle analyzer.

The conducted studies revealed that the combustion of the granulated SHS Ti + C + 25% Ni mixture with PTM titanium showed a long afterglow following the passage of the combustion front. This effect was discovered in granulated systems for the first time. In powdered mixtures Ti + C + 25% Ni of bulk density experiments confirmed the existence of the afterglow effect as well. This kind of

B. S. Seplyarskii et al.

combustion was explained by the fact that nickel having a lower melting point (1726 K) than titanium (1933 K) melted in the combustion front and spread over titanium particles, preventing the interaction of titanium with black. The inhibitory action of the nickel layer on the surface of titanium particles upon combustion of a mixture of Ti + C + 20% Ni was previously shown in [2]. However, due to the low volume content of nickel in the mixture (≤ 8 wt %), only a portion of the titanium particles were covered by the nickel melt. The remaining titanium particles melted in the combustion wave and spread over the black, forming titanium carbide upon interaction. It was this reaction that was the leading one in the combustion front, because the combustion wave in a Ti + Ni mixture does not propagate without preheating. Behind the combustion front, nickel carbon was displaced from its melt with titanium to form titanium carbide, accompanied by the release of heat, giving the afterglow effect. According to the XRD data, the phase composition of the final product (TiC, Ni) both for powdered and granulated mixtures corresponded to the results of thermodynamic calculations (carried out using THERMO program). The experiments showed that in the combustion of granulated Ti + C + 25% Ni mixtures, the granules unlike powders retained their dimensions and were not sintered.

The microstructure of the condensed products (granules) obtained was studied using a Zeiss Ultra Plus scanning electron microscope. The average grain size of titanium carbide was 2–4 μm, which was smaller by an order of magnitude than the initial size of titanium particles (70 μm), i.e. in the combustion process, the titanium particles were dispersed, and the nickel binder prevented the growth of titanium carbide grains after synthesis. Attention was drawn to the fact that despite the small volume fraction in the charge, Ni was uniformly distributed over the granule after synthesis.

The video recording of the combustion of a Ti + C + 25% Ni granulated mixture in a concurrent flow of inert (argon) and active (nitrogen) gas showed the preserving of the afterglow effect associated with the presence of Ni. According to the chemical analysis, the combustion products of Ti + C + 25% Ni mixtures in the nitrogen flow contained 2.5–3.0 wt % nitrogen. XRD analysis shows no intermetallices due to close vicinity of $TiC_xN_{(1-x)}$ phase angles to the titanium carbide phase angular position [3].

It turned out that combustion of mixture based on PTM-1 grade titanium led to the change in the combustion behavior and composition of the products as compared to the PTM-based titanium blend. In the combustion of the granulated mixture, no afterglow stage was observed, and the burning velocity of PTM titanium mixture decreased from 27 to 11 mm/s. According to the XRD data, the combustion products had a more complex composition and included Ti_xNi_y intermetallics. The Ti + C + 25% Ni granules retained their dimensions after synthesis and were not sintered. To test the hypothesis that replacing part of PTM-1 titanium can lead to a decrease in the content of intermetallic compounds in products, the experiments were conducted to burn powdered and granulated Ti + C + 25% Ni mixtures, in which 50% of PTM-1 titanium was replaced with PTM titanium. The studies showed that for this mixture the combustion process proceeded with afterglow. The XRD analysis showed the presence of intermetallics in products, an amount of which is smaller than that for PTM-1 titanium mixture.

Upon combustion in a nitrogen flow, the synthesis product was a porous sample of slightly sintered granules, which crumbled during cutting. It should be noted that filtrating nitrogen made it possible to change the composition of the combustion products of PTM-1 and PTM/PTM-1 titanium mixtures. XRD analysis revealed no intermetallic compounds. Thus, granulation of the mixture Ti + C + 25% Ni followed by combustion in a nitrogen flow made it possible to neutralize the influence of the titanium grade on the phase composition of the final products of synthesis.

The synthesis products prepared from granulated charge without a gas flow were unsintered granules that facilitated the process of their processing into powder. For powdered system in the presence and absence of a gas flow, and for granulated mixture in an argon stream, the combustion products independing on titanium grades were a sintered mass that was impossible to grind under laboratory conditions.

1. B. S. Seplyarskii, R. A. Kochetkov, S. G. Vadchenko, Burning of the Ti + xC (1 > x > 0.5) powder and granulated mixtures, *Combust. Explos. Shock Waves*, 2016, vol. 52, iss. 6, pp. 665–672; doi: 10.1134/S001050821606006X.

B. S. Seplyarskii et al.

2. N. A. Kochetov, A. S. Rogachev, Yu. S. Pogozhev, The effect of mechanical activation of a reaction mixture on the velocity of the wave propagation of shs reactions and microstructure of the TiC-Ni hard alloy, *Russ. J. Non-Ferr. Met.*, 2010, vol. 51, iss. 2, pp. 177–181.

3. B. S. Seplyarskii, A. G. Tarasov, R. A. Kochetkov, I. D. Kovalev, Combustion behavior of a Ti +TiC mixture in a nitrogen coflow, *Combust. Explos. Shock Waves*, 2014, vol. 50, iss. 3, pp. 300–305; doi: 10.1134/S001050S214030071

THE INFLUENCE OF GAS FLOW ON THE MANIFESTATION OF THE PERCOLATION PHASE TRANSITION IN GRANULAR MIXTURES Ti + C

B. S. Seplyarskii, R. A.Kochetkov, and T. G. Lisina

Merzhanov Institute of Structural Macrokinetics and Materials Science, Russian Academy of Sciences, Chernogolovka, 142432 Russia

e-mail: lisina@ism.ac.ru

The study of critical phenomena of combustion is one of the most important and still urgent problem of combustion theory. Earlier we investigated the combustion of granular mixture Ti + C diluted with Al_2O_3 pellets without gas flow [1]. It was shown that critical combustion parameters near the concentration limit, i.e. the maximum degree of dilution, the ratio of the burning velocities at the limit and without dilution, the presence of the non-complete burning of mixture, are consistent with the percolation theory predictions [2].

In the present work, experimental researches of regularities of the combustion of mixtures consisting of active (Ti + C) and inert (Al_2O_3) granules in a flow of inert (argon) and active (nitrogen) gas are carried out. Comparison of the burning velocities in the nitrogen and argon flow allows to divide the influence of convective heat transfer by the filtered gas and the chemical interaction of nitrogen with titanium on the combustion process near the propagation limit.

The initial substances used in the work and the method of preparation of granules and diluted mixtures are described in [3]. Experimental setup [3] allows to burn the mixture in the gas flow or without flow and to measure the flow and pressure of gas in the combustion process. The burning velocity was determined with time-lapse processing of video recordings of the combustion process. The gas supply was carried out from the upper end of the sample under pressure of 2 atm; at the lower end, the pressure was equal to 1 atm.

Before each experiment, an argon purge through the filling was performed to avoid shrinkage of the initial mixture during combustion.

In the gas flow (active and inert), in the entire range of dilution of the initial granulated mixture, burning velocities increase and are higher by several times than the value calculated by the theory of filtration combustion. To determine the reasons of this increase in velocities, experiments on combustion of the active mixture separated by a continuous layer of inert granules with a thickness of 1–2 particles were carried out. When burning without gas stream, the lower part of the backfill did not ignite. In the gas flow, the filling burned down completely, but there was a delay of ignition of the lower part by 1.5 s in nitrogen and by 12 s in argon. The delay time is comparable to or exceeds the combustion time of the full backfill in the absence of the inert jumper. Thus, the straightening of the combustion wave path in the diluted mixture by the gas flow cannot explain a greate increas in the burning velocity. However, the experiments show the possibility of additional transformation of the active granules after passing the combustion front, which increases the final degree of transformation. To explain a greate increase in the burning velocity, the authors suggest that the roughness of active granules affects strongly the heat exchange process with a filtered gas, which can lead to their rapid local heating and ignition.

Quantitative analysis of combustion products, which was carried out by the method of "corundum numbers", showed the appearance of free titanium in combustion products with an increase in the diluent concentration over 50%, which is a characteristic feature of the front propagation through the percolation cluster. Possible reason of incomplete combustion of the active mixture is a decrease in the combustion temperature below the melting point of titanium with an aluminum oxide content of more than 47% (calculations were carried out using THERMO program).

Al_2O_3 concentration equal to 75 wt % is concentration limit of combustion observed in experiments. The measured ratio of burning velocities of undiluted mixtures at the propagation limit of 2.3÷2.8 corresponds to the predictions of percolation theory. The same concentration limit of combustion in the inert and active gas flow and without the flow indicates common reason to stop combustion — percolation phase transition.

The results should be taken into account when solving the problem of fire explosion safety when handling granular mixtures. Since the percolation model is exploited to study the self-spread of forest fires [4], the combustion of granular mixture in a co-flow of active gas could be a useful model for studying this phenomenon.

1. L. A. Andreevskikh, Yu. P. Dedenkov, O. B. Drennov, A. L. Mikhailov, N. N. Titova, A. A. Deribas, Explosive mixture for explosive welding of thin foils, *Propell. Explos. Pyrotech.*, 2011, vol. 36, no. 1. pp. 48–50.
2. V. M.Aulchenko, A. E. Bondar, V. N. Kudryavtsev, D. M. Nikolenko, P. A. Papushev, E. R. Pruuel, I. A. Rachek, K. A. Ten, V. M. Titov, B. P. Tolochko, V. N. Zhilich, V. V. Zhulanov, L. I. Shekhtman, GEM-based detectors for SR imaging and particle tracking**, *J. Instrum.*, 2012, vol. 7, no. 3, pp. 1–18.
3. E. R. Pruuel, K. A. Ten, B. P. Tolochko, L. A. Merzhievskii, L. A. Luk'yanchikov, V. M. Aul'chenko, V. V. Zhulanov, L. I. Shekhtman, V. M. Titov, Implementation of the capability of synchrotron radiation in a study of detonation processes, *Dokl. Phys.*, 2013, vo. 58, no. 1, pp. 24–28.
4. V. M. Titov, E. R. Pruuel, K. A. Ten, L. A. Luk'yanchikov, L. A. Merzhievskii, B. P. Tolochko, V. V. Zhulanov, L. I. Shekhtman, Experience of using synchrotron radiation for studying detonation processes, *Combust. Explos. Shock Waves*, 2011, vol. 47, no. 6, pp. 3–15.

HARDENING OF ALUMINUM–NICKEL REACTIVE MATERIALS

S. A. Seropyan, I. V. Saikov, S. G. Vadchenko, and M. I. Alymov

Merzhanov Institute of Structural Macrokinetics and Materials Science, Russian Academy of Sciences, Chernogolovka, Moscow, 142432 Russia

e-mail: revan.84@mail.ru

The creation and testing of reactive materials combining a required set of physico-mechanical characteristics and high energy release are associated with a number of physico-chemical limitations and technological difficulties. Such research, as a rule, are purely experimental and are distinguished by the complexity of studying fast-acting physicochemical processes directly in the process of explosive loading of the reaction mixture, which is characterized by high deformation rates, pressures and temperatures [1, 2].

The aim of this investigation is the formation of metallic reactive materials with high structural strength. The reactivity of a mixture of powders is determined by their composition, contact area between the particles, temperature, speed, method of application of the external pressure, ratio of volume and shear components of the deformation, particle surface state and other factors. Thus, the actual task is to develop methods of consolidation, which would allow preserving the reactivity of the given compositions, when sufficient contact strength between the powder particles is reached, which determines the structural strength of the material as a whole. The object of the study was a powder mixture based on Ni and Al with a particle size of less than 50 μm in the equiatomic ratio. The studies were carried out using compact samples in the form of a cylinder and a parallelepiped with a relative density of 70% and 80%. Samples with the addition of an inert component (tungsten) and reinforced with tungsten wire and boron fibers were made.

As a result, the data on the strength, heat generation, ignition parameters and burning velocity of composite materials based on nickel and aluminum with inert additives of tungsten, fillers from tungsten wires, and active fillers in the form of boron fibers were obtained.

1. N. A. Imkhovik, A. V. Svidinsky, A. S. Smirnov, V. B. Yashin. Foreign investigations of new high-density reactive materials for different advanced munitions, Gorenie i Vzryv (Moskva) – Combustion and Explosion, 2017, vol. 10, no. 1, pp. 93–101.
2. I. V. Saikov, M. I. Alymov, S. G. Vadchenko, I. D. Kovalev. Investigation of shock-wave initiation in metal-teflon powder mixtures Letters on materials, 2017, vol. 7, no. 4. pp. 465–468.

S. A. Seropyan et al.

POSSIBILITY OF PREPARATION Ta$_4$ZrC$_5$–CrB AND Ta$_4$HfC$_5$–CrB COMPOSITES BY SHS PRESSING

V. A. Shcherbakov and A. N. Gryadunov

Merzhanov Institute of Structural Macrokinetics and Materials Science, Russian Academy of Sciences, Chernogolovka, Moscow, 142432 Russia

e-mail: vladimir@ism.ac.ru

Development of refractory ceramic composites retaining their functionality under extreme conditions at high temperatures in corrosive environments is an importan task of developing modern technologies of machine building, metal working, metallurgy, power engineering, and aircraft industry. Promising materials for solving these problems are high-temperature ceramic composites based on (Ta,Zr)C and (Ta,Hf)C solid solutions. They are characterized by high melting point, heat resistance, hardness, strength, and low coefficient of thermal expansion and corrosion resistance under extreme conditions.

SHS is a promising method to produce ceramic composites. Advantages of this method are simplicity of design, low power consumption and high purity of the target product.

The aim of the paper is to investigate optimal modes of synthesis and consolidation of high-temperature ceramic composites based on solid solutions (Ta$_4$Zr)C$_5$ and (Ta$_4$Hf)C$_5$ by SHS pressing.

To determine optimum synthesis conditions thermodynamic analysis of the Ta–Zr–C and Ta–Hf–C chemical systems were carried out. Depending on reaction mixture composition and initial temperature, the compositions of equilibrium synthesis products and adiabatic combustion temperatures are calculated. Thermodynamic analysis showed that the equilibrium synthesis products are solid refractory compounds TaC, ZrC, and HfC.

Chromium monoboride was proposed as a ceramic binder for the SHS product to improve consolidation efficiency. The synthesis conditions allowing to produce SHS product containing the solid carbides (TaC, ZrC, HfC) and molten binder (CrB) were determined.

It can be concluded that optimum condition to carry out synthesis of $(Ta_4Zr)C_5$–CrB and $(Ta_4Hf)C_5$–CrB composites is thermoelectric explosion under pressure.

V. A. Shcherbakov and A. N. Gryadunov

SHS PRESSING AND PROPERTIES OF B_4C–TiB_2 AND B_4C–ZrB_2 COMPOSITES

V. A. Shcherbakov and A. N. Gryadunov

Merzhanov Institute of Structural Macrokinetics and Materials Science, Russian Academy of Sciences, Chernogolovka, Moscow, 142432 Russia

e-mail: vladimir@ism.ac.ru

This paper presents the results of experimental study to produce B_4C–TiB_2 and B_4C–ZrB_2 composites by SHS pressing.

Based on thermodynamic data, equilibrium product compositions and adiabatic combustion temperatures of Ti–B–C and Zr–B–C SHS-systems were calculated. It has been shown that an increase in B_4C content in the final product to 25 wt % favors to a decrease in the adiabatic combustion temperature from 3300 to 2500 K. At the conditions, synthesized product contains solid TiB_2 and ZrB_2 as dispersed phase and molten B_4C as ceramic binder.

The influence of reaction mixture composition on the microstructure and physicomechanical characteristics of SHS composites was studied. It has been shown that during exothermic synthesis an equilibrium SHS product containing phases B_4C, TiB_2 and ZrB_2 is formed. The binder content (B_4C) was found to affect singnificantly the microstructure of SHS composites. At low B_4C content, homogeneous SHS composites with a grain size of 10–12 μm are formed. SHS composites with high B_4C content are inhomogeneous and are represented by hollow particles consisting of TiB_2 and ZrB_2 (Figs. 1, 2).

The formation of hollow particles is caused by fact that at the initial stage of interaction at temperature below melting point of titanium or zirconium, a product layer containing titanium or zirconium diborides is formed at the surface of particles. When combustion temperature reaches the melting point of titanium or

zirconium, the inner part of the particles (core) consisting of titanium or zirconium melts. The molten metal flowing out and spreads over outer surface of the product layer that lead to the formation of hollow particles. It should be noted that the melt spread only over surface of the product layer and did not infiltrate into porous layer formed by boron and soot particles. This is caused by good wetting which did not allow the molten metal leave off the product surface.

Vickers microhardness and bending strength of B_4C–TiB_2 composites obtained with a binder content (B_4C) of 30–40 wt % are 39.1–44.8 GPa and 140–210 MPa, respectively.
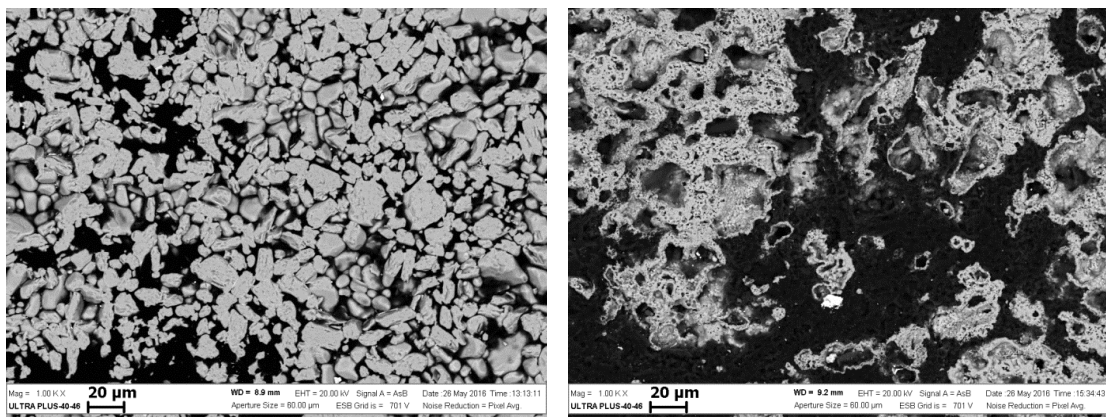
Fig. 1. Microstructure of (a) TiB_2–$20B_4C$ and (b) TiB_2–$50B_4C$ composites. The light phase is TiB_2; the dark phase is B_4C.
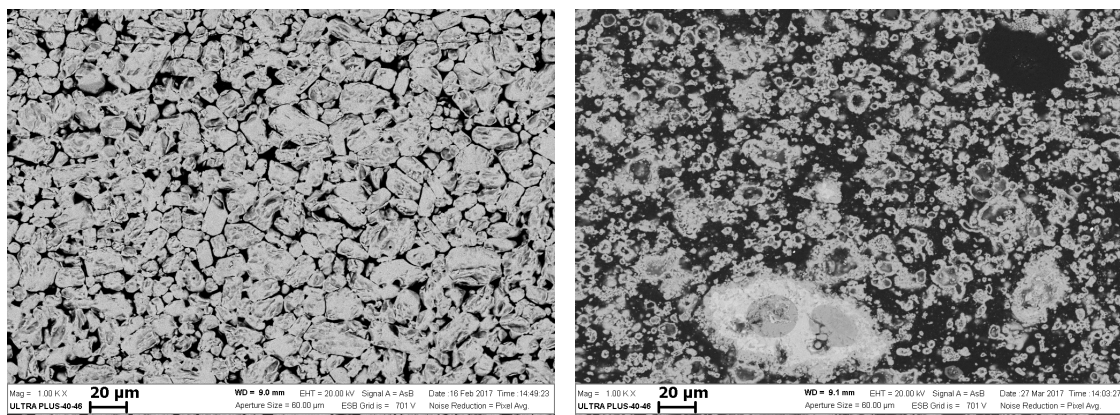
Fig. 2. Microstructure of (a) ZrB_2–$10B_4C$ and (b) ZrB_2–$20B_4C$ composites. The light phase is ZrB_2; the dark phase is B_4C.

ELECTRO-THERMAL EXPLOSION IN W–Ni–Al SYSTEM

A. S. Shchukin[1], S. G. Vadchenko[1], A. V. Shcherbakov[1], A. E. Sytschev[1], V. A. Shcherbakov[1], and A. N. Svobodov[2]

[1] Merzhanov Institute of Structural Macrokinetics and Materials Science, Russian Academy of Sciences, Chernogolovka, Moscow, 142432 Russia

[2] Pribor SPA, JSC, Moscow, 117519 Russia

e-mail: shchukin@ism.ac.ru

It is known that the high-temperature strength of alloys and composites based on Ni−Al solid solutions is achieved through the formation of an intermetallic γ'-phase (NiAl), which is characterized by an anomalous dependence of the strength on temperature [1]. Investigation of alloys in the ternary Ni−Al−W system was carried out in a number of works including those performed in recent years [2−5]. The possibility of production of NiAl-based intermetallic compounds containing more than 10% molybdenum or tungsten by hot isostatic pressing of powders is shown in [6]. Tungsten alloys [7] are widely used for the manufacture of various kinds of weighting agents, electrical contacts, devices for the disposal of nuclear waste, and components for the defense industry [8]. The purpose of this research was to produce the composite W−10NiAl alloy by an electro-thermal explosion (ETE) under pressure.

Preliminary studies of the combustion process were carried out using 90 wt % W + 10 wt % (Ni + Al) samples in an argon atmosphere at different heating rates. At relatively low heating rates of the mixture (120 °C/s), aluminum melting is observed in the experimental thermograms but no ignition occurred (Fig. 1). Heating of samples to 850°C does not lead to the initiation of SHS reactions.

An increase in the heating rate from 120 to 520 °C/s leads to an increase in the ignition temperature of samples from 1000 to 1300°C. Heating of the mixture from the ignition temperature to maximum one

is about 250°C. Figure 2 shows the dependence of the relative change in the electrical resistance of the sample and pressing pressure during ETE. It can be seen that ETE includes three stages: pre-explosive heating of an inhomogeneous mixture (0 s < t < 2.6 s), thermal explosion (2.6 s < t < 3.1 s) and post-process (3.1 s < t < 20 s). At the pre-explosive heating stage, R/R_0 decreased to 0.45 (R is the current value and R_0 is the initial value of the electrical resistance of the sample).
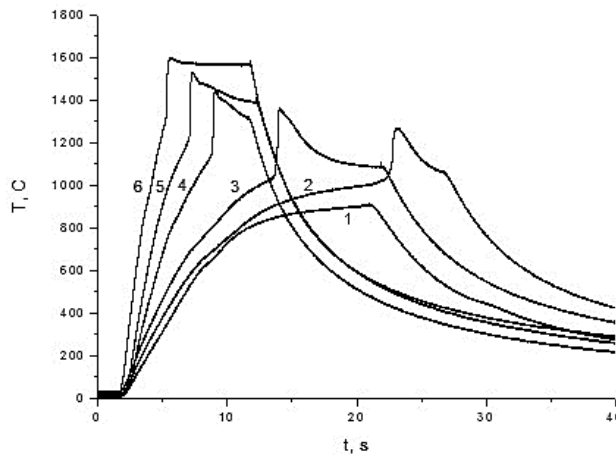
Fig. 1. Thermograms of 90W + 10(Ni + Al) mixture at different heating rates: 1 100; 2 120; 3 140; 4 250; 5 350; and 6 500 °C/s.
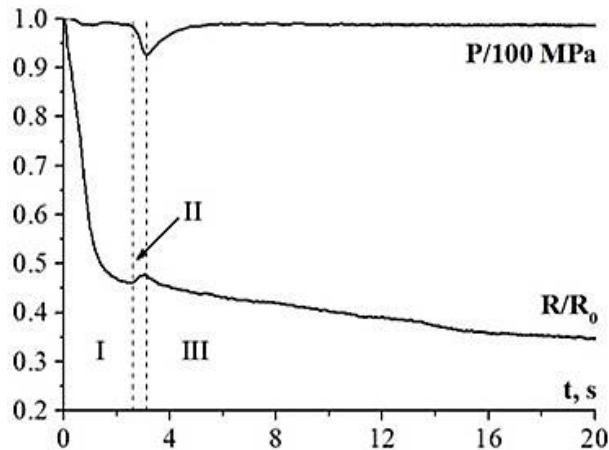
Fig. 2. Dependences of the relative change in R/R0 of sample and pressing pressure during ETE.

At the thermal explosion stage, there is a slight increase in R/R_0 due to the formation of chemical interaction products whose electrical resistance is slightly higher than that of the initial reagents. At this stage, as a result of the shrinkage of the test sample, a slight decrease

in the pressing pressure occurs. The post-process stage occurs after the completion of the exothermic reaction and continues until the sample cools completely. Under these conditions, R/R_0 decreases by 0.1, which is caused by the shrinkage of the hot synthesis product under pressure.

According to the X-ray diffraction data, the synthesized compact sample contains tungsten and a small content of Ni. Analysis of the powdered sample showed also the presence of a small amount of TiC. No Al traces and intermetallic compounds were detected. The microstructure of the synthesized composite consists of uniformly distributed tungsten grains about 5 μm in size, which are surrounded by binder in the form of fine intergranular layers or regions of a solid solution based on nickel and aluminum containing a small amount of Si with a size of up to 10 μm (Fig. 3). The sample contains impurities of silicon, oxygen, and magnesium, which are the components of an ASP-35AlSi10Mg aluminum alloy.

The microstructure of the fracture surface shows the shape anisotropy of W grains (Fig. 3b). The deformation of W grains occurred under applied load (compression pressure of 96 MPa) during ETE. The fracture surface has an essentially intergranular character (Fig. 3b).

The synthesized alloy is practically nonporous, has a density of 15.7 kg/m³, an open porosity of no more than 0.2%, a compressive strength of 2430÷2600 MPa, and a microhardness H_μ of 4820 MPa.
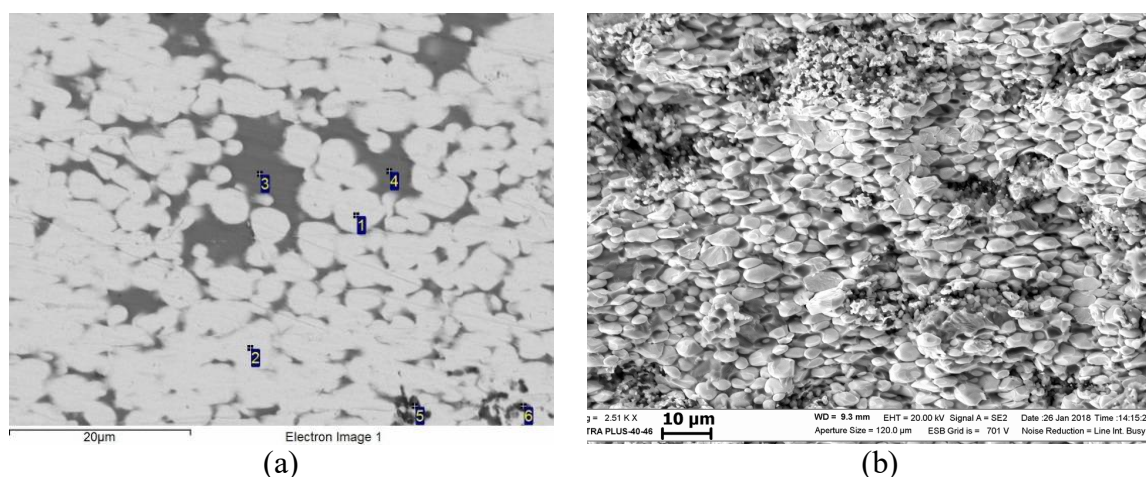
Fig. 3. Microstructure of the (a) composite and (b) fracture surface of the synthesized sample.

1. N. M. Matveeva, E. V. Kozlov, *Ordered Phases in Metallic Systems*, New York: Nova Science Publishers, 1996.
2. Yu. R. Kolobov, *Diffusion-Controlled Processes at Grain Boundaries and Plasticity of Metallic Polycrystals*, Novosibirsk: Nauks, 1998 (in Russian).
3. Yu. R. Kolobov, E. N. Kablov, E. V. Kozlov, *Structure and Properties of Intermetallic Materials with Nanophase Strengthening*, Moscow: MISiS, 2008 (in Russian).
4. J. Popovič, P. Brož, J. Buršík, Microstructure and phase equilibriums in the Ni–Al–W system, *Intermetal.*, 2008, vol. 16, no. 7, pp. 847–942.
5. S. Milenkovic, A. Schneider, G. Frommeyer, Constitutional and microstructural investigation of the pseudo-binary NiAl–W system, *Intermetal.*, 2011, vol. 19, no. 3, pp. 342–349.
6. T. Takahashi, D. C. Dunand, Nickel aluminide containing refractory-metal dispersoids: Microstructure and properties, *Mater. Sci. Eng. A*, 1995, vols. 192–193, pp. 195–203.
7. V. N. Chuvil'deev, A. V. Nokhrin, A. V. Moskvicheva, et al. Study of the structure and mechanical properties of nano- and ultradispersed mechanically activated heavy tungsten alloys, *NanoTech. Rus.*, 2013. vol. 8, no. 1–2. C. 108–121.
8. E. M. Savitskii, K. B. Povarova, P. M. Makarov, *Metal Science of Tungsten*, Moscow: Metallurgiya, 1978 (in Russian).

A. S. Shchukin et al.

MICROSTRUCTURE AND DYNAMIC MECHANICAL PROPERTIES OF MULTILAYER Ti–Al EXPLOSIVELY WELDED PLATE

Z. Sheng, P. Chen, and Q. Zhou

State Key Laboratory of Explosion Science and Technology, Beijing Institute of Technology, Beijing 100081 China

e-mail: m15090359861@163.com; pwchen@bit.edu.cn; 847564608@qq.com

Over the past several years, various investigations were performed on Ti–Al explosively welded clad, because it has a number of excellent features such as low density, high hardness, good corrosion resistance and high strength [1]. In this work, explosive welding was used to obtain a multilayer plate, which is consist of pure titanium and aluminum layers. The welded samples were annealed at 903 K for 5 h and 10 h. The microstructure and intermetallic phase were investigated by optical microscopy, scanning electron microscopy and TEM. The dynamic compression tests were carried out using Split Hopkinson Pressure Bar (SHPB) systems at room temperature.

The well welded interface parallel to the direction of detonation were investigated using optical microscopy. Figure 1a shows an optical micrograph of the composite plates interface after explosive welding. The experimental results demonstrate that the cladding of 1060 Al and TA2 was achieved by the explosive welding technique. Wavy morphology with vortex appears on the bonding interface. After 5-h annealing at 903 K, a uniform intermetallic layer was formed at the interface which is mainly consist of $TiAl_3$ [2, 3].

To investigate the effect of annealing on the microstructure variation, vortex and interfaces were observed after annealing shown in Fig. 2. As can be seen from Fig. 2, some voids and cracks were

formed inside the intermetallic layer after annealing [4].

The dynamic compression tests were carried out on a modified split Hopkinson pressure bar test system. As can be seen from Fig. 3, after the compression, the sample have a significant deformation, the aluminum layer have an obviously plastic deformation. More study on its microstructure transformation will be carried out soon.
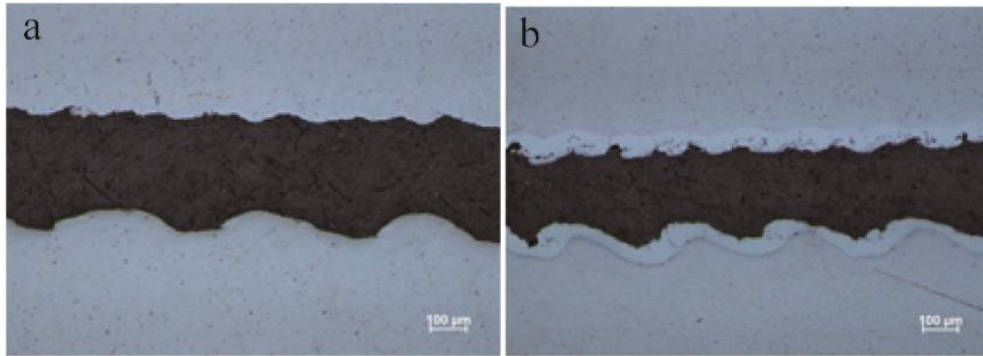
Fig. 1 The growth of the intermetallic at the Ti–Al composite interface: (a) after explosion welding, (b) annealing during 5 h.
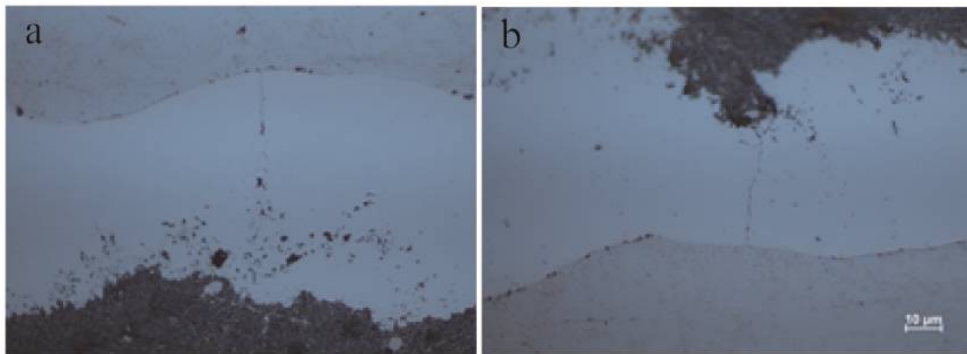
Fig. 2. (a) Voids and (b) cracks after annealing at 903 K for 5 h.
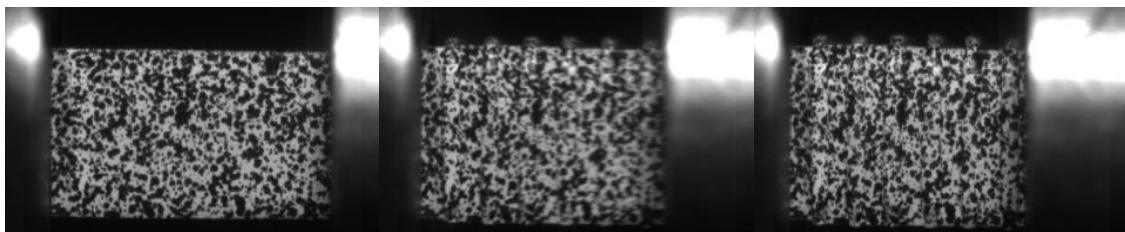
Fig. 3 Samples for dynamic compression tests: before and after compress.

1. I. A. Bataev, A. A. Bataev, V. I. Mali, D. V. Pavlyukova, Structural and mechanical properties of metallic-intermetallic

laminate composites produced by explosive welding and annealing, *Materials & Design*, 2012, vol. 35, no. pp. 225–234.

2. F. Foadian, M. Soltanieh, M. Adeli, M. Etminanbakhsh, The kinetics of $TiAl_3$ formation in explosively welded Ti–Al multilayers during heat treatment, *Metall. Mater. Trans. B*, 2016, vol. 47, no. 5, pp, 2931–2937.

3. M. Fan, W. Yu, W. Wang, X. Guo, K. Jin, R. Miao, J. Tao, Microstructure and mechanical properties of thin-multilayer Ti/Al laminates prepared by one-step explosive bonding, *J. Mater. Eng. Perform.*, 2016, vol. 26, no. 1, pp. 277–284.

4. D. M. Fronczek, R. Chulist, L. Litynska-Dobrzynska, Z. Szulc, P. Zieba, J. Wojewoda-Budka, Microstructure changes and phase growth occurring at the interface of the Al/Ti explosively welded and annealed joints, *J. Mater. Eng. Perform.*, 2016, vol. 25, no. 8, pp. 3211–3217.

TOPOLOGICAL STATES OF STRUCTURAL CHEMISTRY OF NEW SUBSTANCES AND MATERIALS

V. Ya. Shevchenko

Grebenshchikov Institute of Silicate Chemistry, Russian Academy of Sciences, St. Petersburg, 199034 Russia

e-mail: Shevchenko@isc.nw.ru

Strange topological effects might be hiding inside the perfectly ordinary materials. Until recently, chemists have received little attention to topology — the mathematical study of objects and their arrangement in space. The term "topochemistry" in organic chemistry was used unlike inorganic one and especially materials science to describe and predict a number of fundamentally important substances. Recently chemists have found that topology provides unique insight into the physical chemistry and structural chemistry of substances and has trended to focus on tangible problems of solid materials. Many researchers say that the real reward of topological structural chemistry will be a deeper understanding of the nature of matter itself.

Here mention should be made of two fundamentally different states of substances: nanostate implying the appearance of new and strange effects (centaur particles, violations of Gibbs classical phase rule) and macrostate where it is reasonable to expect unexpected physical properties (triply periodic minimal surfaces).

In the early 1800s, J. Gergonne derived the T family of triply periodic minimal surface. In 1853, D surface was described by Riemann. In the 1880s, H. Schwarz constructed H, CLP, and P surfaces. His student E. R. Neovius found new surface (NS) and revealed that P and D surfaces are related to each other by the Bonnet transformation.

To generate periodic surfaces, we select cells that are asymmetric units of three-dimensional space groups. These cells are equivalent to kaleidoscopic cells with flat faces of the Coxeter system for reflection

groups, which were used by A. Schoen to obtain the classical known infinite periodic minimal surfaces (IPMS).

The 43 families of surfaces obtained by this way are thus balanced. There is an indefinite number of unbalanced triply periodic surfaces, which, although everywhere minimal, divide the space into two unequal regions. An example of such surfaces is the Fermi surface of the coinage metal alloys.

Thus, by the middle of past century, the general theoretical framework for triply periodic minimal surfaces was developed. With the advent of computer graphics, it is possible to proceed to a new stage of this problem, which can be formulated briefly: How does nature provide periodic minimal surfaces in chemical structures? Does the surface in which there are atoms, clusters or molecules have any place in a real crystal? Are they a characteristic feature of the structure?

The main idea on the use of these concepts is that the intrinsic properties of these surfaces in molecules and crystalline solids should provide us the information on the relationship between the curvature and the chemical bond, i.e., is to describe the chemical bond by differential geometry. This will help to understand how molecules stand or move in solids and how porous solids such as zeolites, barrel-like proteins, and spiral-shaped molecules (cellulose, collagen and starch) absorb and/or convert other molecules or catalyze reactions. The structure in its bond and relationship follows the metric of its surface. It is known that complex structures can be described as simple structures constructed from small units.

The following conclusions may be drawn: (1) Periodic nodal surfaces (PNSs) of Fourier series are fundamental invariants of structured matter, which are organically bound with periodic minimal surfaces (PMSs) and periodic zero potential surfaces (P0PSs); (2) Interpenetrating (and nonoverlapping) structures can be described by surfaces parallel to minimal surfaces; (3) The properties of PNSs and P0PSs allow to describe the chemical bond by differential geometry.

EXPLOSIVE SYNTHESIS OF NANOSCALE DETONATION CARBON

A. A. Shtertser*, V. Yu. Ul'yanitskii, I. S. Batraev, and D. K. Rybin

Lavrent'ev Institute of Hydrodynamics, Siberian Branch, Russian Academy of Sciences, Novosibirsk, 630090, Russia

*e-mail: asterzer@mail.ru

Various forms of technical carbon (carbon black) can be produced by the burning or by the thermal decomposition of hydrocarbon fuels. There are methods for the production of acetylene carbon black (acetylene black) based on the explosive decomposition of acetylene [1, 2]. At this, the product made by detonation of rich hydrocarbon and oxygen gaseous mixtures is of keen interest because of its particular properties [3]. The pulse gas-detonation device (PGDD) developed in Lavrent'ev Institute of Hydrodynamics on the base of detonation spraying facility CCDS*2000* gives the new possibilities in manufacturing of a kind of carbon black – nanoscale detonation carbon (NDC) [4]. PGDD works in a continuous cyclic mode with automatic repetition of cycles so that the process as a whole consists of a sequence of shots (Fig. 1). The used gases (fuels, oxidizer and nitrogen) pass from gas balloons to the gas-distribution unit *3*. In every cycle (shot), the computer *6* sends the control signals to the valves in the gas distribution unit *3*, and through the open valves the fuel and oxygen pass separately into the mixing-ignition chamber *4*, where the said gases are mixed. Then the ready explosive mixture *5* fills the barrel *2*, which plays the role of a reactor, and the spark plug *7* initiates the process of detonation.

A. A. Shtertser et al.
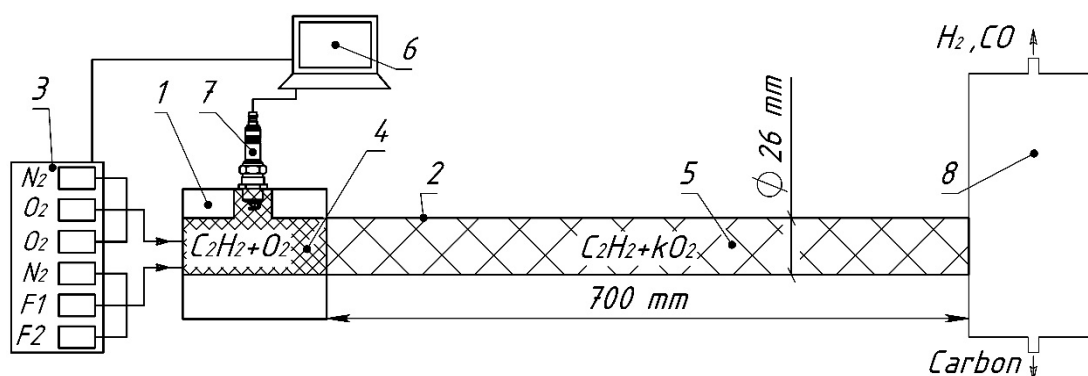
Fig. 1. Pulse Gas-Detonation Device: *1* mixing-ignition chamber, *2* water-cooled barrel, *3* gas-distribution unit, *4* booster explosive charge, *5* main explosive charge, *6* control computer, *7* spark plug, *8* receiver. Gas supply valves: *F1* and *F2* – fuels, O_2 – oxygen, N_2 – nitrogen.

After initiation, the detonation front passes along the barrel, and finally the cycle ends with the ejection of detonation products into the receiver *8* and purging of the barrel with nitrogen. Gaseous products pass through the receiver *8* to the exhaust system, while the solid-phase carbon accumulates there.

PGDD can work on various gaseous hydrocarbons, however in Fig. 1 as an example the explosive mixture of acetylene and oxygen $C_2H_2 + kO_2$ is pictured. When oxygen content in the main mixture *5* is low ($k < 0.4$), the spark plug discharge energy (≈ 10 mJ) is insufficient for initiation of detonation. In this case, it is necessary to create a two-layer explosive charge consisting of the booster charge *4* at the barrel breech end and the main charge *5* in the rest barrel volume. Any easily initiated explosive mixture, i.e. acetylene + oxygen equimolar composition $C_2H_2 + O_2$ can be employed as a booster explosive charge (see Fig. 1). Unlike [1–3], the process in PGDD proceeds in a flowing-gas mode so that a pressure of incoming acetylene is less than 0.14 MPa and a gas pressure in the barrel-reactor is 0.1 MPa. These parameters meet the explosion safety requirements established for common gas welding and cutting techniques.

In the experiments on NDC synthesis, the PGDD barrel with a length of 700 mm and a diameter of 26 mm was used, so the barrel had a volume of 372 cm³. The rich acetylene and oxygen $C_2H_2 + kO_2$ mixtures with k varying from 0.11 to 0.68 served as a main charge. These limit values of k correspond to ≈ 10 and $\approx 40\%$ of the oxygen molar content in the mixture, respectively. A detailed study of

detonation process in rich hydrocarbon + oxygen mixtures is described in [5]. The detonation velocities of rich acetylene + oxygen mixtures are given in Table 1. At $k < 0.11$, the mixture does not detonate, and at $k > 0.7$, the output of solid carbon is very small. At $k \geq 1$, the oxygen content is sufficient for the complete oxidation of carbon, and there is a lack of solid substance in detonation products. Figure 2a shows the solid carbon emission from the barrel during the shot. Figure 2b shows the image of NDC produced at $k = 0.68$. The productivity of PGDD at the operation rate of 5 shots per second is maximal at $k = 0.26$ and is 2.7 kg/h.

(a)	(b)
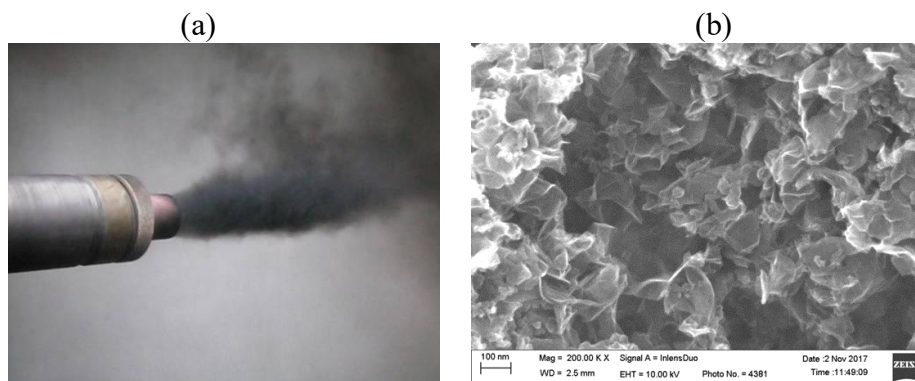
Fig. 2. (a) Solid carbon emission from the PGDD barrel and (b) the morphology of NDC particles.

The investigation of NDC produced at different k shows that the morphology of particles depends significantly on this parameter. At $k = 0.11$, the particles have a rounded shape and a size of dozens of nanometers, whereas at $k = 0.68$ they take a scale shape with a size of more than 100 nm and thickness of about 10 nm (see Fig. 2b). This material can be classified as carbon nanosheets [3]. As one can see in Table 1, the dependence of the acetylene + oxygen mixture detonation velocity and NDC density on k is nonmonotonic. This demonstrates the complexity of the detonation process in rich hydrocarbon + oxygen mixtures.

Table 1. Dependence of acetylene + oxygen detonation velocity D and NDC bulk density ρ on oxygen/acetylene molar ratio k.

k	0.11	0.18	0.26	0.30	0.42	0.57	0.68
D, m/s	1871	2003	2167	2158	2144	2386	2541
ρ, g/cm^3	0.013	0.014	0.020	0.041	0.055	0.024	0.020

The acetylene black commercially produced by Denka Company (Japan) has an average particle size $d = 35$ nm and a bulk density $\rho = 0.04$ g/cm^3; and the product of Soltex Company (USA) is characterized by $d = 25$–45 nm and $\rho = 0.05$–0.09 g/cm^3. The density of NDC produced on PGDD at k ranging from 0.11 to 0.26 and from 0.57 to 0.68 is much lower than densities of Denka and Soltex products. Therefore, we can expect that NDC functional properties (specific surface area, electric conductivity, electrochemical characteristics, etc.) will differ from those of above commercial products.

Presently the properties of NDC are being studied in order to determine the applications of this product.

1. G. B. Kistiakovsky, et al, Detonation process of making carbon black, *US Patent No. 2690960*, date of publication Oct. 5, 1954.

2. V. G. Knorre, V. E. Nizovtsev, E. A. Pryadkina, V. N. Sidorov, Method of Industrial Carbon Production, *RU Patent No. 2325413*, date of publication May 27, 2008.

3. C. Sorensen, A. Nepal, G. P. Singh, Process for high-yield production of graphene via detonation of carbon-containing material, *US Patent No. 9440857*, date of publication Sept. 13, 2016.

4. I. S. Batraev, A. A. Vasil'ev, A. V. Pinaev, et al, Method of nanocarbon production, *RU Patent Application No. 2016132962*, the decision on the grant of Patent dated Nov. 22, 2017.

5. I. S. Batraev, A. A. Vasil'ev, V. Yu. Ul'yanitskii, A. A. Shtertser, D. K. Rybin, The study of gas detonation in rich mixtures of hydrocarbons with oxygen, *Combust. Explos. Shock Waves*, 2018, vol. 54, No. 2, accepted for publication.

REGULARITIES OF COMBUSTION AND CHEMICAL CONVERSION OF A WO$_3$/Al/Ca/C MIXTURE

S. L. Silyakov, V. I. Yukhvid, T. I. Ignat'eva, N. V. Sachkova, N. Yu. Khomenko, A. F. Belikova, and P. A. Miloserdov

Merzhanov Institute of Structural Macrokinetics and Materials Science, RAS, Chernogolovka, Moscow, 142432 Russia

e-mail: ssl@ism.ac.ru

Tungsten carbides are widely used in industry to produce protective coatings on parts of machinery and mechanisms, which are subjected to intensive wear and strong impact. The main methods for obtaining these materials are powder metallurgy and high-temperature melting in furnaces. This report presents the first results of studies on the synthesis of these materials by the methods of SHS metallurgy.

Green high-exothermic mixtures of the thermite type consisted of tungsten oxide (VI) powder, aluminum powder (ASD-1 brand), calcium granules (CAS 7440-70-2, 99.1% pure), and graphite (GMZ, grain size d_c = 315/63 μm). Before mixing, these components were dried. These green exothermic mixtures (25 and 50 g, bulk density of 2.00 g/cm^3) placed in graphite and quartz glasses (40 and 20 mm in diameter, respectively, and 60 mm in height) were burned in a constant pressure bomb fiilled nitrogen gas at initial gas pressure varying within the range of 0.1–6.0 MPa. Green mixture was ignited with tungsten coil. In experiments, we find average linear burning velocity (U), relative mass loss (η_1) and relative yield of cermet phase in the ingot (η_2). Expressions for determination of U, η_1, and η_2 are given in [1]. The synthesis products were characterized by SEM, EDS, and XRD. The calculation of adiabatic combustion temperatures was carried out using a Thermo program. The preliminary thermodynamic analysis of compositions [α(WO$_3$/Ca/C) + (100–α)(WO$_3$/Al/C)] shows that the calculated adiabatic combustion temperatures for all α values are in the range of 2900–3500K (Fig. 1).

S. L. Silyakov et al.
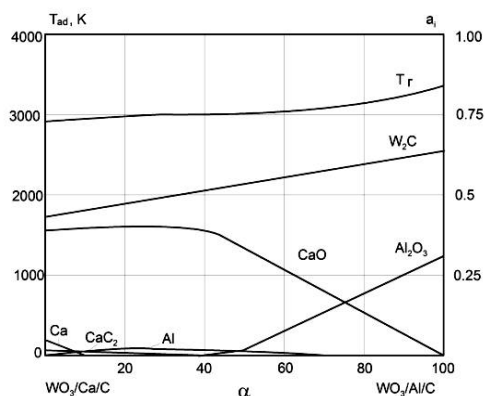
Fig.1. Calculated adiabatic combustion temperature (T_{ad}), total amount of gaseous reaction products (a_g), and composition of condensed reaction products as a function of ratio of mass fractions (α) for $WO_3:Ca:C=0.647:0.336:0.017$ and $WO_3:Al:C=0.790:0.180:0.030$. $P_o = 5MPa$. Initial mixture: $[\alpha(WO_3/Ca/C) + (100-\alpha)(WO_3/Al/C)]$.

At the same time, the total amount of gaseous reaction products (a_g) does not exceed 2 wt %. The low calculated values of a_g allow to expect relatively low range of values in the experiment. The calculated adiabatic combustion temperatures for all α values exceed the melting point of synthesis products ($T(W_2C) = 3053$ K, $T(CaO) = 2853$ K, $T(Al_2O_3) = 2318$ K) which ensures the synthesis of combustion products in a cast form. However, the insignificant difference between the calculated combustion temperatures and the melting points of the synthesis products complicates the process of obtaining cast tungsten carbides. In the experiment, this difference can be significantly reduced. To improve yield of target product, we must strengthen the process of alloy–slag ($CaO–Al_2O_3$) separation. According to the phase diagram of $CaO–Al_2O_3$, a vitreous eutectic with a melting point of 1573–1773 K forms at Al_2O_3 content of 44 to 56%. Thus, favorable conditions for improving phase separation (gravity separation) during synthesis of cast carbide–tungsten materials were created.

The exothermic mixture combustion $[\alpha(WO_3/Ca/C) + (100-\alpha)(WO_3/Al/C)]$ proceeds at any ratio (α), and the synthesis of cast carbide–tungsten materials is possible only in the range $0 \leq \alpha \leq 0.75$ (Fig. 2). The average linear burning velocity for this series of experiments varies from 0.8 to 2.8 cm/s. According to the EDS data, the total carbon content in the cast ingots varies from 0.5 to 2.1 wt %, and the content of aluminum impurity decreases from 2.7 to 0.7 wt % (Fig. 3).
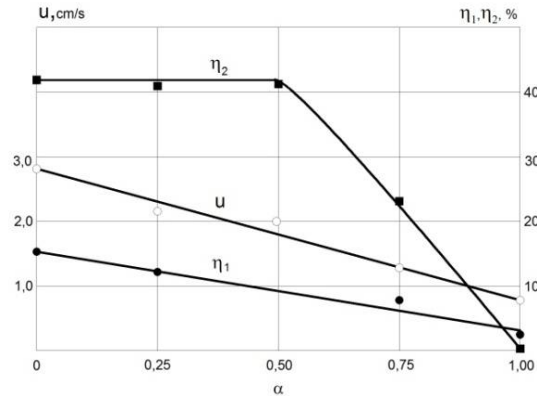
Fig. 2. Influence of the ratio of mixture mass fractions (α) [α(WO$_3$/Al/C) + (1−α)(WO$_3$/Ca/C)] on the relative yield of carbide−tungsten material in the ingot (η_2), relative mass loss (η_1), and average linear burning velocity (U). $P_0 = 5.0$ MPa, $d_c = 90/63$ μm, $M_o = 25$ g.
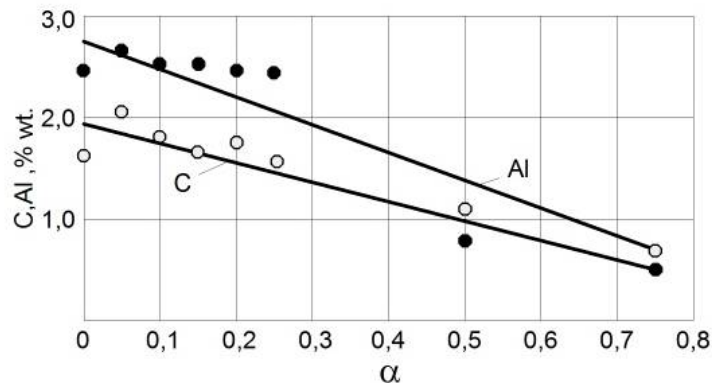
Fig.3. Aluminum impurity and carbon content in the cast carbide−tungsten ingot vs. ratio of mass fractions (α) for WO$_3$:Al:C = 0.794:0.185:0.021 and WO$_3$:Ca:C = 0.647:0.336:0.017. Initial mixture: [α(WO$_3$/Al/C)+(1−α)(WO$_3$/Ca/C)]. $P_0 = 5.0$ MPa, $d_c = 90/63$ μm, $M_o = 50$ g.

The XRD analysis shows that cast materials synthesized from WO$_3$/Al/Ca/C mixture for $0 \le \alpha \le 0.75$ contain two main phases W$_2$C$_{0.48}$ and W. The microstructure of the synthesized cast materials consists of grains W$_2$C$_{0.48}$ and eutectic W + W$_2$C$_{0.48}$. Hardness for W$_2$C$_{0.48}$ grains is 156–176 GPa, for eutectic is 70–93 GPa, and for mixture of small grains of the phase W$_2$C$_{0.48}$ and eutectic is 82–138 GPa.

1. S. L. Silyakov, V. I. Yukhvid, combustion of iron aluminum thermite with ammonium chloride and sodium hydrogen tarbonate, *Comb. Explos. Shock Waves*, 2015, vol. 51, no. 6, pp. 656–658.

S. L. Silyakov et al.

SiAlON-BASED CERAMIC COMPOSITES FROM COMBUSTION-SYNTHESIZED RAW MATERIALS BY SPARK PLASMA SINTERING

K. L. Smirnov[1], E. G. Grigor'ev[2], and E. V. Nefedova[2]

[1] Merzhanov Institute of Structural Macrokinetics and Materials Science, Russian Academy of Sciences, Chernogolovka, Moscow, 142432 Russia

[2] National Research Nuclear University MEPhI, Moscow, 115409 Russia

e-mail: kosm@ism.ac.ru

Solid solutions of general formula $Si_{6-z}Al_zO_zN_{8-z}$ ($z = 0.0–4.2$) are known for their excellent hardness, strength, and wear/corrosion resistance, which explains their wide use in various engineering applications such as refractory materials, bearings, and cutting instruments. Functionality of β-SiAlON ceramics can be markedly improved upon addition of other refractory compounds with strongly different physical parameters such as Young modulus, thermal/electrical conductivity, thermal expansion, etc. The addition of hexagonal boron nitride (h-BN), TiN, and SiC to ceramic composites is known to improve their fracture toughness, thermal shock resistance, tribological properties, thermal/electrical conductivity, and machinability.

Combustion synthesis (CS) is a rapidly developing area of R & D oriented on fast and energy efficient production of high-melting compounds and materials. For example, infiltration-mediated CS in nitrogen is a convenient technique for production of α- and β-SiAlON powders with different phase and elemental composition, particle size, and morphology. Spark plasma sintering (SPS) is a newly developed process that uses dc pulses for sample heating. Compared to conventional hot pressing, SPS ensures higher heating rates and very short holding times and has been widely recognized as a rapid and

effective method for densification of various materials. Thus, the combination of CS and SPS techniques seems rather promising to fabricate β-SiAlON-based ceramic composites with improved functional properties.

Infiltration-mediated CS of β-Si$_5$AlON$_7$ and h-BN powders in nitrogen gas was carried out by the following schemes:

$$4.5Si + Al + 0.5SiO_2 + 3.5N_2 \rightarrow \beta\text{-Si}_5AlON_7 \qquad (1)$$

$$B + 0.5N_2 \rightarrow h\text{-BN} \qquad (2)$$
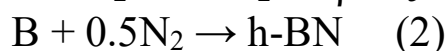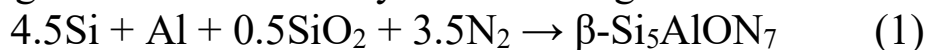
Green mixtures also contained some amount of homemade diluents, β-Si$_5$AlON$_7$ and h-BN respectively, in order to improve extent of conversion. Combustion was performed in a 2-L reactor at $P(N_2) = 8–10$ MPa. The CS of β-SiC was carried out using multistep chemical reactions in the Si–C–N system and TiN fine powders with added NH$_4$Cl as a gasifying agent. Aliquot amounts of combustion-synthesized raw powders were intermixed in a high-energy planetary steel-ball mill. Ball milling time (800 rpm, ball/mill ratio 10:1) was 5 min. Then milled powders (about 0.5 g) were sintered in a Labox 625 SPS facility under vacuum (below 10 Pa). The heating rate was 50 deg/min. The sintered compacts were heated from room temperature to 600°C without applied load and then to 1550–1800°C at a compressive stress of 50 MPa. The compacts were held at a desired temperature for 5 min before the power was turned off.

According to XRD results, the raw powders of β-Si$_5$AlON$_7$, h-BN, and TiN did not contain impurity phases while β-SiC had trace amounts of Si$_3$N$_4$. According to SEM results, all as-synthesized powders appeared largely as agglomerates. Their specific surface was about 1.3 m^2/g for β-Si$_5$AlON$_7$ powders, and from 9.8 to 22.8 m^2/g for h-BN, β-SiC, and TiN fine powders. After ball milling, the specific surface increased by a factor of 4–6. Figure 1 shows relative density ρ_{rel} of sintered samples as a function of temperature T. The sintering of pure β-Si$_5$AlON$_7$ was accompanied by marked intensification of the consolidation process at temperatures above 1400°C probably due to formation of SiO$_2$ and Al$_2$O$_3$ eutectics. Upon further increase in T, relative density of sintered β-Si$_5$AlON$_7$ gradually grows up to 87% (curve *1* in Fig. 1). The addition of h-BN improves the compactibility of sintered powder mixtures. Under a compressive stress of 50 MPa at 600°C, the initial value of ρ_{rel} exceeds 80% for the compact containing 30 wt % BN and 60% for that of pure β-Si$_5$AlON$_7$. In

parallel, an increase in h-BN content suppresses the consolidation processes due to formation of liquid eutectics. At 30 wt % BN, an increase in ρ_{rel} becomes insignificant at temperatures above 1400°C. In case of 10 and 20 wt % h-BN, the processes associated with formation of liquid eutectics are more or less pronounced, so that high relative density (close to theoretical one) can be attained (see curve *3* in Fig. 1). The addition of fine β-SiC and TiN powders worsens the compactibility of sintered powder mixtures under a compressive stress at the initial stage. As a result, the highest value of relative density for sintered ceramic composites containing β-SiC can only be achieved at 1750°C (curve *2* in Fig. 1). Meanwhile, the addition of TiN powder is seen to facilitate the efficiency of sintering above 900°C and the highest values of ρ_{rel} can be achieved already at 1550°C (curve *4* in Fig. 1).

Figure 2a illustrates flexural strength σ_f as a function of ρ_{rel}. SPS method affords to produce ceramic composites with higher relative density and flexural strength (up to 400 MPa). In our case, the flexural strength of sintered ceramic composites was found to depend on the BN content only slightly (Fig. 2b). A marked increase in σ_f (up to 40%) can be achieved upon replacement of 40 wt % of β-Si₅AlON₇ in sintered ceramic composites by β-SiC and TiN (curve *2* in Fig. 2a).
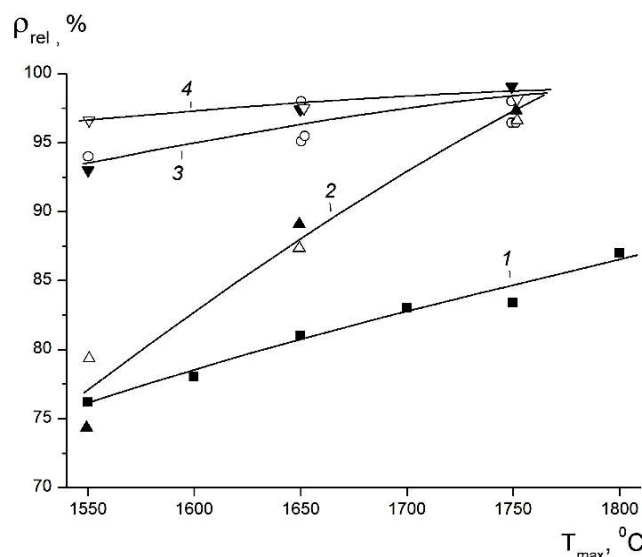
Fig. 1. Relative density ρ_{rel} as a function of T_{max} for: (■) β-Si₅AlON₇ (*1*), (○) β-Si₅AlON₇–BN (10–30 wt %) (*3*), (▼) β-Si₅AlON₇–TiN (20 wt %)–BN (10 wt %) –(*3*), (▽) β-Si₅AlON₇–TiN (40 wt %)–BN (10 wt %) (*4*), (▲) β-Si₅AlON₇–SiC (20 wt %)–BN (10 wt %) (*2*), (Δ) β-Si₅AlON₇–SiC (40 wt %)–BN (10 wt %) (2).
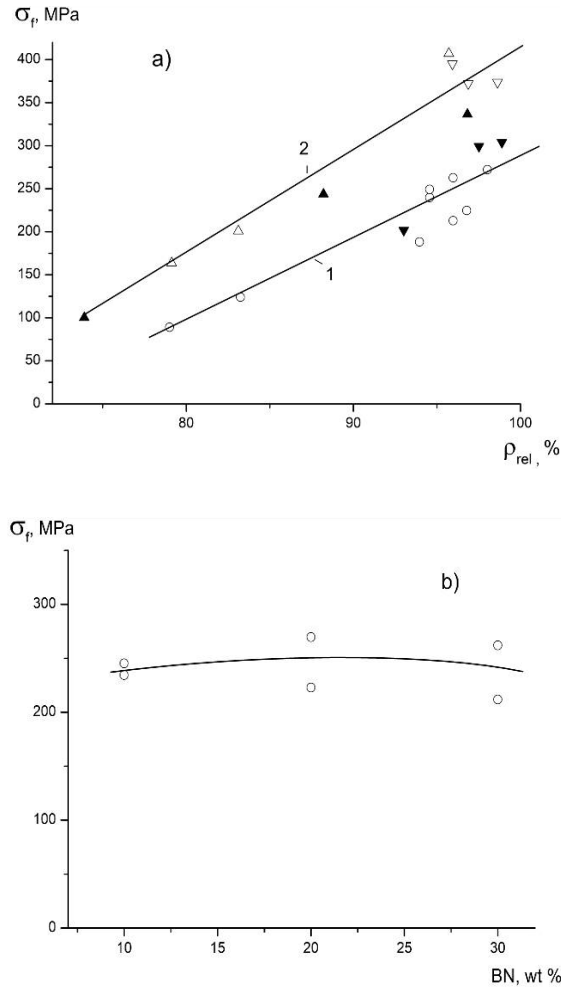
Fig. 2. Flexural strength σ_f as a function of: (a) relative density ρ_{rel} for (○) β-Si$_5$AlON$_7$–BN (0–30 wt %) (*1*), (▼) β-Si$_5$AlON$_7$–TiN(20 wt %)–BN(10 wt %), (∇) β-Si$_5$AlON$_7$–TiN(40 wt %)–BN(10 wt %) (*2*), (▲) β-Si$_5$AlON$_7$–SiC(20 wt %)–BN(10 wt %), (Δ) β-Si$_5$AlON$_7$–SiC(40 wt %)–BN(10 wt %) (*2*), and (b) BN content in β-Si$_5$AlON$_7$–BN (10–30 wt %) (ρ_{rel} = 95–98%).

HIGH-TEMPERATURE SYNTHESIS IN MECHANICALLY ACTIVATED Ti–Al POWDER MIXTURE IRRADIATED BY GAMMA-QUANTA

**A. V. Sobachkin[1], M. V. Loginova[1], A. A. Sitnikov[1],
V. I. Yakovlev[1], V. Yu. Filimonov[1], S. G. Ivanov[1],
A. Yu. Myasnikov[1], and A. V. Gradoboev[2]**

[1] Polzunov Altai State Technical University, Barnaul, 656038 Russia
[2] National Research Tomsk Polytechnic University, Tomsk, 634050 Russia

e-mail: anicpt@rambler.ru

Mechanical activation is one of the ways to influence the powder mixture. It makes it possible to implement the ideal contact between reagents and to increase the mixture reactivity [1]. However, low diffusion rate in solids prevents the rapid averaging of the concentration of components and the production of monophasic products. Chemical heterogeneity of mechanocomposites leads to the staging of chemical transformations and to the multiphase SHS product during rapid heating and cooling of the reaction mixture. Therefore, the annealing of samples at high temperatures will occur due to rapid diffusion recrystallization and product formation close to monophasic [2]. It should be noted that the duration of exposure during mechanoactivation is measured in minutes, and the possibilities of "fine" structure control are limited [3]. Therefore, the use of γ-irradiation systems in a non-equilibrium state for realizing "fine" structure control is of particular interest [4].

Synthesis in mechanically activated irradiated Ti + Al powder mixture was achieved through thermal explosion by induction heating with varying the time of isothermal annealing after reaching the maximum temperature of the charge [5]. Optimal modes for mechanical activation of the Ti + Al powder mixture were determined by the formation of the highest possible microdeformation without

emerging mechanically alloyed products at a given grinding mode [6]. Then mechanically activated powder mixture was subjected to irradiation by gamma quanta ^{60}Co with different absorption doses [7]. The synthesis was conducted under identical conditions in mechanically activated powder mixtures and mechanically activated irradiated powder mixtures of the same Ti + Al composition. After reaching the maximum synthesis temperatures, the heating element was not disconnected; the process of rapid synthesis was continuously shifting to isothermal annealing process. The heating source was switched off at regular intervals.

Figure 1a shows X-ray diffraction patterns of synthesis products for different annealing times (τ, min) corresponding to 7-min mechanical activation.

When turning the system off immediately after the completed chemical reaction, the result of the synthesis in the activated mixtures is a multiphase product in a non-equilibrium state. The system stabilizes with increasing exposure. The same happens with 2-min annealing. The X-ray diffraction patterns show the prevailing reflections of TiAl and a small amount of metastable Ti$_3$Al$_5$ phase. The main TiAl phase decays at a further increase in the annealing time.

(a)   (b)
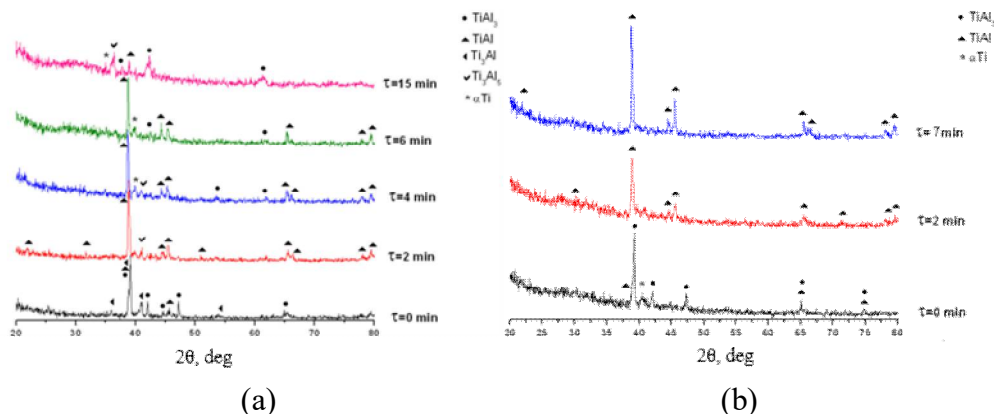
Fig. 1. X-ray diffraction patterns of synthesis products in powder mixture Ti + Al: (a) mechanically activated; (b) mechanically activated and irradiated.

Figure 1b shows the characteristic X-ray diffraction patterns of the products obtained by high-temperature synthesis of Ti + Al powder mixture preliminarily mechanically activated for 7 min and then irradiated by gamma quanta at $D_\gamma = 5 \cdot 10^4$ Gy. The X-ray diffraction

patterns of the powder mixture after isothermal annealing at $\tau = 0$, 2 and 7 min are presented. The annealing for $\tau = 0$ min produces a multiphase synthesis product. The synthesis product after 2-min annealing is represented by monophase TiAl intermetallic compound; the stabilization of system is observed. It should be noted that with an increase in the annealing time to 7 min, there is no decomposition of TiAl phase, as it was observed upon synthesis of mechanically activated Ti + Al mixtures without exposure to gamma irradiation. Thus, with the increase in the annealing time to 7 min the composition of the synthesis product remains unchanged. In the X-ray diffraction pattern, the monophasic TiAl product is observed. Moreover, as can be seen in Fig. 1b, the intensity of phase reflections increases, the narrow peaks and the diffuse background level decreases. This indicates the stabilization of TiAl. In other words, long-term high-temperature annealing does not lead to the decomposition of the compound and the formation of an intermetallic equilibrium phases set at the annealing temperature. On the contrary, the increase of the annealing time promotes the stabilization of the compound. Thus, the influence of gamma radiation on the initial mixture under certain conditions leads to the formation of a structurally homogeneous product of TiAl composition.

Figure 2 presents characteristic component distribution patterns in the volume of the composite after 7-min mechanical activation, γ-irradiation at $D_\gamma = 5 \cdot 10^4$ Gy and annealing for $\tau = 7$ min. The system is characterized by a high degree of uniformity in the distribution of components in the volume of the mechanical composite in accordance with the stoichiometry of the TiAl compound. The composition changes are 50±3 at %, which are in the range of the TiAl phase homogeneity region. Thus, the monophase product γ(TiAl) can be synthesized in mechanically activated mixture after exposure to γ-irradiation.
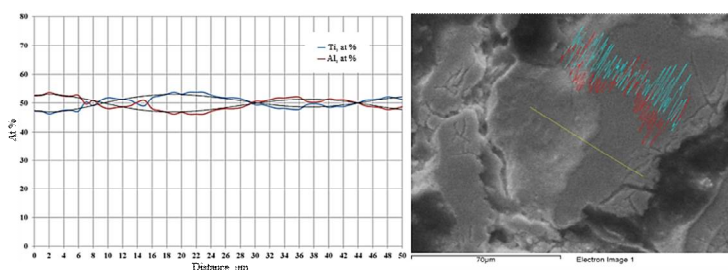
Fig. 2. Patterns of distribution of components in the volume of the product of high-temperature synthesis.

1. A. S. Rogachev, N. F. Shkodich, S. G. Vadchenko, F. Baras, D. Yu. Kovalev, S. Rouvimov, A. A. Nepapushev, A. S. Mukasyan, Influence of the high energy ball milling on structure and reactivity of the Ni + Al powder mixture, *J. Alloys Comp.*, 2013, vol. 577, pp. 600–605.
2. A. A. Popova, A. V. Sobachkin, I. V. Nazarov, V. I. Yakovlev, M. V. Loginova, A. A. Sitnikov, M. R. Sharafutdinov, N. Z. Lyakhov, Dynamic diffractometry of phase transformations during high-temperature synthesis in mechanically activated powder systems in the thermal explosion mode, *Bull. Russ. Acad. Sci.: Phys.*, 2013, vol. 77, no. 2, pp. 120–122.
3. M. A .Korchagin, T. F. Grigorieva, B. B. Bokhonov, M. R. Sharafutdinov, A. P. Barinova, N. Z. Lyakhov, Solid-phase combustion in mechanically activated SHS systems. I. Influence of duration of mechanical activation on the process characteristics and the composition of the combustion, *Combust. Explos. Shock Waves*, 2003, vol. 39, no. 1, pp. 51–59.
4. A. M. Shalaev, *Radiation-stimulated diffusion in metals*, M.: Atomizdat, 1972, 148 p.
5. V. Yu. Filimonov, A. A. Sitnikov, A. V. Afanas'ev, M. V. Loginova, V. I. Yakovlev, A. Z. Negodyaev, D. V. Schreifer, V. A. Solov'ev, Microwave Assisted Combustion synthesis in mechanically activated 3Ti + Al powder mixtures: Structure formation issues, *Int. J. Self-Propag. High-Temp. Synth.*, 2014, vol. 23, no. 1, pp. 18–25.
6. M. V. Loginova, V. Yu. Filimonov, V. I. Yakovlev, A. A. Sitnikov, A. Z. Negodyaev, D. V. Shreifer, Analysis of the influence of high temperature synthesis parameters on the structure formation in the mechanically activated 3Ti+Al powder mixture, *Appl. Mech. Mater.,* 2015, vol. 788, pp. 117–122.
7. M. V. Loginova, V. I. Yakovlev, A. A. Sitnikov, A. V. Sobachkin, S. G. Ivanov, A. Z. Negodyaev, A. V. Gradoboev, The evolution of structural and phase states of titanium aluminides after γ irradiation in small doses, *Phys. Met. Metallogr.,* 2017, vol. 118, no. 2, pp. 170–175.

IMPLEMENTATION OF NEW OPPORTUNITIES FOR OBTAINING LARGE-SIZED COMPACT PLATES FROM CERAMIC POWDER MATERIALS BY FREE SHS COMPRESSION

A. M. Stolin, P. M. Bazhin, and A. S. Konstantinov

Merzhanov Institute of Structural Macrokinetics and Materials Science, Russian Academy of Sciences, Chernogolovka, Moscow, 142432 Russia

e-mail: amstolin@ism.ac.ru

One of the most important problems in the field of SHS is the direct production (in one technological stage and in one installation) of products with a given shape, size, composition, structure and, finally, with predetermined performance properties from brittle and hard-deformable powders of refractory inorganic compounds.

In 1975, studies relating to the development of the method, which combines self-propagating high temperature synthesis (SHS) with compression of the combustion products have been initiated. The advantages of SHS, arising from the nature of this process, become most evident when producing large products whose overall dimensions are more than 100 mm.

It is difficult to manufacture such products by the method of free sintering. The method of hot pressing in electrically heated graphite molds is also expensive and time-consuming.

Since the powders of refractory compounds are fragile and difficult to deform, at first it is seemed to be possible to implement the SHS-pressing method for large-sized products only on powerful presses using special press equipment. However, the complexity of specialized equipment was an obstacle to the introduction of this technology in the industry.

New opportunities in obtaining products from powders of refractory inorganic compounds are opened by using the combined

action of high-temperature shear deformation and pressure in the SHS process. This idea was used in the method of free SHS compression [1]. The essence of this method is to compact and mold the synthesized material under the influence of a constant low pressure (~ 10–50 MPa) without using special molds. This is an important advantage of the method of free SHS compression while production of large plates.

In this paper, we present the results of the study of free SHS compression process for the production of large-sized compact plates with dimensions of more than 100 mm from powders of refractory inorganic compounds from a material based on titanium diboride [2]. For this purpose, a hydraulic press with a force of 120 kN was used, that is 166 times less than the force of the press in 20 MN used early for SHS-pressing of large-sized products. Material-research studies of the obtained plates have been carried out and their physical and mechanical properties have been studied. The obtained materials are stable at the temperatures up to 1100°C.

1. A. M. Stolin, D. Vrel, S. N. Galyshev, A. Hendaoui, P. M. Bazhin, A. E. Sytschev, Hot forging of MAX compounds SHS-produced in the Ti–Al–C system, *Int. J. Self-Propag. High-Temp. Synth*., 2009, vol. 18, no. 3, pp. 194–199.
2. A. S. Konstantinov, P. M. Bazhin, A. M. Stolin, E. V. Kostitsyna, A. S. Ignatov, Ti–B-based composite materials: properties, basic fabrication methods, and fields of application (review), *Compos. Part A: Appl. Sci. Manuf.*, 2018, vol. 108, pp. 79–88; DOI: 10.1016/j.compositesa.2018.02.027.

SELF-PROPAGATING HIGH-TEMPERATURE SYNTHESIS OF Ni−Al BASED ALLOY WITH NANOLAMINATE CARBON-CONTAINING COMPONENTS

A. E. Sytschev, N. A. Kochetov, S. G. Vadchenko, and A. S. Shchukin

Merzhanov Institute of Structural Macrokinetics and Materials Science, Russian Academy of Sciences, Chernogolovka, Moscow, 142432 Russia

e-mail: sytschev@ism.ac.ru

Ni–Al-based intermetallics despite their advantages exhibits an insignificant ductility especially at room temperature. There are various methods for reducing the tendency to embrittlement of these alloys [1–5]. The addition of a negligible amount of carbon can significantly affect the strength, modulus of elasticity, and viscosity of materials [6–8]. The presence of carbon in the Ni–Al alloy (30 weight ppm) leads to an increase in the yield strength by 30% [9]. The formation of a chemical bond between fiber and matrix, which strongly affects the mechanical properties of the composite, can changed depending on conditions for obtaining the material [10]. It is possible to produce eutectic alloys containing metallic nanowires of less than 100 nm in size [11]. The presence of the melt greatly accelerates the process of mutual diffusion of the reaction components and increases the contact area due to the capillary spreading of the liquid over the solid particles. The formation of the melt in the Ni–Al system is easily realized during SHS process [12, 13]. The most important stage in the preparation of the reactive blends can also be mechanical activation (MA), the parameters of which ultimately affect the kinetics of solid-phase combustion (sintering) [14–18].

In this paper, we studied the peculiarities of formation of the structure in intermetallic Ni−Al alloys modified by carbon

components (nanofibers, soot) in the regime of self-propagating high-temperature synthesis (SHS) and the influence of preliminary MA on the structure.

SHS experiments in the Ni−Al−C system showed the possibility of obtaining a material using carbon components in the combustion regime. The reaction mixture consisted of ASD-1 aluminum powder containing about 99.7% Al with a size of about 20 μm and PNK metallic carbonyl nickel powder (no less than 99.9 wt %) of about 10 μm in size. Carbon (0−6 wt %) in the form of carbon soot was added to the mixture of Ni and Al powders. The reaction mixture was exposed to MA for 1 min using an ATO-2 attritor. Cylindrical samples with a diameter of 1 cm were pressed from activated mixtures by cold pressing. Combustion of pressed samples was carried out in a constant pressure chamber in an inert atmosphere of argon under a pressure of 1 atm. The combustion process was recorded on a video camera. Burning velocity of samples was determined by the time-lapse processing of obtained video recordings. The burning velocity decreased noticeably with increasing soot content.

XRD analysis of the synthesized material showed only the presence of the NiAl phase. Because of a low amount of soot in the green mixture (2–6 wt %), no carbon in the synthesized product was detected. For graphite-containing sample, a weakly expressed peak at $2\theta = 27°–28°$ was revealed. However, the fact that the amount of carbon-containing phase is close to the limit of detection of XRD does not allow observing this reflection more clearly.

The microstructural studies showed that as a result of the synthesis, a close-packed intermetallic matrix based on NiAl with a grain size of about 5−10 μm was formed. In the case of using carbon soot in the synthesis product, the carbon predominantly located along the boundaries of intermetallic NiAl grains forms a continuous/ continuous multilayer coating/ film on the their surface with a thickness of about 66 nm (Fig. 1). In [14], the possibility of forming a supersaturated carbon nanocrystalline solid solution of Ni(Al,C) is indicated.

It can be assumed that the formation of multilayer carbon nanofilms occurred as a result of allotropic conversion of carbon soot into graphite only at the point of direct contact of the Ni–Al melt with soot (Fig. 2).

The graphitic layer is thin enough to serve as a window for 10 KeV electron pass along (Fig. 3).

The compressive strength of NiAl/C synthesized samples at a carbon soot content of 1 wt % is 290 MPa. The formation of carbon films on the surface of intermetallic grains increases the plastic properties of synthesized materials as compared to pure NiAl.
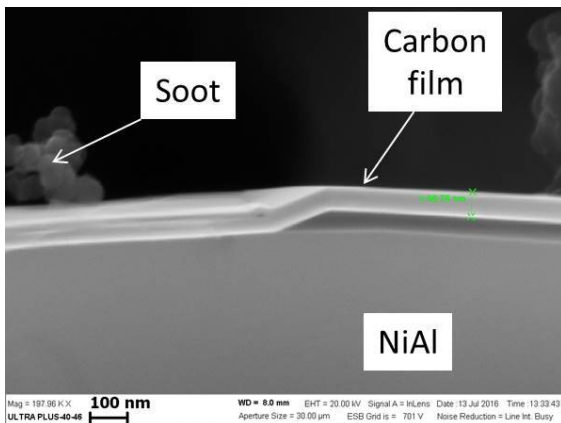
Fig.1. Cross section of NiAl/C alloy.
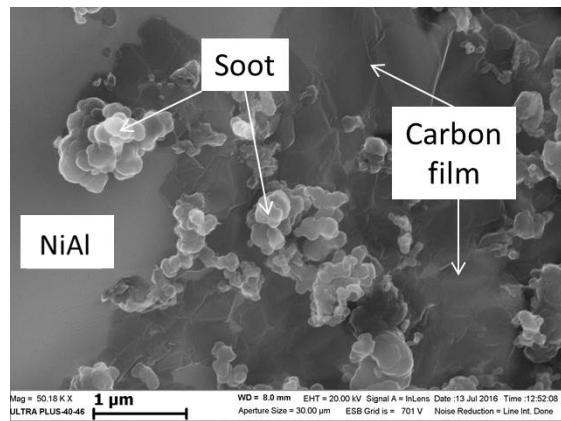
Fig. 2. Formation of a carbon film on the NiAl surface.
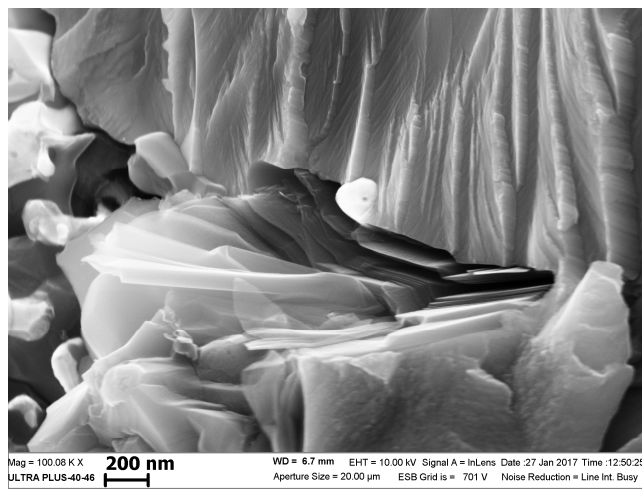
Fig. 3. Transparency graphitic layer on NiAl.

1. A. V. Ponomareva, Yu. Kh. Vekilov., I. A. Abrikosov, Effect of Re content on elastic properties of B2 NiAl from ab initio calculations, *J. Alloy. Compd.*, 2014, vol. 586, pp. 274–278.

2. A. V. Ponomareva, E. I. Isaev, Yu. Kh. Vekilov, I. A. Abrikosov, Site preference and effect of alloying on elastic properties of ternary B2 NiAl-based alloys, *Phys. Rev. B*, 2012, vol. 85, 144117.

3. K. Parlinski, P. T. Jochym, H. Schober, A. Jianu, J. Dutkiewicz, Local modes of Fe and Co atoms in NiAl intermetallics. *Phys. Rev. B*, 2004, vol. 70, 224304.

4. X. L. Hu, Y. Zhang, G.-H. Lu, T. Wang, Role of the alloying element in suppressing the negative effect of O in NiAl: Cr as an example, *Scr. Mater.*, 2009, vol. 61, 189.

5. P. Lazar, R. Podloucky, Ab initio study of the mechanical properties of NiAl microalloyed by X = Cr, Mo, Ti, Ga, *Phys. Rev. B*, 2006, vol. 73, 104114.

6. Y.-L. Liu, Z.-H. Dai, W.-T. Wang, Influence of carbon–vacancy interaction on carbon and vacancy diffusivity in tungsten, *Comput. Mater. Sci.*, 2014, vol. 83, pp. 1–4.

7. Y.-L. Liu, H.-B. Zhou, Y. Zhang, C. Duan, Point defect concentrations of impurity carbon in tungsten, *Comput. Mater. Sci.*, 2012, vol. 62, 282.

8. Y.-L. Liu, H.-B. Zhou, G.-H. Y. Zhang, G.-N. Lu, Luo, Interaction of C with vacancy in W: A first-principles study, *Comput. Mater. Sci.*, 2011, vol. 50, pp. 3213–3217.

9. X. Hu, J. Ma, H. Dou, Y. Niu, Y. Zhang, Q. Song, Effects of C impurities on the elastic properties of NiAl intermetallics, *Prog. Nat. Sci. Mater. Int.*, 2016, vol. 24, pp. 637–641.

10. R. R. Bowman, *Influence of Interfacial Characteristics on the Mechanical Properties of Continuous Fiber Reinforced NiAl Composites*, Materials Research Society Spring Meeting, San Francisco, CA, 1992.

11. D. Frankel, S. Milenkovic, A. J. Smith, A. W. Hassel, Nanostructuring of NiAl–Mo eutectic alloys by selective phase dissolution, *Electrochim. Acta*, 2009, vol. 54, pp. 6015–6021.

12. E. A. Levashov, A. S. Rogachev, V. V. Kurbatkina, Yu. M. Maksimov, V. I. Yukhvid, *Promising Materials and Self-Propagating High-Temperature Synthesis*, Moscow: MISiS, 2011 (in Russian).

13. A. S. Rogachev, A. S. Mukasyan, Combustion for Synthesis of Materials, Boca Raton, London, New York: CRC Press Taylor & Francis Group, 2015.

14. V. K. Portnoi, A. V. Leonov, V. I. Fadeeva, S. A. Fedotov. Mechanochemical synthesis in the Ni–Al–C system, *Bull. Russ. Acad. Sci. Phys.*, 2007, vol. 71, no. 12, pp. 1693–1696.

15. N. A. Kochetov, S. G. Vadchenko, Mechanically activated SHS of NiAl: Effect of Ni morphology and mechanoactivation conditions, *Int. J. Self-Propag. High-Temp. Synth.*, 2012, vol. 21, no. 1, pp. 55–58.

16. A. E. Sytschev, S. G. Vadchenko, A. S. Shchukin, SHS in mechanoactivated Ni–Al–W blends: some structural aspects, *Int. J. Self-Propag. High-Temp. Synth.*, 2013, vol. 22, no. 3, pp. 166–169.

17. N. A. Kochetov, Combustion and characteristics of mechanically activated Ni + Al mixture: Effects of the weight and size of the milling balls, *Russ. J. Phys. Chem. B*, 2016, vol. 10, no. 4, pp. 639–643.

18. A. E. Sytschev, S. G. Vadchenko, O. D. Boyarchenko, A. S. Shchukin, Ni_3Al/C Composites by thermal explosion, *Int. J. Self-Propag. High-Temp. Synth.*, 2018, vol. 27, no. 1, pp. 64–65; DOI: 10.3103/S1061386218010090.

THE INFLUENCE OF HEAT TREATMENT ON CHANGES IN THE STRUCTURE, CHEMICAL COMPOSITION AND MECHANICAL PROPERTIES OF EXPLOSIVELY CLADDED TITANIUM ON STEEL PLATE

M. Szmul[1,2], A. Chudzio[2], Z. Szulc[3], and J. Wojewoda-Budka[1]

[1] Institute of Metallurgy and Materials Science, Polish Academy of Sciences, Reymonta Str. 25, Krakow, 30-059 Poland
[2] FAMET S.A., Szkolna Str. 15a, Kedzierzyn-Kozle, 47-225 Poland
[3] Z.T.W. EXPLOMET S.J., Oswiecimska Str. 100H, Opole, 45-641 Poland

e-mail: marcin.szmul@wp.pl

For the construction of apparatus and process devices (e.g. steam condensers, heat exchangers, pressure vessels) high corrosion resistance materials are used. Explosively cladded titanium–steel bimetal belongs to this group. As a result of the explosive welding process, zones of stress concentration (strengthening) are formed in both the base material and the cladding material. They cause strong decrease in plastic properties in the area of the welded joint, which disqualify the use of bimetal for further production operations such as plastic working. The improvement of plasticity is obtained by reducing the internal stresses by application of stress relief annealing and only such prepared materials are subjected to the processes of plastic forming and/or welding. In addition, in some cases, it is necessary to perform another heat treatment after the welding process in order to reduce the resultant internal stresses and achieve the desired structural changes. An example of the typical interface microstructure of the Ti/steel after explosive welding made in Z.T.W. EXPLOMET is shown in Fig. 1. In the experiment, these plates were then subjected to an annealing treatment by using different annealing process parameters. For some of them, an additional heat treatment was also performed to simulate the influence of the potential stress

relief annealing after welding of explosively plated materials. The influence of annealing in the presence of the atmospheric gases on the properties of the cladding material (titanium) was also investigated depending on the method of surface preparation for heat treatment, which is schematically shown in Fig. 2.

In addition, the microstructure and chemical composition changes of the explosively welded clads resulting from the diffusion processes occurring due to the various heat treatment were correlated with the results of mechanical properties obtained in bending and microhardness tests.
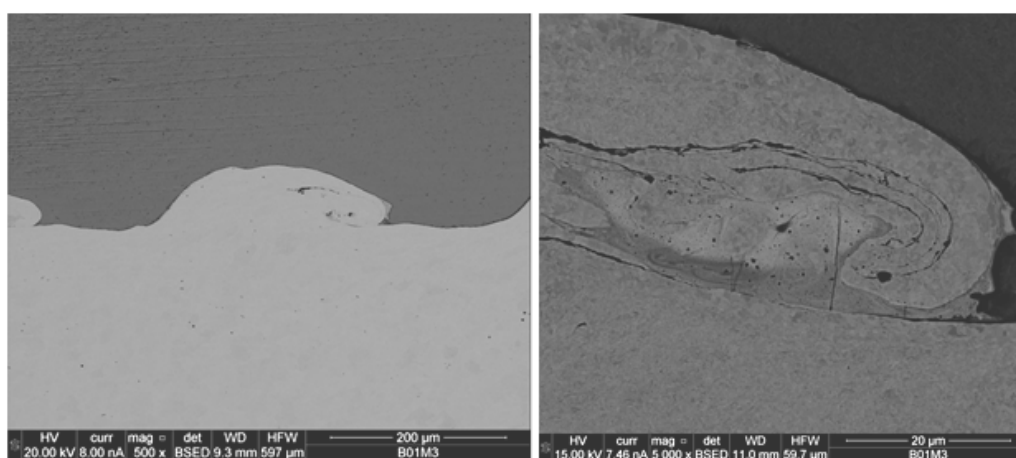
Fig. 1. The characteristic wavy interconnection between Ti and steel (left) and the enlarged view of the melted area inside of the wave.
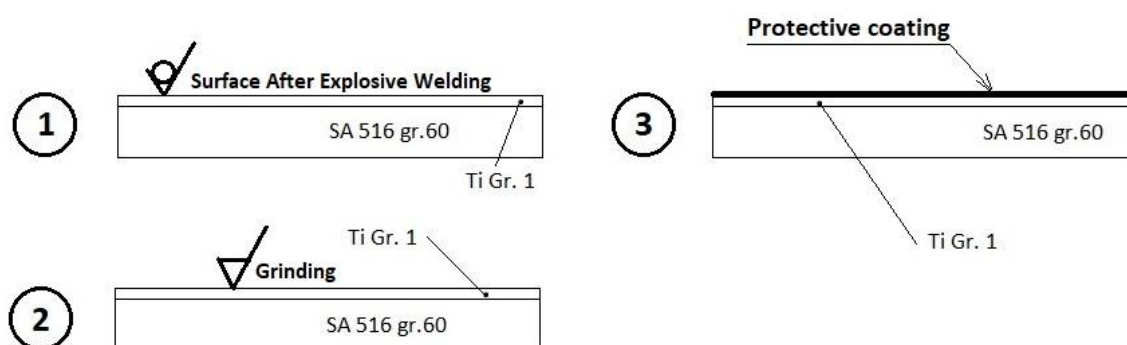
Fig. 2. Variants of Ti surface preparation before the heat treatment: *1* surface in the state after explosive welding; *2* grinded surface; *3* surface with the protective coating.

Microstructure and chemical composition examination was performed in the Accredited Testing Laboratories at the Institute of Metallurgy and Materials Science of the Polish Academy of Sciences

1. H. Jiang, X. Yan, J. Liu, X. Duan, Effect of heat treatment on microstructure and mechanical property of Ti−steel explosive-rolling clad plate**,** *Trans. Nonferrous Met. Soc. China*, 2014, vol. 24, pp. 697−704.
2. T. N. Prasanthi, C. Sudha, Ravikirana, S. Saroja, Explosive cladding and post-weld heat treatment of mild steel and titanium, *Materials and Design*, 2016, vol. 93, pp. 180–193.
3. M. Wachowski, M. Gloc, T. Ślężak, T. Płociński, K. J. Kurzydłowski, The effect of heat treatment on the microstructure and properties of explosively welded titanium-steel plates, *JMEPEG*, 2017, vol. 26, pp. 945–954.

M. Szmul et al.

PROCESS OF TUNGSTEN WIRE EXPLOSION AND SYNTHESIS OF CARBIDE BY PULSED WIRE DISCHARGE

S. Tanaka[1], I. Bataev[2], H. Oda[3], and K. Hokamoto[4]

[1] Institute of Pulsed Power Science (IPPS), Kumamoto University, 2-39-1 Kurokami, Chuo-Ku, Kumamoto, 860-8555 Japan
[2] Novosibirsk State Technical University, K. Marks 20, Novosibirsk, 630073 Russia
[3] Graduate School of Science and Technology, Kumamoto University, 2-39-1 Kurokami, Chuo-Ku, Kumamoto, 860-8555 Japan

e-mail: tanaka@mech.kumamoto-u.ac.jp

WC is widely used for manufacturing cutting tools, metal forming tools, mining tools, and wear resistant surfaces with a wide range of applications. There are a number of processes for the synthesis of WC powders including direct carburization of tungsten powder, solid-state metathesis, reduction-carburization, mechanical milling and polymeric precursor routes using metallic alkoxide; each process produces powders with different characteristics [1–4]. The main drawbacks to these methods are high production costs and long processing times. Jiang and Yatsui [5] have demonstrated that it is possible to produce nanometer-sized particles in a cost-effective way by using wire explosion process. Hokamoto and co-workers [6] successfully synthesized nanometer-sized TiN powder using wire explosion process under relatively high energy at 10 kJ. Liquid nitrogen was used to react with the exploded titanium wire by the same wire explosion process. The present paper investigates the possibility of synthesizing tungsten carbide through electric wire explosion of tungsten under a stored energy of 10 kJ in liquid paraffin. Paraffin is known to be harmless for human body and the use of paraffin as a carbon source has never been investigated before because the atomic ratio of carbon is relatively lower than other hydrocarbons.

The experiments were performed in a steel container as illustrated in Fig. 1. The tungsten wire used for this experiment was provided by Niraco Co., Ltd. (99.5 mass % tungsten). The liquid paraffin was provided by Nakarai Tesque Co., Ltd. (0.86–0.88 g/ml). A high-capacity oil condenser capable of storing energy up to 10 kJ (12.5 μF, 40 kV) made by Nichicon Corporation and equipped at Institute of Pulsed Power Science, Kumamoto University was employed for the experiments. The length and the diameter of the tungsten wire were 180 mm and 0.5 mm, respectively.
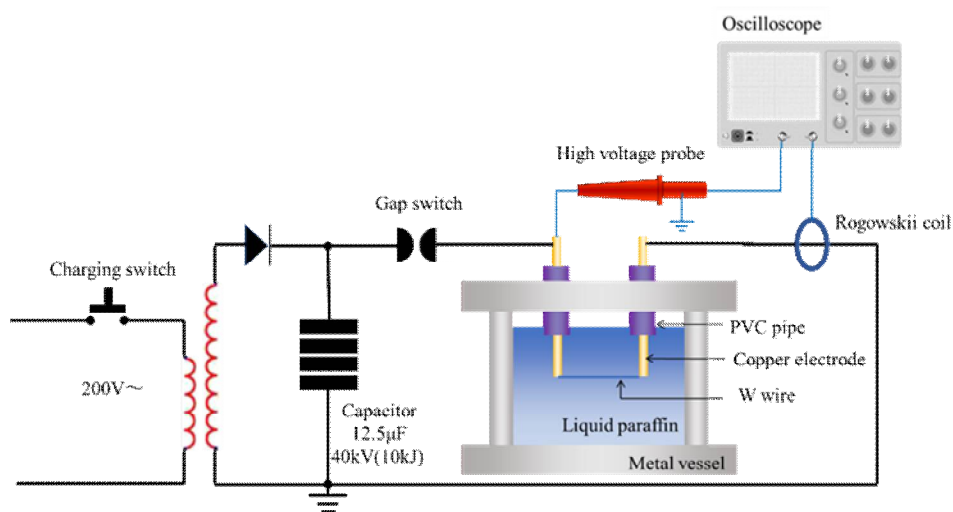
Fig. 1. Schematic illustration of assembly used for wire explosion.

A small amount of powder was recovered from container and it was processed by diethyl ether dissolution treatment, and then, dried at room temperature. X-ray Diffraction (XRD) pattern of the powders reflected the peaks of cubic meta-stable tungsten carbide and small amount of tungsten, which is shown in Fig. 2. It is worth to note that γ-WC_{1-x} is a superconducting material [7] with a cubic crystal structure, which is synthesized through quenching of molten condition.
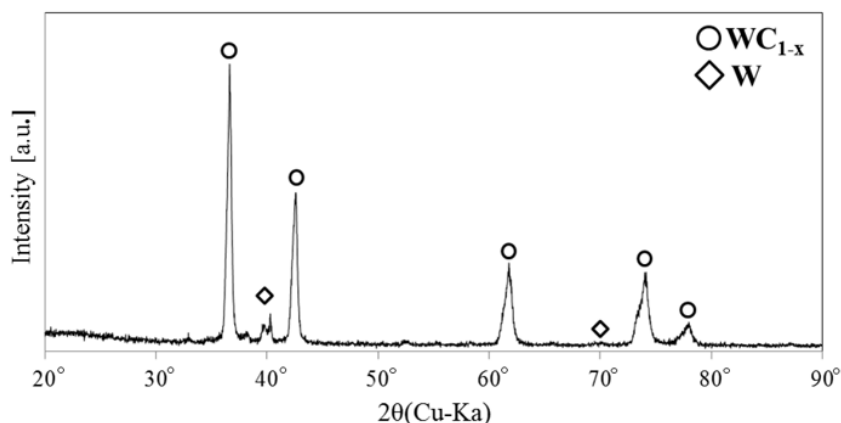
Fig. 2. X-ray diffraction pattern for recovered powder.

The quantity of carbon in the WC_{1-x} can be estimated using the following equation [7]:

$$a(y) = 0.4015 + 0.0481y - 0.0236y^2$$

where $a(y)$ is the lattice constant, y is the carbon quantity equal to $(1-x)$. Based on average values of the main five peaks, the lattice constant was 0.4242 nm and the carbon quantity (y) was 0.734.

The Williamson–Hall plot by the X-ray peaks is shown in Fig. 3. The plot is drawn using the following equation [8]:

$$\beta \frac{\cos\theta}{\lambda} = 2\eta \frac{\sin\theta}{\lambda} + \frac{1}{\varepsilon}$$

where β is the half height width of the peaks, λ is the wavelength of the X-ray, ε is crystalline size and η is crystalline strain. All five plots are almost on the straight line.
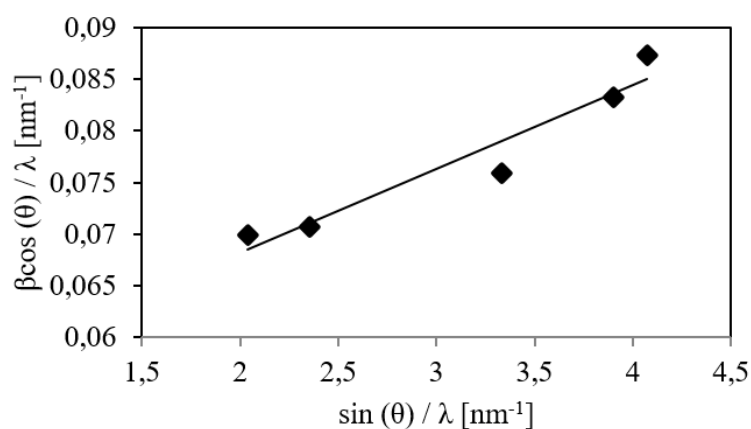
Fig. 3. Williamson–Hall plot of recovered γ-WC_{1-x} powder.

The calculated crystalline size and the strain for the recovered WC_{1-x} particle were 19.3 nm and 0.405%, respectively. As a result, the WC_{1-x} particle obtained by this process was greatly-strained as suggested for explosively consolidated diamond powders [9].

1. F. H. Ribeiro, R. A. D. Betta, G. J. Guskey, M. Boudart, Preparation and surface composition of tungsten carbide powders with high specific surface area, *Chem. Mater.*, 1991, 3, pp. 805–812.
2. R. Koc, S. K. Kodambaka, Tungsten carbide (WC) synthesis from novel precursors, *J. Eur. Ceram.*, 2000, vol. 20, pp. 1859–1869.
3. R. Koc, S. K. Kodambaka, New process for producing submicron tungsten monocarbide powders, *J. Mater. Sci. Lett.*, 1999, vol. 18, pp. 1469–1471.
4. F. F. P. Medeiros, S. A. D. Oliveira, C. P. D. Souza, A. G. P. D. Silva, U. U. Gomes, J. F. D. Souza, Synthesis of tungsten carbide through gas-solid reaction at low temperatures, *Mater. Sci. Eng. A*, 2001, 315, pp. 58–62.
5. W. Jiang, K. Yatsui, Pulsed wire discharge for nanosize powder synthesis, *IEEE Trans. Plasma Sci.*, 1998, vol. 26, 5, pp. 1498–1501.
6. K. Hokamoto, N. Wada, R. Tomoshige, S. Kai, Y. Ujimotod, Synthesis of TiN powders through electrical wire explosion in liquid nitrogen, *J. Alloy. Compd.*, 2009, vol. 485, pp. 573–576.
7. A. S. Kurlov, A. I. Gusev, Phase equilibria in the W–C system and tungsten carbides, *Russ. Chem. Rev.*, 2006, vol. 75, no. 7, pp 617–636.
8. G. K. Williamson, and W. H. Hall, X-ray line broadening from filed aluminium and wolfram, *Acta Metall.*, 1953, vol. 1, 1, pp. 22–31.
9. K. Hokamoto, R. A. Pruemmer, R. Knitter, K. Taira, Hot explosive compaction of diamond powder using cylindrical geometry, *J. Mater. Sci.*, 2008, vol. 43, no. 2, pp. 684–688.

PICOSECOND-EXPOSURE DYNAMIC MEASUREMENTS OF FORMATION OF ULTRA-DISPERSED DIAMONDS IN DETONATION WAVES

K. A. Ten[1], E. R. Pruuel[1], A. O. Kashkarov[1], I. A. Rubzov[1], L. I. Shekhtman[2], V. V. Zhulanov[2], and B. P. Tolochko[3]

[1] Lavrent'ev Institute of Hydrodynamics, Siberian Branch, Russian Academy of Sciences, Novosibirsk, 63009 Russia
[2] Budker Institute of Nuclear Physics, Siberian Branch, Russian Academy of Sciences, Novosibirsk, 630090 Russia
[3] Institute of Solid State Chemistry and Mechanochemistry, Siberian Branch, Russian Academy of Sciences, Novosibirsk, 630128 Russia

e-mail: ten@hydro.nsc.ru

Detonation processes in condensed high explosives (HEs) last less than 1 µs, and thus, their investigation necessitates dynamic methods with nanosecond exposures. This is particularly true for the processes of carbon condensation upon detonation of oxygen-deficient explosives. Such activity began at Lavrent'ev Institute of Hydrodynamics in 1983 in connection with works on the synthesis of detonation nanodiamonds. These works were continued at many scientific centers, and to date there are more than 800 works devoted to this topic in the world [1]. The weight of investigated explosive charges was varied from 200 g to hundreds of kilograms, and their diameter was 40 mm and more. The object of investigation was mainly the retained detonation products (soot) collected in the explosion chamber after explosion. At that time, it was impossible to study experimentally the kinetics (dynamics) of the carbon condensation process. Therefore, the place and time of condensation were considered to coincide with the chemical reaction zone, since the parameters of the medium there corresponded to the stable phase of the diamond state. In the early 2000s, a new method for studying fast processes on high-energy accelerators was begun to develop. The high intensity of synchrotron radiation (SR) enabled recording the

dynamics of the diffraction scattering distribution with an exposure of 1 ns [2]. The intensity of small-angle X-ray scattering (SAXS) is proportional to the fluctuations in the electron density, which depends on the carbon condensation upon detonation of oxygen-deficient explosives. Model calculations show that measured SAXS distributions can provide the data on the sizes of carbon nanoparticles, which are condensed in the chemical reaction zone and beyond [3]. In 2016, a new installation SYRAFEEMA (Synchrotron Radiation Facility for Exploring Energetic Materials) based on VEPP-4 was commissioned at BINP [4]. The VEPP-4 collider has an energy of 4.7 GeV and a pulse length of 100 ps. The SAXS measurement method applied at this installation enables recording the dynamics of nanoparticles with a size from 4 to 200 nm with picosecond exposure.

In this paper, we present results of SYRAFEEMA experiments on the dynamics of carbon condensation in TNT–HMX mixtures (Fig.1), new TATB-based formulations, and a hydrogen-free HE of benzotrifuroxane (BTF). The geometric dimensions of all HE charges investigated in these experiments were the same, as well as the geometric dimensions of all experimental assemblies. That was to ensure identical expansion of the detonation products. Another feature of these experiments is the small size of all HE charges (diameter of 20 mm, length of 30 mm, and weight of ~ 20 g). In the literature, however, there are data only for large charges [1]. For the sake of comparison, the same HEs of the same sizes were exploded in the explosion chamber in an ice shell; the explosion products were retained and then subjected to analysis by microscopic and diffraction methods.

1. V. V. Danilenko, *Synthesizing and sintering of diamond by explosion,* Moscow: Energoatomizdat, 2003, 272 p.
2. V. M. Titov, E. R. Pruuel, K. A. Ten, Experience of using synchrotron radiation for studying detonation processes, *Combust. Explos. Shock Waves*, 2011, vol. 47, no. 6, pp. 3–15.
3. E. R. Pruuel, K. A. Ten, B. P. Tolochko, Implementation of the capability of synchrotron radiation in a study of detonation processes, *Dokl. Phys.*, 2013, vol. 58, no. 1, pp. 24–28.
4. B. P. Tolochko, A. V. Kosov, K. A. Ten, The synchrotron radiation beamline 8-b at VEPP-4 collider for SAXS, WAXS and micro tomography investigation of fast processes at extreme condition of high temperature and pressure with nanosecond time resolution, *Physics Procedia,* 2016, vol. 84, pp. 427–433.

K. A. Ten et al.

FUNCTIONAL PROPERTIES OF SINTERED POWDER Fe–Cr–Co ALLOY OBTAINED BY LOW-TEMPERATURE SINTERING WITH SUBSEQUENT HOT ROLLING

A. S. Ustyukhin[1], A. B. Ankudinov[1], V. A. Zelenskii[1], and I. M. Milyaev[1]

[1] Baikov Institute of Metallurgy and Materials Science, Russian Academy of Sciences, Moscow, 119991 Russia

e-mail: fcbneo@yandex.ru

In conventional production of magnetic alloys in the Fe–Cr–Co system by powder metallurgy methods, the sintering temperature of compacts is high (about 1400°C) [1–3]. The high sintering temperature requires high power consumption. At these conditions, the components of the initial mixture (especially Cr) partially evaporate from the surface of the compacts, the overall chemical composition changes, and the bulk of the material becomes chemically heterogeneous [4]. This process may impair properties, especially in small samples, where the bulk of the material is contained in surface layers.

In present work, we showed that addition of a hot rolling stage after the sintering stage allows one to reduce the sintering temperature to 1200°C. The process was carried out at temperatures of 1100 and 1200°C. Because of the reduced sintering temperature, the density of the sintered material was insufficient and was increased by subsequent hot rolling at 1150°C. As a result, the relative density of the samples was raised to 97–98%, which is comparable to the densities of alloys with the same compositions that were sintered at temperatures above 1300°C.

Table 1 presents the results of measuring the magnetic hysteresis properties of the studied alloy samples both immediately after sintering without hot rolling and after subsequent hot rolling. It is seen that the magnetic properties of all the samples sintered at 1100°C are

low, whether they were rolled or not. Note that the rolling of these samples almost inclusively impaired their magnetic characteristics; only the density of the material increased. The magnetic properties of the samples sintered at 1200°C are suitable for technical applications. The rolling improved the remanence B_r while retaining the same coercivity H_c, with the density of the material increasing significantly.

Table 1. Density and magnetic properties of sintered and rolled samples.

Sintering temperature,°C	Hot rolling	Relative density, %	B_r, T	H_{cB}, kA/m	$(BH)_{max}$, kJ/m³
1100	Without rolling	85–87	0.79–0.83	40–44	11–14
	With rolling	97–98	0.47–0.58	40–41	8.8–10.8
1200	Without rolling	89–91	1.04–1.06	51–53.5	27.6–28.7
	With rolling	97–98	1.19–1.21	51–52	29.6–31.3

The X-ray powder diffraction analysis of the samples detected the presence of the γ-phase in the rolled samples sintered at 1100°C for 150 min (Fig. 1). Most probably, under these conditions, there is not enough time for redistribution of components, and even after quenching to a single-phase α-solid solution, a significant part of the nonmagnetic γ-phase remains in the alloy. The undesirable presence of the γ-phase influences the further thermomagnetic treatment and leads to a considerable decrease in the magnetic hysteresis properties of the alloy.

The tensile strength tests of the rolled sintered material demonstrated a substantial effect of the sintering temperature on the strength of the samples. The tensile strength of the samples sintered at 1100°C (700–930 MPa) exceeded that of the samples sintered at 1200°C (520–590 MPa). The decrease in the strength of the samples sintered at 1200°C is likely to be explained by the structure of the material, in which grain growth is observed at this temperature.
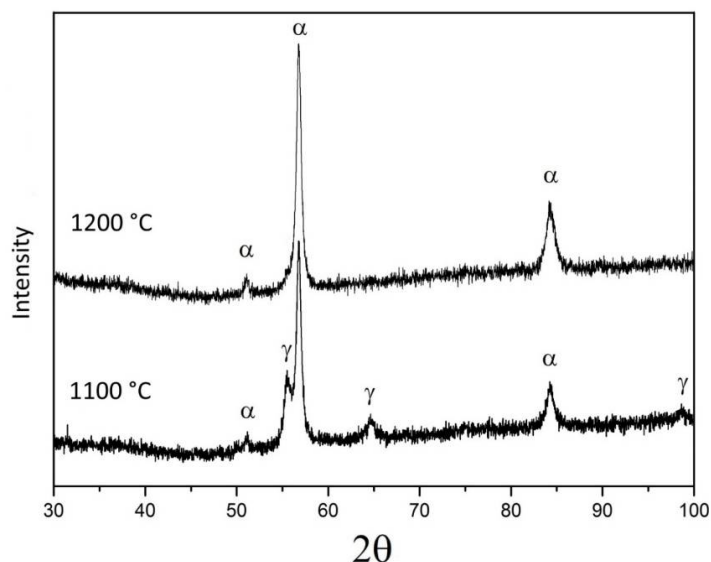
Fig. 1. X-ray powder diffraction patterns of rolled samples of an alloy of composition Fe–26% Cr–16% Co–2% Mo–2% W.

1. M. L. Green, R. C. Sherwood, C. C. Wong, Powder metallurgy processing of CrCoFe permanent magnet alloys containing 5–25 wt. % Co, *J. Appl. Phys*., 1982, vol. 53, no. 3, pp. 2398–2400.
2. A. A. Shatsov, Powder Materials of the Fe–Cr–Co System, *Met. Sci. Heat Treat*., 2004, vol. 46, pp. 152–155.
3. M. I. Alymov, A. B. Ankudinov, V. A. Zelenskii, I. M. Milyaev, V. S. Yusupov, A. S. Ustyukhin, Effect of alloying and sintering regime on magnetic hysteresis properties of Fe–Cr–Co powder alloy, *Fiz. Khim. Obrab. Mater*., 2011, no. 3, pp. 34–38.
4. S. Schiller, U. Heisig, S. Panzer, *Electron Beam Technology*, New York: Wiley, 1982.

MANUFACTURING AND TESTING OF BIMETALLIC BLANKS FOR ITER PF1 COIL JOINTS

V. S. Vakin[1] and E. L. Marushin[2]

[1] AO ENERGOMETALL, Saint Petersburg, 195220 Russia
[2] Efremov Institute of Electrophysical Apparatus (NIIEFA), Metallostroy, Saint Petersburg, 196641 Russia

e-mail: egor.marushin@mail.ru

The PF1 coil [1] is incorporated into one of four main subsystems of the ITER electromagnetic system (EMS) and is made as a complex unit consisting of eight pancakes interconnected by joints. The joints consist of two halves – termination boxes, which are bimetal (stainless steel (SS)–copper) structural components produced by explosive welding. The joints shall ensure the high mechanical, hydraulic and electrical performance in the range of PF1 operating temperatures and the applied magnetic fields. The initial design of the termination box was updated on the basis of deviation requests of the ITER Organization (IO). As a result, the previously developed techniques [2] for bimetallic blanks manufacturing were updated and qualified.

The main design modifications (Fig. 1) were changing of the radius profile of 200 mm to 500 mm, changing of the material used and changing of acceptance criteria. To meet the AC losses criterion, the material grade of the termination box copper sole was changed from OFE copper to Cu-DHP with RRR = 6 [3]. Reducing the copper RRR decreases its temperature from 9 K to 7.4 K after 1 s of 0.4 T/s field variation under a scenario for coil operation during 15 MA plasma pulse. The acceptance criteria were changed as regards the ultrasonic technique (UT), penetrant tests (PT) and mechanical tests, in order to guarantee the defect free interface and high quality connection.
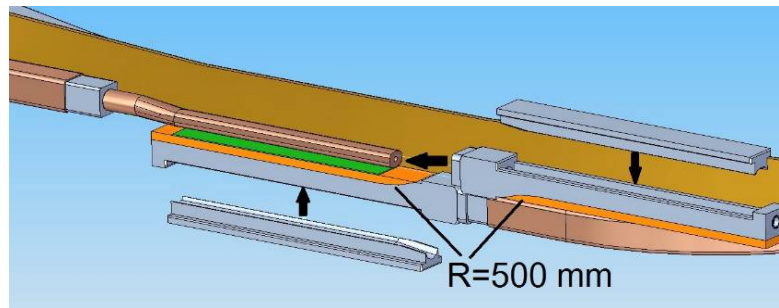
Fig. 1. Joint and termination box designs

Preliminary calculations performed with the help of the ANSIS software package [2] made it possible to determine the dynamic properties of the welding package during the bonding process and correct the technological process. Later, additional process adjustments were made, which made it possible to guarantee the vacuum tightness of the product under critical temperature conditions.

To qualify the updated procedure, two plates ((90 of SS + 18 of Cu) * 450 * 450 mm) were explosion welded. The manufactured plates were ultrasonically tested with Ø1.6 mm flat bottom hole calibration to detect the bond zone. The obtained results demonstrated that the used technological parameters provided the bonded area, sufficient for the future tests and obtaining the finished product. The height of the wave is less than 1 mm, which is convenient for using UT calibration up to Ø1.2 mm.

Four specimens were taken along each side of the acceptable area of the plate and examined under a metallurgical microscope with up to x500 magnification. The result showed the absence of entrapped oxides, pores, and intermetallic compounds at the interface (Fig. 2).

Fig. 2. The bimetallic interface

Three samples were taken for tensile test from three areas of the plate. Prior to test, the samples were subjected to three thermal cycles from 293 K to 77 K. The samples were machined and destructive tensile tested at room temperature. The obtained tensile results met the

acceptance criterion to be more than 255 MPa (Fig. 3). In addition, two kinds of specimens were taken: one perpendicular and one parallel to wave front. Prior to test, the samples were subjected to three thermal cycles from 293 K to 77 K. The samples were machined and tested according to ASTM B432 at room temperature. The obtained tensile results met the acceptance criterion to be more than 140 MPa. The shear test results of samples were similar for both transverse and longitudinal directions. This fact demonstrates the mechanical strength of the bimetallic interface.

After the successfully passed test, the plate was bent to the required radius. The radius control was done by the calibration template. The finished blank was trimmed by a saw to the required width of 66 mm (Fig. 3). Then PT was performed on 100% of the lateral surfaces (including the bonding interface on them) of each blank according to ISO 3452–1. Any indications are not allowed. The results demonstrated the high quality of bimetallic interface (Fig. 4).
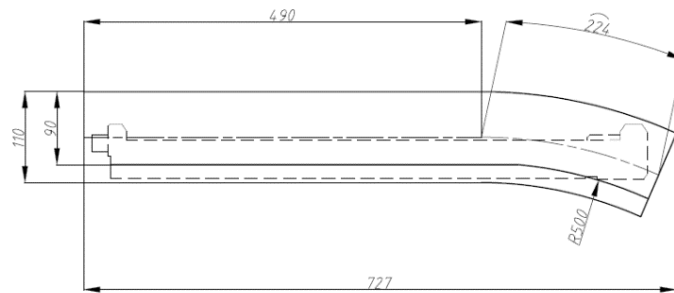
Fig. 3. The dotted line shows the final manufactured termination box.

Fig. 4. The bimetallic blank tested by PT.

The updated technology and parameters of explosive welding were qualified on the basis of the obtained successful test results. The required QA documentation was issued and approved by IO, which was necessary to start manufacturing of the whole amount of the bimetallic blanks for termination boxes of the PF1 coil.

1. B. Lim, F. Simon, Y. Ilyin, C. Y. Gung, J. Smith, Y. H. Hsu, C. Luongo, C. Jong, N. Mitchell, Design of the ITER PF coils, *IEEE Trans. Appl. Supercond.*, 2010, vol. 21, no. 3, pp. 1918–1921.

2. V. Vakin, A. Krasilnikov, Y. Marushin, Calculation and cladding of the profiled surface of the superconducting coil PF1 ITER contacts, *Arch. Metal. Mater.,* 2014, vol. 59, iss. 4., pp. 1579–1585.

3. Yu. Ilyin, G. Rolando, B. Turck, A. Nijhuis, F. Simon, B. Lim, N. Mitchell, Analysis of ITER PF coil joint design under reference operating scenario, *IEEE Trans. Appl. Supercond.*, 2016, vol. 26, no. 4, 4201305.

INFLUENCE OF STRAIN RATE ON THE RATE OF CHEMICAL TRANSFORMATION WITHIN A SHOCK WAVE

V. A. Veretennikov and V. S. Trofimov

Merzhanov Institute of Structural Macrokinetics and Materials Science, Russian Academy of Sciences, Chernogolovka, Moscow, 142432 Russia

e-mail: veret@ism.ac.ru

Available experimental results on shock-induced detonation in cast and pressed TNT [1] were analyzed with special emphasis on the observed marked difference in the processes of the evolution of initiating shock into an ideal wave of self-sustained detonation propagating over the charge.

In this work, we demonstrated that the strain rate of medium can affect the rate of chemical transformation within a shock wave to an extent exceeding that of temperature. This circumstance should be taken into account in modeling the processes of detonation initiation.

1. A. Dremin, S. Koldunov, Shock initiation of detonation in cast and compacted TNT, in *Vzryvnoe delo* (Explosive Business), Moscow: Nedra, 1967, no. 63/20, pp. 37–50.

MICROWAVE ABSORPTION PROPERTIES OF THE CARBON-ENCAPSULATED IRON-BASED NANOPARTICLES

H. Yin[1], Q. Du[1], P. Chen[2], and M. Cao[3]

[1] Institute of Systems Engineering, China Academy of Engineering Physics, Mianyang 612900, Sichuan Province, China
[2] State Key Laboratory of Explosion Science and Technology, Beijing Institute of Technology, Beijing 100081, China
[3] School of Material Science and Engineering, Beijing Institute of Technology, Beijing 100081, China

e-mail 412yinh@caep.cn

Carbon-encapsulated iron-based nanoparticles were produced by detonation of mixtures of high explosive and iron tristearate in a vacuum chamber. The mass ratio of high explosive to iron tristearate, leading to different detonation pressures and temperatures, has played an important role in the formation of carbon encapsulated nanoparticles. With the increase of the mass ratio, the number of the graphitic coating layers and the size of carbon encapsulated nanoparticles decreases. The number of the coating layers and the size of nanopartices are two important factors affecting the dielectric permittivity and reflection loss of as-synthesized samples.Carbon-encapsulated iron-based nanoparticles exhibit strong EM-wave absorption properties ($R < -10$ dB) in the 3.2–18 GHz range and a minimum reflection loss (-43.5 dB) at 9.6 GHz with a 3.1mm thick layer.

SHS METALLURGY OF REFRACTORY MATERIALS BASED ON MOLYBDENUM

V. I. Yukhvid, V. A. Gorshkov, V. N. Sanin, D. E. Andreev, and Yu. S. Vdovin

Merzhanov Institute of Structural Macrokinetics and Materials Science, Russian Academy of Sciences, Chernogolovka, Moscow, 142432 Russia

e-mail: yukh@ism.ac.ru

Mo is refractory metal and has a melting point of 2900 K. Compounds of Mo with C, B and Si have unique properties and are widely used in engineering for manufacturing hard alloys, heat-resistant composite materials, high-temperature heaters, etc. [1]. Machine parts of Mo-based materials are most often made by powder metallurgy methods [2]. In this report, the authors considered the possibilities of SHS metallurgy for the production of carbides, borides, silicides of molybdenum, as well as composite materials based on them.

High-exothermic mixtures of molybdenum oxides with metal reducers (Al and Mg) and nonmetals (C, B and Si) were used to synthesize compounds. To prepare multicomponent materials, other metals and non-metals or their oxides were additionally introduced into the base mixtures. Such mixtures are capable of burning. The final products of their combustion are molybdenum, its compounds or composite materials. The combustion temperature of mixtures can exceed 3500–4000°C [3]. High temperature allows to obtain carbides, borides, silicides of molybdenum and composite materials based on molybdenum in cast form. The high temperature of combustion leads to gas formation. The release of gas from the melt during combustion leads to its sputtering, therefore, the processes of SHS metallurgy are carried out under gas pressure (in reactors) or under centrifugal action [4].

SHS metallurgy of molybdenum carbides. Cast molybdenum carbide obtained from a stoichiometric mixture of MoO_3 with soot and Al has a carbon deficit and contains up to 5–10% by weight aluminum

as an impurity. Note that Al_2Mo_3C impurity is localized at the boundaries of granules of molybdenum carbide.

Deficit of aluminum and excess carbon in the initial mixture, replace of part of soot with graphite granules and part of Al in the mixture with an equivalent amount of Mg leads to a decrease in the Al concentration in cast molybdenum carbide. It is possible to change the carbon content in the ingot from 1 to 7 wt % (Fig. 1) and to obtain cast Mo_2C and Mo_3C_2 by varying the content of graphite in the initial mixture containing Al and Mg as reducing agents.
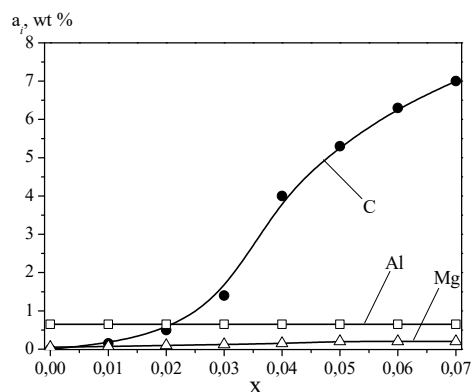
Fig. 1. Influence of the carbon content in the initial mixture (x) on the composition of molybdenum carbide (a_i). Initial mixture: MoO_3/Al/Mg/C. $x = m(C)/[(m(C) + m(MoO_3)) + m(Al) + m(Mg)]$, $m = 100$ g, $P = 5$ MPa.

SHS metallurgy of molybdenum borides. The most "pure" borides can be obtained from two-component systems $MeO_x + B$, where B is a reducing agent and a boride forming element. The loss of B during synthesis of molybdenum borides from the mixture $MoO_3 + Al + B$ is small, therefore, stoichiometric mixtures can be used to obtain MoB, MoB_2, and Mo_2B_5. A noticeable amount of Al appears in the cast boride when B is replaced by B_2O_3 (Table 1).

Table 1. Initial mixtures and composition of cast molybdenum borides.

	Initial mixtures	Chemical composition of boride, wt %			Phase composition of boride
		Mo	B	Al	
1	MoO_3/Al/B=0.63:0.23:0.14	rest	18.6	0.5	MoB_2
2	MoO_3/Al/B_2O_3=0.63:0.23:0.14	rest	15.4	3.2	MoB_2, MoB, MoAlB

SHS metallurgy of molybdenum silicides. Two chemical schemes were used to prepare molybdenum disilicide:

$$MoO_3 + 2Al + 2Si \rightarrow Al_2O_3 + MoSi_2 \quad (1)$$
$$MoO_3 + 3.5Si \rightarrow 1.5SiO_2 + MoSi_2 \quad (2)$$
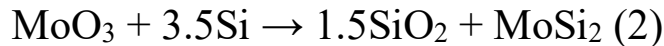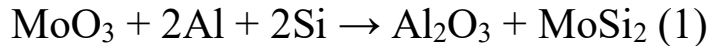
The experiments showed that the combustion of the $MoO_3 + 2Al + 2Si$ mixture is accompanied by complete sputtering of combustion products under an initial gas pressure in a reactor of 0.1 MPa. The increased pressure of nitrogen or argon in the reactor suppresses sputtering of the mixture, while the yield of molybdenum silicides in the ingot reaches the calculated value.

Combustion of the $MoO_3 + 3.5Si$ mixture is not possible despite the high calculated combustion temperature. However, combustion is realizing when a combination of mixtures *1* and *2* is used. It follows from the chemical analysis data that the chemical composition of the Mo–Si ingot change significantly with variation in the ratio of mixtures *1* and *2* (Fig. 2).
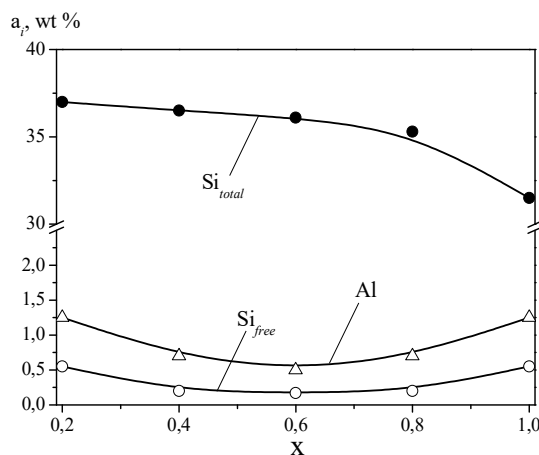
Fig. 2. Influence of the ratio of mixtures *1* and 2 (*x*) on the composition of cast molybdenum silicide (a_i). $x = m_1/(m_1 + m_2)$, a_i is the content of the element in the alloy. Mass of the mixture is 100 g, nitrogen pressure is 5 MPa.

It was shown in experiments on a centrifugal installation that overload suppresses the sputtering of the mixture (Fig. 3) and significantly changes the chemical composition of cast molybdenum silicides (Table 2).

SHS metallurgy of composite materials. The melting point of composite materials based on molybdenum silicides with doping additives (Nb, B, C, etc.) can exceed 1950°C. Operating temperature

of the composite is higher by 150°C than that of nickel superalloys and have a large potential for implementation in aircraft engines.

The report presents the results of studies on the synthesis of these materials by the centrifugal SHS metallurgy method.
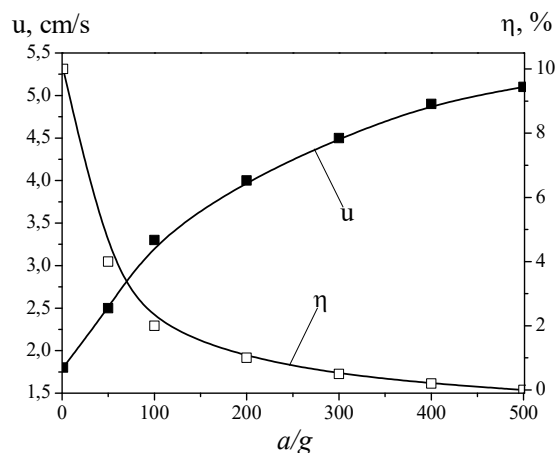
Fig. 3. Effect of overload (a/g) on the burning rate (u) of the mixture and the yield of molybdenum silicide in the ingot (η). Initial mixture: $MoO_3/Al/Mg/C$. $x = 0.06$, $m = 100$ g.

Table 2. Effect of overload on the chemical composition of cast Mo–Si. Initial mixture, $x = 0.06$, $m = 100$ g.

a/g	Mo	Si_{com}	Al	O
1	rest	28.2	3.6	0.2
100	rest	30.1	0.1	0.1

1. S. Drawin, J. F. Justin, Advanced lightweight silicide and nitride based materials for turbo-engine applications, *AerospaceLab*, 2011, p. 1–13.
2. .P. Jéhanno, M. Heilmaier, H. Kestler, M. Böning, A. Venskutonis, B. P. Bewlay, M. R. Jackson, Assessment of a powder metallurgical processing route for refractory metal silicide alloys, *Metall. Mater. Trans. A*, 2005, vol. 36, pp. 515–523.
3. I. S. Gordopolova, A. A. Chiriaev, V. I. Yukhvid, *Effect of Pressure on the Composition of Condensed and Gaseous Combustion Products in Metal Oxide–Aluminum–Carbon Systems*, Preprint ISMAN, 1990 (in Russian).
4. V. I. Yukhvid, High-temperature liquid-phase SHS-processes: new trends and missions, *Tsvet. Metall.*, 2006, no.5, pp. 62–78 (in Russian).

SYNTHESIS OF Ni–W NANOPOWDERS FROM OXIDE AND SALT PRECURSORS IN COMBUSTION MODE BY USING THERMO-KINETIC COUPLING APPROACH

M. K. Zakaryan[1,2], S. V. Aydinyan[3], and S. L. Kharatyan[1,2]

[1] Nalbandyan Institute of Chemical Physics NAS RA, P. Sevak 5/2, 0014, Yerevan, Armenia
[2] Yerevan State University, A. Manukyan 1, 0025, Yerevan, Armenia
[3] Department of Mechanical and Industrial Engineering, Tallinn University of Technology, Ehitajate tee, Tallinn, 19086, Estonia

e-mail: zakaryan526219@gmail.com

Interest in nickel–tungsten (Ni–W) alloys has expanded unusually rapidly in recent years due to their unique combination of tribological, magnetic, electrical and electro-erosion properties (e.g., high tensile strength and premium hardness, as well as superior abrasion resistance, good resistance to strong oxidizing acids, and high melting temperature) [1]. Ni–W alloys successfully compete even with ceramics and graphite by virtue of high thermo-resistance. Current and possible future applications of Ni–W alloys include barrier layers or capping layers in copper metallization for ultra-large-scale integration (ULSI) devices or micro-electromechanical systems (MEMS). They can be also applied in mold inserts, magnetic heads and relays, bearings, resistors, electrodes accelerating hydrogen evolution from alkaline solutions, environmentally safe substitute for hard chromium plating in the aerospace industry, etc [2]. Ni–W alloys are usually electroplated from aqueous solutions containing $NiSO_4 \cdot 6H_2O$ and $Na_2WO_4 \cdot 2H_2O$ as the electroactive species, and organic acids as complexing agents [1].

Here we report the preparation of Ni–W composite powder by energy-saving self-propagating high-temperature synthesis (SHS) or combustion synthesis (CS) method [3] by using reactions thermo-kinetic coupling approach [4]. Its essence consists in the coupling of

low exothermic reduction reaction (*Me*O + C) with a high caloric (*Me*O + Mg) one with possible change of reaction pathway. It will allow performing the processes in mild conditions which is important for preparing nanomaterials. Furthermore, using (Mg + C) combined reducer will allow to control the reaction temperature in a wide range at synthesis of Ni–W composite powders. Byproduct magnesia can be removed by acid treatment with hydrochloric acid ($\omega = 10\%$).

We have envisaged the synthesis of W–Ni composite powder from nikel tungstate to provide considerable advantages of excellent chemical homogeneity of the final product thanks to the presence of both metals in the same crystalline structure of nickel tungstate. Therefore, except of oxides mixture nickel tungstate was used as precursor too. Nickel tungstate was prepared by calcinations of NiO and WO_3 powders mixture in air at $850^{\circ}C$ for 6.5 h. First of all thermodynamic calculations were carried out to reveal the possibility of combustion in $NiO–WO_3–yMg–xC(I)$ and $NiWO_4–yMg–xC(II)$ systems and for determining optimal conditions for joint and complete reduction, aimed to obtain Ni–W alloy (Fig. 1). Based on the results of thermodynamic calculations magnesio-carbothermic co-reduction of nickel and tungsten oxides (I) and nickel tungstate (II) were performed with such amount of magnesium corresponding to low temperature area ($y = 1.7–1.8$ mol). To find out the effect of carbon amount on the behavior of combustion perameters (temperature and velocity) a series of experiments were performed with changing carbon amount. According to the results the growth of carbon amount leads to a decrease both the combustion temperature and velocity (Fig. 2).
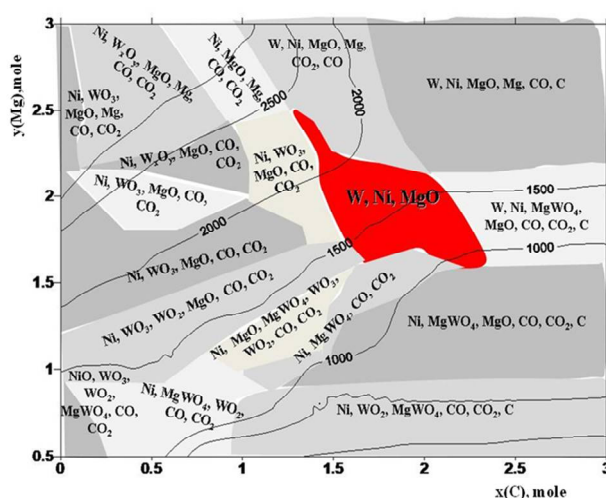
Fig. 1. Thermodynamic analysis results for the $NiO–WO_3–yMg–xC$ system, $P = 0.5$ MPa.
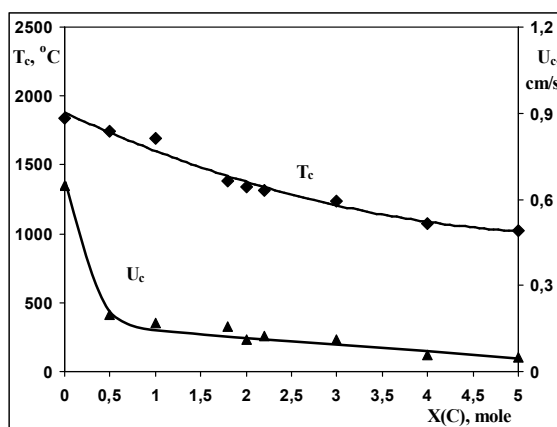
Fig. 2. Combustion temperature and velocity vs carbon amount for the NiO–WO$_3$–1.7Mg–xC system, P = 0.5 MPa.

According to XRD analysis results, the variation of carbon amount makes possible to reduce completely precursors (at x = 2.1–2.2) up to desired Ni and W metals. After acid treatment of completely reduced sample, byproduct magnesia was removed and the products contain only target metals (Fig. 3).
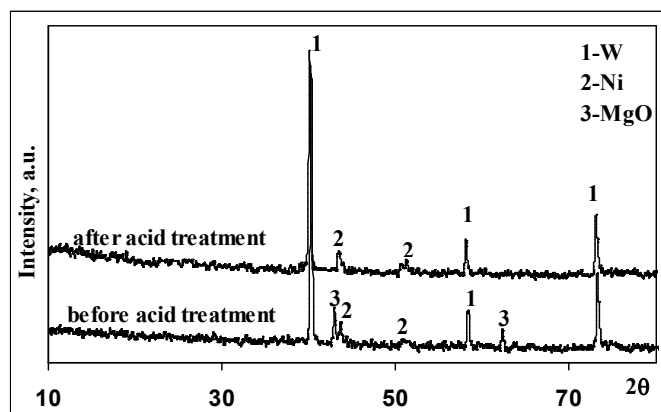
Fig. 3. XRD pattern of the combustion product of the NiO–WO$_3$–1.7Mg–2.2C mixture after acid treatment.

1. N. Eliaz, T. M. Sridhar, E. Gileadi, Synthesis and characterization of nickel tungsten alloys by electrodeposition, *Electrochim. Acta*, 2005, vol. 50, pp. 2893−2904.
2. O. Younes, E. Gileadi, Electroplating of Ni / W alloys, *J. Electrochem. Soc.*, 2002, vol. 149, no. 2, pp. 100−112.
3. S. T. Aruna, A. S. Mukasyan, Combustion synthesis and nanomaterials, *Curr. Opin. Solid State Mater. Sci.*, 2008, vol. 12, pp. 44–50.
4. S. L. Kharatyan, A. G. Merzhanov, Coupled SHS Reactions as a useful tool for synthesis of materials: An overview, *Int. J. Self-Propag. High-Temp. Synth.*, 2012, vol. 21, no. 1, pp. 59–73.

M. K. Zakaryan et al.

CHROMIUM LOSS DURING VACUUM SINTERING OF IRON-BASED ALLOYS

V. A. Zelenskii[1], M. I. Alymov[1,2], A. G. Gnedovets[1], and A. S. Ustyukhin[1]

[1] Baikov Institute of Metallurgy and Materials Science, Russian Academy of Sciences, Moscow, 119991 Russia
[2] Merzhanov Institute of Structural Macrokinetics and Materials Science, Russian Academy of Sciences, Chernogolovka, Moscow, 142432 Russia

e-mail: zelensky55@bk.ru

Vacuum sintering of stainless steels by powder metallurgy (PM) route caused the surfaces of sintered parts to be depleted of chromium because of the high vapor pressure of chromium at elevated temperature [1]. Vacuum sintering gives poor corrosion resistance because of chromium losses. Partial pressures of an inert gas were applied during sintering to eliminate chromium loss. The commercially available Fe-based alloys for solid oxide fuel cell (SOFC) interconnects are best characterized as ferritic stainless steel alloyed with a Cr content greater than 20 wt.% to form a protective Cr-rich oxide layer and, thereby, secure high temperature oxidation resistance [2]. At producing Fe-based alloys for solid oxide fuel cell (SOFC) interconnects Cr can partially evaporate from the surface of the SOFC, the overall chemical composition changes, and the bulk of the material becomes chemically heterogeneous. It was also found that chromium evaporation from the specimen surface occurs during sintering of hard magnetic Fe–Cr–Co alloys, which results in mass losses and nonuniform chemical composition and has a negative impact on the magnetic properties of the sintered material [3].

This work is aimed at studying the effect of sintering conditions on the chromium distribution in the near-surface layer of a Fe–22Cr alloy. Green compacts of the Fe–22Cr composition with a diameter of

13 mm and a height of 20 mm were produced from industrially used high-purity metal powders of iron and chromium with particle sizes < 70 μm. They were blended in an S2.0 turbulent mixer and compacted using a manual press in a composite die with an inner diameter of 13.6 mm under a pressure of 600 MPa. Sintering was carried out in a SSHV-1.255/24-I1 shaft furnace under a vacuum of ~ 10^{-3}–10^{-2} Pa for 2.5 h at temperatures 1300 and 1400°C. In comparison one sample additionally was covered with a crucible with a diameter of 15 mm and a height of 30 mm (Fig. 1)

As seen in Fig. 1, the samples differ markedly in shape under different sintering conditions at the same temperature. The weights of samples are also different: 19.81 g for sample sintered under crucible and 8.54 g without a crucible.

The decrease in the chromium concentration at the surface and in the near-surface layer of the sample during vacuum sintering is associated with evaporation and diffusion of the alloy components. The changes in the chromium concentration in the sample during sintering are governed by two factors: supply of Cr atoms to the surface via diffusion and evaporation of the metal atoms from the surface.

In a vacuum, free evaporation of chromium atoms from the surface occurs. As a result of measurements, mass losses from the surface during sintering at 1400°C was 0.4 kg/m². The use of a crucible leads to changes in evaporation mechanism. When sintered, an atmosphere of saturated chromium vapor is created under the crucible and the reverse flow of chromium atoms compensates their evaporation from the surface.
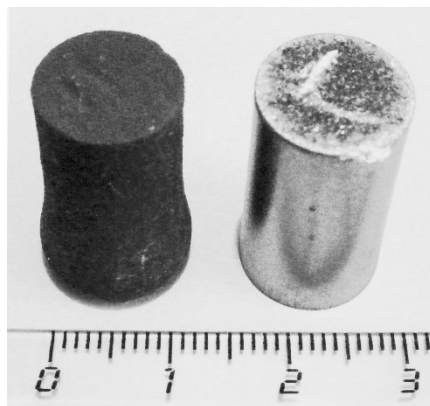
Fig. 1. Cylindrical Fe–22Cr samples sintered in vacuum at 1400°C without a crucible (left) and under a crucible (right).

1. E. Klar, P. K. Samal, *Powder Metallurgy Stainless Steels: Processing, Microstructures, and Properties*, ASM international, 2007.
2. B. K. Kim, D. Kim, K.-W. Yi, *Corrosion Science*, 2018, vol. 130, pp. 45–55.
3. A. S. Ustyukhin, M. I. Alymov, P. M. Krishenik, Y. V. Levinsky, A. S. Rogachev, Chromium concentration profiles in vacuum-sintered Fe–Cr–Co alloys, *Inorg. Mater. Appl. Res.*, 2017, vol. 8, no. 3, pp. 464–468.

MICROSTRUCTURE AND DYNAMIC BEHAVIOR OF EXPLOSIVELY CONSOLIDATED Ni–Al COMPOSITES

Q. Zhou, P. W. Chen, Z. M. Sheng, and Y. Y. Li

State Key Laboratory of Explosion Science and Technology, Beijing Institute of Technology, Beijing, 100081 China

e-mail: zqpcgm@gmail.com

Energetic structural materials (ESMs) constitute a new class of materials that provide dual functions of strength and energetic characteristics [1]. The reactive precursor powders must be processed and combined in some way so as to provide structural integrity, while not compromising on the chemical reactivity under dynamic loading [2].

In this work, the Ni–Al reactive mixture with an equivolumetric ratio was explosively consolidated to obtain near full-density compacts, as shown in Fig. 1. The as-produced samples went through heat treatment (HT) to achieve higher ductility. The mechanical response and failure mechanisms of Ni/Al before and after HT were studied using a split Hopkinson bar combined with high-speed digital photograph. The Ni/Al composite before HT fractured into pieces with a yield strength of ~ 350 MPa at 2500 s^{-1}, showing obvious brittleness. The HT-Ni/Al composite maintained integrity with a lower yield strength of 320 MPa at 2500 s^{-1}, and showed apparent strain hardening during yield stage, as shown in Fig. 2. It indicates the Ni–Al bonding was enhanced through heat treatment. For the Ni/Al composite fabricated in this work, both phases (Ni and Al phase) are continuous, as shown in Fig.3. Two distinct failure mechanisms, axial splitting and shear failure, were observed for the samples before and after HT, respectively. It was found that the failure mode was determined by the bonding strength, which was not consistent with the results of Wei [3]. When the bonding is strong, it shows shear failure, otherwise, axial splitting. The DSC and XRD analysis were also

conducted, showing no intermetallic was formed during the heat treatment and the chemical reactivity was not affected by the heat treatment, as shown in Fig. 4.

Fig. 1. (a) As recovered compacted containers with reduced diameter and (b) the specimen machined out from container.
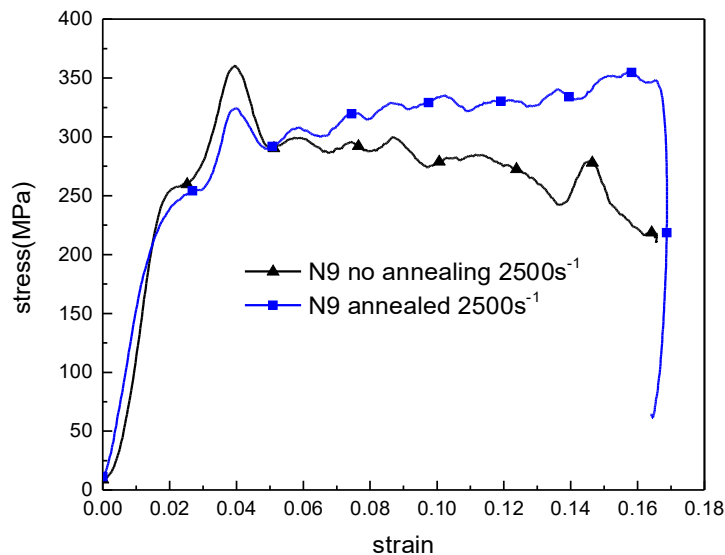
Fig. 2. Split Hopkinson pressure bar test (strain rates ≈ 2500 s^{-1}).
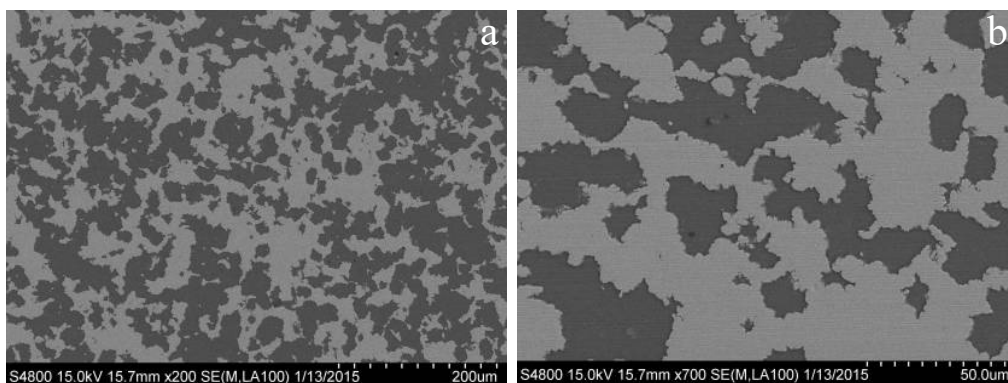
Fig. 3. (a) The SEM images of Ni–Al composites; and (b) magnified view.
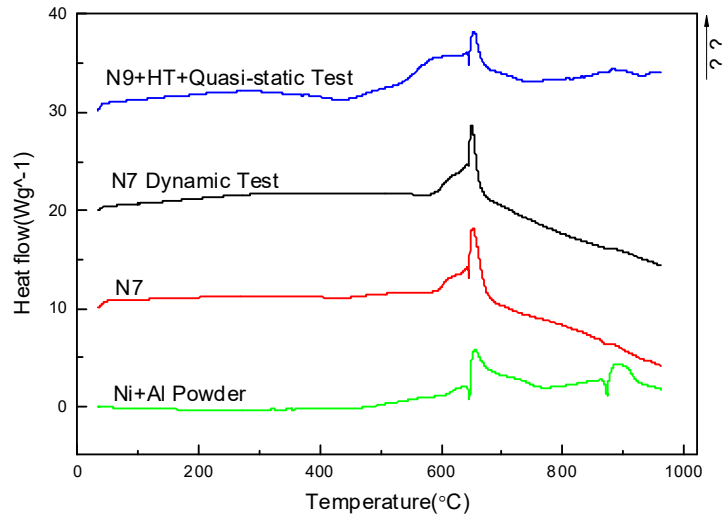
Fig. 4. Heating curves obtained by differential scanning calorimetry (DSC): original powders, as recovered, heat-treated, quasi-statically and dynamically tested Ni–Al composites.

1. D. J. Reding, *Shock induced chemical reactions in energetic structural materials*, 2009.
2. M. Gonzales, *The mechanochemistry in heterogeneous reactive powder mixtures under high-strain-rate loading and shock compression*, 2015.
3. C. T. Wei, E. Vitali, F. Jiang, S. W. Du, D. J. Benson, K. S. Vecchio, N. N. Thadhani, M. A. Meyers, Quasi-static and dynamic response of explosively consolidated metal–aluminum powder mixtures, *Acta Mater.,* 2012, 60, pp. 1418–1432; doi:10.1016/j.actamat.2011.10.027.

Q. Zhou et al.

SHS TECHNOLOGY OF COMPOSITE ALLOYS

M. Kh. Ziatdinov

National Research Tomsk State University, Tomsk, 634050 Russia

e-mail: ziatdinovm@mail.ru

The work addresses to the practical development of a novel process of production of SHS materials — metallurgical SHS process. The replacement of high-purity starting powders with less expensive and accessible alloys afforded for transition from existing actually laboratory-scale fabrication of SHS materials to industrial SHS manufacture. Until recently, the main advantages of SHS—low energy requirements, high rate, and simplicity—remained unclaimed in metallurgy for several reasons. One is the absence of commercially available equipment and properly designed process technologies. Another is the nonavailability of the industrial sector to work with often-unique SHS products. In addition, the use of highly reactive powders (as raw materials) in combination with high pressure/temperature in some cases turned out extremely dangerous. Finally, the self-sustaining process of combustion synthesis practically has no means of control in the course of its evolution. However, the main reason for the rejection of metallurgical SHS production of materials is their high production cost because of expensive raw powders used. Thus, the main advantage of SHS technology, energy saving, is smash up by high cost of fine raw powders. Moreover, the large-tonnage demand of metallurgical industry for potentially important SHS products was incompatible with the output volume of SHS production existing to date. A solution to the problem was found by development of so-called metallurgical SHS technology for production of materials suitable for use in steel-smelting and blast-furnace production. A distinctive feature of this technique is that it uses the raw materials produced by metallurgical industry that is alloying agents and master alloys.

Metallurgical SHS. The multitude of exothermic inorganic reactions can be subdivided into three groups: conventional SHS reactions,

metallothermic reactions, and metallurgical SHS reactions. The latter ones are the exchange reactions most of which involve ferroalloys as reagents; these reactions are close in their nature to metallothermic redox reactions. The reactants of metallurgical SHS—ferroalloys and alloying agents—are inorganic compounds such as silicides (FeSi, $FeSi_2$, $MnSi_2$), intermetallics (VFe, TiFe, $Nb_{19}Fe_{21}$), borides (FeB, FeB_n), as well as solid solutions such as Cr(Fe). Metallurgical SHS reactions yielding inorganic metal–matrix composites can also be subdivided into gasless, gas-absorbing, and gas-releasing systems (Table 1) [1]. The combustion modes taking place in metallurgical SHS systems are exemplified in Table 1.

Table 1. SHS reactions.

	Synthesis from the elements	Synthesis from alloys
Gasless systems	$Hf + C \rightarrow HfC$	$FeB + Ti \rightarrow TiB_2 + Fe$
Gas-absorbing systems	$B + N_2 \rightarrow BN$	$FeTi + N_2 \rightarrow TiN + Fe$
Gas-releasing systems	$Mo + S \rightarrow MoS_2$	$CrN + Ti \rightarrow TiN + Cr$

Chemical oven. Most frequently, metallurgical SHS reactions may need preliminary heating to some certain temperature T_0, which can be achieved by holding in furnace. Another approach is the use of the so-called chemical oven [2]. This principle was first applied to metallurgical SHS reactions in [3]. In view of this, it seemed reasonable to apply the method of chemical oven (Table 2) to the synthesis of complex alloying agents and boron-containing master alloys. External chemical oven is used in the case of chemical incompatibility between constituent components. Their use makes it possible to produce steels with different nitrogen content varying from low to extra-high. Metallic master alloys are environment-friendly. For this reason, the nitriding of V, Cr, Si, and Mn alloys with nitrogen-containing ferroalloys remains to be a main process in modern metallurgy.

Table 2. Syntheses in chemical oven.

SHS process	Internal oven	External oven
Conventional	$(Ti + C) + (W + C) \rightarrow$ $TiC + WC$	$[\mathbf{Ti + B \rightarrow TiB_2}] + [B + C \rightarrow B_4C]$ $[\mathbf{Ti + C \rightarrow TiC}] + [Nb + C \rightarrow NbC]$
Metallurgical	$(\mathbf{Ti + Si}) + (FeTi + FeB)$ $\rightarrow TiB_2 + Ti_5Si_3 + Fe$ $\mathbf{Fe{-}Ti} + FeMn + N_2 \rightarrow$ $TiN + Mn_4N + Fe$	$[\mathbf{FeTi + C \rightarrow TiC + Fe}] +$ $[FeTi + FeB \rightarrow TiB_2 + Fe]$ $[\mathbf{FeSi + N_2 \rightarrow S_3N_4 + Fe}] +$ $[FeCr + N_2 \rightarrow CrN + Fe]$

Chemical furnaces are highlighted in bold.

Combustion of ferrovanadium. For nitrogen pressures below 15 MPa, combustion was infiltration-mediated. The burning velocities U of the model and commercially available powders, as well as of Fe–V powder mixtures, were essentially the same. On going from 60 to 55% V, U spasmodically increases. This is accompanied by a decrease in the nitrogen content of combustion product and an increase in the extent of product nitriding. The reached values of T_{max} were 1780–2060°C for FeV80, 1630–1830°C for FeV60, and 1480–1560 and 1420–1490°C for FeV50 and FeV40, respectively. The larger nitrogen uptake, the higher T_{max}.

Combustion of ferrochromium. For P = 2.0–10.0 MPa, the combustion temperature varied in the range of 1220–1300°C (at $T_{ad} \approx$ 1680°C). The smaller the particle size of Fe–Cr powder, the higher burning velocity U, and the greater nitrogen uptake. The nitriding conditions can be improved by either preliminary heating or by conducting combustion in a coflow of inert or reactive gas [4, 5]. For the ferrochromium studied, the nitrogen uptake reached a value of 13% (nominal 16.8%); the extent of nitriding, 77%. For industrial-scale implementation in steel-making plants, we worked out four master alloys (Table 3). The nitrogen-containing master alloys have been tested at several steel plants of Russia and abroad. The nitrogen uptake was above 90%.

Table 3. SHS-produced nitride alloys for implementation in steel-making plants.

		Ferrochromium nitride		Chromium nitride	
		Melted	Sintered	Melted	Sintered
Elements (wt %)	N	6–8	8–13	8–12	16–20
	Cr	62–76	60–72	88–91	79–82
	C	0.05–0.10	0.05–0.10	0.03–0.06	0.03–0.06
	O	0.3	0.3	0.2	0.2
Phase composition		$(Fe,Cr)_2N$, Fe	$(Fe,Cr)_2N$, CrN, Fe	Cr_2N	CrN, Cr_2N
Density, g/cm^3		6.0–7.0	4.3–5.3	5.5–6.6	3.4–4.6

Combustion of ferroboron. Commercial powders of ferroboron and Ti powders of different granulometry were used to prepare green mixtures for Reaction *1* and Reaction *2* (Table 4). At Ti/B = 0.86, the combustion temperature attained a value of 1950°C in case of preheating and only 1370°C without preheating. In all cases, an increase in T_0 led to a marked

increase in U. It has been found that a relatively small preheating ($T_0 \geq$ 300°C) can be used in order to involve coarse Ti powders ($d > 0.4$ mm) into cost-effective and safe SHS reaction with ferroboron. For industrial-scale production of boron-containing master alloys, ferroborons with maximal boron content can be recommended. The alloys containing 6–14% B and 30–60% Ti can be readily fabricated upon variation in Ti/B ratio.

Table 4. Calculated composition of combustion products derived from different FeB–Ti mixtures.

Composition of model ferroboron	Boron content, wt %	Reaction 1 $FeB + Ti \rightarrow TiB_2 + Fe$			Reaction 2 $FeB + Ti \rightarrow TiB_2 + FeTi$		
		Calculated composition of combustion product					
		B	Ti	Fe	B	Ti	Fe
Fe$_2$B	8.8	7.36	16.32	76.32	5.44	38.12	56.44
FeB	16.2	11.66	28.0	60.34	7.69	52.54	39.77
FeB–FeB$_n$	25.6	16.34	36.17	47.49	11.61	54.64	33.75

1. A. G. Merzhanov, Solid-flame combustion: Fundamentals, advance, and prospects, *Izv. Ross. Akad. Nauk, Ser. Khim.*, 1997, vol. 46, no. 1, pp. 7–31.
2. V. M. Maslov, I. P. Borovinskaya, M. Kh. Ziatdinov, Combustion of the systems niobium–aluminum and niobium–germanium, *Combust. Explos. Shock Waves*, 1979, vol. 15, no. 1, pp. 41–47.
3. M. Kh. Ziatdinov, I. M. Shatokhin, *SHS technology of ferroalloys nitriding*, Proc. Int. Congress INFACON XII, Helsinki, 2010, pp. 899–909.
4. M. Kh. Ziatdinov, A. G. Gubar, *Combustion of titanium powders with forced filtration*, Abstr. Int. Symp. on the Chemistry of Flame Front, Almaty, 1997, pp. 59–61.
5. M. Kh. Ziatdinov, Chromium combustion in a nitrogen coflow, *Combust. Explos. Shock Waves*, 2016, vol. 52, no. 4, pp. 418–426.

M. Kh. Ziatdinov

THE PECULARITIES OF WAVE FORMATION AT EXPLOSIVE WELDING VIA THIN INTERLAYER

B. S. Zlobin[1], V. V. Kiselev[1], A. A. Shtertser[1,2]*, and A. V. Plastinin[2]

[1] Design and Technology Branch of Lavrent'ev Institute of Hydrodynamics, Siberian Branch, Russian Academy of Sciences, Novosibirsk, 630090 Russia
[2] Lavrent'ev Institute of Hydrodynamics, Siberian Branch, Russian Academy of Sciences, Novosibirsk, 630090 Russia

*e-mail: asterzer@mail.ru

The wave formation phenomenon upon explosive welding (EW) is well known and there are more than a dozen models devoted to its description [1]. However, there is as yet no satisfactory theory for prediction of wave size considering the strength and physical properties of colliding materials, while experiments show that their hardness and density affect the length and amplitude of generated wave [2]. Note that the control of wave formation is very important in welding of low-plasticity metals when the problem of cracking arises. Our experiments show that the wave size can reduced when a flyer plate is in advance clad with a thin copper layer [2, 3]. This is an effective way to get bonding without cracking. Furthermore, the same experiments have shown the existence of two types of waves occurring in the bond zone and differing in wavelength λ and wave amplitude a (Fig. 1) [3].

The possible existence of two types of waves has previously been discussed in [4], but experimentally proved for the first time in [3]. The weld zone in Fig. 1 has appeared in result of explosive welding performed in two steps. First, the 3 mm thick steel plate with a hardness HV of 4600 MPa was clad with the 0.3 mm thick copper band with $HV = 600$ MPa. Then, the copper layer was removed from the part of the surface of bimetal by milling and the plate obtained was

welded onto the steel plate with $HV = 3200$ MPa. Evidently, Fig. 1 illustrates that the use of thin interlayer makes it possible to reduce the size of waves.
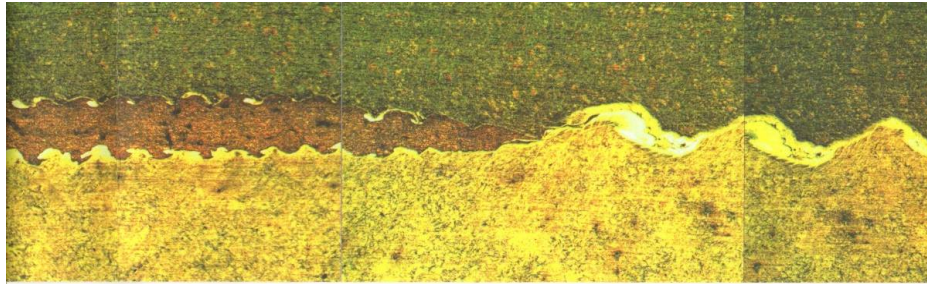
Fig. 1. Small (left) and large (right) waves in the bond zone of steel plates welded via copper interlayer (left) and directly (right) in one experiment at a collision point velocity $v_c = 2.5$ km/s and collision angle $\gamma \approx 10^0$.

Our further experiments with the use of Cu, Ti, Al and mild steel interlayers have shown that there are not only two types of waves. It was discovered that the experimental values of wavelength λ drop in the interval between the upper (λ_{max}) and the lower (λ_{min}) bounds defined by the following equations

$$\lambda_{max} = \delta(0.76R + 18.5)\sin^2(\gamma/2) \quad (1)$$

$$\lambda_{min} = \delta(0.73R - 1.70)\sin^2(\gamma/2) \quad (2)$$

$$R = \frac{(\rho_1 + \rho_2)v_c^2}{2(HV_1 + HV_2)} \quad (3)$$

where δ is the flyer plate full thickness, ρ_1 and ρ_2 are the densities of flyer and base plates, respectively, v_c is the contact point velocity, γ is the collision angle, HV_1 and HV_2 are the Vickers hardness of flyer and base plate, respectively, R is the Reynolds number as it is accepted among specialists in explosive welding [4, 5]. When the flyer plate is clad with an interlayer, the subscript 1 relates to the interlayer material. Let's introduce the parameter $F = \lambda/(\delta\sin^2(\gamma/2))$ and apply experimental points and theoretical lines corresponding to $\lambda_{max}(R)$ and $\lambda_{min}(R)$ on the F–R diagram (Fig. 2).

It follows from Eqs. (1) and (2) that upper and lower bounds are described in the F–R diagram by the straight lines $F(R) = 0.76R + 18.5$ and $F(R) = 0.73R - 1.70$, respectively. For the proper use of Eqs. (1–3) upon calculation of R, the following measure units should be taken: kg/m^3 for density, m/s for velocity, and Pa for Vickers hardness.

B. S. Zlobin et al.
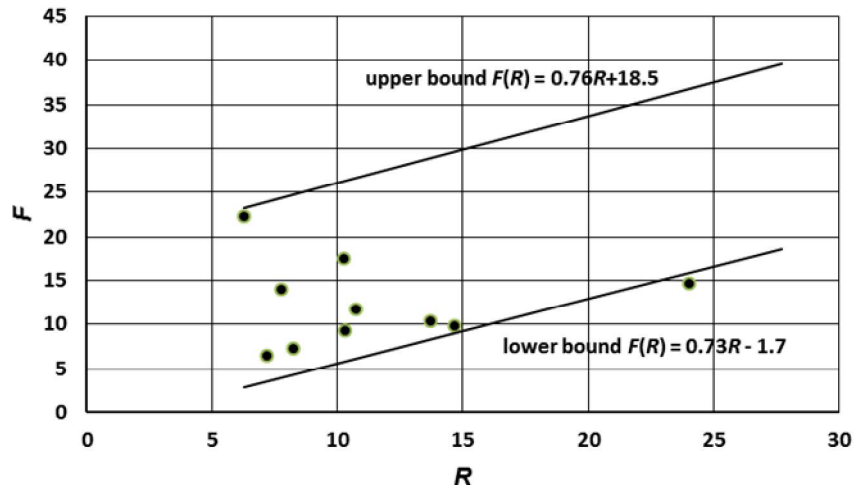
Fig. 2. Dependence of $F = \lambda/(\delta\sin^2(\gamma/2))$ on R. The points corresponding to experimental values of F lay between the lines representing the upper and lower bounds.

As for the wave amplitude a, there are inequalities $0.14 \leq a/\lambda \leq 0.30$ previously suggested in [4] and based mostly on experiments when ρ_1 and ρ_2 did not differ much. However, it is known that the strong bond can be obtained even in the absence of waves, especially when plates with different density colliding. This means that the wave amplitude $a \to 0$ when ρ_1/ρ_2 or $\rho_2/\rho_1 \to 0$ (depending on what density is less) and a becomes less than can be measured due to limitations of the measurement method. Our experiments have confirmed this. With new experimental data on explosive welding via thin interlayer the above inequalities from [4] can be updated and written in the following form

$$0.14\left(\rho_{min}\Big/\rho_{max}\right)^{2.6} \leq a\Big/\lambda \leq 0.30\left(\rho_{min}\Big/\rho_{max}\right)^{2.6} \qquad (4)$$

where ρ_{min} is the lower value among the two related to densities of colliding plates, and ρ_{max} is the higher one.

So we can conclude that it is impossible to predict explicitly λ and a because there is a wave size spectrum limited by the Eqs. (1), (2), and (4). However, the use of thin interlayers welded previously onto the flyer plate enables to get waves with decreased values of λ and a so that the corresponding point (F, R) is close to the lower boundary in Fig. 2. This is important in welding of low-plasticity metals and alloys.

At our glance the uncertainty in the wave size is associated with the uncertainty in the thickness of cumulative jet arising between the colliding surfaces because it (jet) is not solid but dispersed at $\gamma < 30^\circ$ [6].

1. I. V. Yakovlev, V. V. Pai, *Explosive Welding of Metals*, Novosibirsk: Izd. SO RAS, 2013 (in Russian).
2. B. S. Zlobin, A. A. Shtertser, V. V. Kiselev, A. V. Plastinin, *Bonding and wave formation at the explosive welding of low-plastic materials*, in Explosive Production of New Materials: Science, Technology, Business, and Innovations (Proc. EPNM-2016 Symp.), A. A. Deribas, Yu. B. Scheck, Eds., Coimbra: ACIV, 2016. pp. 219–221.
3. B. S. Zlobin, V. V. Kiselev, A. A. Shtertser, A. V. Plastinin, Use of emulsion explosives in experimental investigations of flows in the bonding zone at explosive welding, *Combust. Explos. Shock Waves*, 2018, vol. 54, no. 2, accepted for publication.
4. A. A. Deribas, *Physics of explosive hardening and welding*, Novosibirsk: Nauka, 1980 (in Russian).
5. B. Crossland, *Explosive Welding of Metals and its Application*, Oxford: Clarendon Press, 1982.
6. A. A. Shtertser, B. S. Zlobin, Flows, strains, and the formation of joints in oblique collision of metal plates, *J. Appl. Mech. Tech. Phys.,* 2015, vol. 56, no. 5, pp. 927–935.

APPLICATION OF THE IDENTATION METHOD TO THE EVALUATION OF TITANIUM STRUCTURES

W. Żórawski[1], M. Makrenek[2], A. Góral[3], and S. Kowalski[1]

[1] Kielce University of Technology, Laser Processing Research Centre, al. Tysiąclecia Państwa Polskiego 7, 25-314 Kielce, Poland
[2] Kielce University of Technology, Faculty of Management and Computer Modelling, al. Tysiąclecia Państwa Polskiego 7, 25-314 Kielce, Poland
[3] Institute of Metallurgy and Materials Science Polish Academy of Science, Reymonta 25, 30-059 Cracow, Poland

e-mail: ktrwz@tu.kielce.pl

Titanium structures were deposited by explosive welding and cold spraying technique onto titanium substrate. The main advantage of cold spraying is elimination of influence of temperature on the particles of the spraying material and the substrate that occurs in conventional thermal spraying methods. Therefore, the properties of such formed structures are not available in other technologies. In the cold spray process, the structure is deposited by grains of powder hitting with supersonic velocity (500÷1200 m/s) onto the surface of the substrate [1–3]. These grains undergo great deformation, which consequently causes the deformed particles to adhere closely to each other. As a result of the strong plastic deformation at very high velocity, bonding mechanism is created by mechanical interlocking and adiabatic shear instability. This last phenomenon refers to shear occurrence at high pressure followed by increase of temperature at a high strain rate deformation. The low temperature of cold spray process prevents the harmful effects of particle oxidation, phase change, grain growth and other problems occurring during the plasma, supersonic or arc spraying processes [4–7]. The ability of particles to plastic deformation depends on their mechanical (e.g. tensile strength) and thermal properties (e.g. melting point) as well as the parameters of

the spraying process (gas temperature and pressure) [8]. The relatively low temperature of the process also allows for preservation of the original chemical and phase composition of the particles in the resulting structure, which is not possible in the other thermal spraying processes.

Titanium structures were sprayed onto the titanium substrate by means of cold spray system Impact Innovations 5/8 equipped with the Fanuc M-20iA robot at Kielce University of Technology. Two titanium powders with different morphology (spheroidal and angular) and the same grain size range of 15÷45 μm were applied in experiment (Fig. 1).
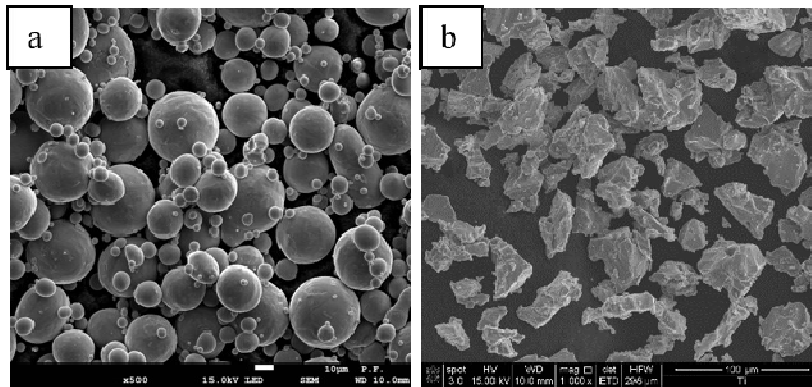
Fig. 1. Ti powder: (a) spheroidal, (b) angular.

The microstructure of the Ti powders and the cold sprayed and explosive structures were analysed with the microscope SEM FEI Nova NanoSEM 200. The phase composition was studied using D8 Discover Bruker (as sprayed deposits) and X'Pert Philips PW 1710 (powder feedstock) diffractometers with Co-Kα radiation of wavelength λ = 1.78897 Å. The micromechanical testing of titanium structures was carried out with the use of nanoindentation technique (Nanovea) with a Berkovitz indenter (the Olivier and Pharr methodology). Forty nine readings were taken for each structure.

Figure 2 shows the microstructure of the cold sprayed titanium structure with no apparent splat boundaries. The sprayed titanium particles formed a very dense structure and the deformed particles strongly adhered to the substrate and to each other.

As in explosive welding in cold spray process to achieve good the impact velocity of sprayed particles must exceed a critical velocity. It is necessary to create phenomenon of adiabatic shear instability at the

bond interface. Velocity of particles influences on microstructure and mechanical behaviour of cold sprayed structures.

Figure 3 presents the indentation tests of the titanium structure cold sprayed with angular powder (nanohardness and Young's modulus). It was observed the change of these properties in the measured area caused by varying deformation degree of titanium powder consisting of grains with different sizes, which at the time of impact had different speeds. Tests carried out onto explosive welding and cold spraying (spheroidal) structures showed significant differences in theirs mechanical properties.
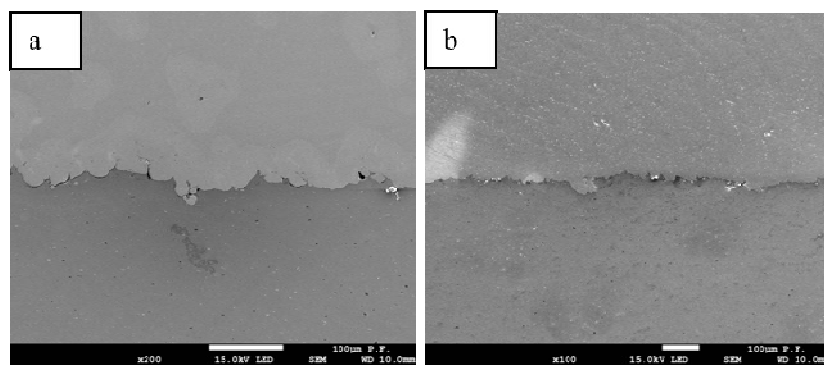
Fig. 2. Microstructure of the cold sprayed titanium structure: (a) spheroidal powder, (b) angular powder.
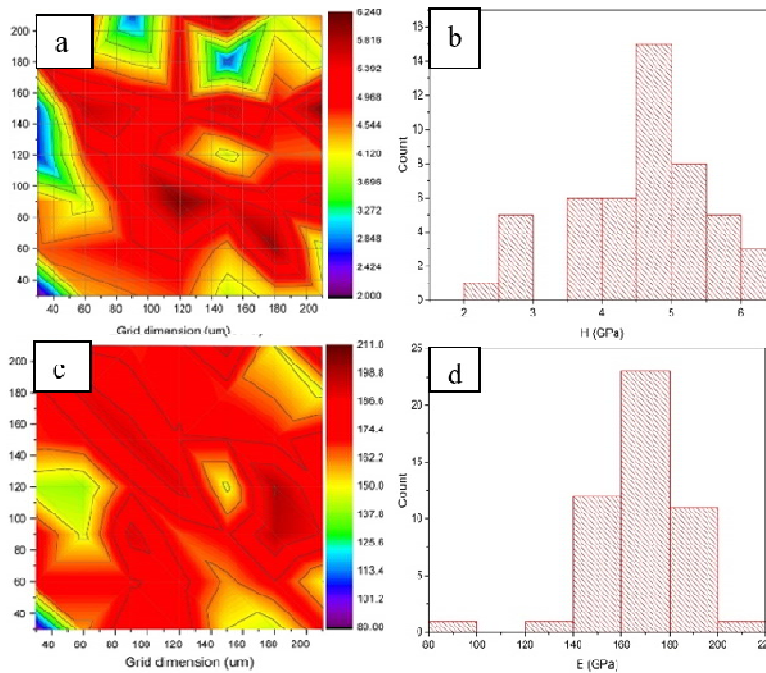
Fig. 3. Distribution of titanium structure cold sprayed with angular powder: (a) hardness map, (b) hardness histogram and probability, (c) Young's modulus map, (d) Young's modulus histogram and probability.

1. A. Papyrin, *Cold Spraying*, Elsewier Ltd, 2007.
2. J. Villafuerte, *Modern Cold Spray, Materials, Process and Applications,* Springer, 2015.
3. T. Klassen, et al., Cold spraying – new developments and application potential. 8. Kolloquium HVOF Spraying, Erding 2009, 9–16.
4. H. Assadi, H. Kreye, F. Gartner, T. Klassen, Cold spraying – a materials perspective, *Acta Materialia*, 2016, vol. 116, pp. 382–407.
5. W. Żórawski, Mikrostruktura powłok miedzianych natryskanych zimnym gazem, *Inżynieria Powierzchni*, 2006, 1, pp. 29–34.
6. R. Kromer, J. Cormier, S. Costil, Role of powder granulometry and substrate topography in adhesion strength of thermal spray coatings, *J. Therm. Spray Tech.*, 2016, vol. 25, pp. 933–945.
7. A. Góral, W. Żórawski, Charakterystyka mikrostruktury natryskanych zimnym gazem powłok Ni-Al2O3, *Przegląd Spawalnictwa*, 2015, 5, pp. 34–37.
8. S. Yin, M. Meyer, W. Li, H. Liao, R. Lupoi, Gas flow, particle acceleration, and heat transfer in cold spray: A review, *J. Therm. Spray Tech.*, 2016, vol. 25, pp. 874–896.

Author Index

TECHNICAL PROGRAM

**XIV International Symposium
on Explosive Production of New Materials:
Science, Technology, Business,
and Innovations (EPNM-2018)**

**May 14–18, 2018
Saint Petersburg, Russia**

International Advisory Committee

Alymov M.I.	(Russia)	Peikrishvili A.	(Georgia)
Babul T.	(Poland)	Pervukhin L.B.	(Russia)
Banker J.G.	(USA)	Prothe C.	(USA)
Campos J.	(Portugal)	Pruemmer R.	(Germany)
Carton E.	(Netherlands)	Remond Y.	(France)
Chen P.	(China)	Ribeiro J.	(Portugal)
Deribas A.A.	(Russia)	Rozen A.E.	(Russia)
Fortov V.E.	(Russia)	Shtertser A.A.	(Russia)
Galka A.	(Poland)	Szulc Z.	(Poland)
Hokamoto K.	(Japan)	Tavadze G.F.	(Georgia)
Ivanov V.V.	(Russia)	Thadhani N.N.	(USA)
Kecskes L.J.	(USA)	Veehmayer M.	(Germany)
Levashov E.A.	(Russia)	Yücel O.	(Turkey)
Lis J.	(Poland)	Yukhvid V.I.	(Russia)
Mendes R.	(Portugal)	Vakin V.S.	(Russia)
Moon J.G.	(Korea)	Zieba P.	(Poland)
Nesvadba P.	(Czechia)		

Organizing Committee

Alymov M.I., co-chairman	(Russia)
Vakin V.S., co-chairman	(Russia)
Likhanova O.O., coordinator	(Russia)
Tarasova L.E., executive secretary	(Russia)
Sanin V.N.	(Russia)
Sytschev A.E.	(Russia)
Amelina O.V.	(Russia)
Alymova A.M.	(Russia)

Scientific Committee

Sanin V.N., chairman	(Russia)
Deribas A.A.	(Russia)
Shtertser A.A.	(Russia)
Golosova O.A.	(Russia)

MONDAY, MAY 14

9.00–10.00   Registration

10.00–10.20 Opening ceremony
Welcoming speeches of Co-chairmen of Organizing Committee:
  Prof. M. I. Alymov   (ISMAN, Russia)
  V. S. Vakin   (EnergoMetall Co, Russia)

10:20 *M. I. Alymov* (Russia)
ISMAN – NEW RESULTS ON THE SYNTHESIS OF NEW
MATERIALS

11.00–11.20 │Coffee Break

Session I
Explosive Welding

11:20 *J. G. Banker* (USA)
GLOBAL EVOLUTION OF THE COMMERCIAL EXPLOSION
METALWORKING INDUSTRY: PAST, PRESENT AND FUTURE

11:40 *R. Kosturek, M. Wachowski, L. Śnieżek, and A. Gałka* (Poland)
THE INFLUENCE OF THE HEAT LOAD ON THE
MICROSTRUCTURE AND MECHANICAL PROPERTIES OF
CHOSEN NIOBIUM-CLAD STEELS AND NICKEL ALLOYS
OBTAINED BY EXPLOSIVE WELDING

12:00 *A. M. Fedorov, I. A Schastlivaya, V. A. Mezhonov,
and D. E. Oderyshev* (Russia)
GROWTH OF DEFECTS OF DISCONTINUITY OF BIMETALLIC
STEEL-TO-TITANIUM PLATE BILLET JOINT DURING
MANUFACTURING EQUIPMENT AND ITS OPERATION

12:20 *P. Chen, C. Xu, H. Yin, X. Gao, Q. Zhou, and L. Qu* (China)
SHOCK SYNTHESIS OF FEW-LAYER GRAPHENE AND
NITROGEN-DOPED GRAPHENE MATERIALS

12:40 <u>H. Paul</u>, M.M. Miszczyk, M. Prażmowski, A. Gałka, Z. Szulc, P. Bobrowski, and Ł. Maj (Poland)
INTERFACIAL REACTIONS DURING ANNEALING OF EXPLOSIVELY WELDED SHEETS

13.00–14.00 │ Lunch

14:00 R. R. Mulyukov (Russia)
THE INFLUENCE OF SEVERE PLASTIC DEFORMATION ON THE PROPERTIES OF METALS AND ALLOYS

14:40 <u>R. Mendes</u>, G. Sena, J. Ribeiro, A. Campos, and A. Loureiro (Portugal)
EXPLOSIVE WELDING OF METAL/Al AND PROCESS LIMITATIONS

15:00 A. A. Deribas, <u>A. A. Shtertser</u>, and E. E. Zubkov (Russia)
EXPLOSIVE HARDENING AND ITS APPLICATION IN PRODUCTION OF RAILROAD SWITCH FROGS

15:20 S. Liu, <u>V. Petr</u>, J. Banker and C. Prothe (USA)
CHARACTERIZATION OF TEMPERATURE EXCURSION IN EXPLOSIVE STEEL–COPPER BONDS

15:40 <u>V. P. Efremov</u> and E. I. Zakatilova (Russia)
THE MECHANISM OF DETONATION NANODIAMONDS GRAPHITISATION UNDER HEATING AND IRRADIATION

16.00–16.20 │ Coffee Break

16:20 A. G. Bryzgalin, E. D. Pekar, <u>P. S. Shlonskii</u>, G. D. Shirkov, Yu. A. Budagov, and B. M. Sabirov (Ukraine)
THE EXPLOSION WELDING OF Ti + SS + Ti TRIMETAL FOR THE MANUFACTURING OF LINEAR COLLIDER ADAPTORS

16:40 <u>K. Saksl</u>, Š. Michalik, D.M. Fronczek, K. Šuľová, M. Šuliková, A. Lachová, Z. Szulc, M. Fejerčák, Z. Molčanová, and D. Daisenberger (Slovakia)
RESIDUAL STRESSES IN BIMETAL PREPARED BY EXPLOSION WELDING

17:00 *M. Blakely* (USA)
REVIEW OF HYDROGEN INDUCED CLAD DISBOND TESTING

17:20 *I. A. Bataev* (Russia)
SUPERHIGH COOLING RATES AND FORMATION OF
STRUCTURE AT THE INTERFACE OF EXPLOSIVELY
WELDED MATERIALS

18.00–20.00 │ Welcome Party

TUESDAY, MAY 15
Session I
Explosive Welding

9:00 *S. Tanaka, I. Bataev, H. Oda, and K.* Hokamoto (Japan)
PROCESS OF TUNGSTEN WIRE EXPLOSION AND SYNTHESIS
OF CARBIDE BY PULSEDWIRE DISCHARGE

9:20 *A. E. Rozen, A. V. Dub, G. V. Kozlov, S. I. Kamyshanskii,
A. V. Khorin, I. A. Safonov, A. A. Rozen, V. V. Mamontov,
and E.F. Lezhneva* (Russia)
SCIENTIFIC BASIS OF CREATION OF NEW MATERIALS BY
EXPLOSION WELDING TO PROVIDE SAFE HANDLING OF
RADIOACTIVE WASTE

9:40 *V. Petr, J. Banker, S. Liu, and C. Prothe* (USA)
INFLUENCE OF EXPLOSIVE CHARGE DENSITY AND SIZE OF
PRILLS ON THE VELOCITY OF DETONATION OF ANFO
EXPLOSIVES

10:00 *A. A. Shtertser, V. Yu. Ul'yanitskii, I. S. Batraev,
and D.K. Rybin* (Russia)
EXPLOSIVE SYNTHESIS OF NANOSCALE DETONATION
CARBON

10:20 *Z. Sheng, P. Chen, and Q. Zhou* (China)
MICROSTRUCTURE AND DYNAMIC MECHANICAL
PROPERTIES OF MULTILAYER Ti–Al EXPLOSIVELY WELDED
PLATE

10:40 *T. Schlothauer, C. Schimpf, G. Heide, and E. Kroke* (Germany)
CHEMICAL REACTIONS, EOS-CALCULATIONS AND
MECHANICAL BEHAVIOR OF SHOCKED POROUS TUNGSTEN
CARBIDE IN THE MBAR-RANGE

11.00–11.20 │ Coffee Break

11:20 *R. Prümmer and D. Kochsiek* (Germany)
IMPORTANCE OF MORPHOLOGY OF POWDER IN EXPLOSIVE
COMPACTION FOR PRODUCTION OF INTERMETALLIC
ALLOYS

11:40 *B. S. Zlobin, V. V. Kiselev, A. A. Shtertser,
and A. V. Plastinin* (Russia)
THE PECULARITIES OF WAVE FORMATION AT EXPLOSIVE
WELDING VIA THIN INTERLAYER

12:00 *I. Lendiel, P. Shlonskii, and A. Cherkachin* (Ukraine)
INITIATION OF THERMAL EXPLOSION IN Ni/Al REACTION
MULTILAYER FOILS BY ELECTRIC CURRENT PULSE

12:20 *K. A. Ten, E. R. Pruuel, A. O. Kashkarov, I. A. Rubzov,
L. I. Shekhtman, V. V. Zhulanov, and B. P. Tolochko* (Russia)
PICOSECOND-EXPOSURE DYNAMIC MEASUREMENTS OF
FORMATION OF ULTRA-DISPERSED DIAMONDS IN
DETONATION WAVES

12:40 *V. O. Belko, P. N. Bondarenko, K. A. Kurkin,
and A. D. Lukyanchikov* (Russia)
DETECTION OF INTERLAYER DEFECTS IN BIMETALLIC
MATERIALS BY ELECTRIC FOUR-PROBE METHOD

13.00–14.00 │ Lunch

14:00 *A. Mori, S. Tanaka, and K. Hokamoto* (Japan)
PHENOMENA OF WELDING FOR SIMILAR AND DISSIMILAR
MATERIALS IN THE OBLIQUE COLLISION

14:20 *Ch. G. Pak, A. V. Pryshchak, and G. A. Koshkin* (Russia)
INVESTIGATION OF THE INFLUENCE OF SHOCK
ACTIVATION ON MAIN PROPERTIES OF PIEZOELECTRIC
CERAMICS

14:40 *I. S. Los', S. Yu. Kireev, and A. V. Pryshchak* (Russia)
EVALUATION OF MECHANICAL PROPERTIES AND
CORROSION RESISTANCE OF EXPLOCLAD MULTILAYER
MATERIALS

15:00 *M. Szmul, A. Chudzio, Z.Szulc,
and J. Wojewoda-Budka* (Poland)
THE INFLUENCE OF HEAT TREATMENT ON CHANGES IN
THE STRUCTURE, CHEMICAL COMPOSITION AND
MECHANICAL PROPERTIES OF EXPLOSIVELY CLADDED
TITANIUM ON STEEL PLATE

15:20 *O. L. Pervukhina* (Russia)
INFLUENCE OF THERMAL PROCESSING ON STRUCTURAL
CHANGES OF STEEL–TITANIUM BIMETAL OBTAINED BY
EXPLOSIVE WELDING IN ARGON MEDIUM

15:40 *E. V. Petrov, I. V. Saikov, and G. R. Saikova* (Russia)
INVESTIGATION OF INITIATION OF $Zn + S$ STOICHIOMETRIC
MIXTURE BY PULSE IMPACT

16.00–16.20 │ Coffee Break

16:20 *I. V. Saikov, M. I. Alymov, and S. G. Vadchenko* (Russia)
INITIATION OF COMBUSTION OF METAL–TEFLON SYSTEMS
WITH EXPLOSIVE ACTION

16:40 *A. G. Bryzgalin, P. S. Shlonskii, S. D. Ventsev,
and E. D. Pekar* (Ukraine)
PROBLEMS OF EXPLOSION WELDING OF LONG-LENGTH
COAXIAL Cu+Al RODS WITH A THIN CLADDING LAYER

17:00 *A. Yu. Malakhov, I. V. Saikov, and I. V. Denisov* (Russia)
EXPLOSIVE WELDING OF STAINLESS STEEL PIPE TO
CARBON STEEL

17:20 _D. V. Nonyak, O. L. Pervukhina, and L. B. Pervukhin_ (Russia)
DETERMINATION OF LEVEL OF THE STRESSED-DEFORMED
CONDITION OF BIMETALS PRODUCED BY EXPLOSION
WELDING USING METAL MAGNETIC MEMORY METHOD

17:40 _H. Yin, Q. Du, P. Chen, and M. Cao_ (China)
MICROWAVE ABSORPTION PROPERTIES OF THE CARBON-
ENCAPSULATED IRON-BASED NANOPARTICLES

WEDNESDAY, MAY 16
Session II
Compaction, Composite Materials

9:00 _T. Babul and A. Olbrycht_ (Poland)
COMPOSITE COATINGS MANUFACTURED IN THE RESULT
OF THE DETONATION SPRAYING OF THE COPPER POWDER
COATED WITH GRAPHENE

9:20 _A. B. Peikrishvili, L. J. Kecskes, G. F. Tavadze, B. A. Godibadze,
E. Sh. Chagelishvili, and G. Sh. Oniashvili (_Georgia/USA_)_
HOT SHOCK WAVE CONSOLIDATION OF
NANOSTRUCTURED TUNGSTEN BASED COMPOSITES

9:40 _D. V. Lazurenko, V. I. Mali, A. A. Kashimbetova, M. A. Esikov,
I. A. Bataev, A. Stark, and F. Pyczak_ (Russia)
FORMATION OF Ti–Al$_3$Ti MULTILAYER COMPOSITES WITH
TETRAGONAL AND CUBIC STRUCTURES OF
INTERMETALLIC BY EXPLOSIVE WELDING AND
SUBSEQUENT ANNEALING

10:00 _V. A. Grachev, A. E. Rozen, A. V. Dub, Yu. P. Perelygin,
I. A. Safonov, A. E. Korneev, I. L. Kharina, S. Yu. Kireev, A. A. Rozen,
and N. N. Ratsuk_ (Russia)
INNOVATIVE SOLUTION IN THE AREA OF
MANUFACTURING MULTILAYERED COMPOSITE
MATERIALS BY EXPLOSION WELDING FOR THE ATOMIC,
CHEMICAL, OIL AND GAS INDUSTRY

10:20 _A. G. Knyazeva_ (Russia)
BASIC MODELS OF VOLUME SYNTHESIS OF Ti-BASED
COMPOSITES

10:40 _T. Minasyan, S. Aydinyan, L. Liu, S. Cygan,_
and I. Hussainova (Armenia)
SINTERING BEHAVIOR OF ZrC–TiC–MoSi$_2$ CERAMIC
COMPOSITE

11.00–11.20 | Coffee Break

11:20 _Q. Zhou, P. W. Chen, Z. M. Sheng, and Y. Y. Li_ (China)
MICROSTRUCTURE AND DYNAMIC BEHAVIOR OF
EXPLOSIVELY CONSOLIDATED Ni–Al COMPOSITES

11:40 _A. E. Rozen, Yu. P. Perelygin, S. G. Usatyi, A. V. Khorin,_
I. A. Safonov, O. N. Loginov, A. A. Rozen,
and E. V. Zavartseva (Russia)
STRUCTURING OF INTERLAYER BOUNDARIES DURING
EXPLOSION WELDING OF LAYERED COMPOSITE
MATERIALS AND MODELING OF WAVE FORMATION
CONDITIONS

12:00 _T. Minasyan_, _H. Kirakosyan, S. Aydinyan, L. Liu,_
I. Hussainova, and S. Kharatyan (Armenia)
SYNTHESIS AND CONSOLIDATION OF Mo–Cu COMPOSITE
NANOPOWDER

12:20 _B. Godibadze, A. Peikrishvili, T. Gegechkori,_
and G. Mamniashvili (Georgia)
DEVELOPMENT OF SUPERCONDUCTIVE MgB$_2$ HYBRID
COMPOSITES AND INVESTIGATION THEIR
STRUCTURE/PROPERTY RELATIONSHIP

12:40 _A. B. Peikrishvili, E. Sh. Chagelishvili, B. A. Godibadze,_
G. I. Mamniashvili, L. I. Qurdadze, and A. A. Dgebuadze (Georgia)
LIQUID PHASE SHOCK WAVE CONSOLIDATION OF
NANOSTRUCTURED Ta–Ag COMPOSITES

13.00–14.00 | Lunch

14:00 *A. B. Peikrishvili, L. J. Kecskes, G. F. Tavadze, B. A. Godibadze, and E. Sh. Chagelishvili* (Georgia/USA)
SHOCK ASSISTED LIQUID-PHASE CONSOLIDATION OF Ta(Nb,V)–Al COMPOSITES

14:20 *G. H. S. F. L. Carvalho, I. Galvão, R. M. Leal, R. Mendes, J. B. Ribeiro, and A. Loureiro* (Portugal)
WELDING STAINLESS STEEL AND ALUMINIUM BY EXPLOSION WELDING: EFFECT OF THE MATERIALS POSITION

14:40 *G. H. S. F. L. Carvalho, I. Galvão, R. M. Leal, R. Mendes, J. B. Ribeiro, and A. Loureiro* (Portugal)
BONDING INTERFACE CHARACTERISTICS OF STEEL-TO-ALUMINIUM EXPLOSION WELDS

15.00–16.00 │ Poster Session

16.00–18.00 │ Boat Tour - sightseeings of Saint Petersburg

THURSDAY, MAY 17

9:00 *V. Ya. Shevchenko* (Russia)
TOPOLOGICAL STATES OF STRUCTURAL CHEMISTRY OF NEW SUBSTANCES AND MATERIALS

Session II
Compaction, Composite Materials

9:40 *A. Yu. Dolgoborodov, B. D. Yankovskii, V. G. Kirilenko, A. N. Streletskii, S. Yu. Anan'ev, I. V. Kolbanev, and G. A. Vorob'eva* (Russia)
INITIATION AND COMBUSTION OF MECHANOACTIVATED MIXTURES OF ALUMINUM AND COPPER OXIDE

10:00 *M. K. Zakaryan, S. V. Aydinyan, and S. L. Kharatyan* (Armenia)
SYNTHESIS OF Ni–W NANOPOWDERS FROM OXIDE AND SALT PRECURSORS IN COMBUSTION MODE BY USING THERMO-KINETIC COUPLING APPROACH

10:20 *A. V. Sobachkin, M. V. Loginova, A. A. Sitnikov, V. I. Yakovlev, V. Yu. Filimonov, S. G. Ivanov, A. Yu. Myasnikov, and A. V. Gradoboev* (Russia)
HIGH-TEMPERATURE SYNTHESIS IN MECHANICALLY ACTIVATED Ti–Al POWDER MIXTURE IRRADIATED BY GAMMA-QUANTA

10:40 *S. V. Ganin, O. G. Zotov, A. I. Shamshurin, V. A. Markov, and V. A. Sokolova* (Russia)
INVESTIGATION OF STRUCTURE FORMATION AT GAS DYNAMIC COLD SPRAY OF ALUMINUM–ZINC POWDER

11:00 *S. V. Karpov, A. M. Stolin, L. S. Stelmakh, and A. O. Glebov* (Russia)
MATHEMATICAL MODELING OF NON-STATIONARY HEAT PROCESSES DURING FREE SHS COMPRESSION OF MATERIALS

11:20 *A. E. Sytschev, N. A. Kochetov, S. G. Vadchenko, and A. S. Shchukin* (Russia)
SELF-PROPAGATING HIGH-TEMPERATURE SYNTHESIS OF Ni–Al-BASED ALLOY WITH NANOLAMINATE CARBON-CONTAINING COMPONENTS

11:40 *V. N. Sanin, D. M. Ikornikov, D. E. Andreev, N. V. Sachkova, and V. I. Yukhvid* (Russia)
REPROCESSING OF MILL SCALE WASTES BY SHS METALLURGY FOR PRODUCTION OF CAST FERROSILICON, FERROSILICO ALUMINUM AND FERROBORON

12.00–12.40 │ Lunch

12.40 │ Excursion to Peterhof

<div align="center">

FRIDAY, MAY 18
Session III
SHS

</div>

9:00 *M. Kh. Ziatdinov* (Russia)
SHS TECHNOLOGY OF COMPOSITE ALLOYS

9:20 *V. I. Yukhvid, V. A. Gorshkov, V. N. Sanin, D. E. Andreev, and Yu. S. Vdovin* (Russia)
SHS METALLURGY OF REFRACTORY MATERIALS BASED ON MOLYBDENUM

9:40 *A. M. Stolin, P. M. Bazhin, and A. S. Konstantinov* (Russia)
IMPLEMENTATION OF NEW OPPORTUNITIES FOR OBTAINING LARGE-SIZED COMPACT PLATES FROM CERAMIC POWDER MATERIALS BY FREE SHS COMPRESSION

10:00 *G. Oniashvili, Z. Aslamazashvili, T. Namicheishvili, G. Tavadze, Z. Melashvili, A. Tutberidze, and G. Zakharov* (Georgia)
STUDY OF TECHNOLOGICAL PARAMETERS IN Ti–Cr–C–STEEL, Ti–B, Ti–B–Me SYSTEMS FOR OBTAINING PRODUCTS BY SHS–ELECTRICAL ROLLING

10:20 *A. Yu. Potanin, I. V. Yatsuk, S. Vorotilo, Yu. S. Pogozhev, D. Yu. Kovalev, and E. A. Levashov* (Russia)
SHS OF ADVANCED HEAT-RESISTANT CERAMICS IN THE $Me^{IV}(–Me^{VI})–Si–B(C)$ SYSTEM

10:40 *V. A. Shcherbakov and A. N. Gryadunov* (Russia)
POSSIBILITY OF PREPARATION OF Ta_4ZrC_5–CrB AND Ta_4HfC_5–CrB COMPOSITES BY SHS PRESSING

11:00 *E. I. Patsera, V. V. Kurbatkina, E. A. Levashov, Yu. Yu. Kaplanskii, and A. V. Samokhin* (Russia)
OBTAINING CLOSE-CUT-FRACTION SPHERICAL MICROPOWDERS OF HEAT-RESISTANT ALLOY BASED ON NICKEL MONOALUMINIDE

11:20 *V. A. Gorshkov and P. A. Miloserdov* (Russia)
SHS METALLURGY OF CAST OXIDE MATERIALS

11:40 *E. G. Grigor'ev, V. Yu. Goltsev, V. S. Kashirin, A. V. Osintsev, K. Yu. Ochkov, A. S. Plotnikov, and A. V. Yudin* (Russia)
PULSED HIGH-VOLTAGE WELDING OF MAGNETIC CORES FROM MAGNETICALLY SOFT ALLOY

12:00 *P. M. Bazhin and* <u>*A. M. Stolin*</u> (Russia)
SHS OF POWDER MATERIALS OF REFRACTORY INORGANIC
COMPOUNDS UNDER THE COMBINED ACTION OF
PRESSURE AND SHEAR

12.20–13.00 │ Closing Ceremony

13.00–14.00 │ Lunch

POSTER SESSION
15:00–16:00
Wednesday, May, 16, 2018

M. I. Alymov, S. G. Vadchenko, and I. S. Gordopolova
INFLUENCE OF ALUMINUM ADDITIVES ON IGNITION OF
TUNGSTEN/TEFLON POWDER MIXTURE

*M. I. Alymov, S. G. Vadchenko, I. S. Gordopolova,
and I. V. Saikov*
EFFECT OF MECHANICAL ACTIVATION ON THE
THERMAL AND SHOCK-WAVE INITIATION OF THE
REACTION BETWEEN REFRACTORY METALS AND
TEFLON

A. F. Belikova, S. N. Buravova, and E. V. Petrov
FEATURE OF FORMATION OF LOCALIZED DEFORMATION
BANDS UPON PULSE LOADING

V. N. Borshch and I. M. Dement'eva
ZSM-5 SUPPORTED CATALYSTS PRODUCED BY LOW-
TEMPERATURE COMBUSTION

*V. N. Borshch, E. V. Pugacheva, S. Ya. Zhuk, V. N. Sanin,
D. E. Andreev, and V. I. Yukhvid*
STRUCTURE FEATURES OF SHS INTERMETALLICS AS
PRECURSORS FOR HIGHLY ACTIVE POLYMETALLIC
CATALYSTS

S. N. Buravova, E. V. Petrov, N. I. Mukhina, and A. S. Shchukin
DISSOLUTION OF STRENGTHENING PHASE PARTICLES IN
THE LOCALIZED DEFORMATION BANDS

S. V. Dudin, V. A. Sosikov and S. I. Torunov
EXPLOSIVE LABORATORY INSTALLATION FOR
CYLINDRICAL COMPRESSION

V. I. Goltsev, E. G. Grigor'ev, N. A. Gribov, L. A. Degadnikova,
V. Osintsev, and A. S. Plotnikov
INVESTIGATION OF STRENGTH OF MATERIALS OBTAINED
BY ELECTRIC PULSE CONSOLIDATION OF POWDERS

R. D. Kapustin, I. V. Denisov, and I. V. Saikov
EXPLOSION WELDING Of Al + Cu BIMETALLIC JOINTS FOR
ELECTRICAL CONTACTS

S. V. Konovalikhin, V. I. Ponomarev, D. Yu. Kovalev, and
S. A. Guda
MONOCLINIC BORON CARBIDE FROM SHS

D. Yu. Kovalev and V. I. Ponomarev
DIAGNOSTICS OF SHS: TIME RESOLVED X-RAY
DIFFRACTION METHOD

M. Kowalski, M. Böhm, and A. Kurek
NUMERIC SIMULATIONS OF THE STEEL–ALUMINIUM
TRANSISTION JOINT UNDER MONOTONIC LOADING

P. M. Krishenik, S. V. Kostin, N. I. Ozerkovskaya, and
K. G. Shkadinskii
THE UNSTEADY CELLULAR MODES OF FILTRATION
COMBUSTION

O. N. Kryukova and A. G. Knyazeva
THE FORMATION OF COATINGS USING SYNTHESIZED
MODIFYING POWDERS AND THE ENERGY OF ELECTRON
BEAM

M. I. Alymov, O. A. Golosova
**Explosive Production of New Materials:
Science, Technology, Business, and Innovations**

М. И. Алымов, О. А. Голосова
**Получение взрывом новых материалов:
наука, технологии, бизнес и инновации**